Unsolved problems in QCD: a lattice approach

Alejandro Vaquero Avilés-Casco

Departamento de Física Teórica
Universidad de Zaragoza

Contents

Agradecimientos

Esta compilación del trabajo realizado a lo largo de cuatro años no hubiera sido posible sin la ayuda de multitud de personas, tanto en el ámbito científico como en lo personal. Puesto que la Tésis sólo la firmo yo, voy a decicar unas páginas, en ejercicio de justicia, a todos aquellos que, de una manera u otra, la habéis hecho posible.

En primer lugar debo agradecer a mi director de tesis, Vicente, su apoyo y guía, tanto a nivel científico como personal. Siempre ha sido enormemente comprensivo con mis compromisos, y su preocupación por mí nunca se limitó a la física teórica. Todo esto hace que ahora lo considere más un amigo que un colega.

Algo parecido se puede aplicar a mis otros colaboradores cercanos, como Eduardo y Giuseppe, a los que además debo agradecer su hospitalidad, y a Fabrizio, por su sabio consejo. Estos cuatro años no hubieran sido lo mismo de no ser por Pablo, cuyas conversaciones, qué sólo de cuándo en cuándo versaban sobre física y a menudo me hacían mirar al mundo desde otro punto de vista, y su compañía en el despacho han hecho que desarrolle una relación con él que va más allá de lo profesional. Tampoco podría olvidarme de mis otros compañeros de pasillo, en particular Fernando Falceto y Jose Luis Alonso, que siempre han estado dispuestos a echarme una mano con cualquier problema que me surgiera, y me han animado a participar en proyectos nuevos que mantuvieran vivo mi interés en la investigación; así como de Diego Mazón y Victor Gopar, con quienes he compartido algunos buenos momentos que me han ayudado a hacer más ligero mi trabajo. Críticos para sobrevivir a la inmensa burocracia española han sido Pedro Justes, Esther Hernández y Esther Labad. Sin ellos probablemente aún estaría haciendo papeleo.

Fabio y Paula merecen un lugar aparte: Además de ofrecerme una ayuda inestimable en temas de física, son capaces de transformar cada escuela de física o cada nuevo congreso en una fiesta. Aunque casi siempre se encontraran a varios cientos de kilómetros de distancia, han estado muy presentes desde que nos conocimos en aquella escuela de Seattle en 2007.

Al capitán Jul y a Anuchi la princesa les debo miles de horas de buenos y malos momentos. Para mí es una inmensa suerte el poder contar con vosotros. Y contigo, Julieta, que no te olvido, a pesar de la enorme distancia que nos separa. A Irenilla por saber escucharme como nadie jamás lo ha hecho nunca, una pena que te mudaras a Barcelona. Y a Carlos Sánchez, Cristina Azcona, Pepa Martínez (siempre tan dulce y tan macarra al mismo tiempo) y Enrique Burzurí, que aunque os vea sólo de cuando en cuando, siempre son agradables vuestras visitas.

No podían faltar ente estas líneas mis compañeras de patinaje, en particular mi entrenadora Laura, Luci y Sara, mi pareja de patinaje, con las que he compartido infinitas alegrías, lloros y peleas. En cuanto a mi carrera pianística, a Luis debo agradecerle su inagotable comprensión por todos eso deberes inacabados. Y a Laura Rubio le debo mucha inspiración, tanto para la física como para la música. Todos ellos me han ofrecido otra vía de escape para descansar un poco la mente cuando los problemas físicos no encontraban solución. Mis inseparables compañeros de aventuras, Juan, Dano, Marta, Fabio y el Leas, también se merecen unas líneas, por estar allí (casi) todos los domingos, dispuestos a ayudarme a desconectar machacando orcos o lo que conviniera en el momento.

Por último, a mis padres, mi hermano Carlos y mi prima Ana por su apoyo incondicional y constante.

Zaragoza, March 22, 2012

Alejandro Vaquero Avilés-Casco ha realizado su tesis gracias al programa FPU del ministerio de Educación, a la colaboración INFN-MEC, a la colaboración europea STRONGnet, y al grupo de Altas Energías de la universidad de Zaragoza.

Introduction

Quantum Chromo-Dynamics (QCD) is a challenging theory: the strong CP problem or its behaviour for very high densities are some of the yet-unsolved problems that worry the QCD practitioners all along the world. Even some of its fundamental properties, like the confinement of quarks, remain unproved[1].

One of the points that makes the analysis of QCD so intrincate is its non-perturbative behaviour at low energies. Contrary to what happens in Quantum Electro-Dynamics (QED), whose coupling constant α_{QED} is small, QCD is only accessible to perturbative techniques in the high energy region, where its coupling constant α_{QCD} becomes small, due to the property of asymptotic freedom. For low energies, α_{QCD} takes very high values, and the perturbative expansion does not converge any more: we need an infinite number of Feynmann diagrams to compute any observable. Moreover, perturbation theory is unable to give account for all the topological properties of QCD. Since the topology plays a fundamental role in the theory, the availability of a non-perturbative tool to study QCD is very desirable.

The most prominent tool to investigate non-perturbative theories is the lattice. Logically, in this work, which is about QCD, the lattice is the underlying basis for every development. Lattice QCD and numerical simulations usually come together: in most cases, lattice theories are very complex to study analitically, but surprisingly easy to put in a computer. Taking into account the increasingly high computer power available nowadays, lattice QCD simulations are becoming a powerful and accurate tool to measure the relevant quantities of the theory. Unfortunately, the lattice is far from perfect, and there are still obstacles (like the sign problem) which prevent some simulations to be performed.

The title of this thesis summarizes the aim seeked along these four years of research: to tackle some of the yet-unsolved problems of QCD, to explore or create techniques to study the nature and the origin of the problem, and in some isolated cases, to find the desired solution. As the topics developed in this work have been the responsible of the headaches and frustrations of many scientist during the last decades, only in very few cases a reasonable solution to the problem exposed is found. In any case, the effort put into these pages constitute valuable information to those who decide to embark themselves in such a similar task.

The work exposed here can be divided in two parts. The first one (comprising chapters one to five) is related to the chiral anomaly, the strong CP problem, and the discrete symmetries of QCD, mainly Parity. All these topics are introduced very briefly in chapter one, to make the manuscript as self contained as possible. The second chapter is devoted to the key tool used to study all the aforementioned phenomena: the Probability Distribution Function ($p.d.f.$) formalism, a well-known technique used to study the spontaneous symmetry breaking (SSB) phenomena in statistical mechanics, brought to quantum field theories. Of particular interest is the extension of the domain of application of this technique to fermionic bilinears, well explained at the end of the second chapter. This chapter thus establish the theoretical framework required to understand the analyses performed in the following pages.

The third chapter is the first one containing original contributions. It begins with an introduction to the Aoki phase, explaining its origin and properties from several points of view. The Aoki phase is a consequence of the explicit chiral symmetry breaking of Wilson fermions. In this phase, Parity and Flavour symmetries are spontaneously broken, and even if the Aoki phase is not physical, its existence represents an obstacle to the proof of Parity and Flavour conservation in QCD. The new research performed here is the application of the $p.d.f.$ to the study the breaking of Parity and Flavour. Surprisingly we obtain unusual predictions: new

[1] At this moment, only numerical 'proof' of the confinement exists. In fact, the confinement of quarks is one of the *millenium problems*, awarded with a substantial prize by the *Clay Mathematics Institute*.

undocumented phases appear, that seem to contradict the standard picture of the Aoki phase; more exactly, the χPT and the $p.d.f.$ predictions clash and become difficult to reconcile. Since χPT is one of the pillars of the lattice QCD studies, it is quite important to find if one of the approaches is giving wrong results. The resolution to the contradiction is seeked –without much success- in a dynamical simulation of the Aoki phase without a twisted mass term, an outstanding deed never done before, due to the small eigenvalues of the Dirac operator that cause the Aoki phase.

The chapter four is, in some way, a continuation of chapter three. It tries to answer a question that arises after a careful examination of the Aoki phase: are Parity and Flavour spontaneously broken in QCD? The old Vafa and Witten theorems on Parity and Flavour conservation are reviewed and critiziced, and a new and original proof for massive quarks, within the frame of the $p.d.f.$, is developed. This proof makes use of the Ginsparg-Wilson regularisation, which lacks the problems of the Wilson fermions, despite of being capable of reproducing the anomaly on the lattice without doublers: its nice chiral properties depletes the spectrum of small eigenvalues for massive fermions and forbids the appearance of an Aoki-like Parity or Flavour breaking phase.

The fifth chapter drifts from the trend established in chapters three and four, in order to deal with the simulations of physical systems with a θ term. Although the main goal behind this chapter is to study QCD with a θ term, it is devoted entirely to the antiferromagnetic Ising model within an imaginary magnetic field, which is used as a testbed for our simulation algorithms. The first half of the chapter introduces the Ising model and the techniques used to avoid the sign problem inherent to the imaginary field. The second part, which contains the new contributions to the scientific world, applies the aforementioned algorithms to the two- and three-dimensional cases with success. The complete phase diagram of the model is sketched with the help of a mean-field calculation and, despite the simplicity of the model, its θ dependence proved to be more complicated than what one expects for QCD, featuring a phase transition for $\theta < \pi$ for some values of the coupling. The chapter ends with the commitment to apply these methods to QCD, in order to find out what would be the behaviour of nature if θ departed from zero, and to try to find out what it behind the strong CP problem.

The possibility to overcome the sign problem in the numerical simulations of QCD with a θ term inspired us to deal with another long-standing problem of QCD suffering from the same handicap: finite density QCD. This difficulties take us to the second part of this work, which deals with the polimerization of fermionic actions. The polimerization as a technique was born around thirty years ago, with the purpose of performing simulations of fermions on the lattice. Nowadays, fermion simulations are carried out by means of the effective action, obtained after the integration in the full action of the Grassman variables[2]. This integration yields the fermionic determinant, characterized by its high computational cost, for it usually reaches large dimensions[3]. The polymeric alternative transforms the quite expensive computationally determinant of the effective theory into a simple statistical mechanics system of monomers, dimers and baryonic loops, easy to simulate. Although this formulation naively displays a severe sign problem, it can be solved in some cases by clustering configurations, being the most notorious one the MDP model of Karsch and Mütter for QCD in the strong coupling limit.

That is why the sixth chapter of this work is completely devoted to the MDP model of Karsch and Mütter. When this model appeared, it was claimed that it allowed the performance of numerical simulations of finite density QCD in the strong coupling limit, for the sign problem within this model was mild in the worst case. Some doubts were raised when the analysis of Karsch and Mütter was carefully revised and extended, and in analyzing these objections we

[2]Direct simulation of the Grassman fields in the computer is not feasible at this moment.

[3]The most impresive numerical simulations involving dynamical fermions invert a $\sim 10^8 \times \sim 10^8$ fermionic matrix.

found a serious problem with the original simulation algorithm, which was not ergodic for small masses. In particular, the chiral limit $m \to 0$ was not simulable at all. Our contribution to the field is the improvement of the simulation algorithm to enhance its ergodicity, matching the good properties of the new so-called worm algoriths, to whom it is compared. The results are disappointing: the sign problem is recovered once the ergodicity is restored, so it was the lack of ergodicity the responsible of the reduction of the sign problem's severity. This result opposses that of Philippe de Forcrand in his last papers, were he claims to solve the sign problem in the same model by using a worm algorithm. Theoretical arguments explaining why the sign problem for high values of the chemical potential can not be solved within the $p.d.f.$ framework are then given.

On the other hand, the MDP model should suffer from a severe sign problem even at zero chemical potential, but from the experience of Karsch and Mütter, it seems that a clever clustering might be able to remove the sign problem completely, or at least to reduce its severity. This fact takes us to the seventh chapter, which successfully tries to apply the polimerization technique to a pure, abelian Yang-Mills action[4], in an attempt to take the MDP model beyond the strong coupling limit. The polymeric abelian gauge model is simulated and it is found to perform at least as well as the standard heat-bath procedure, besting it in some areas. A reduction of the critical slowing down for some systems featuring a second order phase transition is also observed. Nevertheless, the complete system featuring fermions plus Yang-Mills fields has a severe sign problem, even at zero chemical potential, and can not be simulated in the computer. In the last chapter, which can be viewed as an extension of chapter seven, the polymerization procedure is generalized and applied to other systems, mixing failure with success, being the most important of the latter the Ising model under an imaginary field $h = i\pi/2$ for any value of the dimension, which takes us back to the fifth chapter and the theories with a θ term.

Hence, the underlying topic of these four years of research has been the sign problem inherent to complex actions, in particular finite density QCD and QCD with a θ term, and any deviation from this point (mainly chapters two, three, four, seven and eight) is a side-work which ended up giving interesting results. These are long-standing problems to which hundreds of scientist have devoted half their lives without too much success. My collaborators and me are no exception, and although some significant advances were made within these four years, we are still very far from finding a solution to these problems.

[4]Although we regarded at first this application of the polymerization as an original contribution never done before, we discovered afterwards that we were wrong. The polymerization for abelian gauge theories was proposed some years ago, but it was never simulated in a computer.

Part I

Symmetries of QCD and θ-vacuum

Chapter 1

QCD and θ-vacuum: the strong CP problem

"Science never solves a problem without creating ten more"

—George Bernard Shaw

1.1 The symmetries of QCD lagrangian

The full[1] QCD lagrangian for N_F-flavours is

$$\mathcal{L} = \frac{1}{4} F^a_{\mu\nu} F^{\mu\nu}_a + \sum_{m,n}^{N} \left[i\bar{q}^m \gamma^\mu D_\mu q^m - \bar{q}^m M_{mn} q^n \right] \tag{1.1}$$

where the mass matrix is diagonal and real. The quark fields q belong to the $\left(\frac{1}{2}, 0\right) \oplus \left(0, \frac{1}{2}\right)$ representation of the Lorentz group, i.e., they are *Dirac spinors*. This representation is reducible and give rise to two sets of *Weyl spinors* by application of the *chiral projectors* P_L and P_R,

$$\begin{array}{rclcrcl} q_L &=& P_L q & & \bar{q}_L &=& \bar{q} P_L \\ q_R &=& P_R q & & \bar{q}_R &=& \bar{q} P_R, \end{array} \tag{1.2}$$

so we could write the lagrangian in terms of left and right handed fields,

$$\mathcal{L} = \frac{1}{4} F^a_{\mu\nu} F^{\mu\nu}_a + \sum_{m,n}^{N} \left[i\bar{q}^m_L \gamma^\mu D_\mu q^m_L + i\bar{q}^m_R \gamma^\mu D_\mu q^m_R - \bar{q}^m_L M_{mn} q^n_R \right]. \tag{1.3}$$

The key point to notice here is the absence of interactions between the left and the right weyl spinors, except for the mass term. In a world of massless quarks, the whole lagrangian would enjoy an $U(N_F)_L \times U(N_F)_R$ symmetry,

$$\begin{array}{rclcrcl} q^m_L &\to& U_{mn} q^n_L & & \bar{q}^m_L &\to& \bar{q}^m_L \left(U_{mn}\right)^\dagger \\ q^m_R &\to& V_{mn} q^n_R & & \bar{q}^m_R &\to& \bar{q}^m_R \left(V_{mn}\right)^\dagger \end{array} \qquad U, V \in U\left(N_F\right), \tag{1.4}$$

including the so called *chiral group*, represented by the $SU(N_F)_L \times SU(N_F)_R$ rotations, and allowing independent transformations of the left and right fields. Nonetheless, this is not the case of the universe.

[1] The θ-term will be introduced later.

Given an arbitrary diagonal, real mass matrix M with unequal eigenvalues, the only surviving symmetry for each quark field q_m is the $U(1)$ phase transformation, associated to fermion number conservation:

$$\begin{aligned} q' &= e^{i\alpha} q, \\ \bar{q}' &= e^{i\alpha} \bar{q}. \end{aligned} \tag{1.5}$$

As far as we know, the quarks up and down are not massless in Nature, but their masses are quite small, and it is usually a good approximation to work in the massless limit[2], where the light quark masses vanish. The strange quark, although much more massive, usually fits well in the chiral limit as well. This approximation brings up a $U(3)_L \times U(3)_R$ symmetry group in the theory, widely decomposed as $SU(3)_L \times SU(3)_R \times U(1)_B \times U(1)_A$. This symmetry is not preserved: its subgroup $SU(3)_L \times SU(3)_R \times U(1)_V$ is thought to be spontaneously broken to $SU(3)_V \times U(1)_V$, where the V subindex (vector) indicates a coherent rotation in both the L and the R fermions, whereas the A subindex (axial) denotes an opposite rotation. The chiral limit becomes a good approximation for those quarks whose mass is much smaller than the QCD scale $m_q << \Lambda_{QCD} \sim 300MeV$.

In this context, the $SU(2)_V \in SU(3)_V$ subgroup of the symmetry, associated to rotations mixing the up and down quarks, amounts to the old *isospin symmetry*[3]. In general, the whole $SU(3)_V$ is understood as *flavour symmetry*: being the three quarks massless in the chiral limit, they become indistinguishable from the QCD point of view; indeed the existence of this symmetry does not require massless but degenerated quarks. This vector symmetry is expected to generate multiplets of 'equivalent' hadrons related to the different representations of the group. The most widely-known are the baryonic decuplet and the meson octet. In fact, this is what approximatively happens in nature.

Regarding the remaining symmetries, the $U(1)_V$ group entails, as explained above, *fermion number conservation*, and the resting $U(1)_A$ is known as *axial symmetry*, and forces the difference of the number of fermions of each chirality $N_L - N_R$ to be preserved. As both, $N_L + N_R$ and $N_L - N_R$ are to be preserved, we should infer that both N_L and N_R are conserved separately. However, this is not what actually happens, I will come back to this point later.

The facts supporting the spontaneous breaking of the $SU(3)_L \times SU(3)_R$ symmetry for the up, down and strange quarks are related to the particle spectrum of the world: were the full symmetry realized, we should observe in Nature larger 'equivalent' particle multiplets, including positive parity partners of the standard mesons with similar masses. Up to now, none of these have been found, and there are no scalar particles with masses anywhere close to those of the pseudoscalar meson octet.

On the other hand, what we do observe is the existence of *light mesons*, in this case, the three pions. These can be understood in the framework of the spontaneous breaking of isospin symmetry $SU(2)_L \times SU(2)_R$ down to a $SU(2)_V$: the symmetry breakdown generates three massless Goldstone bosons; as the up and down quarks are not massless in Nature, the pions are assimilated in the theory as *approximate Goldstone bosons*, which should be strictly massless in the chiral limit.

The strange quark enlarges this picture with the four *Kaons*. These feature masses higher than the pions, for the strange quark is further from the chiral limit than the up and down

[2] Also called *chiral limit*, for at $m = 0$ the chiral group becomes a symmetry of the Lagrangian again, but this is not the end of the story...

[3] The wisdom that the isospin (interchange of up and down quarks) is a good symmetry of Nature has a long tradition in nuclear physics. Many relationships among cross-sections have been found using this symmetry.

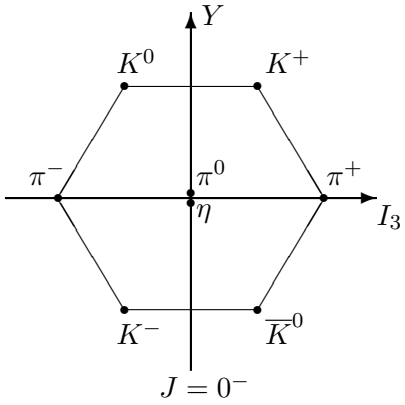

Figure 1.1: Mesonic octet of three flavoured QCD. These are aproximate Goldstone bosons of the spontaneous breaking of the $SU(3)_L \times U(3)_R \to SU(3)_V$ symmetry, which leaves eight broken generators.

quark, but the underlying phenomena giving rise to the low mass of the Kaons is the same. What puzzled the physicists during the 70's was the absence of a ninth Goldstone boson (or a fourth, in the context of only isospin symmetry with up and down quarks), coming from the spontaneous breaking of the $U(1)_A$ axial symmetry. Manifestations of this breaking were observed in the dynamical formation of diquark condensates $\langle \bar{u}u \rangle = \langle \bar{d}d \rangle \neq 0$. The spectrum of mesons revealed no ninth light meson that could be assimilated to the breaking of the $U(1)$ axial symmetry of QCD. The best candidate was the η', for it has the right quantum numbers to be the ninth meson, but its mass is too high to be considered a vestige of a Goldstone boson. People began to think that, after all, there was no true $U(1)_A$ symmetry in QCD, but this fact was not reflected in the lagrangian. The $U(1)_A$ problem was born [1].

1.2 Solution to the $U(1)_A$ problem

To understand the current solution to the $U(1)_A$ problem we must review the theory a bit more deeply. Let's begin with a free spinor of mass m

$$S_F = \int d^4x \left(\bar{\psi} \gamma^\mu \partial_\mu \psi + m \bar{\psi} \psi \right),$$

and consider both $U(1)_V$ and $U(1)_A$ internal transformations of the field ψ

$$U(1)_V \left\{ \begin{array}{rcl} \psi & \to & e^{i\alpha}\psi \\ \bar{\psi} & \to & \bar{\psi} e^{i\alpha} \end{array} \right. \qquad U(1)_A \left\{ \begin{array}{rcl} \psi & \to & e^{i\gamma^5\theta}\psi \\ \bar{\psi} & \to & \bar{\psi} e^{i\gamma^5\theta} \end{array} \right. . \tag{1.6}$$

For small values of α and θ

$$\begin{array}{rcl} e^{i\alpha} & \approx & 1 + i\alpha \\ e^{i\gamma^5\theta} & \approx & 1 + i\gamma^5\theta, \end{array}$$

and direct application of the Nöther theorem (A.3) produces

$$U(1)_V \left\{ \begin{array}{rcl} j^\mu & = & \bar{\psi}\gamma^\mu\psi \\ \partial_\mu j^\mu & = & 0 \\ Q & = & \psi^\dagger\psi = N_L + N_R \end{array} \right. \tag{1.7}$$

$$U(1)_A \left\{ \begin{array}{rcl} j_5^\mu & = & \bar{\psi}\gamma^\mu\gamma^5\psi \\ \partial_\mu j_5^\mu & = & 2im\bar{\psi}\gamma^5\psi \\ Q_5 & = & \psi^\dagger\gamma^5\psi = N_L - N_R. \end{array} \right. \tag{1.8}$$

Therefore, the massless free theory is $U(1)_A$ invariant. As j_μ and j_5^μ are both conserved, the following currents and charges

$$\begin{array}{rclcrcl} j_L^\mu & = & \frac{1}{2}\left(j^\mu - j_5^\mu\right) & \qquad & Q_L & = & N_L \\ j_R^\mu & = & \frac{1}{2}\left(j^\mu + j_5^\mu\right) & & Q_R & = & N_R \end{array} \tag{1.9}$$

are preserved, and the number of left-handed and right-handed fermions is constant over time.

What happens if we switch on a gauge field? As our transformation deals only with the fermionic degrees of freedom, the naive conclusion would be that the conservation of both currents holds. Nevertheless we know that there are gauge contributions to the anomaly, which can be computed in perturbation theory [2]. In fact, the so-called triangle diagrams

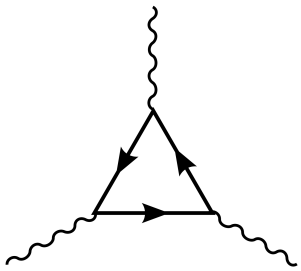

Figure 1.2: Example of triangle diagram contributing to the anomaly.

give rise to the equation

$$\partial_\mu j_5^\mu = 2im\bar{\psi}\gamma^5\psi - \frac{N_F g^2}{16\pi^2}\epsilon^{\alpha\beta\mu\nu}F^c_{\alpha\beta}F^c_{\mu\nu}. \tag{1.10}$$

The new term

$$\mathcal{P} = -\frac{N_F g^2}{16\pi^2}\epsilon^{\alpha\beta\mu\nu}F^c_{\alpha\beta}\left(x\right)F^c_{\mu\nu}\left(x\right) \tag{1.11}$$

is the *Pontryagin density* $\mathcal{P}$, which encodes the *topological properties of the Yang-Mills potentials and fields*, i.e., defects, dislocations and instanton solutions of the gauge fields, deeply related to the winding number of the configurations. Thence, chiral symmetry is only preserved at the classical level, for the quantum corrections of the fermion triangle diagrams break it explicitly. This phenomenon is known as the *Adler-Bell-Jackiw anomaly*, honoring the discoverers [2].

The path integral formulation

$$Z = \int \left[dA_\mu^a\right] d\psi d\bar{\psi}\, e^{\int d^4x\mathcal{L}} \tag{1.12}$$

can also give account of the anomaly. Although the massless action is invariant under a chiral transformation, the integral measure is not, and its Jacobian

$$J = e^{-i\int d^4x\theta(x)\frac{N_F g^2}{16\pi^2}\epsilon^{\alpha\beta\mu\nu}F^c_{\alpha\beta}(x)F^c_{\mu\nu}} \tag{1.13}$$

reproduces exactly the anomalous contribution of the Adler-Bell-Jackiw triangle diagrams.

The chiral transformation introduces a new parameter in the theory, the θ-angle associated to the chiral rotation, and one might wonder which value θ should take. As the term in the action arising from the anomaly violates CP-symmetry, most scientist assume $\theta = 0$ on experimental grounds[4], for as far as we know, CP is a good symmetry of QCD. Nonetheless, there are no theoretical arguments favouring the vanishing value of θ. This mystery, being know as *the strong CP problem*, still bewilders the theoretical physicists[5].

1.3 The role of the topological charge in the anomaly

An amazing property of this construction is the fact that the Pontryagin index can be written as a total divergence

$$\mathcal{P} = -\partial_\mu K = \\ -\frac{1}{16\pi^2}\epsilon^{\mu\alpha\beta\gamma}\partial_\mu \mathrm{Tr}\left[\frac{1}{2}A^a_\alpha(x)\,\partial_\beta A^a_\gamma(x) + \frac{1}{3}A^a_\alpha(x)\,A^a_\beta(x)\,A^a_\gamma(x)\right]; \quad (1.14)$$

thence, the modification of the action induced by $\mathcal{P}$ is a pure surface integral

$$\delta S = -\int d^4x \partial_\mu K^\mu = \int d\sigma_\mu K^\mu; \quad (1.15)$$

which becomes zero when the naive boundary condition $A^a_\mu = 0$ at spatial infinity is used. Furthermore, the redefinition of the axial current as

$$\mathcal{J}^\mu_5 = j^\mu_5 + K^\mu \quad (1.16)$$

implies that the new current is conserved in the chiral limit

$$\partial_\mu \mathcal{J}^\mu_5 = 2im\bar{\psi}\gamma^5\psi \underset{m\to 0}{=} 0. \quad (1.17)$$

Nonetheless, K^μ is not gauge invariant, so in principle, the conservation of the current $\mathcal{J}^\mu_5$ might seem an empty statement. We should wonder, what is the meaning of the equation (1.17) in the chiral limit. There are different points of view to address this phenomenon, being maybe the one introduced by 't Hooft [3] the most insightful: he showed that the correct boundary condition to be used is that A^a_μ should be a pure gauge field at spatial infinity, which comprises $A^a_\mu = 0$ *and its gauge transformations*. But K^μ is not gauge invariant, and there are pure gauge configurations, equivalent to $A^a_\mu = 0$, for which $\int d\sigma_\mu K^\mu \neq 0$.

Another way to see it, more practical, is the incompatibility of the regularisation schemes and the realization of the symmetries of the theory. We usually desire to apply a regularisation scheme which preserves gauge invariance, as this symmetry is what defines the QCD interactions. Equation (1.17) implies that this regularisation breaks the chiral symmetry explicitly. On the other hand, if we use a regularisation conserving chiral symmetry, we must give up gauge invariance. In other words, there is no regularisation scheme that can preserve gauge invariance and the chiral symmetry at the same time.

As exposed previously, the current $\mathcal{J}^\mu_5$ receives two apparently uncorrelated contributions: The first coming from the fermionic terms in the lagrangian, j^μ_5, is related to the chiralities of the fermions; and the second one, K^μ, is a pure gauge contribution, associated to the presence of

[4]The current experimental upper-bound of the θ parameter, based on measurements of the neutron electric dipole moment, is quite small $\theta \lesssim 10^{-10}$ (see [4]).

[5]For a review on this topic, see [5].

topological structures in the vacuum. Equation (1.17) relates both through the new conserved charge of the full symmetry. Integrating (1.17),

$$\mathcal{Q}_5 = Q_5 + Q_{Top}. \tag{1.18}$$

Thence, what is conserved is the quantity $N_L - N_R + Q_{Top}$, that simply is the celebrated Atiyah-Singer index theorem. It seems that there is an interplay between the fermionic and the pure gauge degrees of freedom, and the change of chirality in the fermions of the vacuum carries a modification of the topological structure of the gauge fields. In fact, there exist solutions for the gauge fields which are capable of changing the vacua, modifying Q_{Top}, and hence $N_L - N_R$. This solutions are called instantons, from *instant·on*, because they appear briefly in time. The instantons are quite important to define the theory, for the pure vacua of QCD is not the state of fixed Q_{Top}, but a linear combination of them

$$|\theta\rangle = \int e^{i\theta Q_{Top}} |Q_{Top}\rangle \,. \tag{1.19}$$

The picture is completely analogous to that of the electrons in a periodic cristalline structure, where θ would be the Bloch momentum and $|Q_{Top}\rangle$ would represent the position of the electron.

Summing up the former points, it is widely assumed that chiral symmetry is spontaneously broken in QCD, giving rise to the octet of light mesons, a remnant of the Goldstone bosons that should appear if the mass of the up, down and strange quarks was set to zero. The ninth particle (the η'), too massive to come from a Goldstone boson, adquires its mass from the anomaly, which, in the end, is not a true symmetry of the theory, thus has no effects and generates no Goldstone boson. Nonetheless, the axial transformation still maps solutions of the equations of motion into solutions of the equations of motion. The behaviour of the $U(1)_A$ symmetry reminds to spontaneous symmetry breaking, in the sense that the current $\mathcal{J}_5^\mu$ is preserved, and the ground state of the theory is degenerated. But in this case the η' cannot be considered as the remnant of a Goldstone boson, for the symmetry transformation associated to it is not gauge invariant; thus, the different vacua are essentially disconnected. The final structure of the theory is a discrete set of equivalent vacua, differing in the values of Q_{Top} and $N_L - N_R$, but conserving the charge $Q_{Top} + N_L - N_R$. The system can move through these vacua through the instanton solutions, which would be (in some sense) an analogous to the Goldstone boson, allowing tunneling between the vacua.

This way, the fluctuations of the topological charge produced by the instantons, those of the transverse susceptibility[6], related to $N_L - N_R$, and the chiral condensate are physically related, and the equation relating the transverse susceptibility χ_5, the topological susceptibility χ_T and the chiral condensate $\langle\bar{\psi}\psi\rangle$,

$$\chi_5 = -\frac{\langle\bar{\psi}\psi\rangle}{m} + \frac{\chi_T}{m^2} \tag{1.20}$$

acquires its full sense.

1.4 Discrete symmetries

Any Lorentz invariant local quantum field theories with an hermitian Hamiltonian is CPT invariant [6][7], where CPT is a combination of three discrete symmetries:

[6]The transverse susceptibility is defined as $\chi_5 = V\left[\left\langle\left(i\bar{\psi}\gamma_5\psi\right)^2\right\rangle - \left\langle i\bar{\psi}\gamma_5\psi\right\rangle^2\right]$, that is, the $i\bar{\psi}\gamma_5\psi$ correlation function integrated to all the points of the lattice.

[7]In the work of Schwinger, the theorem is implicitly proved, as an intermediate step to demonstrate the spin-statistics theorem. For a more recent and systematic proof, see [7].

- **Charge conjugation** C

  This symmetry relates a fermion with its corresponding antifermion.

- **Parity** P

  Parity inverts the spatial coordinates $\mathbf{x} \to -\mathbf{x}$, that is, it inverts the momentum of a particle while keeping its spin. Were the universe symmetric under Parity, the physic laws would not change if the whole universe was reflected in a mirror.

- **Time reversal** T

  The effect of a T transformation is to reverse the time $t \to -t$, flipping spin and momentum.

Even if a theory preserves CPT, each one of the symmetries might be violated separately; for instance, the electro-weak theory, due to its chiral nature, violates the T and CP symmetries.

In the early days of the strong interaction, when most of the work was undertaken by phenomenologist and nuclear physicist, each one of the symmetries (C, P and T) was though to be preserved separately. The aparition of the θ term in the action was quite disturbing, for this term explicitly violates CP symmetry, and such a violation in the strong force was not observed. On the other hand, and although the experiments seem to confirm that C, P and T are good symmetries of QCD, there is no theoretical proof of this fact. A symmetry preserved at the action level (and including the integration measure of the path integral) might not be realized in the vacuum, for spontaneous symmetry breaking might occur. Therefore, and although there are convincing indications assuring that these three symmetries are conserved in the strong interaction, this is still unclear from a theoretical point of view. I will deal with this topic later on, for now, let us go back to the anomaly.

1.5 The anomaly on the lattice

Arguably, the most successful regularisation of QCD so far is the lattice. Its ability to take into account the non-perturbative phenomena associated to the strong interactions allows the theoreticians to explore the low-energy dynamics and spectrum of QCD, an impossible deed to those devoted to QCD perturbation theory. Unfortunately, and in spite of the fact that the discretization of the pure gauge theory works perfectly, the introduction of the fermions is not so seamless, as the Nielsen-Ninomiya no-go theorem [8] asserts. The theorem states that no fermionic action can verify the four following conditions at the same time

(i.) The Fourier transform of the Dirac operator $\tilde{D}(p)$ is an analytic, periodic function of p.

(ii.) The operator $\tilde{D}(p) \propto \gamma^\mu p_\mu$ for $a|p_\mu| << 1$. This property forces D to be the fermionic operator for a Dirac fermion.

(iii.) The operator $\tilde{D}(p)$ must be invertible for an p_μ except $p_\mu = \mathbf{0}$.

(iv.) The anticommutator $\left\{\gamma^5, D\right\} = 0$ vanishes.

The first property is equivalent to require locality for the fermionic action. The second one forces D to be the the fermionic operator associated to Dirac fermions. As we know, each pole of D accounts for a fermion in the $a \to 0$ limit, thus the third requisite ensures that only one fermion is recovered in the continuum limit. And finally the fourth rule is the realization of chiral symmetry on the lattice.

The naive discretisation of fermions, first proposed by Wilson [9], violates the third point of the theorem, and its continuum limit produces 2^D Dirac fermions. This is not difficult to prove, one just need to write the naive action for a single flavour,

$$S_F\left[\psi,\bar{\psi}\right] = a^4 \sum_x \bar{\psi}(x) \Bigg(\sum_{\mu=1}^{4} \gamma_\mu \frac{U_\mu(x)\,\psi(x+\hat{\mu}) - U_\mu^\dagger(x-\hat{\mu})\,\psi(x-\hat{\mu})}{2a} - m\psi(x) \Bigg), \quad (1.21)$$

with a the lattice spacing. Here, the Dirac operator is

$$D(x,y)_{\substack{a\ b\\ \alpha\ \beta}} = \sum_{\mu=1}^{4} (\gamma_\mu)_{\alpha\beta} \frac{U_\mu(x)_{ab}\,\delta_{x+\hat{\mu},y} - U_\mu^\dagger(x-\hat{\mu})_{ab}\,\delta_{x-\hat{\mu},y}}{2a} + m\delta_{ab}\delta_{\alpha\beta}\delta_{x,y}. \quad (1.22)$$

where a and b are colour subindices, and α and β represent Dirac subindices. The fourier transform of D allows us to compute the poles of the propagator and see the doublers in this formulation. This is

$$\begin{aligned}\tilde{D}(p,q) &= \frac{1}{V}\sum_x e^{-i(p-q)xa} \left(\sum_{\mu=1}^{4} \gamma_\mu \frac{e^{iq_\mu a} - e^{-iq_\mu a}}{2a} + m\mathbf{1} \right) \\ &= \delta(p-q) \left[m\mathbf{1} + \frac{i}{a}\sum_{\mu=1}^{4} \gamma_\mu \sin(p_\mu a) \right] = \delta(p-q)\,\tilde{D}(p), \end{aligned} \quad (1.23)$$

and the propagator becomes

$$\tilde{D}^{-}1(p) = \frac{m\mathbf{1} - \frac{i}{a}\sum_{\mu=1}^{4}\gamma_\mu \sin(p_\mu a)}{m^2\mathbf{1} + a^{-2}\sum_\mu \left(\sin(p_\mu a)\right)^2}, \quad (1.24)$$

which has $2^D = 16$ poles at $m = 0$ in the four-dimensional case, given by $p_\mu = (k_1, k_2, k_3, k_4)$, where $k_i = 0, \frac{\pi}{2}$.

Wilson noticed the problems of the naive action shortly after the publication of [9], and proposed a simple way to fix it: he added a term to the action, the so-called Wilson term, which is a discretization of $-\frac{ra}{2}\partial_\mu\partial_\mu$, where ∂_μ is the full covariant derivative and r is usually $r = 1$:

$$S_F\left[\psi,\bar{\psi}\right] = a^4 \sum_x \bar{\psi}(x) \Bigg[\left(m + \frac{4r}{a}\right)\psi(x) - \sum_{\mu=1}^{4} \frac{(\mathbf{1}-\gamma_\mu)\,U_\mu(x)\,\psi(x+\hat{\mu}) - (\mathbf{1}+\gamma_\mu)\,U_\mu^\dagger(x-\hat{\mu})\,\psi(x-\hat{\mu})}{2a} \Bigg]. \quad (1.25)$$

The Wilson term generates a mass proportional to $\frac{1}{a}$ to $2^D - 1$ fermions [10]; therefore the degrees of freedom associated to these fermions become frozen in the continuum limit, and only

a single fermion is recovered. But in doing so, the new action violates chiral symmetry explicitly, even at zero mass of the quark, for the Wilson term mixes chiralities, and behaves in the same way as a mass term under chiral transformations.

One might think that an explicit violation of chiral symmetry should not be quite problematic, as in the end we have to cope with massive quarks. Sadly, the problem is a bit more complicated. An explicit violation of chiral symmetry not induced by the quark mass terms produces a *mixing* of the chiral violating operators with the mass terms. In the end we have to substract these contributions to the mass terms to find out the right value for the masses of the particles of our theory, i.e., the masses are renormalized additively, and to worsen the problem, the terms to be substracted diverge, giving in the end a finite contribution. This fact renders the measurements of some observables quite difficult. On the other hand, a fermionic action complying with chiral symmetry protect the masses from additive renormalisations, so only multiplicative renormalisation occurs, and the relationship between the measured quantities on the lattice and the physical observables is simplified greatly.

So at first, one is tempted to think that chiral symmetry is quite a desirable property. Indeed it is, and a quite successful action for lattice fermions is the Kogut-Susskind action, also known as staggered fermions. The problem with the exact realization of chiral symmetry in the lattice is the fact that, as the regulator does not violate chiral symmetry, the anomaly is not accounted for in the continuum limit. In fact, it seems that there is no simple resolution to this matter: the anomaly requires an infinite number of degrees of freedom to happen, and can not be observed on the lattice. The only way to reproduce the anomaly is use a regulator which breaks the chiral symmetry explicitly on the lattice, and recover it in the continuum limit[8].

A great advance was done on this topic by the introduction of the *Ginsparg-Wilson* fermions [11]. These break explicitly the chiral symmetry in the mildest possible way: the anticommutator $\{\gamma_5, D\}$ equals something that is *local*,

$$\{\gamma_5, D\} = aRD\gamma_5 D \tag{1.26}$$

with R a constant depending on the particular version of the regularisation, and a the lattice spacing. This locality allow the fermions to behave *as if the anticommutator was realized for long distances*, as we will see in chapter 4. Therefore, the Ginsparg-Wilson regularisation for fermions is capable of reproducing the anomaly in the continuum limit, while keeping the good properties of the chiral fermions and keeping the theory free of doublers.

[8] Actually, some authors [12] claim that the staggered fermions can reproduce the correct continuum limit (and therefore, the anomaly) by using *rooting trick*, which escapes the Nielsen-Nimoyima no-go theorem by imposing the non-locality of the action. In some cases, even numerical agreement has been reached [13], although it is still unclear if all the aspects of the anomaly are correctly reproduced by the rooting approach [14]. The subject is quite controversial and completely out of the scope of this work.

Chapter 2

The analysis of Spontaneous Symmetry Breaking phenomena

"A child of five would understand this.
Send someone to fetch a child of five."

—Groucho Marx

2.1 Introduction to Spontaneous Symmetry Breaking (SSB)

In some models, the symmetries of the action (or the Hamiltonian, if we are working with statistical mechanics models) do not always show up in the ground state, but instead, the system may choose among many degenerated ground states, related to each other by the original symmetry.

For instance, the spins inside a magnet are free to point everywhere. The Hamiltonian of the system exhibits an $SO(3)$ symmetry, that should lead to a vanishing magnetization. But this scenario only happens at high temperatures, where the spins are disordered. At low temperatures, long range ordering appears, and spontaneous magnetization is developed. It seems that there is a preferred direction for the system, but this is in clear contradiction with the $SO(3)$ symmetry of the Hamiltonian. What happened to the symmetry? The answer is... nothing. The symmetry is still there, and it is manifested in the degeneration of the ground state. The different possible ground states are related by the original $SO(3)$ symmetry, which means that if we rotate all the spins at the same time, the energy does not change. Thus the total magnetization taking into account all the possible outcomes (directions) is zero.

The following thought experiment might help: imagine that a large set of equal magnetic samples is available to us, and that we can isolate each sample in a different chamber, where no magnetic fields are allowed. Then we heat each sample in a different chamber, until the magnetization of each one is completely lost, and then, let them cool down and regain magnetization. At the end, we should find a set of samples whose magnetization vectors are non-zero, but point randomly, and averaging magnetizations we would find a vanishing vector.

Strictly speaking, spontaneous symmetry breaking phenomena can only happen in systems with an infinite number of degrees of freedom. The reason is simple: if the number of degrees of freedom is finite, the system can jump from vacuum to vacuum in a finite amount of time, and in an effective way, the symmetry is realized. If, on the contrary, the number of degrees of freedom is infinite, the degenerated vacua become disconnected and the system is trapped in an asymmetric state. This fact is well known in statistical mechanics systems.

For quantum mechanical systems with a finite number of degrees of freedom, the arguments are a bit more complex: although there are systems in which the different ground states do not enjoy the same symmetry level as the Hamiltonian, all these vacua lie in the same Hilbert space of square-integrable funcions L_2[1]. The creation and annihilation operators of the vacua are related among each other through unitary transformations. Therefore, the symmetry transformations, which commute with the Hamiltonian by definition, amount to a redefinition of the fields and observables, there is only just one vacuum and the breaking of the symmetry was impossible to observe at the physical[2] level[3].

On the contrary, in theories with infinite degrees of freedom, like quantum field theories (QFT), the different symmetric vacua feature a different representation of the algebra of the operators. Although every vacua relates to the same dynamical system, their representations are essentially inequivalent, and cannot be connected by using unitary transformations. In other words: the system can not evolve from one vacuum to another, and the SSB is realized[4].

In fact, the former though experiment was flawed. If we are patient enough, we will see variations in the magnetization of the samples as time goes by, even if they are kept at very low temperatures. Averaging over an infinite time, we will find a vanishing magnetization vector. The reason that makes the system evolve so slowly is the large number of degrees of freedom in a natural magnet, of the order of Avogadro's number ($N_A \approx 10^{23}$). The system can move from one vacuum to another, but it takes indeed a remarkable long time to do so.

Spontaneous symmetry breaking might happen in system with discrete and with continuous symmetries. In the case of a continuous symmetry, the Goldstone theorem [16, 17] states that:

In a Lorentz and translational invariant local field theory with conserved currents related to a Lie group G, the spontaneous breaking of the symmetry G generates massless and spinless particles called Goldstone bosons, which couple to both, currents and fields.

In simpler words, the breaking of a continuous symmetry implies the existence of massless particles [18], one for each generator of the symmetry that does not annihilate the vacuum. This set of generators build up the symmetry transformations that relate all the degenerate vacua.

The Goldstone bosons represent long wavelength vibration modes of low-energy. In fact, being the Goldstone bosons massless, it defines a transformation of infinite wavelength which modifies the ground state of the system at zero energy cost. But we stated earlier that whenever SSB occurs, the system is trapped in a single ground state, because this transformation is ill-defined in the Fock space of our theory. Nonetheless, the Goldstone bosons describe and define the low-energy spectrum of the theory, thus they define the dynamics of the broken phase.

2.2 The $p.d.f.$ formalism

The analysis of the properties of the ground state of a theory can become a tricky exercise. The ground state need neither be unique, nor respect all the symmetries announced in the action

[1] For instance, one can take two completely different theories, like an Hydrogen atom and an harmonic oscillator, to find that the action of the Hydrogen atom Hamiltonian H_H on the harmonic oscillator grond state $|0\rangle_{HO}$ is perfectly defined.

[2] See the first chapter of [15].

[3] Another way to look at this property is to use the Feynmann path integral formulation to transform the quantum mechanical system into a one-dimensional statistical system with a local interaction. A theorem forbids SSB on such statistical system.

[4] In this case, the action of the Hamiltonian of a theory in the ground state of a different theory (let's take, for instance, two Klein-Gordon bosons with different masses), is not well defined. The reason is that the Fock spaces of the two theories are disconnected in the thermodynamic limit, and an expansion of the ground state of the first theory in terms of particles belonging to the second theory requires an infinite number of terms.

(or the Hamiltonian), for SSB may take place. With a degenerated ground state, the direct analysis becomes complicated and normally offers no useful information, and we need to couple the system to external sources that break explicitly the symmetry, in order to select a vacuum. Then, we compute the pertinent order parameters of the symmetry for a given value of the external field in the thermodynamic limit, and finally we take the zero external field limit, and see how the order parameters behave. This approach is quite sensible in analytical calculations, and it is, in fact, a standard procedure.

The numerical simulations of statistical systems and QFT's (particularly, QCD) share the same problem. If we try to measure the mean magnetization in a simulation of the Ising model, we find after a large number of iterations that $\langle m \rangle \to 0$, even if we are in the ordered phase where Z_2 is spontaneously broken. The reason is the fact that system is enclosed in a finite volume, with a finite number of degrees of freedom, and tunneling between the two degenerated vacua occurs, averaging the magnetization to zero. The easy solution in this case is to measure $\langle m^2 \rangle$, which is always non-vanishing at finite volume, but takes very small values (of order $O\left(\frac{1}{V}\right)$ in the disordered phase, whereas in the magnetized phase $\left\langle m^2 \right\rangle \approx 1$. This procedure might seem quite surprising at first, for $\left\langle m^2 \right\rangle$ is invariant under Z_2 transformations, thus it does not look like a good order parameter for spontaneous Z_2 breaking. However, we have to keep in mind that m and its higher powers are intensive operators. As the odd powers of m are good order parameters of the Z_2 symmetry, in the symmetric vacuum case $m \to 0$ when $V \to \infty$. Since intensive operators do not fluctuate in the thermodynamic limit, $m^2 \to 0$ as well.

Unfortunately, this recipe is only valid for the Ising model, and similar models featuring a Z_2 broken symmetry. There are other situations, far more complex, where it would be desirable to find a systematic way to deal with the order parameters. The first attemps are a shameless copy of the analytical procedure, and basically consist on (*i.*) adding an external source to the action, which breaks explicitly the symmetry, (*ii.*) performing many simulations of the same system at different values of the volume and the external field, (*iii.*) finding the infinite volume limit for the order parameter at each fixed value of the field, and (*iv.*) finding the zero field limit of the set of values of the order parameter in the $V \to \infty$ limit. This process involves many simulations, as we have to take two different limits, thermodynamic and zero external source, and the extrapolations required to reach both limits are usually arbitraly, a fact that enlarges the systematic errors. In addition, for some systems the external source method introduces a severe sign problem in the simulation. Examples of this are the addition of a θ vacuum term in the QCD action, or the addition of a diquark source in two-coloured QCD. It seems that the analytical approach is not so clean when we put it on the computer.

There is an alternative, well-known in statistical mechanics, the *Probability Distribution Function* (*p.d.f.*) *formalism*. The *p.d.f.* formalism amounts to the calculation of the probability distribution function $P(c)$ of the interesting order parameter c at vanishing external field. Once the function $P(c)$ is known, the mean value of any power of the order parameter c^n is easily computable as

$$\langle c^n \rangle = \int_{-\infty}^{\infty} dc\, c^n\, P(c)$$

In contrast with the external source approach, the *p.d.f.* requires only one long simulation to measure $P(c)$ and no extrapolations at all, so the systematic errors are strongly suppressed. Moreover, external sources introducing a sign problem can be treated normally [20].

Fermions are a specially complicated case. As Grassman variables are not directly simulable in the computer[5], the common strategy is to integrate them out, yielding an effective action

[5]Some efforts in this direction have been done by M. Creutz [19]. Although the results indicate –as expected– an exponential growing of the computation time with the number of d.o.f., the increasing computer power

proportional to the determinant of the fermionic matrix. The key point here is the fact that, in many cases, the integration of the Grassman variables is equivalent to an averaging over all the possible degenerated vacua[6]; thence, all the order parameters which are fermionic bilinears vanish by force, configuration per configuration, and the $P(c)$ of the bilinear is not measurable directly. The external source method allows the system to accommodate in one of the vacua, breaking the degeneration, but as stated before, even if this procedure is quite standard and widespread, it is not as clean as we would like.

It would be much better to be able to measure the $P(c)$ for these fermionic bilinears. It happens that a way to compute this function was devised fifteen years ago in [21]. Although quite advantegeous, the *p.d.f.* is unfortunately not the standard approach to deal with SSB of systems with fermionic bilinears as order parameters. That is why I have considered pertinent to sketch the procedure and introduce the notation in the following sections.

The *p.d.f.* formalism for fermionic bilinears

Let

$$\mathcal{O}(x) = \bar{\psi}(x) O \psi(x) \tag{2.1}$$

be the order parameter of an interesting symmetry of our fermionic system, where O is a constant matrix, so the only dependence on the lattice site is gathered in the Grassman fields. If the symmetry is spontaneously broken, we expect the ground state to be degenerate. Each different vacuum can be labeled with an index α, so the expectation value c of the order parameter becomes vacuum-dependent c_α

$$c_\alpha = \frac{1}{V} \int d^4x \, \mathcal{O}_\alpha(x) \,. \tag{2.2}$$

An expression for the $P(c)$ follows from (2.2)

$$P(c) = \sum_\alpha \omega_\alpha \delta(c - c_\alpha) = \left\langle \delta\left(c - \frac{1}{V} \int d^4x \, \mathcal{O}(x) \right) \right\rangle , \tag{2.3}$$

where ω_α is the weight of the vacuum labeled as α, and the brackets $\langle \cdot \rangle$ stands for mean value, computed with the integration measure

$$[dU] \, e^{-S_G} \det(D + m) \,,$$

which defines the partition function of the theory

$$Z = \int [dU] \, e^{-S_G} \det(D + m) \,, \tag{2.4}$$

with $(D + m)$ as the fermionic matrix with mass terms, S_G as the bosonic action and U aglomerating every bosonic degree of freedom.

The rightmost expression of equation (2.3) involves the dirac delta of a fermionic bilinear. This kind of object is –in principle- defined only formally, thus equation (2.3) is empty of meaning for fermionic order parameters; were $\mathcal{O}(x)$ a bosonic operator, no objections to (2.3) could be raised. The solution to this problem is not straightforward, and involves another ill-defined step: The computation of the Fourier transform $P(q) = \int dc \, e^{iqc} P(c)$,

available for simulations is making this approach interesting for some unsolved scenarios featuring sign problem (i.e. chemical potential, or θ–vacuum).

[6] Parity is a notable exception, for it acts on the gauge fields as well; ergo the determinant cannot contain all the possible vacua.

$$P(q) = \frac{\int [dU] \left[d\bar{\psi} d\psi\right] e^{-S_G + \bar{\psi}(D+m)\psi + \frac{iq}{V}\int d^4x\, \mathcal{O}(x)}}{\int [dU] \left[d\bar{\psi} d\psi\right] e^{-S_G + \bar{\psi}(D+m)\psi}}. \tag{2.5}$$

Again, nothing wrong can be found in this equation for bosonic order parameters, but in the case of a fermionic bilinear, we have to postulate $P(q)$ directly, skipping (2.3), in order to keep the discussion rigurous.

After integration of the Grassman variables, the expression for the $P(q)$ is simplified

$$P(q) = \left\langle \frac{\det\left(D + m + \frac{iq}{V}\mathcal{O}\right)}{\det(D+m)} \right\rangle, \tag{2.6}$$

and the different moments of the $p.d.f.$ are easily calculated as the $q-$derivatives at the origin of the generating function,

$$\langle \mathcal{O}^n \rangle = \left. \frac{d^n P(q)}{dq^n} \right|_{q=0}. \tag{2.7}$$

This way we can postulate (2.5) or (2.6) directly as the *generation function of all the moments of the distribution function* and render the formalism rigorous, even for fermionic fields, and we can define a $P(c)$ as the inverse Fourier transform of the postulated $P(q)$ [21, 20].

We have to take into account that, due to the anticommuting nature of the Grassman variables, $P(q)$ is a polynomial of degree the lattice volume V, so all the moments of $P(c)$ higher than V vanish, for they involve an integral of a product of Grassman variables with a repeated index.

Chapter 3

The Aoki phase

"Research is what I'm doing when I don't know what I'm doing."

—Wernher von Braun

Spontaneous chiral symmetry breaking plays a distinguished role in the properties of QCD at low energies. One expects that the theory of two flavours develops three massless pions and a massive η as the mass of the quarks is driven towards zero: at $m = 0$ a first order phase transition takes place, for chiral symmetry is recovered, and then spontaneously broken, giving rise to three Goldstone bosons (the massless pions). Nonetheless the Wilson regularization for fermions breaks chiral symmetry explicitly, and behaves in a very different way. First of all, (i.) the critical line marking the 'chiral transition' must be non-chiral, i.e., the critical line can not mark spontaneous chiral symmetry breaking, for chiral symmetry is violated explicitly. But if the action behaves well (i.e., it leads to QCD in the continuum limit), we expect the pions to become massless at the critical line, whereas the η should stay massive. On the other hand, (ii.) the critical line lies not at $m = 0$, but the Wilson r term mixes with the mass term, displacing the critical line towards a value $m_c(\beta)$ which depends on the lattice spacing. As there is nothing wrong in using mass values below the critical mass m_c, there must be a region beyond the critical line with maybe new properties. These two features are combined in the so called Aoki phase.

The Aoki phase is a region, appearing only[1] in actions with Wilson fermions, quenched and unquenched [25, 26, 27, 28, 29, 30, 31], which extends beyond the critical line, and breaks Parity and Flavour symmetries (the latter only in case the number of flavours $N_F > 1$) spontaneously. The usual sketch of the Aoki phase for two flavours[2] is shown in fig. 3.1, where the QCD continuum-like phase (that conserving Parity and Flavour) is labeled as A, whereas the Aoki phase is marked as B. The Aoki phase develops five fingers at weak coupling, associated to ten critical lines –where the masses of the three pions vanish– which shrink swiftly to isolated points as $g \to 0$, leading to different continuum limits. These limits differ in the number of fermions, as can be seen computing the poles of the free propagator: equaling to zero its denominator

$$\left(\cos\left(p_\nu a^\nu\right) - 4 - m\right)^2 + \sin^2\left(p_\nu a^\nu\right) = 0, \tag{3.1}$$

we find that for each border of the Brillouin zone there is a different continuum limit at a different value of the mass. For $m = 0$ only the value $p_\nu = (0, 0, 0, 0)$ is a pole of the propagator, so there

[1] So far, no other regularization has exhibited the same properties. Although in [22, 23] an Aoki phase for staggered fermions was proposed theoretically, it was never confirmed in simulations. On the other hand, other models involving Wilson fermions, but different from QCD, display an Aoki-like phase, see [24].

[2] The most studied case of the Aoki phase is $N_F = 2$ for obvious reasons.

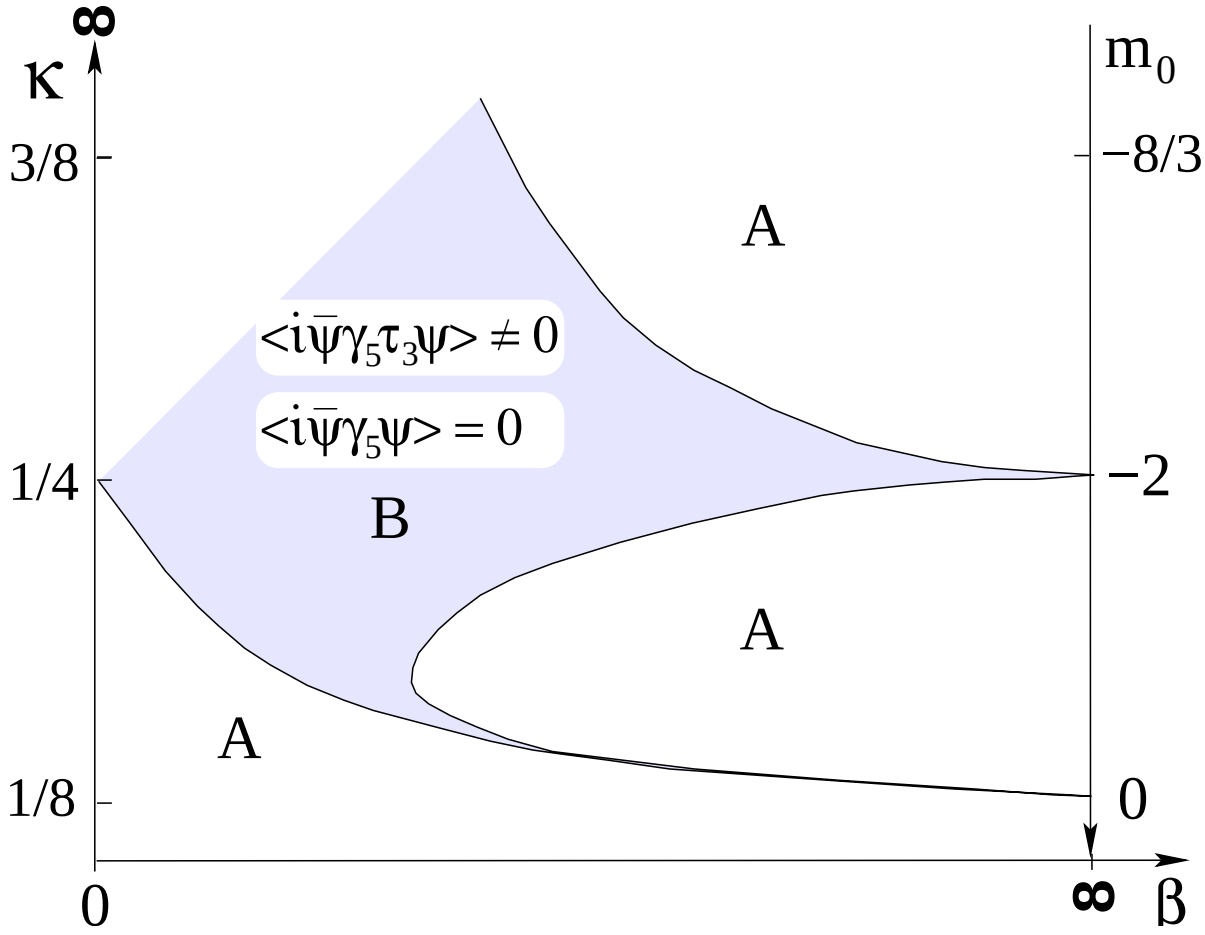

Figure 3.1: Aoki (B) and physical (A) region in the (β, κ) plane. The mean values refer to a single vacuum, among all the possible ones. Adapted from [41] with courtesy of the authors.

is only one fermion (per flavour) in the continuum limit. However, for $m = -2$ the condition is satisfied by the vector $p_\nu = \left(\frac{\pi}{2}, 0, 0, 0\right)$ and its equivalents $\left(0, \frac{\pi}{2}, 0, 0\right)$, $\left(0, \frac{\pi}{2}, 0, 0\right)$ and $\left(0, 0, 0, \frac{\pi}{2}\right)$, giving rise to four fermions. In the case $m = -4$ the family of vectors $p_\nu = \left(\frac{\pi}{2}, \frac{\pi}{2}, 0, 0\right)$ leads to a continuum limit with six fermions, for $m = -6$ there are again four vectors similar to $p_\nu = \left(\frac{\pi}{2}, \frac{\pi}{2}, \frac{\pi}{2}, 0\right)$ and finally at $m = -8$ only one fermion $p_\nu = \left(\frac{\pi}{2}, \frac{\pi}{2}, \frac{\pi}{2}, \frac{\pi}{2}\right)$ appears as $a \to 0$. It is clear from this picture that the degenerated two-flavoured action features a symmetry $4 + m \leftrightarrow -(4 + m)$, that is, $\kappa \leftrightarrow -\kappa$.

For the two flavoured case, Flavour breaking propiciates the apparition of massless particles in the thermodynamic limit, even if there is no spontaneous chiral symmetry breaking: two massless Goldstone bosons at the critical line (the two charged[3] pions) plus a massless mode associated to the continuous second order phase transition $A \leftrightarrow B$[4].The fact that these Goldstone bosons are the pions is related to Parity breaking as well. As we know, the operators associated to the pions in this case are $i\bar{\psi}\gamma^5\tau_j\psi$ with $j = 1, 2, 3$, for the pions are $P = -1$ particles. Only the spontaneous breaking of Parity would allow these operators to develop long-range ordering and non-zero disconnected parts. The η still stays massive, this is reflected in the fact that there

[3]Which pions become massless depends on the vacuum chosen after the SSB leading to the Aoki phase has taken place. We will use in this introduction the standard Aoki vacuum, that is, the one selected after adding the external source $hi\bar{\psi}\gamma_5\tau_3\psi$.

[4]Since the transition is continuous, and the two charged pions become massless at the critical line, the neutral pion must also be massless in the transition, so as to recover Flavour symmetry in phase A.

are no more Goldstone bosons, and thence there is no massless η. Thence the η is thought not to play further role in the Aoki phase, and the expectation value of any moment of the operator $i\bar{\psi}\gamma_5\psi$ is expected to vanish. In fact, and as stated by S. Sharpe and R. Singleton Jr. in [32], there is a conserved discrete symmetry

$$P' = P \times i\tau_1 \tag{3.2}$$

which consist of a combination of flavour interchange and Parity transformation, multiplied by a phase to keep the operator hermitian. This symmetry, which is not a replacement for Parity, forces any power of the operator $i\bar{\psi}\gamma_5\psi$ to take zero expectation value inside the Aoki phase, even if Parity is broken. The operator $\bar{\psi}\tau_3\psi$, which could be used to check Flavour symmetry breaking, vanishes as well because of symmetry P'.

Thence, the Aoki phase is characterized by the following properties in the thermodynamic limit

$$\begin{aligned} \left\langle i\bar{\psi}\gamma_5\tau_3\psi \right\rangle &\neq 0, \\ \left\langle i\bar{\psi}\gamma_5\psi \right\rangle &= 0. \end{aligned} \tag{3.3}$$

This unambiguously implies an antiferromagnetic ordering of the two condensates $i\bar{\psi}_u\gamma_5\psi_u$ and $i\bar{\psi}_d\gamma_5\psi_d$, verifying the relation

$$\left\langle i\bar{\psi}_u\gamma_5\psi_u \right\rangle = -\left\langle i\bar{\psi}_d\gamma_5\psi_d \right\rangle.$$

The standard picture of the Aoki phase does not allow any other kind of ordering of the $P = -1$ condensates.

3.1 Arguments supporting the standard picture of the Aoki phase

χPT analysis

The theory of chiral Lagrangians indeed supports this standard picture, and is fully compatible with the existence of the Aoki phase [32, 33][5]. Let us see this at work. When close to the continuum limit, the lattice theory can be described by an effective continuum Lagrangian, plus some terms depending on the finite lattice spacing a. Not all terms are allowed to supplement the original continuum Lagrangian, but only those complying with the symmetries of the lattice action, i.e., chiral symmetry in this case. Up to first order in a, the result is

$$\begin{aligned} \mathcal{L}_{Eff} \sim \mathcal{L}_G + \bar{\psi}\left(D + \frac{m_0}{a}\right)\psi - \frac{\tilde{m}_c}{a}\bar{\psi}\psi + b_1 ia\bar{\psi}\tau_{\mu\nu}F_{\mu\nu}\psi + b_2 a\bar{\psi}\left(D+m\right)^2\psi \\ + b_3 am\bar{\psi}\left(D+m\right)\psi + b_4 am\mathcal{L}_G + b_5 am^2\bar{\psi}\psi + O\left(a^2\right), \end{aligned} \tag{3.4}$$

where $\mathcal{L}_G$ is the pure gluonic Lagrangian, m is the physical mass, which will be defined shortly, and $\tau_{\mu\nu} = [\gamma_\mu, \gamma_\nu]$. In this analysis, there is no attempt to control factors of order unity, like renormalization factors with logarithmic dependence on a. That is why we use the symbol $\sim$.

Now we proceed to the analysis of every single term of (3.4). The first two sumands on the r.h.s. correspond to the naive continuum limit of the lattice Lagrangian. The next one is the

[5] Although the exposition contained here is based in the work of S. Sharpe and R. J. Singleton, Jr., the pioneer on the topic was M. Creutz [34] with an analysis based on the linear $\sigma-$model, which predicted the existence of an Aoki phase as well.

most important correction, the additive mass renormalization term, and it is usually absorbed in a redefinition of the mass

$$m = \frac{m_0 - \tilde{m}_c}{a}, \tag{3.5}$$

which is the aforementioned physical mass m. Two comments are in order: (i) the divergence $\frac{1}{a}$ is absorbed in the definition, so we are renormalizing the mass term, and (ii) $\tilde{m}_c$ is close to $m_c\left(g^2\right)$, the mass at which the pion masses vanish, but slightly different. That is why the $\tilde{x}$ notation is used.

The terms proportional to b_2 and b_3 vanish by virtue of the leading order equations of motion, as one can find a redefinition of the quark variables that makes both terms zero. The term proportional to b_4 only adds a dependency of the gauge coupling on the renormalized mass, and the term b_5 complicates the dependency of the physical mass on the bare quark mass. These two last contributions are not relevant for the analysis we are carrying out, so they will be subsequently ignored. As a result, only the Pauli term b_1 survives, and our effective Lagrangian reads

$$\mathcal{L}_{Eff} \sim \mathcal{L}_G + \bar{\psi}\left(D + m\right)\psi + iab_1\bar{\psi}\tau_{\mu\nu}F_{\mu\nu}\psi + O\left(a^2\right). \tag{3.6}$$

So what we need to do is to modify the standard χPT Lagrangian to accomodate the Pauli term.

The standard chiral Lagrangian for two flavours is defined as a $SU\left(2\right)_L \times SU\left(2\right)_R$ invariant theory, describing the low energy dynamics of QCD. Its degrees of freedom are the pion fields, gathered in the $SU\left(2\right)$ matrix Σ as

$$\Sigma = \begin{pmatrix} \frac{\pi^0}{\sqrt{2}} & \pi^+ \\ \pi^- & -\frac{\pi^0}{\sqrt{2}} \end{pmatrix}. \tag{3.7}$$

The Lagrangian of the massless case is simply

$$\mathcal{L}_\chi = \frac{f_\pi^2}{4}\mathrm{Tr}\left(\partial_\mu\Sigma^\dagger\partial^\mu\Sigma\right). \tag{3.8}$$

The field Σ transforms under the $SU\left(2\right)_L \times SU\left(2\right)_R$ chiral group as

$$\Sigma \to L\Sigma R^\dagger, \tag{3.9}$$

where L and R are two independent $SU\left(2\right)$ matrices.

In the ground state, the field Σ acquires a non-zero expectation value $\langle\Sigma\rangle = \Sigma_0 \neq 0$, signaling chiral symmetry breaking from $SU\left(2\right)_L \times SU\left(2\right)_R \to SU\left(2\right)_V$. The lowest excitations of the vacuum are associated to the Goldstone bosons, in this case, the pions

$$\Sigma = \Sigma_0 e^{i\sum_{j=0}^{3}\frac{\pi_a\tau_a}{f_\pi}}, \tag{3.10}$$

with τ_a the Pauli matrices. The addition of a mass term breaks explicitly chiral symmetry. Up to second order in m, this rupture is achieved by adding the potential

$$\mathcal{V}_\chi = -\frac{c_1}{4}\mathrm{Tr}\left(\Sigma + \Sigma^\dagger\right) + \frac{c_2}{16}\left[\mathrm{Tr}\left(\Sigma + \Sigma^\dagger\right)\right]^2, \tag{3.11}$$

where the mass dependence is introduced in the coefficients $c_1 \sim m\Lambda_{QCD}^3$ and $c_2 \sim m^2\Lambda_{QCD}^2$. All the terms containing derivatives of the field Σ have been dropped in (3.11): as we are

interested in the vacuum state only (not in the dynamics) these terms are irrelevant, thus only powers of $\mathrm{Tr}\left(\Sigma+\Sigma^{\dagger}\right)$ appear[6].

The inclusion of the Pauli term does not modify the structure of this Lagrangian, but only the value of the coefficients. The reason is the fact that the Pauli term and the mass term transform in the same way under the chiral group, so the introduction of the Pauli term only amounts to a shift in the mass $m \to m + a\Lambda_{QCD}^2$. Consequently, neglecting terms of order unity,

$$c_1 \sim m\Lambda_{QCD}^3 + a\Lambda_{QCD}^5 \qquad c_2 \sim m^2\Lambda_{QCD}^2 + am\Lambda_{QCD}^4 + a^2\Lambda_{QCD}^6.$$

This mass shift of order $a\Lambda_{QCD}$ due to the Pauli term is expected: for values of m of order a, we should observe a competition between the explicit breaking of chiral symmetry coming from the Wilson discretization, and the breaking coming from the mass term. As we see, terms of order $O\left(a^2\right)$ are kept in the expression for c_2. To be consistent, we should compute all the $O\left(a^2\right)$ corrections to the underlying Lagrangian, but these turn out to be either negligible (suppressed by higher powers of $a\Lambda_{QCD}$) or proportional to $a^2\Lambda_{QCD}^6$, thence the expressions for c_1 and c_2 remain valid.

According to the values of the quark masses, three different possibilities may arise

(i.) **The mass take physical values $m << \Lambda_{QCD}$ and the mass terms dominate c_1 and c_2:** then, $c_1 \sim m\Lambda^3$ and $c_2 \sim m^2\Lambda^2$ as $a \to 0$, the discretization errors become negligible, and the contribution of the c_2 term is strongly suppressed, as $\frac{c_1}{c_2} \sim \frac{m}{\Lambda}$. The symmetry breaking pattern occurs as in the continuum.

(ii.) **The mass is of order $O(a)$ and the mass terms compete against the discretization terms in c_1 and c_2:** so the contributions of c_2 are strongly suppressed, but c_1 is affected by discretization errors, which amount to a shift in the value of the critical mass. It is usually easier to work with the 'shifted mass' $m' = m - a\Lambda_{QCD}^2$, that vanishes as c_1 vanishes. Then, c_1 and c_2 have new expressions

$$c_1 \sim m'\Lambda_{QCD}^3 \qquad c_2 \sim m'^2\Lambda_{QCD}^2 + am'\Lambda_{QCD}^4 + a^2\Lambda_{QCD}^6.$$

(iii.) **The shifted mass m' is of order $O\left(a^2\right)$ and the discretization terms dominate:** in such a case, $am' \sim (a\Lambda_{QCD})^3$ and

$$c_1 \sim m'\Lambda_{QCD}^3 \qquad c_2 \sim a^2\Lambda_{QCD}^6,$$

so $c_1 \sim c_2$, the two terms in the potential $\mathcal{V}_\chi$ are of the same order of magnitude, and this competition can lead to the Aoki phase, as it is explained in the following lines.

The value of the condensate $\Sigma = \Sigma_0$ at the ground state minimizes the potential $\mathcal{V}_\chi$. Assuming a general expresion for $\Sigma = A + i\tau \cdot \mathbf{B}$ with $A^2 + \mathbf{B}^2 = 1$, the potential becomes

$$\mathcal{V}_\chi = -c_1 A + c_2 A^2 \qquad A \in [-1, 1]\,. \tag{3.12}$$

This expression is invariant under $SU(2)_V$ rotations ($L = R$ in (3.9)), although the $\mathbf{B}$ components of the condensate rotate as a vector. Therefore, a non-zero value of these vector components of the condensate in the ground state $\Sigma_0 = A_0 + i\tau \cdot \mathbf{B}_0$ indicates Flavour symmetry breaking $SU(2)_V \to U(1)$, where the $U(1)$ subgroup of allowed rotations is

$$e^{i\theta\tau\mathbf{B}_0}.$$

[6] Any term invariant under $SU(2)_V$ symmetry can be written as a function of $\mathrm{Tr}\left(\Sigma+\Sigma^{\dagger}\right)$.

As Σ_0 is an $SU(2)$ matrix, it must verify the condition

$$A^2 + \mathbf{B} \cdot \mathbf{B} = 1.$$

Thus, Flavour symmetry breaking occurs if and only if $|A_0| < 1$.

The value of A_0 is defined by the potential $\mathcal{V}_\chi$, which in turn depends on the coefficients c_1 and c_2. So depending on the value of these coefficients, Flavour symmetry breaking might or might not take place. Let us analyze the different possibilities.

There are two scenarios, depending on the sign of c_2. If $c_2 > 0$, then the potential is a parabola with a minimum at $A_m = \frac{c_1}{2c_2} \sim \frac{m'}{a^2 \Lambda_{QCD}^3}$, which is a function of the mass m' and the coupling g through a. This minimum may or may not lie in the $(-1, 1)$ range; if it is outside the range, A_0 is forced to take the values ± 1, lying at the boundaries, and Flavour symmetry is preserved. If, on the contrary, $|A_m| < 1$, then $A_0 = A_m$ and $\mathbf{B}_0$ acquires a non-zero value at the minimum. Therefore Flavour symmetry is spontaneously broken to $U(1)$ and the properties of the vacuum are those of the Aoki phase.

Let us go deeper into the details of this phase. Without any lose of generality, we assume that the $\mathbf{B}_0$ component of the condensate is aligned to the $(0, 0, 1)$ direction[7]. Then $\Sigma_0 = \cos\theta_0 + i\tau_3 \sin\theta_0$, where

$$\cos\theta_0 = \begin{cases} -1 & A_m \leq -1 \\ A_m & -1 \leq A_m \leq 1 \\ +1 & 1 \leq A_m \end{cases} . \tag{3.13}$$

Thence, inside the Aoki phase the vacuum interpolates smoothly between the two possible values of the condensate in the continuum limit. In order to compute the pion masses, we perturbate the condensate Σ around its equilibrium point Σ_0 and work out the value of A. This can be done expanding equation (3.10), and taking the trace. The result is

$$A = \cos\theta_0 - \frac{\sin\theta_0}{f_\pi}\pi_3 - \frac{\cos\theta_0}{2f_\pi^2}\sum_{j=1}^{3}\pi_j^2 + O\left(\pi_j^3\right). \tag{3.14}$$

Then we put A in the potencial $\mathcal{V}_\chi$ to obtain

$$\mathcal{V}_\chi = \begin{cases} \frac{c_2}{f_\pi^2}\left(1 - A_m^2\right)\pi_3^2 - c_2 A_m^2 + O\left(\pi_j^3\right) & |A_m| < 1 \\ \frac{c_2}{f_\pi^2}\left(|A_m| - 1\right)\sum_{j=1}^{3}\pi_j^2 & |A_m| \geq 1 \end{cases} . \tag{3.15}$$

The coefficient of the quadratic term in the pion fields π_j is the physical mass m_j,

$$\begin{array}{cc} m_1 = m_2 = 0, \qquad m_3 = \frac{c_2}{f_\pi^2}\left(1 - A_m^2\right) & |A_m| < 1 \\ m_j = \frac{c_2}{f_\pi^2}\left(|A_m| - 1\right) & |A_m| \geq 1 \end{array} . \tag{3.16}$$

The picture is the following: outside the Aoki phase and the critical line, the three pions share the same value of the mass. As they approach the critical line, their masses decrease, until it vanishes exactly at the critical line. If we cross the critical line, the pions $\pi_{1,2}$ remain massless, whereas the pion π_3 acquires a non-vanishing mass (this is a consequence of the polarization of the vacuum in the τ_3 direction, and could happen in any other direction). This picture is in complete agreement with the standard expectations on the behaviour of the Aoki phase. In addition, the χPT analysis makes some new predictions

[7]Since most numerical simulations done inside the Aoki phase add an external source term $hi\bar{\psi}\gamma_5\tau_3\psi$, this assumption also allows us to connect directly the results exposed here with numerical simulations.

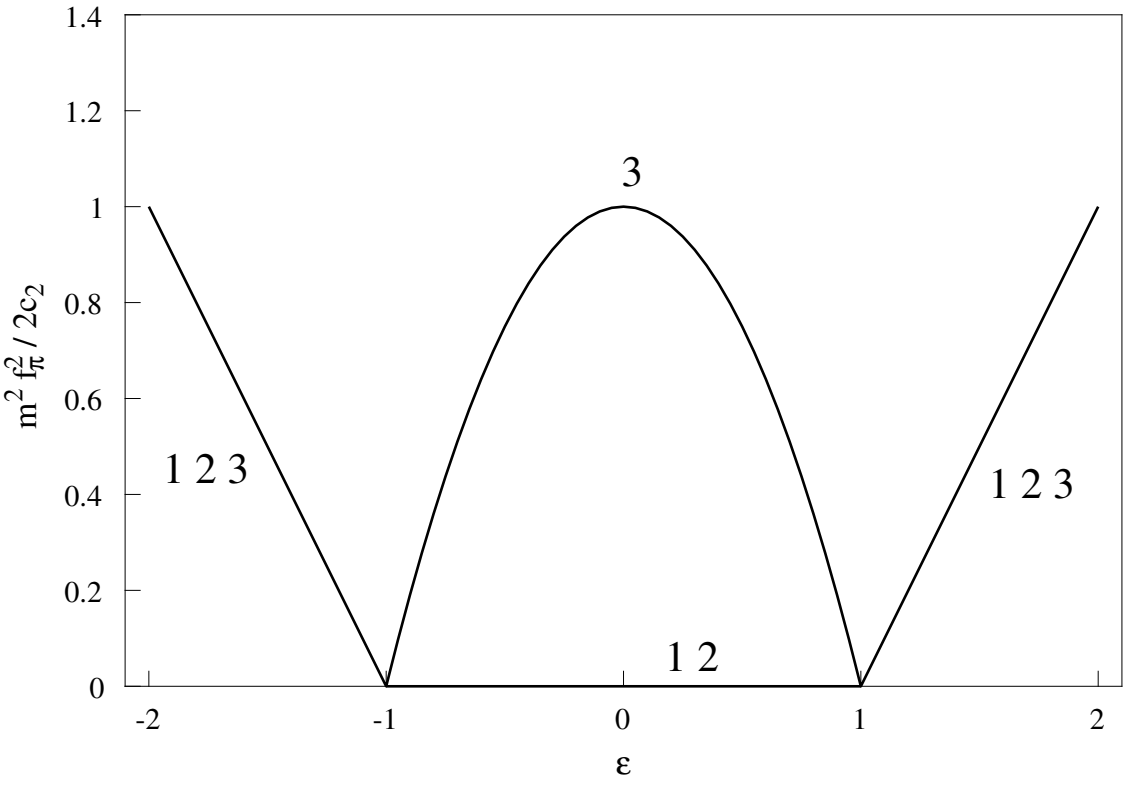

Figure 3.2: Dependence of the pion masses for the case $c_2 < 0$, QCD with an Aoki phase. Figure taken from [32] with courtesy of the authors.

(i.) The width of the fingers in which the Aoki phase occurs is $\Delta m_0 \sim a\Delta m' \sim \left(a\Lambda_{QCD}^3\right)$. This result comes from the fact that only in the region where there is a competition between c_1 and c_2 can an Aoki phase exist[8]. The result is consistent with the fact that, in the continuum limit, it should not be important if we approach the chiral limit from positive or negative masses, so the Aoki phase should shrink to a point. Moreover, as the Aoki phase is not observed in perturbation theory, one expects for the width of the phase a power-law dependency on a. This should hold up to logarithmic corrections in the lattice spacing (which have been ignored thorough the analysis), when we are close enough to the continuum limit.

(ii.) The mass of the neutral pion π_3 is predicted in terms of quantities computable outside the Aoki phase. It can be measured and contrasted against simulations.

(iii.) The expectation value of $i\bar{\psi}_u\gamma_5\psi_u$ is connected to the spectral density of the hermitian Dirac-Wilson operator $\gamma_5 D$ in the origin, through the Banks and Casher relation

$$\left\langle \bar{\psi}_u\gamma_5\psi_u \right\rangle = -\pi\rho\left(0\right).$$

[8]In principle, there is no need to worry for higher order terms in the expansion, or the existence of a third coefficient c_3. One could argue that, being the two first terms of the expansion comparable, a third term might become important, but a third term would have an order $c_3 \sim a^3\Lambda_{QCD}^7$, thus well suppressed when close enough to the continuum limit. A region might arise where these three terms cancel, but it must be a very small region of width $\Delta m_0 \sim a^4$, much smaller than the region of the Aoki phase, of order $\sim a^3$. In the same spirit, an $a^2\Lambda_{QCD}^2$ contribution to c_1 would shift the mass m' again by $O\left(a^2\right)$, but the analysis remains the same.

In other words, the Aoki phase features *small eigenvalues* and a *closing gap*. The calculations reproducing these results can be checked in [32].

The second possibility, $c_2 > 0$, leads to a very different scenario. The parabolic potential $\mathcal{V}_\chi$ changes sign and the former minimum becomes a maximum. Therefore, the global minimum within the range $[-1, 1]$ lie at the borders, and $\Sigma_0 = \pm 1$, according to the sign of m' (or c_1). The expansion of (3.10) in this case is

$$A = \pm \left(1 - \frac{1}{2f_\pi^2}\right) \sum_{j=1}^{3} \pi_j^2 + O\left(\pi_j^3\right),$$

where the sign depends on the sign of m' or c_1. Calling $\epsilon = \frac{c_1}{2c_2}$ (the A_m of the previous case), the potential around the minima develops the behaviour

$$\mathcal{V}_\chi = \frac{|c_2|}{f_\pi^2} (1 + |\epsilon|) \sum_{j=1}^{3} \pi_j^2 + c_2 - |c_1| + O\left(\pi_j^3\right), \tag{3.17}$$

and the three pions share the same non-zero mass

$$\frac{m_j^2 f_\pi^2}{2|c_2|} = 1 + |\epsilon| \tag{3.18}$$

in a world where Flavour symmetry is not spontaneously broken. Note that the pions never become massless in this case, but there is a minimum value for the pysical mass

$$m_{Min,j}^2 = 2|c_2| f_\pi^2. \tag{3.19}$$

Three comments regarding this analysis are in order:

(i.) This analysis is also valid for improved Wilson fermions, for the discretization errors contribute as $O\left(a^2\right)$ to c_2.

(ii.) The sign of c_2 is not predicted by this analysis, and must be found out by numerical simulations. As the above point stresses, the coefficient c_2 might vary from improved to unimproved Wilson fermions, so it might happen that these two cases are different.

(iii.) The results of this analysis rely on the assumption that we are close enough to the continuum limit, so that higher terms in the expansions are negligible.

Numerical simulations

Extensive numerical work was done to find out if the phase diagram of QCD with one and two flavours of Wilson fermions coincided with Aoki's proposal. Most of the computational results were obtained by Aoki himself and collaborators during the 80's and the 90's. Aoki (and collaborators) succeded in proving that $i\bar{\psi}_u \gamma_5 \psi_u \neq 0$ for a single Wilson fermion in the quenched approximation with [35, 36] and without external sources [37]. They also pursued dynamical simulations of two flavours of Wilson fermions with an added external source, and show numerically the existence of a Parity breaking phase [38, 39], even at finite temperature [40], although in this latter case the Aoki region at some point developed a cusp and was pinched out in the (β, κ) phase diagram. The standard picture was further reinforced by simulations by other groups. In particular, the group of E.-M. Ilgenfritz and collaborators found for two

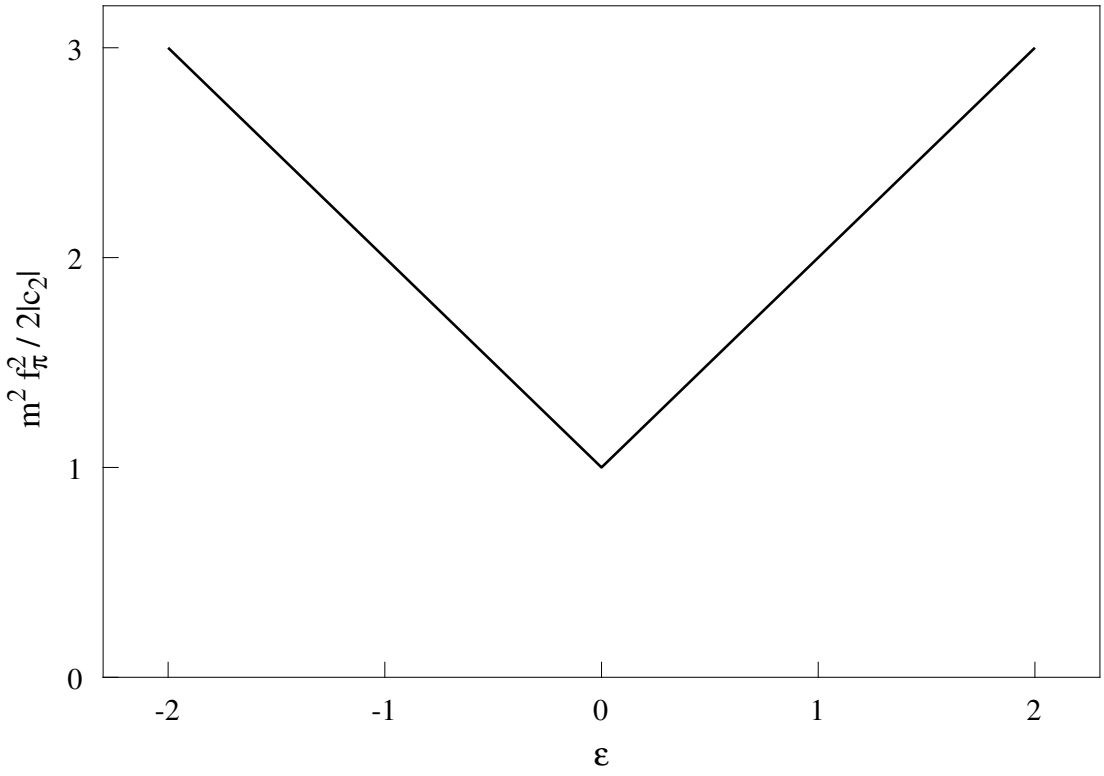

Figure 3.3: Dependence of the pion masses for the case $c_2 > 0$, where no Aoki phase exists. Figure taken from [32] with courtesy of the authors.

flavoured QCD at zero [41] and finite temperature [42] very similar results to that obtained by Aoki.

All these simulations (except [37], which is quenched and features a single Wilson fermion) have been done using the external source procedure to analyze the spontaneous symmetry breaking phenomena. It would be desirable to obtain some results without any contamination coming from external sources, and here a problem arises: as in the effective action for fermions on the lattice the Grassman variables are integrated out, the outcoming theory averages over all the possible degenerated vacua of the Gibbs state (i.e., without the external source and in the thermodynamic limit), which in the case of spontaneous symmetry breaking means that the expectation values of (3.3) are averaged to zero in a computer simulation, even inside the Aoki phase. As explained in the $p.d.f.$ introductory chapter, this is a scenario where the $p.d.f.$ formalism shines, for it allows to compute easily the higher moments of the probability distribution function, which should not be zero if the symmetries are spontaneously broken.

3.2 The $p.d.f.$ applied to the Aoki phase

The Gibbs state, or the $\epsilon-$regime

The introduction of the $p.d.f.$ point of view for the Aoki phase may cast light on the properties of the Aoki phase. Our starting point is the computation of the generating function of the selected observable. Here we call $P_j(q), P_0(q)$ the generating functions of $i\bar{\psi}\gamma_5\tau_j\psi$ and $i\bar{\psi}\gamma_5\psi$, which are

$$P_1(q) = P_2(q) = P_3(q) = \left\langle \prod_j \left(1 - \frac{q^2}{V^2\mu_j^2}\right)\right\rangle,$$

$$P_0(q) = \left\langle \prod_j \left(1 + \frac{q}{V\mu_j}\right)^2\right\rangle, \tag{3.20}$$

where V is the number of degrees of freedom (including colour and Dirac but not flavour d.o.f.) and μ_j are the real eigenvalues of the Hermitian Dirac-Wilson operator $\bar{D}(\kappa) = \gamma_5 D(\kappa)$, and the mean values $\langle\cdot\rangle$ are computed in the Gibbs state[9]. Notice that $P_3(q)$ has not a definite sign, whereas $P_0(q)$ is always positive definite. As the generating functions are computed at zero value of the external source, we are at the so-called $\epsilon-$regime (see [43]). This means that the zero-momentum modes of the charged pions are unsuppressed. On the other hand, the neutral pion lies in the $p-$regime, as $m_{\pi^3}L \to \infty$, and its fluctuations are completely eliminated.

The $q-$derivatives of $P(q)$ give us the moments of the distribution $P(c)$. As explained before, the first moment of both distributions vanishes, independently of the realization of the symmetries. The first non-vanishing moment, in the case of spontaneous symmetry breaking, is the second one. Thus, for the particular case[10]

$$i\bar{\psi}\gamma_5\psi = \frac{1}{V}\sum_x i\bar{\psi}(x)\gamma_5\psi(x),$$

$$i\bar{\psi}\gamma_5\tau_3\psi = \frac{1}{V}\sum_x i\bar{\psi}(x)\gamma_5\tau_3\psi(x), \tag{3.21}$$

the second moments are

$$\left\langle \left(i\bar{\psi}\gamma_5\psi\right)^2\right\rangle = 2\left\langle \frac{1}{V^2}\sum_j \frac{1}{\mu_j^2}\right\rangle - 4\left\langle \left(\frac{1}{V}\sum_j \frac{1}{\mu_j}\right)^2\right\rangle,$$

$$\left\langle \left(i\bar{\psi}\gamma_5\tau_3\psi\right)^2\right\rangle = 2\left\langle \frac{1}{V^2}\sum_j \frac{1}{\mu_j^2}\right\rangle. \tag{3.22}$$

In the A region of fig. 3.1 (physical) Flavour symmetry is realized. Thence, the *p.d.f.* of $i\bar{\psi}\gamma_5\tau_3\psi$ becomes $\delta\left(i\bar{\psi}\gamma_5\psi\right)$ and $\langle\left(i\bar{\psi}\gamma_5\psi\right)^2\rangle = 0$. For the other order parameter, the equation of the second moment

$$\left\langle \left(i\bar{\psi}\gamma_5\psi\right)^2\right\rangle = -4\left\langle \left(\frac{1}{V}\sum_j \frac{1}{\mu_j}\right)^2\right\rangle$$

should vanish in the thermodynamic limit since Parity is also preserved in this region, even at non-zero lattice spacing. Furthermore, a negative value of $\langle c_0^2\rangle$ would be quite remarkable, since $\left(i\bar{\psi}\gamma_5\psi\right)^2$ is the square of an Hermitian operator. This may render unreliable the simulations far from the continuum limit; we will come back to this point later.

In the Aoki phase (region B) [26] there are vacuum states where the condensate $i\bar{\psi}\gamma_5\tau_3\psi$ takes a non-vanishing vacuum expectation value. This implies that its *p.d.f.*, $P\left(i\bar{\psi}\gamma_5\tau_3\psi\right)$, is not a Dirac delta $\delta\left(i\bar{\psi}\gamma_5\tau_3\psi\right)$, and therefore $\langle\left(i\bar{\psi}\gamma_5\tau_3\psi\right)^2\rangle$ (3.22) does not vanish, due to the

[9] That is, at zero value of the external source and taking into account all the degenerated vacua.

[10] Here we are abusing a bit of the language. We will keep the notation of (3.21) thorough all this work.

apparition of small eigenvalues (near zero modes) of order $O\left(\frac{1}{V}\right)$, which compete against the volume factors. Indeed this aglomeration of small eigenvalues was recognized long time ago as a signal of spontaneous symmetry breaking in the Banks and Casher formula [44], which relates the spectral density of the Hermitian Dirac-Wilson operator at the origin with the vacuum expectation value of $i\bar{\psi}\gamma_5\tau_3\psi$ [32].

Thence the original vacuum splits, giving rise to the Aoki set of vacua, related among them by $P\times SU\left(2\right)/U\left(1\right)$ transformations. As the other interesting bilinear, $i\bar{\psi}\gamma_5\psi$, is invariant under $SU\left(2\right)/U\left(1\right)$ transformation and changes sign under Parity, if its expectation value $\langle i\bar{\psi}\gamma_5\psi\rangle$ vanishes in one of the Aoki vacua, it must vanish in any other Aoki vacua. Therefore, and assuming that these are all the degenerate vacua that exist in the Aoki phase, we conclude that $P\left(i\bar{\psi}\gamma_5\psi\right)=\delta\left(i\bar{\psi}\gamma_5\psi\right)$ and $\langle\left(i\bar{\psi}\gamma_5\psi\right)^2\rangle=0$, which implies the following non-trivial relation

$$\left\langle \frac{1}{V^2}\sum_j\frac{1}{\mu_j^2}\right\rangle = 2\left\langle\left(\frac{1}{V}\sum_j\frac{1}{\mu_j}\right)^2\right\rangle\neq 0. \tag{3.23}$$

Since the l.h.s. of equation (3.23) does not vanish in the thermodynamic limit inside the Aoki phase due to the presence of small eigenvalues, the r.h.s. must be non-zero as well.

A comment is in order here: the *p.d.f.* does not allow us to infer the existence of an Aoki phase. It only predicts the expression of the different moments of the distribution function in terms of the eigenvalues; in fact, equations (3.22) are valid inside and outside the Aoki phase. In order to find out the properties of these expectation values, additional input is needed. Most of the time some general properties of the spectrum are enough. In this case, the existence of the Aoki phase is assumed, thence (3.22) must be non-zero, so there must exist small eigenvalues $\sim O\left(\frac{1}{V}\right)$, a property which has already been observed in numerical simulations.

Outside the Aoki phase, there is a gap in the spectrum around the origin

$$|\mu_j|>\epsilon \qquad \epsilon\in\mathbb{R}^+.$$

Thus the $\frac{1}{V}$ factors kill as $V\to\infty$ the contributions of the inverse of the eigenvalues, all the expectation values are zero, and Flavour symmetry and Parity are preserved. But as noted before, the fact that there is a gap in the spectrum comes not from the *p.d.f.*, but it is deduced from the assumption that Flavour and Parity are realized in the vacuum.

Equation (3.23) is not the only non-trivial relation forced by the vanishing of the bilinear $i\bar{\psi}\gamma_5\psi$ inside the Aoki vacua. According to the well stablished standard wisdom of the Aoki phase, one expects all the even moments of this distribution to vanish

$$\left\langle\left(i\bar{\psi}\gamma_5\psi\right)^{2n}\right\rangle=0, \tag{3.24}$$

which implies a set of infinite independent relations among the eigenvalues of the Hermitian Dirac-Wilson operator. The consequence of this set of equations will be reviewed later.

QCD with a Twisted Mass Term, or the $p-$regime

Non-symmetric Spectral Density of Eigenvalues

Seldom are the numerical simulations inside the Aoki phase performed in the absence of an external source. Although this procedure –the addition of an external source– has its drawbacks when ported to numerical simulations, it is a valid theoretical tool to study analytically spontaneous symmetry breaking. That is why it might seem interesting to predict, from the *p.d.f.* point of view, what happens to the Aoki phase when we add an external source like

$$\sum_x im_t \bar{\psi}(x)\gamma_5\tau_3\bar{\psi}(x), \tag{3.25}$$

that explicitly breaks Flavour and Parity. For this source, the Flavour symmetry is broken from $SU(2)$ to $U(1)$.

Let us compute again the $p.d.f.$'s $\bar{P}_0(q)$ and $\bar{P}_3(q)$ of $i\bar{\psi}\gamma_5\psi$ and $i\bar{\psi}\gamma_5\tau_3\psi$ under the effects of the external source (3.25). Simple algebra gives us the following expressions

$$\begin{aligned}
\bar{P}_0(q) &= \left\langle \prod_j \left(\frac{\frac{q^2}{V^2} + \frac{2q}{V}\mu_j}{m_t^2 + \mu_j^2} + 1 \right) \right\rangle, \\
\bar{P}_3(q) &= \left\langle \prod_j \left(\frac{\frac{q^2}{V^2} + \frac{2q}{V} i m_t}{m_t^2 + \mu_j^2} - 1 \right) \right\rangle,
\end{aligned} \tag{3.26}$$

where again μ_j are the real eigenvalues of the Hermitian Dirac-Wilson operator and the mean values are computed now with the integration measure of the Wilson lattice QCD two-flavoured action, modified with the symmetry breaking source term (3.25).

The condensates are calculated taking the $q-$derivatives at the origin of $\bar{P}_0(q)$ and $\bar{P}_3(q)$

$$\begin{aligned}
\langle i\bar{\psi}\gamma_5\psi\rangle &= \frac{2i}{V}\left\langle \sum_j \frac{\mu_j}{m_t^2 + \mu_j^2} \right\rangle, \\
\langle \left(i\bar{\psi}\gamma_5\psi\right)^2\rangle &= \frac{4}{V^2}\left\langle \sum_j \frac{\mu_j^2}{(m_t^2 + \mu_j^2)^2} \right\rangle - \\
&- \frac{2}{V^2}\left\langle \sum_j \frac{1}{m_t^2 + \mu_j^2} \right\rangle - 4\left\langle \left(\frac{1}{V}\sum_j \frac{\mu_j}{m_t^2 + \mu_j^2} \right)^2 \right\rangle,
\end{aligned} \tag{3.27}$$

and

$$\langle i\bar{\psi}\gamma_5\tau_3\psi\rangle = \frac{2}{V} m_t \left\langle \sum_j \frac{1}{m_t^2 + \mu_j^2} \right\rangle. \tag{3.28}$$

Equation (3.28) is well known: taking first the infinite volume limit and then the $m \to 0$ limit, one can reproduce the Banks and Casher result

$$\langle i\bar{\psi}\gamma_5\tau_3\psi\rangle = -2\pi\rho\left(0\right), \tag{3.29}$$

which relates a non-vanishing spectral mean density of the Hermitian Wilson operator at the origin with the spontaneous breaking of Parity and Flavour symmetries, indicating the presence of small eigenvalues in the spectrum.

The first equation in (3.27) is actually unpleasant since it predicts an imaginary number for the vacuum expectation value of a Hermitian operator. However, the issue is solved by using the remnant P' symmetry (3.2), which is still a symmetry of the action. The P' enforces $\langle i\bar{\psi}\gamma_5\psi\rangle = 0$, nonetheless $\left(i\bar{\psi}\gamma_5\psi\right)^2$ could acquire a nonzero expectation value if P' is spontaneously broken.

Concerning the second equation in (3.27), the m_t term regularizes the denominators of the first and second contributions to $\langle \left(i\bar{\psi}\gamma_5\psi\right)^2\rangle$, forcing them to vanish in the thermodynamic limit for $m_t \neq 0$. The third contribution however, which is negative, vanishes only if the spectral density of eigenvalues of the Hermitian Wilson operator $\rho_U(\mu)$ for any background gauge field U

is an even function of μ. This is actually not true at finite values of V, and some authors [32, 45] suggest that the symmetry of the eigenvalues will be recovered not in the thermodynamic limit, but only in the zero lattice spacing or continuum limit. If we take this last statement as true, we should conclude:

(i.) The Aoki phase, which seems not to be connected with the critical continuum limit point ($g^2 = 0, \kappa = 1/8$) [37] is unphysical since the $\langle c_0^2 \rangle$ would be negative in this phase, being c_0^2 the square of an Hermitian operator.

(ii.) In the standard QCD phase, where Parity and Flavour symmetries are realized in the vacuum, we should have however negative values for the vacuum expectation value of the square of the Hermitian operator $i\bar{\psi}\gamma_5\psi$, except very close to the continuum limit. Since this operator is related to the η-meson, one can expect in such a case important finite lattice spacing effects in the numerical determinations of the η-meson mass.

Symmetric Spectral Density of Eigenvalues

Assuming that the spectral density of eigenvalues of the Hermitian Wilson operator $\rho_U(\mu)$ for any background gauge field U is an even function of μ, the previous picture changes dramatically. In such a case equation (3.27) forces the vanishing of $\langle \left(i\bar{\psi}\gamma_5\psi\right)^2 \rangle$ for any value of m_t

$$\langle \left(i\bar{\psi}\gamma_5\psi\right)^2 \rangle = 0. \tag{3.30}$$

Therefore the *p.d.f.* of c_0 is $\delta\left(i\bar{\psi}\gamma_5\psi\right)$ and

$$\langle i\bar{\psi}\gamma_5\psi \rangle = 0, \tag{3.31}$$

for any m_t, and also in the $m_t \to 0$ limit. Thence $i\bar{\psi}\gamma_5\psi = 0$ in the Aoki vacuum selected by the external source (3.25), as stated in [26]; but since $i\bar{\psi}\gamma_5\psi$ is Flavour invariant, and change sign under Parity, $i\bar{\psi}\gamma_5\psi$ must vanish, not only in the vacuum selected by the external source (3.25), but also in all the Aoki vacua connected to this one by Parity-Flavour transformations. The standard wisdom on the Aoki phase does not contemplate the existence of any more vacua with different properties, but there is no proof of this point.

In fact, if all the vacua are the one selected by the twisted mass term plus those obtained from it by Parity-Flavour transformations, the spectral density of the Hermitian Wilson operator must always be an even function of μ, since the eigenvalues of this operator change sign under Parity and are invariant under Flavour transformations. Then the spectrum density $\rho_U(\mu)$ must also be symmetric at $m_t = 0$, in the Gibbs state. Now let us come back to expression (3.22), which gives us the vacuum expectation values of the square of $i\bar{\psi}\gamma_5\psi$ and $i\bar{\psi}\gamma_5\tau_3\psi$ as a function of the spectrum of the Hermitian Wilson operator, but averaged over all the Gibbs state (without the external symmetry breaking source (3.25) and averaging over all the vacua). Subtracting the two equations in (3.22),

$$\langle \left(i\bar{\psi}\gamma_5\tau_3\psi\right)^2 \rangle - \langle \left(i\bar{\psi}\gamma_5\psi\right)^2 \rangle = 4 \left\langle \left(\frac{1}{V} \sum_j \frac{1}{\mu_j} \right)^2 \right\rangle. \tag{3.32}$$

This equation would *naively* vanish, if the spectral density of eigenvalues of the Hermitian Wilson operator were an even function of μ. Therefore one would reach the following conclusion for the Gibbs state

$$\langle \left(i\bar{\psi}\gamma_5\tau_3\psi\right)^2 \rangle = \langle \left(i\bar{\psi}\gamma_5\psi\right)^2 \rangle. \tag{3.33}$$

Nevertheless, S. Sharpe put into evidence in a private communication (developed deeply in [43]) an aspect that in [51] we somewhat overlooked: a sub-leading contribution to the spectral density may affect (3.33) in the Gibbs state (ϵ-regime, in χPT terminology), in such a way that, not only $\langle\left(i\bar{\psi}\gamma_5\psi\right)^2\rangle$, but every even moment of $i\bar{\psi}\gamma_5\psi$ would vanish, restoring the standard Aoki picture. This is equivalent to the imposition of the infinite set of equations (3.24), announced at the beginning of this chapter. These could be understood as *sum rules* for the eigenvalues, similar to those found by Leutwyler and Smilga in the continuum [46], which relate the topological charge of the configurations with the eigenvalues of the Dirac operator.

Therefore, and *assuming a symmetric spectral density in the thermodynamic limit*, there are two possibilities for the Aoki phase:

(i.) The standard picture of the Aoki phase is right and complete, the Aoki vacua are characterized by

$$\left\langle i\bar{\psi}\gamma_5\tau_3\psi\right\rangle \neq 0,$$
$$\left\langle i\bar{\psi}\gamma_5\psi\right\rangle = 0,$$

and equations (3.24) are verified, thanks to subleading contributions to the spectral density, which conspire to enforce the vanishing of all the even moments of the *p.d.f.* of $i\bar{\psi}\gamma_5\psi$. Thence there exists an infinite number of sum rules among the eigenvalues of the Hermitian Dirac Wilson operator.

(ii.) The standard picture of the Aoki phase is *incomplete*, for there exists a set of vacua verifying $\left\langle i\bar{\psi}\gamma_5\psi\right\rangle \neq 0$, completely disconnected from the standard Aoki vacua. As χPT predicts unambiguously only the standard Aoki vacua, the implications of this second scenario are quite strong: *Chiral Perturbation Theory may be incomplete.*

Since the last scenario implies a confrontation with χPT, it is extremely important to find out which one of the two possibilities is realized.

The New Vacua

To understand the physical properties of these new vacuum states we will assume, inspired by the numerical results reported in the next section, that the spectral density of eigenvalues $\rho_U(\mu)$ is an even function of μ. Then equation (3.33) holds (taking into account the aforementioned discussion raised by S. Sharpe), and hence the *p.d.f.* of the flavour singlet $i\bar{\psi}\gamma_5\psi$ order parameter can not be $\delta\left(i\bar{\psi}\gamma_5\psi\right)$ inside the Aoki phase, therefore new vacuum states characterized by a non-vanishing vacuum expectation value of $i\bar{\psi}\gamma_5\psi$ should appear. These new vacua can not be connected, by mean of Parity-Flavour transformations, to the Aoki vacua, as previously discussed.

In order to better characterize these new vacua, we have added to the lattice QCD action the source term

$$im_t\bar{\psi}\gamma_5\tau_3\psi + i\theta\bar{\psi}\gamma_5\psi, \tag{3.34}$$

which breaks more symmetries than (3.25), but still preserves the $U(1)$ subgroup of the $SU(2)$ Flavour. By computing again the first moment of the *p.d.f.* of $i\bar{\psi}\gamma_5\psi$ and $i\bar{\psi}\gamma_5\tau_3\psi$ and taking into account that the mean value of the first of these operators is an odd function of θ, whereas the second one is an even function of θ, we get

$$\langle i\bar{\psi}\gamma_5\psi\rangle = -\frac{2\theta}{V}\left\langle \sum_j \frac{-\mu_j^2 + m_t^2 - \theta^2}{(\mu_j^2 + m_t^2 - \theta^2)^2 + 4\theta^2\mu_j^2}\right\rangle,$$

$$\langle i\bar{\psi}\gamma_5\tau_3\psi\rangle = \frac{2m_t}{V}\left\langle \sum_j \frac{\mu_j^2 + m_t^2 - \theta^2}{(\mu_j^2 + m_t^2 - \theta^2)^2 + 4\theta^2\mu_j^2}\right\rangle, \tag{3.35}$$

where μ_j are again the eigenvalues of the Hermitian Wilson operator and the mean values are computed using the full integration measure of lattice QCD with the extra external sources (3.34). This integration measure is not positive definite due to the presence of the $i\bar{\psi}\gamma_5\psi$ term in the action, but this should not be a problem for the $p.d.f.$ formalism. In fact, the $p.d.f.$ has been previously applied with success to other systems where a sign problem prevented the direct simulation within an external source [20].

Let us assume that $\theta = rm_t$, so after taking the thermodynamic limit the expressions for the two order parameters

$$\langle i\bar{\psi}\gamma_5\psi\rangle = \int \frac{2rm_t\mu^2 - 2rm_t^3(1-r^2)}{\left(m_t^2(1-r^2)+\mu^2\right)^2 + 4r^2m_t^2\mu^2}\rho(\mu)d\mu,$$

$$\langle i\bar{\psi}\gamma_5\tau_3\psi\rangle = \int \frac{2m_t^3(1-r^2) + 2m_t\mu^2}{\left(m_t^2(1-r^2)+\mu^2\right)^2 + 4r^2m_t^2\mu^2}\rho(\mu)d\mu, \tag{3.36}$$

depend only on m_t and not on θ. Here $\rho(\mu)$ is the mean spectral density of the Hermitian Wilson operator averaged with the full integration measure.

Now the $m_t \to 0$ limit is equivalent to approaching the vanishing external source (3.34) point in the θ, m_t plane on straight line crossing the origin and with slope r. In this limit, the remnant expressions are

$$\langle i\bar{\psi}\gamma_5\psi\rangle = 2\rho(0)\int_{-\infty}^{+\infty} \frac{rt^2 - r(1-r^2)}{(1-r^2+t^2)^2 + 4r^2t^2}dt,$$

$$\langle i\bar{\psi}\gamma_5\tau_3\psi\rangle = 2\rho(0)\int_{-\infty}^{+\infty} \frac{1-r^2+t^2}{(1-r^2+t^2)^2 + 4r^2t^2}dt. \tag{3.37}$$

In the particular case of $r = 0$ ($\theta = 0$) the Banks and Casher formula is recovered

$$\langle i\bar{\psi}\gamma_5\tau_3\psi\rangle = -2\pi\rho(0). \tag{3.38}$$

and the standard Aoki picture is realized, with $i\bar{\psi}\gamma_5\psi = 0$ but for any other finite value of r the flavour singlet acquires a non-zero expectation value proportional to $\rho\,(0)$. Therefore, if $\rho(0)$ does not vanish, many vacua appear, characterized by a non-vanishing value of the two order parameters $i\bar{\psi}\gamma_5\psi$ and $i\bar{\psi}\gamma_5\tau_3\psi$. The special case $r \to \infty$ (equivalent to setting $m_t = 0$) can be computed as well in many ways, and the final result

$$\left\langle i\bar{\psi}\gamma_5\psi\right\rangle = 0$$

$$\left\langle i\bar{\psi}\gamma_5\tau_3\psi\right\rangle = 0$$

indicates symmetry restoration and confirms a point previously exposed in this chapter: if there are new Aoki-like phases, characterized by $\left\langle \left(i\bar{\psi}\gamma_5\psi\right)^2\right\rangle = 0$, these can only exist in presence of the standard Aoki phase. As the external source (3.34) does not lead to the Aoki phase if $m_t = 0$, the symmetries are restored as $\theta \to 0$.

It must be remarked that the value of $\rho(0)$ could depend on the slope r of the straight line along which we approach the origin in the θ, m_t plane, and therefore, even if results of numerical simulations suggest that $\rho(0) \neq 0$ when we approach the origin along the line of vanishing slope, this does not guarantee that the same holds for other slopes. However the discussion in the first half of this section tell us that if $\rho(0) \neq 0$ at $r = 0$ (i.e., standard Aoki vacua), $\rho(0)$ should be non-vanishing for other values of r (other vacua should exist).

Quenched Numerical Simulations

The behaviour of the spectral density of the Hermitian Dirac Wilson operator determines which one of the different scenarios proposed occurs during simulations. It can become symmetric in the thermodynamic limit, or it may be necessary to reach the continuum limit to recover the symmetry. In the latter case, the negative expectation value for the operator $\left(i\bar{\psi}\gamma_5\psi\right)^2$ should hinder the measurements of the $\eta-$meson mass in the physical region, whereas in the first scenario, we find new properties associated to the Aoki phase. These properties comprise, either the existence of phases with non-zero expectation value of $\left(i\bar{\psi}\gamma_5\psi\right)^2$, or the existence of an infinite set of sum-rules for the eigenvalues of the Hermitian Dirac Wilson operator. The possibilities are quite rich, and as far as the author knows, have not been proposed before.

In order to find out the behaviour of the spectral density at the thermodynamic limit (and thus rule out one of the three scenarios), quenched simulations of lattice QCD with Wilson fermions were performed. After generating ensembles of well uncorrelated configurations for $4^4, 6^4$ and 8^4 lattices, we diagonalized the Hermitian Wilson matrix for each configuration and measured the volume dependence of the asymmetries in the eigenvalue distribution, both inside and outside the Aoki phase.

It is important to point out that, because of kinematic reasons, the trace of the firsts odd $p-$powers of the Hermitian Wilson operator $H(\kappa) = \gamma_5 W(\kappa)$ vanish until $p = 7$, this included. This is related to the properties of the gamma matrices: in order to have a non-zero contribution, a term with an even number of annihilating gamma matrices must occurr. Writting $\gamma_5 W(\kappa)$ as $\gamma_5 + \gamma_5\kappa M$, with M traceless, any power of $\gamma_5 W(\kappa)$ is readily computed

$$\mathrm{Tr}\left\{\left[\gamma_5 W(\kappa)\right]^{2n+1}\right\} = \mathrm{Tr}\left[\gamma_5\left(\sum_{i=0}^{2n+1}\left(\frac{n}{i}\right)\kappa^i M^i\right)\right] \qquad n = 0, 1, 2\ldots \tag{3.39}$$

The γ_5 matrix which multiplies the whole expansion makes all the terms zero, unless there is a power of κM containing a γ_5 in the diagonal. The first odd term verifying this condition comes from the ninth power of $\gamma_5 W(\kappa)$, in the term $\kappa^8 M^8$. This means that the asymmetries in the eigenvalue distribution of the Hermitian Dirac Wilson operator start to manifest with a non-vanishing value of the ninth moment of the distribution. Fortunately these asymmetries, even if small, are clearly visible in the numerical simulations.

Figs. 3.4-3.8 show the quenched mean value

$$A(\beta, \kappa, m_t) = \left\langle \left(\frac{1}{V} \sum_j \frac{\mu_j}{m_t^2 + \mu_j^2} \right)^2 \right\rangle_Q , \tag{3.40}$$

multiplied by the volume for the three different analyzed volumes, in order to see the scaling of the asymmetries of the spectrum. As previously discussed, $A(\beta, \kappa, m_t)$ give us a quantitative measure of these asymmetries. We have added an extra V factor to make the plots for the three different volumes distinguishable: since the value of $A(\beta, \kappa, m_t)$ is found to decrease as the volume increases, the plots of the larger volumes are negligible with respect to the plot of

the smaller volume 4^4. Multiplying all the plots by V, they become of the same magnitude order.

The m_t term in the denominator of (3.40) acts also as a regulator in the quenched approximation, where configurations with zero or near-zero modes are not suppressed by the fermion determinant[11]. This is very likely the origin of the large fluctuations observed in the numerical measurements of (3.40) near $m_t = 0$ in the quenched case. That is why our plots are cut below $m_t = 0.05$; in the physical phase, this cutoff is not really needed, but in the Aoki phase it is more likely to find zero modes which spoil the distribution.

Figs. 3.4 and 3.5 contain our numerical results in $4^4, 6^4$ and 8^4 lattices at $\beta = 0.001, \kappa = 0.17$ and $\beta = 5.0, \kappa = 0.15$. These first two points are outside the Aoki phase, the first one in the strong coupling region. The second one intends to be a point where typically QCD simulations are performed.

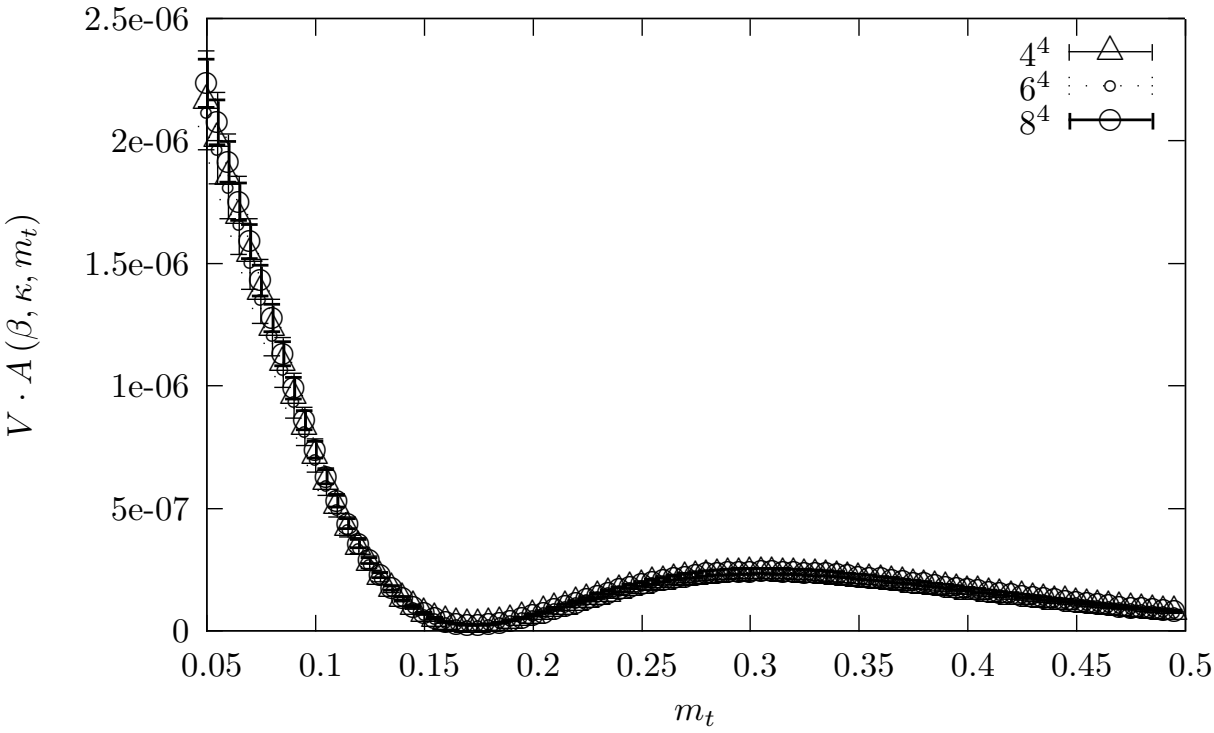

Figure 3.4: Point outside of the Aoki phase ($\beta = 0.001$, $\kappa = 0.17$) and in the strong coupling regime. The superposition of plots clearly states that the asymmetry of the eigenvalue distribution decreases as $\frac{1}{V}$. Statistics: 240 configurations (4^4), 2998 conf. (6^4) and 806 conf. (8^4)

Figs. 3.6, 3.7 and 3.8 represent our numerical results in $4^4, 6^4$ and 8^4 lattices at $\beta = 0.001, \kappa = 0.30$, $\beta = 3.0, \kappa = 0.30$ and $\beta = 4.0, \kappa = 0.24$. These points are well inside the Aoki phase, and the structure of the distribution is different from the structure observed in the previous plots of the physical phase. Nevertheless, the qualitative behaviour as the volume increases is the same.

Large fluctuations in the plotted quantity are observed near $m_t = 0$, specially inside the Aoki phase. However the behavior with the lattice volume may suggests a vanishing value of $A(\beta, \kappa, m_t)$ in the infinite volume limit in both regions, inside and outside the Aoki phase. If this is actually the case in the unquenched model, the spectral symmetry would be recovered

[11] Although we expect small eigenvalues to appear in the Aoki phase, even with dynamical fermions, in the quenched case these can be ridiculously small [47].

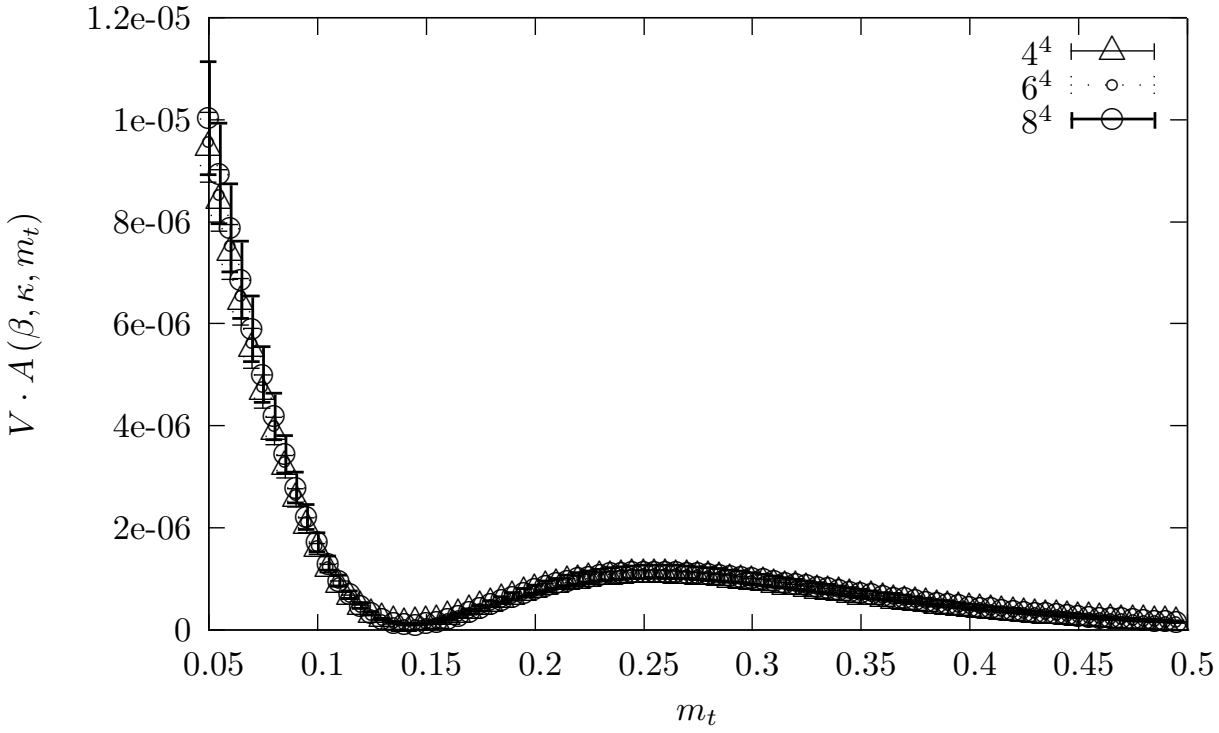

Figure 3.5: Another point outside of the Aoki phase ($\beta = 5.0$, $\kappa = 0.15$) in a region in which QCD simulations are commonly performed. The conclusion is the same as in Fig. 3.4. Statistics: 400 conf. (4^4), 900 conf. (6^4) and 200 conf. (8^4)

in the thermodynamic limit, the $\eta-$meson mass would be measurable reliably at finite lattice spacing and the Aoki phase would display new features: either a richer phase diagram or a set of non-trivial sum rules.

A discussion regarding the effect of the regulator m_t is in order here. The asymmetry inside the Aoki phase becomes important for small eigenvalues $\mu \sim O\left(\frac{1}{V}\right)$, but the regulator smooths out this asymmetry completely. Therefore, and according to our data, the spectral symmetry is recovered for $\lambda \gtrsim m_t$. Our regulator was set to $m_t = 0.05$, which is appropiate for $V = 4^4$, or might be even for 6^4, but runs short for 8^4. On the other hand, the asymmetry for small eigenvalues is expected, for it is related to the topological charge of the configurations[12] [48, 49]. A single small eigenvalue crossing the origin might be enough to spoil the symmetry of ρ_U, hence the only way to keep the symmetry of the spectral density is that those crossing eigenvalues become zero-modes as $V \to \infty$. As we expect the μ's to be of order $O\left(\frac{1}{V}\right)$, this should be a natural consequence. The important point here is the fact that the index theorem is recovered inside the Aoki phase, in the thermodynamic limit [50].

Unquenched Numerical Simulations

Assuming a symmetric spectral density, we are left with two different possibilities. A brief description of each of them follows.

(i.) In the first scenario the conditions

$$\left\langle \left(i\bar{\psi}\gamma_5\psi\right)^{2n} \right\rangle \neq 0 \qquad n \in \mathbb{N} \tag{3.41}$$

[12]This point will be elucidated in detail in the next section.

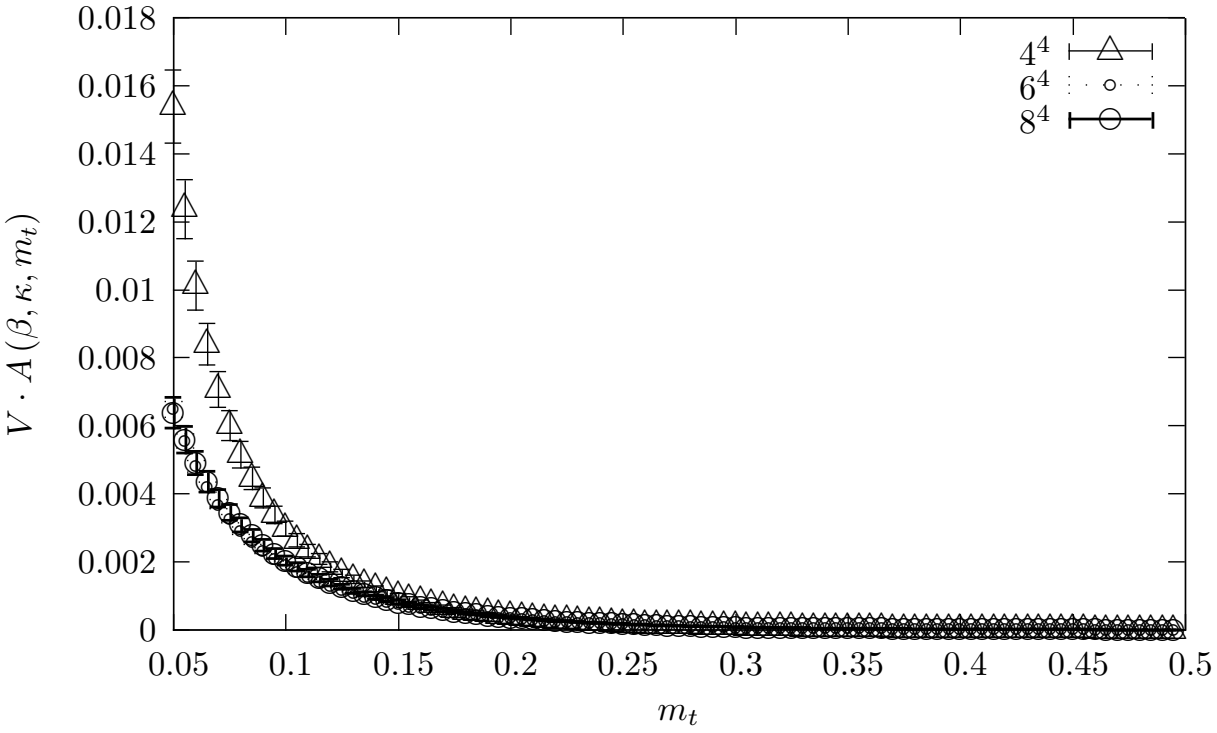

Figure 3.6: Point inside the Aoki phase ($\beta = 0.001$, $\kappa = 0.30$) and in the strong coupling regime. Although there is no clear superposition of plots, it is evident that the asymmetry goes to zero as the volume increases. Statistics: 368 conf. (4^4), 1579 conf. (6^4) and 490 conf. (8^4)

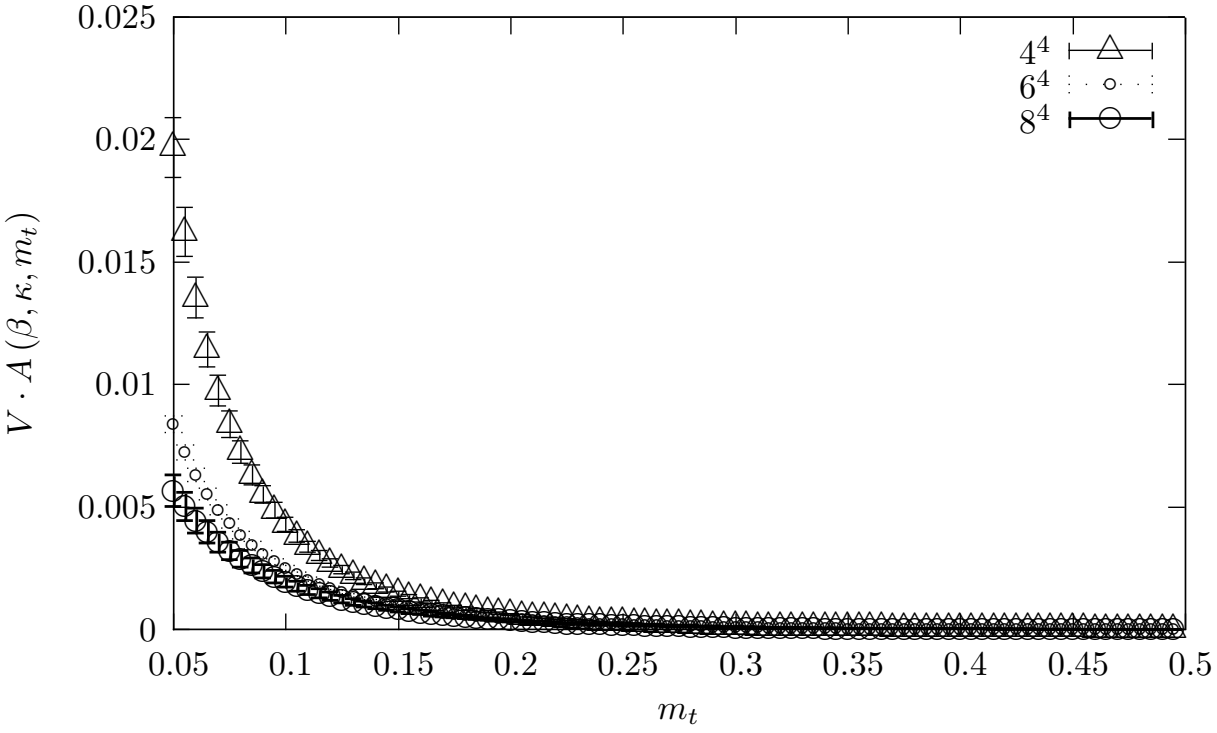

Figure 3.7: Point inside the Aoki phase ($\beta = 3.0$, $\kappa = 0.30$). The asymmetry disappears as the volume increases. Statistics: 400 conf. (4^4), 1174 conf. (6^4) and 107 conf. (8^4)

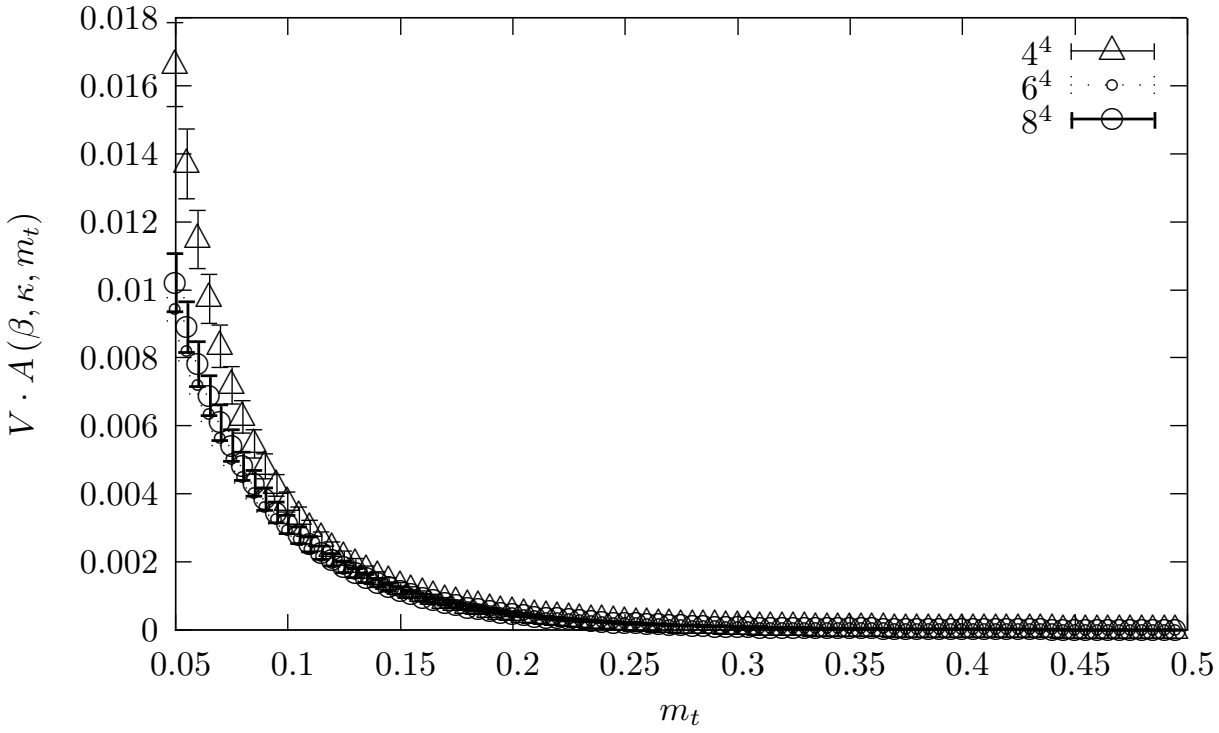

Figure 3.8: Point inside the Aoki phase ($\beta = 4.0$, $\kappa = 0.24$). Same conclusions as in the other Aoki plots. Statistics: 398 conf. (4^4), 1539 conf. (6^4) and 247 conf. (8^4)

are verified as a consequence of the spectral symmetry. To remember how this happens, take the special case $n = 2$. Then we recover equation (3.22)

$$\left\langle \left(i\bar{\psi}\gamma_5\psi\right)^2 \right\rangle = 2\left\langle \frac{1}{V^2}\sum_j \frac{1}{\mu_j^2} \right\rangle - 4\left\langle \left(\frac{1}{V}\sum_j \frac{1}{\mu_j}\right)^2 \right\rangle . \tag{3.42}$$

Inside the Aoki phase, the first member of the r.h.s. of the equation is different from zero, but the second member must be zero (in the $V \to \infty$ limit) due to the spectral symmetry. Therefore the Aoki phase implies $\left\langle \left(i\bar{\psi}\gamma_5\psi\right)^2 \right\rangle \neq 0$. This point contradicts the standard picture of the Aoki phase by predicting new phases, unrelated to the original Aoki phase, and characterized by (3.41). In particular, the prediction $\left\langle \left(i\bar{\psi}\gamma_5\psi\right)^2 \right\rangle \neq 0$ clash to those of chiral lagrangians, where $i\bar{\psi}\gamma_5\psi$ identically vanishes, and thus does any higher power of it.

(ii.) The second scenario is the one predicted by chiral lagrangians. There,

$$\left\langle \left(i\bar{\psi}\gamma_5\psi\right)^{2n} \right\rangle = 0 \qquad \forall n \in \mathbb{N} \tag{3.43}$$

which in turn implies the existence of an infinite set of sum-rules, a different and independent one for each n.

These two predictions are incompatible, yet we could not differentiate which one was realized in our quenched simulations. Therefore, dynamical simulations of the Aoki phase are mandatory.

Technical difficulties

Although the simulations of the Aoki phase with dynamical fermions are nothing new in the lattice QCD panorama, these have always been performed under very special conditions: an external source is added to the action with a twisted mass term

$$hi\bar{\psi}\gamma_5\tau_3\psi \tag{3.44}$$

in order to (i.) regularise the small eigenvalues of the Dirac Wilson operator, which appear only in the Aoki phase and usually spoil any attempt of simulation without the external source, and (ii.) to analyse the pattern of spontaneous Flavour and Parity breaking. As proved before (3.37) (see [51] as well), the use of an external source like (3.44) selects a standard Aoki vacuum, complying with ((3.43)), whereas an external source

$$h_5 i\bar{\psi}\gamma_5\psi \tag{3.45}$$

would introduce a sign problem in the measurement. The only way to investigate the existence of the new phases characterized by (3.41) is to remove the external source, and extract results from direct measurements of the Gibbs state (ϵ-regime). The latter point is solved by the $p.d.f.$ formalism, but the former –the removal of the external source– has been an unexplored option in the Aoki phase dynamical simulations for a number of years. The reason is the appearance of small eigenvalues of the Hermitian Dirac Wilson operator, of order $O\left(\frac{1}{V}\right)$. As far as we know, the technical problems inside the Aoki phase are similar to those faced when trying to reach the physical point: The critical slowing down spoils the efficiency of simulations, the Dirac Wilson operator becomes increasingly harder to invert, and the performance decreases dramatically. In fact, for some values of the parameters (β, κ) in the coupling-mass phase diagram, the standard algorithms to invert the Dirac operator just will not work. This fact called for a research on competent algorithms to simulate inside the Aoki phase.

Inspiration came in the recent results for new algorithms which reduce the critical slowing down for small masses in several orders of magnitude. We successfully implemented a SAP preconditioner in a GCR inverter, as explained in [52]. The new inverter allow us to perform simulations inside the Aoki phase without external sources at a reasonable speed. Unfortunately this is not the whole history.

The simulations done outside the Aoki phase feature a spectral gap around the origin, with a symmetric spectrum[13]. This gap is required to preserve Parity and Flavour symmetry [51]. However, the Aoki phase breaks both of them, so this gap was not present in our simulations, and as explained above, the smallest eigenvalues of each configuration took values of order $O\left(\frac{1}{V}\right)$. As the eigenvalues approach the origin, it may happen that they try to change sign, rendering the spectrum asymmetric, but this movement is forbidden[14] by the Hybrid Montecarlo dynamics, i.e., *the HMC algorithm is not ergodic for Wilson fermions inside the Aoki phase.* Therefore we are introducing artificial constraints in the dynamics, and the final results are bound to be modified. That is why we considered another dynamical fermion simulation algorithm, the Microcanonical Fermionic Average (MFA) [53, 54, 55, 56], which solves the problem of the eigenvalue crossing, but converges poorly as the volume increases.

[13] By symmetric ***here*** we mean that the number of positive and negative eigenvalues are the same.

[14] The movement is not strictly forbidden for higher volumes, as the natural state of the small eigenvalues inside the Aoki phase is very close to the origin. If the value of the stepsize is high enough, an eigenvalue might cross the origin. In fact we observed a couple of crossings in our $V = 6^4$ HMC simulation, but this transformation is without doubt highly improbable, and constitutes a serious bottleneck in the phase space exploration of the algorithm.

The problem was overcome by using an argument developed in [48, 49] and applied to the current case in [43], where the asymmetry of the spectrum n_{Asym} (the difference between the number of positive and negative eigenvalues) is related to the topological charge Q as

$$n_{Asym} \propto Q. \tag{3.46}$$

Then the constraints imposed by the hybrid Montecarlo are equivalent to leaving the topological charge fixed. Since the measurement of the observables should not depend on the value of the topological charge in the thermodynamic limit, we can select the symmetric sector $Q = 0$ and measure our observables there, where one expects to have smaller finite volume effects[15].

Another interesting possibility is (i.) to measure the weight of the different n_{Asym} sectors in the partition function via the MFA algorithm, (ii.) then perform Hybrid Montecarlo simulations within the relevant sectors, and (iii.) do a weighted average of the observables obtained in the HMC using the MFA weights. The results obtained with this method were contrasted to those coming from the direct MFA simulations, and with the HMC simulations at fixed n_{Asym}.

A third proposal for simulations could be the addition of a small (3.44) external source, large enough to regularise the small eigenvalues, but small enough to avoid vacuum selection, would allow us to include the eigenvalue crossing phenomenon in our HMC algoritm. Unfortunately, there exists no value of the external field h capable of this two deeds at the same time. If the field is very small, no vacuum is selected, but the eigenvalues do not cross the origin during the simulations; on the contrary, for larger values of the field h, the standard Aoki vacuum is selected. This third possibility was, thus, forsaken.

Numerical results

We performed measurements of three observables of interest

Table 3.1: Expected behaviour of the analysed observables in the different scenarios as $V \to \infty$.

	$\left\langle \left(i\bar{\psi}_u\gamma_5\psi_u\right)^2 \right\rangle$	$\left\langle \left(i\bar{\psi}\gamma_5\psi\right)^2 \right\rangle$	$\left\langle \left(i\bar{\psi}\gamma_5\tau_3\psi\right)^2 \right\rangle$
Outside Aoki	~ 0	~ 0	~ 0
Aoki Standard Wisdom	$\neq 0$	~ 0	$\neq 0$
Aoki Our Proposal	$\neq 0$	$\neq 0$	$\neq 0$

Our measurements refer always to the second moment of the *p.d.f.*, which should be zero in case of symmetry conservation, and non-zero if the symmetry is spontaneously broken [21]. The first observable signals Parity breaking, and should be non-zero inside the Aoki phase. The second one allows us to distinguish between our proposal –there is an additional *Aoki-like phase* verifying $\left\langle \left(i\bar{\psi}\gamma_5\psi\right)^2 \right\rangle \neq 0$– and the one involving an infinite number of sum rules. Finally, the third observable is the landmark of the Aoki phase, marking spontaneous Flavour and Parity breaking.

The first set of simulations were performed using the HMC algorithm, improved with a SAP-preconditioned solver. The symmetric runs $n_{Asym} = 0$ were performed starting from a

[15] To clarify this point one could have a look at [46], where the probability distribution of Q is calculated explicitly for a finite lattice, and to [57], where the finite volume corrections arising after imposing the constraint $Q = cte$ are computed.

cold (ordered, links close to the identity) and from a hot (disordered, close to strong coupling) configuration, obtaining identical results within errors. We could not find an asymmetric state $n_{Asym} = 1$ in a cold configuration at the values of κ explored, the asymmetric run was started only from a hot configuration.

Table 3.2: Results of the Hybrid Montecarlo measurements. NConf indicates the number of configurations.

	NConf	$\left\langle \left(i\bar{\psi}_u\gamma_5\psi_u\right)^2 \right\rangle$	$\left\langle \left(i\bar{\psi}\gamma_5\psi\right)^2 \right\rangle$	$\left\langle \left(i\bar{\psi}\gamma_5\tau_3\psi\right)^2 \right\rangle$
Outside* Aoki $V = 4^4$	20002	$2.098(3) \times 10^{-3}$	$4.149(4) \times 10^{-3}$	$4.244(4) \times 10^{-3}$
$n_{Asym} = 0^{**}$ $V = 4^4$	19673	$1.90(3) \times 10^{-2}$	$2.69(12) \times 10^{-2}$	$4.90(9) \times 10^{-2}$
$n_{Asym} = 0^{**}$ $V = 6^4$	664	$9.2(30) \times 10^{-3}$	$-4.3(30) \times 10^{-1}$	$4.7(30) \times 10^{-1}$
$n_{Asym} = 1^{**}$ $V = 4^4$	10002	$6.5(7) \times 10^{-3}$	$-4.5(5) \times 10^{-2}$	$7.1(3) \times 10^{-2}$

*Point outside the Aoki phase $\beta = 3.0$, $\kappa = 0.22$.

**Point inside the Aoki phase $\beta = 2.0$, $\kappa = 0.25$.

We expect all the observables to have non-zero expectation values, even outside the Aoki phase, due to finite volume effects. However, the values inside the Aoki phase are an order of magnitude larger than those measured outside the Aoki phase. Outside the Aoki phase, the following approximate rule holds:

$$2\left\langle \left(i\bar{\psi}_u\gamma_5\psi_u\right)^2 \right\rangle \approx \left\langle \left(i\bar{\psi}\gamma_5\psi\right)^2 \right\rangle \approx \left\langle \left(i\bar{\psi}\gamma_5\tau_3\psi\right)^2 \right\rangle,$$

which is a manifestation of (i.) the presence of an spectral gap and (ii.) the high level of symmetry of the spectral density, even at small volumes. This facts can be seen in the $p.d.f.$ expressions for these observables in terms of the eigenvalues μ

$$\left\langle \left(i\bar{\psi}_u\gamma_5\psi_u\right)^2 \right\rangle = \frac{1}{V^2}\left\langle \sum_j^N \left(\frac{1}{\mu_j^2}\right) - \left(\sum_j^N \frac{1}{\mu_j}\right)^2 \right\rangle, \tag{3.47}$$

$$\left\langle \left(i\bar{\psi}\gamma_5\psi\right)^2 \right\rangle = \frac{2}{V^2}\left\langle \sum_j^N \left(\frac{1}{\mu_j^2}\right) - 2\left(\sum_j^N \frac{1}{\mu_j}\right)^2 \right\rangle, \tag{3.48}$$

$$\left\langle \left(i\bar{\psi}\gamma_5\tau_3\psi\right)^2 \right\rangle = \frac{2}{V^2}\left\langle \sum_j^N \left(\frac{1}{\mu_j^2}\right) \right\rangle, \tag{3.49}$$

where the term $\left\langle \left(\sum_j^N \frac{1}{\mu_j}\right)^2 \right\rangle$ almost vanishes outside the Aoki phase. Nonetheless, inside the Aoki phase the gap disappears, the asymmetry near to the origin can become relevant and this rule would break down.

The numerical results are reported in table 3.2. Some comments are in order: inside the Aoki phase, due to the parity and Flavour breaking, we expect to find $\left(i\bar{\psi}_u\gamma_5\psi_u\right)^2$ and $\left(i\bar{\psi}\gamma_5\tau_3\psi\right)^2$ to be large with respect to the case of standard QCD (outside the Aoki phase), and this is exactely

what we get. The crucial point to discriminate between the two scenarios depicted above is the behaviour of $\left(i\bar{\psi}\gamma_5\psi\right)^2$: if we take the results of $n_{Asym}=0$ in the 4^4 lattice at face value we are induced to conclude that the non-standard scenario for the Aoki phase is favoured, being the $\left(i\bar{\psi}\gamma_5\psi\right)^2$ expectation value of the same order of magnitude of the other two observables (and an order of magnitude larger than outside the Aoki phase). The results of the 6^4 lattice seem to add no useful informations due to the large statistical errors (we hope to get better quality results in the future). On the other hand the result for $n_{Asym}=1$ can seem strange at a first sight (a negative number for the expectation value of the square of an hermitian operator), but we have to take into account that we are restricting ourselves to a single topological sector and what is relevant is the relative weight of the various topological sectors to the final result (that should be positive). The evaluation of the weights can not be performed using HMC simulations due to ergodicity problems.

We also observed that, in order to achieve in the asymmetric run the same acceptance ratios ($\sim 90\%$) than in the symmetric runs, we had to reduce the simulation step by a factor of ten, for the forces inside the HMC became much larger than expected. We took this as an indication that the system was trying to return to the symmetric state, pushing the eigenvalues through the origin, thus increasing in an uncontrolled manner the norm of the inverse of the Dirac Wilson operator. In the symmetric run, the eigenvalues certainly tried to cross the origin, however this did not happen continuously, but only from time to time. Hence, although we can not fully rely in any of these results because of the aforementioned problems of the HMC, we find the results of $n_{Asym}=0$ much more believable of those of the asymmetric state. Then we introduced the MFA algorithm [53, 54, 55, 56], with the hope of solving the ergodicity problems. As in the MFA the contributions of fermions is added during the measurement, the eigenvalues can cross the origin at will. So the MFA algorithm allowed us to measure the weights of the different sectors $n_{Asym}=0,1\ldots$, and then use these weights to correctly average the HMC data.

Table 3.3: Weights of the different sectors according to MFA algorithm.

Volume	$n_{Asym}=0$	$n_{Asym}=1$	$n_{Asym}=2$
4^4	$85.9\pm5.8\%$	$14.1\pm5.8\%$	0%

Table 3.4: Results for weighted HMC.

	$\left\langle\left(i\bar{\psi}_u\gamma_5\psi_u\right)^2\right\rangle$	$\left\langle\left(i\bar{\psi}\gamma_5\psi\right)^2\right\rangle$	$\left\langle\left(i\bar{\psi}\gamma_5\tau_3\psi\right)^2\right\rangle$
Weighted HMC $V=4^4$	$1.72(9)\times10^{-2}$	$1.7(6)\times10^{-2}$	$5.2(3)\times10^{-2}$

Conservation of P'

The numerical results are not conclusive in any way. The expectation value of $\left(i\bar{\psi}\gamma_5\psi\right)^2$ suffers from large statistical errors as the volume increases, and we fail to clarify whether the average is zero or not. We must, either increase our statistics, or find new arguments favouring one of the realizations.

The point which favours the standard realization fo the Aoki phase against our proposal is the symmetry P'. As explained before (3.2), P' is a symmetry, composition of Parity P

plus a Flavour interchange transformation, which should be conserved inside the Aoki phase, in spite of Parity being broken. This symmetry forces $i\bar{\psi}\gamma_5\psi$ to be identically zero, thence $\left\langle \left(i\bar{\psi}\gamma_5\psi\right)^2 \right\rangle = 0$ and the standard wisdom is realized. An order parameter for P' is

$$X = \frac{1}{V}\mathrm{Tr}\left(\gamma_5 D^{-1}\right) = \frac{2}{V}\sum_j \frac{1}{\mu_j}, \tag{3.50}$$

which should be $\langle X \rangle = 0$ if the symmetry P' is realized. The expectation value $\langle X^2 \rangle$ is the second piece of $\left\langle \left(i\bar{\psi}\gamma_5\psi\right)^2 \right\rangle$. Recalling (3.22)

$$\left\langle \left(i\bar{\psi}\gamma_5\psi\right)^2 \right\rangle = \left\langle \left(i\bar{\psi}\gamma_5\tau_3\psi\right)^2 \right\rangle - \langle X^2 \rangle, \tag{3.51}$$

and we are left with a contradiction: if we are inside the Aoki phase, $\left\langle \left(i\bar{\psi}\gamma_5\tau_3\psi\right)^2 \right\rangle \neq 0$, and $\left\langle \left(i\bar{\psi}\gamma_5\psi\right)^2 \right\rangle$ would only vanish if $\langle X^2 \rangle$ takes non-zero values. But certainly $\langle X^2 \rangle$ non-zero implies $\langle X \rangle \neq 0$ different from zero as well, breaking explicitly P'[16]. In this discussion we are using the fact that X is an intensive operator which does not fluctuate in the thermodynamic limit, for it scales with the volume like an intensive operator. Thus we have an strong argument to support the new scenario for the Aoki phase shown here. Were X not intensive, then the standard wisdom could be realized.

3.3 Conclusions

Up to now, almost any analysis of the Aoki phase in QCD with two flavours of Wilson fermions relied on the addition of a twisted mass term $hi\bar{\psi}\gamma_5\tau_3\psi$ as an external source, in order to break Parity and flavour explicitly, and then take the limit of vanishing external field $h \to 0$, to see whether the symmetries are restored or not. This approach presents the great handicap of vacuum selection: the addition of an external source chooses a vacuum where the behaviour of some fermionic observables is predefined. Moreover, the method often requires uncontrolled extrapolations to reach the desired results, and sometimes is not applicable at all because of the introduction of a severe sign problem in the external source. The *p.d.f.* formalism avoids these dangerous steps by computing the Fourier transform of the probability distribution function of the interesting fermionic bilinears from the eigenvalues of the Wilson-Dirac operator. As the *p.d.f.* formalism is unable to predict the form of the spectrum, several possibilities appear.

The first possibility deals with a spectral density $\rho_U(\mu, \kappa)$ of the Hermitian Dirac-Wilson operator, in a fixed background gauge field U, which is not symmetric in μ. This is a true property of the spectral density at finite V for the single gauge configurations, even if a symmetric distribution of eigenvalues is recovered by averaging over Parity conjugate configurations. This assumption leads to negative values for the square of the flavour singlet $i\bar{\psi}\gamma_5\psi = i\bar{\psi}_u\gamma_5\psi_u + i\bar{\psi}_d\gamma_5\psi_d$ operator at finite β. Thence, a reliable measurement of the η mass could be only done near enough to the continuum limit, where the symmetry of the spectral density $\rho_U(\mu, \kappa)$ should be recovered. Furthermore assuming that the Aoki phase ends at finite β, as some authors suggest [45, 58], the physical interpretation of the Aoki phase in terms of particle excitations would be lost. Quenched computer simulations at several small volumes (4^4, 6^4 and 8^4) seem to rule out this option. This arguments strongly suggest that the second possibility is realized.

In the second scenario, the symmetric spectral density $\rho_U(\mu, \kappa)$ is assumed to become symmetric in the infinite volume limit. Under this assumption, the existence of the Aoki phase

[16] There is no contradiction outside the Aoki phase, for all the observables take zero expectation values in the thermodynamic limit.

as established by the common lore is linked to the appearance of other phases, in the same parameters region, which can be characterized by a non-vanishing vacuum expectation value of $i\bar{\psi}\gamma_5\psi$, and whose vacuum states are not connected to the Aoki vacua by Parity-flavour symmetry transformations. This scenario is quite unexpected: Aoki's approximated calculations [27, 28] of $i\bar{\psi}\gamma_5\psi$ reveal that this observable vanishes all along the Aoki phase, and χPT supports unambiguously this picture. Nevertheless, the *p.d.f.* calculations are *exact*, hence, (i.) either the approximations used in all the previous calculations of the two-flavoured Aoki phase are not accurate enough to predict $i\bar{\psi}\gamma_5\psi \neq 0$ and χPT is either incomplete or not the right tool to analyze the Aoki phase, or (ii.) there must be a way to reconcile the results of the *p.d.f.* with those of previous calculations. Indeed a way exists, but involve the realization of an infinite set of sum rules.

The χPT practitioners strongly defend their results [32, 33], which predict two possible realizations for lattice QCD with two flavours of Wilson fermions at small values of hte lattice spacing a. These depends on the sign of a coefficient c_2 in a expansion up to second order of the potential energy of the effective Lagrangian. The first possibility $c_2 > 0$ predicts the standard Aoki phase, with spontaneous Parity and Flavour breaking, whereas in the second realization $c_2 < 0$ the three pions remain massive (in lattice units of mass) all thorough the parameters space. The sign of c_2 depends on the lattice action, thus χPT states that unimproved and improved actions might behave differently, and that the Aoki phase might not be present for some versions of the QCD action with Wilson fermions.

A tentative way to harmonise the χPT results with the *p.d.f.* was devised in [43], where a reason why the sum rules must hold is exposed. In simple words, the existence of an unbroken flavour-rotated Parity symmetry, $P' = -i\tau_1 \times P$, is proposed [32], and this symmmetry forces $i\bar{\psi}\gamma_5\psi$ to vanish. On the other hand, $\left\langle \left(i\bar{\psi}\gamma_5\psi\right)^2 \right\rangle$ is composed of the difference of two pieces, both of them strictly non-negative. The first piece is always non-zero inside the Aoki phase, whereas the second piece W^2 can be understood as the square of an intensive hermitian operator, which is an order parameter for the P' symmetry. The realization of the χPT scenario would require $W \neq 0$ to compensate the first piece and let the sum rule be fulfilled. However, $W \neq 0$ implies that the P' symmetry is violated, reaching a contradiction.

At this point we considered to carry out unquenched simulations of the Aoki phase without the aid of external sources. The aim of these simulations is twofold: (i.) to elucidate the conservation or violation of P', and (ii.) to measure the expectation value of the interesting observables in the Aoki region. In addition, these simulations are completely new in the QCD panorama (former simulations inside the Aoki phase for two flavours have always been done with a twisted mass term), and suffer from a critical slowing down, quite similar to that of simulating small masses. In spite of the utilization of a recently developed SAP solver [52] to overcome the slowing down, another severe problem arised, related to the inability of the Hybrid Montecarlo (HMC) algorithm to cross eigenvalues through the origin, due to an appearing divergence in the fermionic force. Thus, the HMC algorithm is not ergodic inside the Aoki phase, in the absence of external sources which regularise the unbounded eigenvalues. The Microcanincal Fermionic Average (MFA) represents a valid alternative to HMC, capable of overcoming the ergodicity problems, although it displays poor convergence for higher volumes. Unfortunately the simulations turned out to be noisy enough to prevent us to extract conclusive results. It seems that $\left\langle \left(i\bar{\psi}\gamma_5\psi\right)^2 \right\rangle$ certainly takes non-zero values for $V = 4^4$, but the scaling of this value with the volume remains unclear.

Chapter 4

Realization of symmetries in QCD

"In all science, error precedes the truth, and it is better it should go first than last."

—Hugh Walpole

4.1 Parity realization from first principles in QCD

Parity P is widely regarded as a symmetry of QCD by the scientific community. There is nothing wrong with this assumption: Indeed Parity is a symmetry of the QCD action in the absence of a θ-term –whose upper bound, established by experimental results, is extremely small–, and experimental data suggest that Parity is not spontaneously broken, at least at the energies investigated. Nonetheless, a proof of Parity realization in QCD was remarkably absent. In fact, it was revealed in lattice simulations with Wilson fermions that, for some values of the parameters, Parity could become spontaneously broken. Being lattice QCD the most successful non-perturbative tool to analyze QCD at low energies, this fact was quite disturbing.

During the mid-eighties, Vafa and Witten published a couple of theorems [59, 60] which seemed to aliviate the concerns of the theoretical people on this matter. These theorems proved that neither Parity nor any vector symmetry (the latter includes Flavour if there is some degeneration in the quark mass) were spontaneously broken in a vector-like theory. Sadly, this theorems were far from perfect, but the effort put into them was not wasted, as they were very important steps in the development of more refined proofs. In the following sections I will review them carefully, point out the flaws, and fix them as well as I can.

Review of the Vafa-Witten theorem

The original theorem was unanimously praised by the scientific community, for it provided a very elegant proof of Parity realization, which required only two pages of explanation. The article was sort and beautiful, and the underlying ideas were brilliant; however the proof was not complete.

The core of the proof is the fact that, if the vacuum expectation value of any P-nonconserving hermitian operator X vanishes, then the underlying theory preserves Parity. Let's assume that X is *any* Lorentz invariant, hermitian, P-nonconserving operator, composed of Bose fields, and let $\hat{\mathcal{L}}(\lambda)$ the original lagrangian of the theory $\mathcal{L}$, plus an external source term $\hat{\mathcal{L}}(\lambda) = \mathcal{L} - \lambda X$. If $\lambda \in \mathbb{R}$, then the new lagrangian is hermitian. The energy $E(\lambda)$ of the ground state is easily deduced to lowest order in λ

$$E(\lambda) = E(0) + \lambda \langle X \rangle$$

where $\langle X \rangle$ is the vacuum expectation value of X at $\lambda = 0$. As X is not invariant under P, the scalar $\langle X \rangle$ can take either sign, in particular the one where $\lambda \langle X \rangle$ is negative, lowering the energy of the ground state. Therefore, if P is violated, there is at least one operator X verifying $\langle X \rangle \neq 0$, and for a small non-vanishing λ this implies $E(\lambda) < E(0)$.

The way to rule out this possibility requires of the path integral formulation in the Euclidean space, but first the operator X must be Wick-rotated. As required before, X is an hermitian Bose scalar. Therefore it must be a combination of the gauge fields A^a_μ, the metric tensor $g_{\mu\nu}$ and the antisymmetric tensor $\epsilon_{\mu\nu\rho\sigma}$. The latter assures that X is P-nonconserving, as long as it appears as an odd power in X. The fields A^a_μ and the tensor $g_{\mu\nu}$ remain real in both, the Euclidean and the Minkowski space, but the tensor $\epsilon_{\mu\nu\rho\sigma}$ picks up a pure imaginary factor i in the Wick rotation. As X is proportional to an odd power of this tensor, the operator X itself pick up an i factor as well. The free energy $E(\lambda)$ then becomes

$$e^{-VE(\lambda)} = \int dA^a_\mu \, d\psi \, d\bar{\psi} \, e^{-\int d^4x (\mathcal{L} + i\lambda X)}, \tag{4.1}$$

where the acquired i factor of X has been made explicit. Integrating out the fermions

$$e^{-VE(\lambda)} = \int dA^a_\mu \, \det(D+m) \, e^{-\beta \int d^4x \mathrm{Tr} F^a_{\mu\nu} F^{\mu\nu}_a} e^{i\lambda \int d^4x X}, \tag{4.2}$$

where $(D+m)$ is the fermionic matrix with a mass term. Since the determinant $\det(D+m)$ is definite positive in vector-like theories, the positivity of the r.h.s. of (4.2) can only be spoiled by the term $e^{i\lambda \int d^4x X}$. This is a pure phase factor, as the hermiticity of X assures that the integral $\int d^4x X$ is real. In fact, the pure phase factor is the only contribution of the external source λX to the free energy. Since a pure phase factor can only *decrease* the value of the integral, the maximum of $e^{-VE(\lambda)}$, and thence the minimum of $E(\lambda)$, lie at $\lambda = 0$. Therefore, $\langle X \rangle = 0$ and Parity is preserved. As a side result, Vafa and Witten state that the same argument could be applied to the QCD lagrangian in the presence of a θ-term, to conclude that the minimum of the free energy is achieved at $\theta = 0$. For other discrete symmetries (charge conjugation C and time reversal T), the argument fails. An extension to fermoinic order parameters is straightforward, according to the authors.

Objections to the theorem

1. *The proof is not valid for fermionic order parameters*

   The proof is so simple and elegant, that it is difficult to find arguments against it. Perhaps, the firsts to notice that something was wrong with so much elegance were S. Sharpe and R. Singleton Jr., in its analysis of the Aoki phase –a quite notable counter-example of the P-preserving theorem– published in 1998 [32]. It is quite remarkable that 14 years were neccessary for the scientific community to acknowledge that the theorem was flawed.

   The remark of Sharpe and Singleton is as simple as deadly for the proof. The theorem has been developed for bosonic operators, but Vafa and Witten argue that the extension to Fermi fields is straightforward: For instance, let us assume that there are two degenerated flavours in our action, and we couple to an external field the P-violating operator $X = i\bar{\psi}\gamma_5\tau_3\psi(x)$. After the integration of the Grassman variables, X becomes

   $$X = \mathrm{Tr}\left[i\gamma_5\tau_3 S_A(x,x)\right],$$

where $S_A(x,y)$ is the fermionic propagator in the background gauge field A. As X is only a function of A, we can apply the argument safely. This is not strictly right: In the presence of fermionic zero-modes, the operator X is ill-defined, and in any other case, since the integration over the Grassman fields averages over all the possible degenerated vacua, X always vanishes, and the eigenvalues of $\gamma_5\tau_3 S_A(x,x)$ come in opposite pairs.

One way to overcome the vacua averaging after the integration of Grassman variables is the addition of a fermionic external source to the original Lagrangian, which breaks Parity explicitly, and then taking the zero external field limit. Then, the fermionic determinant is modified in the integration measure. In order to evaluate the behaviour of the order parameter in the ground state, the determinant must be expanded in small powers of the external field. However, not all the terms of the expansion are odd under Parity, but some of the terms become P-even. As these terms are even under Parity transformations, they do not become purely imaginary after a Wick rotation, and do not amount to a pure phase. Therefore, the argument is not valid for fermionic order parameters.

The clearest way to see it is the fermionic determinant, as first T. D. Cohen pointed out in [61]. Using the last example, it is easy to compute the new determinant

$$\begin{gathered}\det\left(D+m-i\lambda\gamma_5\tau_3\right)= \\ \prod_n\left(\mu_n^2+h^2\right)\geq\prod_n\mu_n^2=\det\left(D+m\right),\end{gathered} \tag{4.3}$$

with μ_n the n eigenvalue of the fermionic matrix, including mass terms. The addition of the external source obviously decreases the value of the energy $E(\lambda)<E(0)$, in contradiction with the Vafa-Witten theorem. The failure is evident, as Xiangdong Ji shown in [62], if we expand the determinant as

$$\begin{gathered}\det\left(D+m-i\lambda\gamma_5\tau_3\right)=e^{\mathrm{Tr}\ln(D+m-i\lambda\gamma_5\tau_3)}= \\ \det\left(D+m\right)e^{\mathrm{Tr}\ln\left[1-(D+m)^{-1}i\lambda\gamma_5\tau_3\right]},\end{gathered} \tag{4.4}$$

so the gluonic operator we have to consider is

$$\mathrm{Tr}\ln\left(1-\left(D+m\right)^{-1}i\lambda\gamma_5\tau_3\right), \tag{4.5}$$

which has Parity-even pieces, contributing to the lowering of the energy. Indeed the Aoki phase is a well documented counter-example of the applicability of this theorem to fermionic bilinears.

2. *The free energy is ill-defined*

Only a year later, V. Azcoiti and A. Galante pointed out [63] that the theorem was only valid if the free energy was well-defined in the presence of the P-breaking term λX. In fact, it is quite surprinsing that the realization of a symmetry depends on the fact that the order parameter X picks up an imaginary i factor under a Wick rotation. As stressed at the beginning of this chapter, although the external source method is an useful tool to analyze the spontaneous breaking of symmetries, the $p.d.f.$ is also a valid formalism to deal with symmetries, so all the information required to know whether a symmetry is spontaneously broken or not is encoded in the ground state, and there is no need to add any external sources.

Let us see the claim of Azcoiti and Galante at work. Here, X is a lorentz invariant, bosonic, hermitian, local operator, verifying the same properties as in the original article

of Vafa and Witten. In order to operate with well-defined mathematical objects, a lattice regularization which ensures the positivity of the determinant (i.e. Kogut-Susskind fermions) is chosen. In addition, since the operator X is intensive, it is assumed that it does not fluctuate when the system rests in a pure vacuum state. In other words: All the connected correlation functions are supposed to verify the cluster property.

Taking into account these assumptions, the partition function of the generalized Lagrangian can be written as a function of the *p.d.f.* of X as

$$Z(\lambda) = Z(0) \int_{-\infty}^{\infty} d\tilde{X}\, P\left(\tilde{X}, V\right) e^{i\lambda V \tilde{X}}, \tag{4.6}$$

with $P\left(\tilde{X}, V\right)$ the *p.d.f.* of X at finite volume.

Now let us assume that Parity is spontaneously broken. Then we will show that the vacuum expectation value $\langle X \rangle$ is ill-defined in the thermodynamic limit. The vacuum structure of a theory with spontaneous Parity breaking can be as complex as one can imagine; the only requisite is that any of the degenerated vacua is related to another different vacuum by the P operator. Here we will assume that the vacuum structure is the simplest possible which breaks Parity, i.e., a couple of symmetric Dirac deltas,

$$\lim_{V\to\infty} P\left(\tilde{X}, V\right) = \frac{1}{2}\delta\left(\tilde{X} + a\right) + \frac{1}{2}\delta\left(\tilde{X} - a\right), \tag{4.7}$$

in the thermodynamic limit, which will translate into a two peak structure with centers at a and $(-a)$ at any finite value of the volume.

As the P symmetry becomes a Z_2 symmetry for scalars like X, we can take advantage of this and write

$$Z(\lambda) = 2Z(0)\,\mathrm{Re}\left[\int_{0}^{\infty} d\tilde{X}\, P\left(\tilde{X}, V\right) e^{i\lambda V \tilde{X}}\right], \tag{4.8}$$

for $P(\tilde{x}, V) = P(-\tilde{x}, V)$. Then we take out a factor $e^{i\lambda V a}$

$$Z(\lambda) = 2Z(0)\,\mathrm{Re}\left[e^{i\lambda V a} \int_{0}^{\infty} d\tilde{X}\, P\left(\tilde{X}, V\right) e^{i\lambda V\left(\tilde{X} - a\right)}\right], \tag{4.9}$$

and operate, expanding the exponential in sines and cosines. In the end we arrive at

$$\begin{aligned}\frac{Z(\lambda)}{2Z(0)} = \cos(\lambda V a) \int_{0}^{\infty} d\tilde{X}\, P\left(\tilde{X}, V\right) \cos\left[\lambda V\left(\tilde{X} - a\right)\right] - \\ \sin(\lambda V a) \int_{0}^{\infty} d\tilde{X}\, P\left(\tilde{X}, V\right) \sin\left[\lambda V\left(\tilde{X} - a\right)\right].\end{aligned} \tag{4.10}$$

The zeroes of the partition function are easily obtained from (4.10), equalling the r.h.s. to zero. The resulting equation can be expressed as

$$\cot(\lambda V a) = \frac{\int_{0}^{\infty} d\tilde{X}\, P\left(\tilde{X}, V\right) \sin\left[\lambda V\left(\tilde{X} - a\right)\right]}{\int_{0}^{\infty} d\tilde{X}\, P\left(\tilde{X}, V\right) \cos\left[\lambda V\left(\tilde{X} - a\right)\right]}. \tag{4.11}$$

Up to now the discussion is quite general for any landscape pattern of Parity breaking, in the sense that this equation is valid for any $P\left(\tilde{X},V\right)$. The only mention to the double-peaked structure anticipated earlier in (4.7) is the apparition of the center of the peak a, which is not strictly neccessary. Now we need the structure defined in (4.7) to carry on our analysis. Although we expect the same behaviour for other patterns, the aim pursued here is to reveal a counterexample for the P-conservation theorem, thus it is enough to show what happens to the simplest case.

It is easy to see that the denominator of the r.h.s. of (4.11) is constant as $V \to \infty$

$$\lim_{V\to\infty} \frac{d}{d\left(\lambda V\right)} \int_0^\infty d\tilde{X}\, P\left(\tilde{X},V\right) \cos\left[\lambda V\left(\tilde{X}-a\right)\right] =$$

$$\lim_{V\to\infty} \int_0^\infty d\tilde{X}\, P\left(\tilde{X},V\right)\left(\tilde{X}-a\right) \sin\left[\lambda V\left(\tilde{X}-a\right)\right] = 0, \tag{4.12}$$

as $P\left(\tilde{X},V\right)$ becomes a Dirac delta and the factor $\left(\tilde{X}-a\right)$ makes everything vanish. The same result applies to the numerator of the expression, but the l.h.s. of (4.11) oscillates wildly, giving rise to an infinite number of solutions in the thermodynamic limit. Thus there are an infinite number of zeroes approaching the origin (i.e., $\lambda = 0$) with velocity V, and the free energy does not converge[1]. For instance, suppose the double peaked structure is gaussian at finite volume

$$P\left(\tilde{X},V\right) = \frac{1}{2}\left(\frac{V}{\pi}\right)^{\frac{1}{2}} \left(e^{-V\left(\tilde{X}+a\right)^2} + e^{-V\left(\tilde{X}-a\right)^2}\right). \tag{4.13}$$

Then, the partition function becomes

$$Z\left(\lambda\right) = Z\left(0\right)\cos\left(\lambda V a\right) e^{-\frac{\lambda^2}{4}V}, \tag{4.14}$$

and the expectation value of the order parameter is

$$i\left\langle X\right\rangle = \frac{\lambda}{2} + a\tan\left(\lambda V a\right), \tag{4.15}$$

which oscillates wildly for $a \neq 0$.

This discussion might seem somewhat artificial, but in fact very simple models fitting in Vafa and Witten's theorem requirements break down in the presence of a $P = -1$ operator. One of the simplest examples is the Ising model with an imaginary magnetic field, which breaks the Z_2 symmetry at low temperatures, in clear contradiction with the result of the theorem. Under these conditions (low temperature, external imaginary field), the free energy is ill-defined in the thermodynamic limit. Although the Ising model is not a vector-like theory, it verifies all the assumptions required for the theorem, even those associated to a vector-like theory (positivity of the measure).

The theorem is only valid if the free energy is well-defined, which implies that the symmetry is realized in vacuum, so it becomes a tautology.

[1]The result derived here can be understood as a generalization of the Lee-Yang theorem [64] for any system featuring a Z_2 symmetry.

3. *The argument fails at finite temperature*

   In 2001 T. D. Cohen cleverly remarked in [61] a number of loopholes in original Vafa and Witten reasoning. The expansion of the free energy

$$E(\lambda) = E(0) + \lambda \langle \mathcal{O} \rangle_{\lambda=0}$$

   is assumed to hold always, but this point must be treated with care. The limits $\lambda \to 0$ and $V \to \infty$ are not interchangeable, and this linear expression might not be valid in the thermodynamic limit. For instance, the free energy

$$E(\lambda) = E_0 + \sqrt{\alpha V_{\text{Space}}^{-\beta} + \gamma \lambda^2}$$

   with α, β and γ constant and positive, has a minimum at $\lambda = 0$, even in the infinite volume limit, but as $V \to \infty$ it develops a cusp at $\lambda = 0$, which signals spontaneous symmetry breaking (the first derivative becomes discontinuous). As Cohen explains, one can rule out this possibility on physical grounds: This kind of behaviour is related to level-crossing, and level-crossing can never happen at a global-minimum. Nonetheless the picture changes at finite temperature.

   The limitation of the temporal length of our box does not seem to affect to Vafa and Witten reasoning, and the fermionic determinant remains non-negative. Thence the argument should be valid for finite temperature, and Lorentz-invariant P-violating operators have vanishing vacuum expectation values. But the argument does not apply to Lorentz-noninvariant operators. As the heat-bath of finite temperature introduces a rest frame, it violates Lorentz symmetry, and allows the introduction of the velocity four-vector u_μ in the operators. Thus, observables like

$$\text{Tr}\left[\left(\vec{D} \times \vec{E}\right) \cdot \vec{E}\right] = \epsilon^{\alpha\beta\gamma\delta} \text{Tr}\left[D_\alpha F_{\gamma\sigma} F_{\delta\rho}\right] u_\beta u^\sigma u^\rho$$

   are not purely imaginary in the Euclidean space, and they do not become a pure phase in the path integral. The Vafa-Witten theorem is useless here.

4. *P-breaking gluonic external sources always increase the free energy*

   This loophole was exposed by Xiangdong Ji in [62], and may invalidate Vafa and Witten's Parity theorem. The argument is the following: The addition of an external source need not decrease the energy of a system, regardless of the realization of the symmetry. A very clever example –which is not completely analogous, and must be understood with care– is the antiferromagnetic Ising model. In the presence of an external magnetic field, the Z_2 symmetry is explicitly broken, nonetheless the energy of the vacuum in the ordered phase increases.

   Of course, the problem with the Ising example is the election of the right order parameter for the symmetry, for not every symmetry breaking term selects a vacuum effectively. The point with Parity-odd gluonic operators, according to Xiangdong Ji, is that they can not select a vacuum either: They contribute as a pure phase factor, whose phase is proportional to the volume in the path integral. The factor oscillates wildly in the thermodynamic limit, sampling over all the possible degenerated vacua, and erasing any effects of the breaking of the symmetry by the external source.

   The solution proposed by Xiangdong Ji is, in some sense, analogous to the role played by the Wick rotation in the path integral formulation. If we allow the external field to be

purely imaginary, the phase factor becomes an exponential, capable of selecting a vacuum. Then, we can asses the effects of the symmetry breaking by the external source.

This is only an incomplete sample of the claims of the wrongness of Vafa and Witten's result on Parity, but there are much more (see, for instance [65, 66]). On the whole, the Vafa and Witten result [59] can not be considered as a true theorem, and maybe the clearest example is the existence of a Parity breaking Aoki phase for two flavours of Wilson fermions, in spite of the theory complying with all the requirements of the theorem.

The *p.d.f.* approach to the problem

Although the arguments against Vafa and Witten theorem are quite serious, they do not rule out Parity conservation in vector-like theories at all, but only state that the theorem is incorrect and must be improved or reformulated. Most of the claims should be solved if the proof is based on the *p.d.f.* formalism, where the degeneration of the vacua is explicitly signaled in the probability distribution function of each observable. Even the point of fermionic bilinears can be addressed by using the extension of the *p.d.f.* developed at the beginning of this chapter.

So let us see now an alternative way of reaching the Vafa-Witten result [67], that makes use of the concept of the *p.d.f.* of a local operator. I will assume hereafter that a quantum theory can be consistently defined with a P-breaking local order parameter term.

Let be $Y(A_\mu^a)$ a local operator constructed with Bose fields. The probability distribution function of this local operator in the effective gauge theory described by the partition function (2.4) is

$$P\left(c\right) = \left\langle \delta\left(c - \frac{1}{V}\int d^4x\, Y(x)\right)\right\rangle \tag{4.16}$$

where V is the space-time volume and the mean values are computed over all the Yang-Mills configurations using the integration measure

$$\left[dA_\mu^a\right] e^{S_B} \det\left(D+m\right),$$

One can define the Fourier transform of the *p.d.f.* as

$$P\left(q\right) = \int dc\, e^{iqc} P(c) \tag{4.17}$$

which, in our case, is given by the following expression

$$P\left(q\right) = \frac{\int \left[dA_\mu^a\right] e^{-S_{PG} + \left(\frac{iq}{V} - \lambda\right)\int d^4x\, Y(x) + \ln\det(D+m)}}{\int \left[dA_\mu^a\right] e^{-S_{PG} - \lambda\int d^4x\, Y(x) + \ln\det(D+m)}} \tag{4.18}$$

or, in a short notation:

$$P(q) = \left\langle e^{\frac{iq}{V}\int d^4x\, Y(x)}\right\rangle \tag{4.19}$$

The distribution function $P(c)$ of a local P-breaking operator in absence of a P-breaking term in the action ($\lambda = 0$) should be a Dirac delta distribution, centered at the origin, only if the vacuum state is non degenerate, so Parity is preserved. On the contrary, if Parity is broken, the vacuum state is degenerate, and the expected form for $P(c)$ is

$$P\left(c\right) = \sum_\alpha w_\alpha\, \delta\left(c - c_\alpha\right), \tag{4.20}$$

where c_α is the mean value of the local order parameter in the vacuum state α and w_α are positive real numbers which give us the probability of each vacuum state ($\sum_\alpha w_\alpha = 1$).

When the degeneration of the vacuum is due to the spontaneous breaking of a discrete Z_2 symmetry like Parity, the system is likely to follow the more standard case of two symmetric vacuum states ($\pm c_\alpha$) with the same weights w_α (or an even number of vacuum states with opposite values of c_α in the most general case). The probability distribution function $P(c)$ will be then the sum of two symmetric Dirac delta's with equal weights:

$$P\left(c\right) = \frac{1}{2}\delta\left(c - c_\alpha\right) + \frac{1}{2}\delta\left(c + c_\alpha\right) \tag{4.21}$$

and its Fourier transform

$$P\left(q\right) = \cos\left(q c_\alpha\right) \tag{4.22}$$

which can take both positive and negative values.

The relevant fact now, as stated in Vafa-Witten's paper, is the fact that the local P-breaking order parameter is a pure imaginary number $Y(A^a_\mu) = iX(A^a_\mu))^2$. In such a case, the $P(q)$,

$$P\left(q\right) = \left\langle e^{-\frac{q}{V}\int d^4x\, X(x)} \right\rangle. \tag{4.23}$$

which is *real* and *positive*, as long as the integration measure is real and positive as well. Were the symmetry spontaneously broken we should get for $P\left(q\right)$ either a cosine function in the simplest case, or a sum of cosines in the most general case. This sum takes positive and negative values, but since the negative values are excluded, $P\left(q\right)$ should be a constant function equal to 1, representing a symmetric vacuum state.

Let us now extend, as much as possible, the Vafa-Witten result for pure gluonic operators to fermion bilinear local operators. To this end we will use the generalization of the *p.d.f.* discussed at the beginning of this chapter, which applies to local operators constructed with Grassmann fields. The main goal of the following lines is to show that all local bilinear $P = -1$ gauge invariant operators of the form $\mathcal{O} = \bar{\psi} O \psi$, with O a constant matrix with Dirac, color and flavour indices, take a vanishing vacuum expectation value in any vector-like theory with N_F degenerate flavours.

Let us start with the one-flavour case since, as it will be shown, it is a special case. The standard hermitian, local and gauge invariant P order parameter bilinear in the fermion fields is

$$\bar{\psi} O \psi = i \bar{\psi} \gamma_5 \psi.$$

Equation (2.6) gives the generation function of all the moments of $\mathcal{O}$

$$P(q) = \left\langle \frac{\det\left(D + m + \frac{q}{V}\gamma_5\right)}{\det\left(D + m\right)} \right\rangle \tag{4.24}$$

The determinant of the Dirac operator in the denominator of (4.24) is positive definite, but the numerator of this expression, even if real, has not well defined sign. The final form for $P\left(q\right)$ will depend crucially on the distribution of the real eigenvalues of $\gamma_5\left(D + m\right)$. Therefore we cannot say *a priori* whether $P\left(q\right)$ will be the constant function $P\left(q\right) = 1$ (symmetric vacuum) or any other function (spontaneously broken P). The matter will be solved as we go on with the N-flavoured case.

[2] As the key of the proof is the pure imaginary nature of the euclidean version of the external source $Y(A^a_\mu) = iX(A^a_\mu)$, Cohen's remark still applies to the *p.d.f.* derivation of the Vafa-Witten Parity theorem.

For N_F flavours ($N_F > 1$), the most general $P = -1$ hermitian and Lorentz and gauge invariant local order parameters $\bar{\psi} O \psi$ that can be constructed are

$$i\bar{\psi}\gamma_5\psi, \quad i\bar{\psi}\gamma_5\bar{\tau}\psi; \tag{4.25}$$

with $\bar{\tau}$ any of the hermitian generators of the $SU(N_F)$ Flavour group. However, since Flavour symmetry cannot be spontaneously broken in a vector-like theory [60], particularly in QCD[3], we will restrict our analysis to the flavour singlet case, which should give us all the information about the realization of Parity

$$i\bar{\psi}\gamma_5\psi = i\bar{\psi}_u\gamma_5\psi_u + i\bar{\psi}_d\gamma_5\psi_d + i\bar{\psi}_s\gamma_5\psi_s + \dots \tag{4.26}$$

Let us assume that $\langle i\bar{\psi}_u\gamma_5\psi_u\rangle = \pm c_0 \neq 0$. Since Flavour symmetry is not spontaneously broken,

$$\langle i\bar{\psi}_u\gamma_5\psi_u\rangle = \langle i\bar{\psi}_d\gamma_5\psi_d\rangle = \langle i\bar{\psi}_s\gamma_5\psi_s\rangle = \dots \tag{4.27}$$

Thus the system will show two degenerate vacua with all the condensates oriented in the same direction. This 'ferromagnetic' behaviour is naturally imposed by the realization of Flavour symmetry in the vacuum. Otherwise one could imagine also 'antiferromagnetic' vacua with antiparallel condensates, or even more complex structures.

The interaction between different flavours in vector-like theories is mediated by the particles associated to the gauge fields, gluons in QCD. Assuming $\langle i\bar{\psi}_u\gamma_5\psi_u\rangle \neq 0$, the fact the Flavour symmetry is conserved [60] suggests that the gauge interaction favours 'ferromagnetic' vacua, with parallel oriented condensates. However the actual dynamics can become more complicated. Indeed, a non vanishing condensate $\langle i\bar{\psi}_u\gamma_5\psi_u\rangle \neq 0$, which would imply spontaneous breaking of P, CP, T and CT, can be excluded. Let us see how in the following lines:

If we apply equation (2.6) to the computation of the $p.d.f.$ in momentum space $P_{ud}(q)$ of $i\bar{\psi}_u\gamma_5\psi_u + i\bar{\psi}_d\gamma_5\psi_d$, the result is

$$P_{ud}(q) = \left\langle \left(\frac{\det\left(D + m - \frac{q}{V}\gamma_5\right)}{\det\left(D+m\right)} \right)^2 \right\rangle, \tag{4.28}$$

where $(D + m)$ in (4.28) is the one flavour Dirac operator and the mean value is computed in the theory with N_F-degenerate flavours.

The r.h.s. of equation (4.28) is the mean value, computed with a positive definite integration measure, of a real non-negative quantity. Thus $P_{ud}\,(q)$ is positive definite, or at least a non negative, definite quantity. Were $\langle i\bar{\psi}_u\gamma_5\psi_u\rangle$ non-zero, one should expect a cosine function for $P_{ud}\,(q)$, since $i\bar{\psi}_u\gamma_5\psi_u$ and $i\bar{\psi}_d\gamma_5\psi_d$ are enforced to take the same $v.e.v.$ because of Flavour symmetry. Since the positivity of $P_{ud}(q)$ excludes such a possibility, we can infer that all the pseudo-scalar condensates $i\bar{\psi}_f\gamma_5\psi_f$ take vanishing expectation values.

The aforementioned considerations indeed complete Vafa and Witten's theorem on Parity conservation on vector-like theories with N_F degenerated flavours[4]. Nevertheless, in both theorems by Vafa and Witten, no regularisation mechanism is applied to the theory. The omission of the regularisation step in what aims to be a general proof of symmetry conservation is a dangerous business, and as we shall see, can lead to inconsistencies when a particular regularisation is chosen.

[3] QCD with Wilson fermions is not an exception, for as we will see, it does not comply with the requirements of the theorem [60].

[4] Except for the finite temperature issue, which will not be addresses in this dissertation.

One steps further: Parity and Flavour conservation in QCD

The last result is not as useful as one would like: It is not valid for N_F non-degenerated flavours, which is the case of QCD at the physical point. Regarding the paper of Vafa and Witten [60] on vector-like symmetries, such as Flavour or baryon number conservation, it does not make references to any particular regularisation either, but this does not imply that the arguments are valid for all the different versions of fermions in the lattice. In fact, the only two regularizations capable of simulating just one quark flavour[5], namely Wilson fermions and Ginsparg-Wilson fermions, do not comply with the requirements of the theorem. In the Ginsparg-Wilson case, the theorem does not apply because, even if the integration measure is positive definite, the other essential ingredient in the proof in [60], the anticommutation of the Dirac operator with γ_5, is not realized. For the case of Wilson fermions neither of the two assumptions in [60], positivity of the integration measure and anticommutation of the Dirac operator with γ_5, are fulfilled, the first of the two failing for an odd number of flavours. Indeed there exists a region of the parameters space where Parity and Flavour symmetries are spontaneously broken: the well known Aoki phase [25, 26], and even a more complex phase structure for lattice QCD with Wilson fermions has been suggested [51, 43], as discussed in the previous chapter. In the end, a theoretical proof of the realization of symmetries of QCD is still lacking.

The standard wisdom is that Vafa and Witten theorems fail, when applied to Wilson fermions, due to the existence of exceptional configurations which have a non-vanishing weight in the Aoki phase. Outside this phase, and in particular in the physical region near the continuum limit, the exceptional configurations would be suppressed and then Parity and Flavour symmetries would be restored in the QCD vacuum. Following this wisdom, and in order to prove Parity and Flavour conservation in QCD [68], it would be very convenient to choose a 'small eigenvalue free' regularization for the fermions. It happens that Ginsparg-Wilson fermions fulfill this requirement.

In order to follow the steps of the proof, some knowledge on the spectrum of the Ginsparg-Wilson operator is needed. This knowledge is exposed in appendix D. Here I restrict the computations to a particular realization of the Ginsparg-Wilson relation ($R = \frac{1}{2}$, see appendix D) verifying

$$\{\gamma_5, D\} = aD\gamma_5 D, \tag{4.29}$$

which is equivalent to overlap fermions. I also use as the mass and pseudoscalar terms the unsubstracted order parameters

$$i\bar{\psi}\left(1 - \frac{aD}{2}\right)\psi \qquad i\bar{\psi}\gamma_5\left(1 - \frac{aD}{2}\right)\psi, \tag{4.30}$$

which transform well under chiral rotations. Finally, the Ginsparg-Wilson operator Δ invoked in the following pages refers to

$$\Delta = \left(1 - \frac{am}{2}\right)D, \tag{4.31}$$

for the reasons explained in appendix D.

[5]There is a polemical controversy around the staggered quarks with the rooting technique. One side argues that they should be able to simulate one flavour and give the right continuum limit [12], and the other explains that some features of the theory in question can not be reproduced by the rooting [14]. The analysis of this discussion is out of the scope of this dissertation.

The one flavour case

Let us start by analyzing the one flavour case with the *p.d.f.*. As before, we work with the P-violating bilinear $\mathcal{O} = i\bar{\psi}\gamma_5\psi$. Our basic tool in the analysis is $P(q)$, the generating function for the moments of O,

$$\begin{array}{lllllll} P(0) & = & 1, & & P'(0) & = & i\langle\mathcal{O}\rangle, \\ P''(0) & = & -\langle\mathcal{O}^2\rangle & \dots & P^n(0) & = & (i)^n\langle\mathcal{O}^n\rangle. \end{array} \tag{4.32}$$

The evaluation of the generating function is straightforward using (4.24)

$$P(q) = \left\langle \frac{\det\left(\Delta + m + \frac{q}{V}\gamma_5\right)}{\det(\Delta + m)} \right\rangle = \left\langle \frac{\det\left(H + \frac{q}{V}\right)}{\det H} \right\rangle, \tag{4.33}$$

where $H = \gamma_5(\Delta + m)$. Let us write the $P(q)$ in terms of the μ_j, the eigenvalues of H

$$P(q) = \left\langle \frac{\prod_j\left(\mu_j + \frac{q}{V}\right)}{\prod_j \mu_j} \right\rangle = \left\langle \prod_j \left(1 + \frac{q}{\mu_j V}\right) \right\rangle. \tag{4.34}$$

In appendix D it is shown that the modulus of the eigenvalues $|\mu_j|$ is bounded from below by the mass, $|\mu_j| \geq m$ (see equation (E.22)). Thence, no zero modes are allowed if $m > 0$, and every factor of the rightmost member of equation (4.34) is well defined and does not diverge. The expansion of the product of the eigenvalues leads to a new expression,

$$P(q) = \sum_{k=0}^{V} q^k \left\langle \frac{1}{V^k} \sum_{(j_1,\cdots,j_k)} \frac{1}{\mu_{j_1},\cdots,\mu_{j_k}} \right\rangle, \tag{4.35}$$

where the sum over $(j_1,\cdots,j_k)$ means that every possible combination of the indices $j_1,\cdots,j_k$ is added to the final result. This sum can be arranged in a simpler fashion up to finite volume effects,

$$\frac{1}{V^k} \sum_{(j_1,\cdots,j_k)} \frac{1}{\mu_{j_1},\cdots,\mu_{j_k}} = \frac{1}{k!}\left(\frac{1}{V}\sum_j \frac{1}{\mu_j}\right)^k + \mathrm{O}\left(\frac{1}{V}\right). \tag{4.36}$$

As the results derived here are only valid in the thermodynamic limit, the residual terms of order $\mathrm{O}\left(\frac{1}{V}\right)$ should not be a problem.

The analysis of the spectrum of the Ginsparg-Wilson operator (see appendix D) reveals that the μ's come in pairs $\pm\mu$, except for the ones corresponding to chiral modes, in case they exist. Therefore, most of the terms in (4.36) cancel out, and the only contribution left is the one coming from the chiral modes,

$$\frac{1}{V}\sum_j \frac{1}{\mu_j} = \frac{1}{V}\left(\frac{1}{m}\left(n^+ - n^-\right) + \frac{a}{2}\left(n'^+ - n'^-\right)\right) = \left(\frac{am}{2} - 1\right)\frac{Q}{mV}, \tag{4.37}$$

where $n^\pm$ is the number of zero modes with chirality ± 1, whereas $n'^\pm$ is the number of real modes $\lambda = \frac{2}{a}$ with chirality ± 1. Putting everything together, we conclude, for non-zero mass

$$P(q) = \sum_{k=0}^{V} \frac{q^k}{k!}\left(\frac{am}{2} - 1\right)^k \frac{1}{m^k}\left\langle \left(\frac{Q}{V}\right)^k \right\rangle + \mathrm{O}\left(\frac{1}{V}\right). \tag{4.38}$$

This relationship implies that the moments of the $p.d.f.$ of $\mathcal{O} = i\bar{\psi}\gamma_5\psi$ and those of the density of topological charge are intimately related. The relationship is somewhat expected, as it is very well known that for Ginsparg-Wilson fermions

$$\chi_5 = -\frac{\langle\bar{\psi}\psi\rangle}{m} + \frac{\chi_T}{m^2}.$$

The exact relation between the moments of these two magnitudes can be easily calculated. For the even moments, the result is

$$\left\langle \left(i\bar{\psi}\gamma_5\psi\right)^n \right\rangle = (-i)^n \left(\frac{am}{2} - 1\right)^n \frac{1}{m^n} \frac{\langle Q^n\rangle}{V^n} + \mathrm{O}\left(\frac{1}{V}\right), \tag{4.39}$$

and all the odd moments vanish by Parity. The first non-trivial moment is the second one

$$\left\langle \left(i\bar{\psi}\gamma_5\psi\right)^2 \right\rangle = -\left(\frac{am}{2} - 1\right)^2 \frac{1}{m^2} \left\langle \left(\frac{Q}{V}\right)^2 \right\rangle + \mathrm{O}\left(\frac{1}{V}\right). \tag{4.40}$$

At this point we require that $i\bar{\psi}\gamma_5\psi$ be an hermitian operator, in order to carry on with the proof. This is a simple requirement, but with important consequences: The expectation value of the square of an hermitian operator must be positive, but from (4.40), this expectation value is manifestly negative in the thermodynamic limit. The only way to fulfill both requirements at the same time is the vanishing of the second moment,

$$\lim_{V\to\infty} \left\langle \left(\frac{Q}{V}\right)^2 \right\rangle = 0, \tag{4.41}$$

but then the probability distribution function of the density of topological charge, $\frac{Q}{V}$, must become a Dirac delta at the origin as V increases,

$$\lim_{V\to\infty} p\left(\frac{Q}{V}\right) = \delta\left(\frac{Q}{V}\right), \tag{4.42}$$

and all the higher moments of both $i\bar{\psi}\gamma_5\psi$ and $\frac{Q}{V}$ vanish as well. Therefore Parity is not broken in lattice QCD with one flavour of Ginsparg-Wilson fermions, at least for the standard order parameter $i\bar{\psi}\gamma_5\psi$.

Let us consider now the case of the unsubstracted order parameter,

$$i\bar{\psi}\gamma_5\left(1 - \frac{aD}{2}\right)\psi. \tag{4.43}$$

Its generating function $P(q)$ is

$$P(q) = \left\langle \frac{\det\left[\Delta + m + \frac{q}{V}\gamma_5\left(1 - \frac{aD}{2}\right)\right]}{\det\left(\Delta + m\right)} \right\rangle. \tag{4.44}$$

The expression (4.44) is immediately simplified, for only the zero modes of D contribute to this last equation (4.44). In order to see it, let us consider the following argument: The matrix corresponding to the numerator is block-diagonal, whose blocks are of the form indicated in (E.24). The contribution to the ratio coming from a pair of complex eigenvalues of D belonging to a 2×2 block is of the form (from (E.25) in appendix D)

$$1 - \alpha\frac{q^2}{V^2}, \tag{4.45}$$

with $|\alpha| \leq m^{-2}$ (E.27). Therefore, the contribution to $P(q)$ corresponding to complex eigenvalues comes solely from the factor $\prod_j \left(1 - \alpha_j \frac{q^2}{V^2}\right)$, where the product extends over all pairs of complex eigenvalues. Expanding this product, the coefficient corresponding to q^{2k} can be computed easily,

$$\left| \frac{1}{V^{2k}} \sum_{(j_1,\ldots,j_k)} \alpha_{j_1} \cdots \alpha_{j_k} \right| \leq \frac{1}{V^{2k}} \left(\sum_j |\alpha_j| \right)^k \leq \frac{V^k m^{-2k}}{V^{2k}} = \frac{m^{-2k}}{V^k}. \tag{4.46}$$

Thence, the contribution from the complex eigenvalues is of order $1 + O\left(\frac{1}{V}\right)$, that is, just 1 in the thermodynamic limit.

Regarding the chiral modes of D with $\lambda = \frac{2}{a}$, and as explained in (E.28), they also contribute with a factor 1. The zero modes of D, on the other hand, give a non-trivial contribution,

$$P(q) = \left(1 + \frac{q}{mV}\right)^{n^+} \left(1 - \frac{q}{mV}\right)^{n^-}. \tag{4.47}$$

If $n^+ < n^-$ $(Q > 0)$, then

$$P(q) = \left(1 - \frac{q^2}{m^2V^2}\right)^{n^+} \left(1 - \frac{q}{mV}\right)^{Q}. \tag{4.48}$$

A similar expression is valid for $n^+ > n^-$. The argument applied to (4.46) can be essentially translated here: The first factor of the r.h.s. of (4.48) goes to 1 in the thermodynamic limit. Therefore we obtain the final result (valid for arbitrary values of n^+ and n^-) when $V \to \infty$

$$P(q) = \left(1 - sign(Q)\frac{q}{mV}\right)^{|Q|}. \tag{4.49}$$

All odd moments vanish as before because of (finite-volume) Parity symmetry. The even moments also vanish because they are trivially related to the ones in (4.38), as can be seen easily by expanding (4.49). In consequence, we see that Parity is not broken for the unsubstracted order parameter either.

It is interesting to give a more physical argument that uses only the vanishing of the second moment. In fact, if Parity were spontaneously broken, we would expect two degenerate vacua α and β, since Parity is a Z_2 symmetry. Let z_α be a complex number which give us the mean value of the pseudoscalar $\mathcal{P}$ in the α state

$$\langle \mathcal{P} \rangle_\alpha = z_\alpha,$$

then we have

$$\langle \mathcal{P} \rangle_\beta = -z_\alpha.$$

Since $\mathcal{P}^2$ is Parity invariant, it takes the same mean value in the two states. Making use of the cluster property in each one of these two states, one can find out that

$$\langle \mathcal{P}^2 \rangle = \frac{1}{2} \langle \mathcal{P}^2 \rangle_\alpha + \frac{1}{2} \langle \mathcal{P}^2 \rangle_\beta = z_\alpha^2,$$

but since $\langle \mathcal{P}^2 \rangle = 0$, z_α must vanish.

In conclusion we have shown rigorously, assuming hermiticity of $i\bar{\psi}\gamma_5\psi$ and using standard properties of Ginsparg-Wilson fermions, that Parity is not spontaneously broken in the one-flavour model, at least for the more standard order parameters, namely $i\bar{\psi}\gamma_5\psi$ and the density of topological charge.

The N_F flavours case

The last arguments apply only to the one-flavoured case, but they can be easily extended to an arbitrary number of flavours N_F. In contrast with the extension of the Vafa-Witten theorem proposed before, these flavours can have different masses, but they must be non-vanishing. Most of the results from the previous section apply here as well with small modifications. The fermionic action is

$$\sum_{\alpha=1}^{N_F} \bar{\psi}_\alpha \left(\Delta + m_\alpha\right) \psi_\alpha. \tag{4.50}$$

The complete spectrum of the Dirac operator consists of N_F copies of the single flavour spectrum, each of them calculated with the mass of the corresponding flavour.

Let us consider the usual pseudoscalar order parameter for a single flavour β, $i\bar{\psi}_\beta\gamma_5\psi_\beta$. The corresponding generating function $P\left(q\right)$ can be computed easily,

$$P\left(q\right) = \left\langle \frac{\det\left(\Delta + m_\beta + \frac{q}{V}\gamma_5\right)}{\det\left(\Delta + m_\beta\right)} \right\rangle_{N_F}. \tag{4.51}$$

The average is taken over the effective gauge theory with N_F flavours, but only the β flavour appears within the average[6]. The calculation is identical to the one for the single flavour case and gives

$$P\left(q\right) = \left\langle \prod_j \left(1 + \frac{1}{\mu_j^\beta}\frac{q}{V}\right) \right\rangle. \tag{4.52}$$

The superindex on the eigenvalues indicate flavour, that is, μ^β belongs to the spectrum of $\gamma_5\left(\Delta + m_\beta\right)$. Equation (4.52) is essentially the same as the one for one flavour, and the moments of $P\left(q\right)$ still are, up to constants, the same as the moments of the density of topological charge $\frac{Q}{V}$. The only difference is that now the average is taken in the theory with N_F flavours. This does not change any of the conclusions: all odd moments vanish by symmetry, the second moment vanish in the thermodynamic limit because of the hermiticity of $i\bar{\psi}\gamma_5\psi$, the density of topological charge goes to a Dirac delta centered on the origin, and therefore all the higher moments vanish as $V \to \infty$. This is valid for any flavour separately, and so will be valid as well for any linear combination $\sum_\alpha A_\alpha i\bar{\psi}_\alpha\gamma_5\psi_\alpha$. The extension to the unsubstracted order parameter is trivial. This result extends the generalization of the Parity Vafa-Witten theorem to fermionic bilienars, but note that the mass of every flavour must be non-zero, otherwise the proof breaks down.

Let us consider now the degenerate case, all flavours with equal nonzero masses. The action now enjoys *Flavour symmetry*. As stated in the introduction of this paper, the Vafa-Witten theorem [60] for vector-like symmetries does not apply to Ginsparg-Wilson fermions because, even if the integration measure is positive definite, the Dirac operator does not anticommute with γ_5. However we can study this symmetry with the *p.d.f.* method as we did for Parity.

Consider first the case of two degenerate flavours and the standard order parameters $\bar{\psi}\tau_3\psi$ and $i\bar{\psi}\gamma_5\tau_3\psi$. Proceeding as before, we find for the first order parameter

$$P\left(q\right) = \left\langle \frac{\det\left(\Delta + m + i\frac{q}{V}\right)\det\left(\Delta + m - i\frac{q}{V}\right)}{\det\left(\Delta + m\right)^2} \right\rangle_{N_F} =$$

[6]Our fermionic determinant (and hence, its eigenvalues) will always refer to a *single flavour*.

$$\left\langle \prod_j \left(1 + \frac{q^2}{\lambda_j^2 V^2} \right) \right\rangle_{N_F}, \tag{4.53}$$

where λ_j are the eigenvalues of $\Delta + m$. By the same argument we have use repeatedly before, i.e., the lower bound of the eigenvalues $|\lambda| < \frac{1}{m}$, $P(q) \to 1$ in the thermodynamic limit[7].

Similarly for $i\bar{\psi}\gamma_5\tau_3\psi$ we obtain

$$P(q) = \left\langle \frac{\det\left(H + \frac{q}{V}\right) \det\left(H - \frac{q}{V}\right)}{\det\left(H^2\right)} \right\rangle_{N_F} =$$

$$\left\langle \prod_j \left(1 - \frac{q^2}{\mu_j^2 V^2} \right) \right\rangle_{N_F}. \tag{4.54}$$

The same argument applies, for $|\mu|$ is bounded from below as well, and we have also that $P(q) \to 1$ as the volume grows to infinity. In fact, the extension of the proof of Flavour conservation to N_F flavours is trivial: since the preceding results apply to any pair of flavours, and we can choose the generators τ_i of the $SU(N_F)$ Flavour symmetry group so as to involve only pairs of flavours, then Flavour symmetry is realized in general. The calculations can be repeated easily for the unsubstracted operators, and the result is the same. We can then conclude that there is no Aoki phase for two flavours of Ginsparg-Wilson fermions with non-zero mass. This conclusion should not be surprising at all, for the spectrum of the hermitian Ginsparg-Wilson operator H with a mass term is depleted of small eigenvalues of order $\approx \frac{1}{V}$.

The following relation

$$\chi_5 = -\frac{\langle \bar{\psi}\psi \rangle}{m} + N_F^2 \frac{\chi_T}{m^2},$$

also holds when taking into account the number of flavours, implicitly in the condensate, and explicitly in the topological susceptibility via the N_F^2 factor.

The chiral limit

The results of the previous sections can not be extended in a straightforward way to QCD in the chiral limit. We lose the non-trivial lower bound on the spectrum of $\Delta + m$, $0 < m < |\lambda|$, and the Dirac operator has exact zero modes corresponding to gauge fields with non-trivial topology. Thence, as the arguments developed in the preceeding sections do not help us finding a definite conclusion on the realization of Parity in the chiral limit from first principles, we will appeal to the standard wisdom.

Let us consider QCD with one massless flavour. In this limit, the action of the model has the chiral $U(1)$ symmetry, which is anomalous because the integration measure is not invariant under chiral $U(1)$ global transformations. The Jacobian associated to this change of variables introduce an extra term to the pure gauge action proportional to the topological charge of the gauge configuration, the θ-vacuum term, which allows one to understand the absence of a Goldstone boson in the model, but this fact generates the well known strong CP problem. All these features of QCD in the continuum formulation are well reproduced in lattice QCD with Ginsparg-Wilson fermions, as discussed in this chapter and appendix E.

[7]This conclusion rests only on the bound on the eigenvalues, and not on any other specific property of the Dirac operator.

Let's consider first the unsubstracted scalar order parameter, $\bar{\psi}\left(1-\frac{aD}{2}\right)\psi$. The corresponding generating function $P(q)$ in the chiral limit and for a generic value of θ[8] is

$$P(q)=\frac{\int[dA]\,e^{-S_{PG}}e^{-i\theta Q}\det\left(D+i\frac{q}{V}\left(1-\frac{aD}{2}\right)\right)}{Z}, \tag{4.55}$$

with $Z=\int[dA]\,e^{-S_{PG}}e^{-i\theta Q}\det D$ and $Q=n^{-}-n^{+}$. The contribution to the determinant in the numerator of (4.55) coming from pairs of complex eigenvalues of D is easily computed and gives a factor

$$f_0(q)=\prod_j\left[|\lambda_j|^2-\frac{q^2}{V^2}\left(1-\frac{a^2|\lambda_j|^2}{4}\right)\right], \tag{4.56}$$

where the product is taken over all different pairs of complex eigenvalues. Each chiral mode corresponding to an eigenvalue $\frac{2}{a}$ contributes a factor of $\frac{2}{a}$ to the determinant, and each chiral mode corresponding to a zero eigenvalue contributes a factor of $\frac{iq}{V}$. The normalization factor Z is computed from the same expressions by setting $q=0$. Therefore we can write $P(q)$ as

$$P(q)=Z^{-1}\int[dA]\,e^{-S_{PG}}e^{-i\theta Q}f_0(q)\left(\frac{2}{a}\right)^{n'^{+}+n'^{-}}\left(\frac{iq}{V}\right)^{n^{+}+n^{-}}, \tag{4.57}$$

where $n^{\pm}$ represent the chiral zero modes, and $n'^{\pm}$ represent the chiral $\frac{2}{a}$ modes. The computation of the generating function for the pseudoscalar order parameter $i\bar{\psi}\gamma_5\left(1-\frac{aD}{2}\right)\psi$ follows the same line,

$$P(q)=Z^{-1}\int[dA]\,e^{-S_{PG}}e^{-i\theta Q}f_0(q)(-1)^{n^{+}}\left(\frac{2}{a}\right)^{n'^{+}+n'^{-}}\left(\frac{q}{V}\right)^{n^{+}+n^{-}}. \tag{4.58}$$

Defining

$$f_{\mathcal{S}}(q)=f_0(q)\left(\frac{2}{a}\right)^{n'^{+}+n'^{-}}\left(\frac{iq}{V}\right)^{n^{+}+n^{-}} \tag{4.59}$$

and denoting by $P_S(q)$ and $P_P(q)$ the generating functions for the scalar and pseudoscalar respectively, we can rewrite the above results in the following way

$$P_{\mathcal{S}}(q) = Z_S^{-1}\int[dA]\,e^{-S_{PG}}e^{-i\theta Q}f_S(q), \tag{4.60}$$

$$P_{\mathcal{P}}(q) = Z_P^{-1}\int[dA]\,e^{-S_{PG}}e^{-i\theta Q}f_S(q)(-i)^{Q}. \tag{4.61}$$

Two comments are in order, regarding these two expressions:

(i.) Only the $Q=\pm1$ sectors verifying $n^{-}+n^{+}=1$ contribute to the chiral condensate $\langle\mathcal{S}\rangle$. As its expectation value is computed as the derivative $\frac{dP_{\mathcal{S}}}{dq}\Big|_{q=0}$, only when $n^{-}+n^{+}=1$ all the q factors are removed from the expression (4.60), giving a non-zero result.

(ii.) The dependence of the expectation value of the scalar order parameter with the θ parameter is $\langle S\rangle\propto\cos\theta$.

[8] Although in the chiral limit the free energy does not depend on θ, the condensate certainly does, as in order to compute it in the chiral limit we need to know the free energy in the neighbourhood of the point $m=0$. This neighbourhood is θ dependent.

For the second moment $\langle S^2 \rangle$, the only non-vanishing contributions come from the sectors with $Q = 0$ and $Q = \pm 2$[9], the first coming from the second derivative of the function $f_0(q)$, and the second appearing as the factor $\left(\frac{iq}{V}\right)^2$ is eliminated by the second derivative. Thence

$$\langle S^2 \rangle = A_0 + A_2, \tag{4.62}$$

where A_0 is the contribution coming from the $Q = 0$ sector and A_2 the contribution coming from the $Q = \pm 2$ sector.

Expression (4.61) for the pseudoscalar condensate tells us that all the odd moments vanish because of Parity symmetry[10]. In contrast, the second moment receives non-zero contributions from the $Q = 0, \pm 2$ sectors

$$\langle P^2 \rangle = A_0 - A_2. \tag{4.63}$$

Looking at moments of higher order we would find an infinite set of relations among the A_i.

Since strictly speaking, due to the chiral anomaly we do not have a new symmetry in the chiral limit of one flavour QCD, the standard wisdom tells us that the vacuum expectation value of the chiral order parameter does not vanish as $m \to 0$. Moreover, the absence of massless particles in the one flavour model suggests that the perturbation series in powers of m does not give rise to infrared divergences [46], the free energy density is an ordinary Taylor series in m [69, 46]; and in what concerns the chiral condensate, the chiral and thermodynamical limits commute.

On the other hand, the free energy density of the model at $m \neq 0$ and $\theta = 0$ can be computed in the thermodynamical limit from the topologically trivial sector $Q = 0$ [69, 46]. But since chiral symmetry in the $Q = 0$ sector is not anomalous, it should be spontaneously broken in that sector, if the chiral condensate takes a non vanishing value when approaching the chiral limit. In such a case, the value of the chiral condensate in the full theory and in the chiral limit will be related to the spectral density at the origin of eigenvalues of the Dirac operator of the topologically trivial sector by the well known Banks and Casher formula [44]

$$\langle S \rangle = -\pi \rho(0) = \Sigma_0.$$

This equation provide us with a non trivial relation between the value of the scalar condensate in the chiral limit in the full theory, which gets all its contribution from the $Q = \pm 1$ sectors, and the spectral density of eigenvalues at the origin of the Dirac operator in the topologically trivial sector $Q = 0$.

The scalar condensate is invariant under Parity, and therefore we expect its probability distribution function to be a delta function $\delta(c - \Sigma_0)$ in the full theory in the chiral limit, irrespective of the realization of Parity in the vacuum. Thence, we expect for the moments

$$\langle \mathcal{S}^n \rangle = \Sigma_0^n. \tag{4.64}$$

For the second moment, this implies

$$A_0 + A_2 = \Sigma_0^2, \tag{4.65}$$

[9] As in the case of $\langle \mathcal{S} \rangle$, only when $Q = \pm 2$ *and* $n^- + n^+ = 2$ there appears a contribution to the second moment of the pseudoscalar. This rule holds for every contribution coming from a sector with non-trivial topology $Q \neq 0$.

[10] Parity symmetry imposes that, given a configuration with topological charge $Q = n$, one always can find a corresponding configuration with topological charge $Q = -n$, and the same weight in the partition function. As the factor $(-i)^Q$ changes sign with Q when Q is odd, the sum of the contributions of every pair of corresponding configurations vanishes for any observable. Even values of Q do not share this property, and $(-i)^{2n} = (-i)^{-2n}$.

but as previously stated, the standard wisdom suggests that the topologically trivial sector break spontaneously the chiral $U(1)$ symmetry, and since A_0 is exactly the second moment of $P_{\mathcal{S}}(c)$ computed in the $Q = 0$ sector, what should happen is

$$A_0 = \frac{1}{2}\Sigma_0^2, \tag{4.66}$$

and consequently

$$A_2 = \frac{1}{2}\Sigma_0^2, \tag{4.67}$$

but this implies that the second moment of the pseudoscalar condensate (4.63) vanishes,

$$\left\langle \mathcal{P}^2 \right\rangle = 0. \tag{4.68}$$

By a similar argument, the relations for the higher (even) moments, $\left\langle \mathcal{S}^{2n} \right\rangle = \Sigma_0^{2n}$ imply the vanishing of the corresponding pseudoscalar moments, $\left\langle \mathcal{P}^{2n} \right\rangle = 0$

Symmetry under Parity is the only obvious reason for the vanishing of the pseudoscalar moments, and therefore the previous result strongly suggests that Parity is also realized in QCD with one massless flavour.

4.2 Conclusion

It is quite well-establish in the scientific community that Parity and vector-like global symmetries remain unbroken in QCD. Nonetheless, no sound theoretical proof of this hypothesis has ever been presented. Vafa and Witten gave convincing arguments against spontaneous breaking of these symmetries in [59, 60], but those were questioned by several groups [32, 63, 61, 62, 65, 66], and now the QCD researchers agree on the lack of a proof for Parity realization in QCD. As far as vector-like symmetries –as Flavour or Baryon number conservation- are concerned, it must be remarked that the staggered fermion discretization is the only known lattice regularization that fulfills the initial conditions of the Vafa-Witten theorem. Indeed, the fact that the theorem is not applicable neither to the Ginsparg-Wilson regularization nor to Wilson's one is quite remarkable. Both regularizations violate the condition of the theorem that the Dirac operator must anticommute with γ_5. Moreover, in the Wilson case positivity for the integration measure cannot be assumed for a single flavour. As a matter of fact, the Wilson regularization features the Aoki phase, where Parity and Flavour symmetries are spontaneously broken.

The $p.d.f.$ formalism, when combined with an appropiate regularization, shows a way to discard spontaneous breaking of these symmetries in QCD. By an appropiate regularization we mean a regularization where the eigenvalues of the Dirac operator are bounded from below for a non-zero fermion mass. This is not the Wilson case, and those arbitrarily small eigenvalues are responsible of the appearance of the Parity and Flavour breaking Aoki phase. Fortunately, the Ginsparg-Wilson regularization has nice chiral properties which protect the masses of the quarks to be renormalized additively. This is translated into our desired lower bound for the eigenvalues, and thence, a proof for Parity and flavour conservation can be constructed. This is a major result that overcomes the difficulties found in [59, 60].

Chapter 5

The Ising model under an imaginary magnetic field

"The distance between insanity and genius is measured only by success."

—Bruce Feirstein

5.1 Introduction to the Ising model

The origins of the Ising model

The Ising model was first proposed[1] by Lenz to his student Ising [72] as a simple model describing ferromagnets. Lenz's original model tried to explain the Curie law of paramagnets [73], evading the widely criticized *molecular-field hypothesis* of Weiss [74]. Although Weiss hypothesis was successful numerically, and in fact, when combined with the Langevin equations [75], was able to predict the Curie law and the phenomenon of spontaneous magnetization, it awoke sharp criticism among many physicists. The most remarkable of them was Stern (1920), who argued that Langevin equations were not applicable to gases at very low temperatures, in a crystaline solid state. The gas molecules carrying magnetic moment were implicitly suppossed to rotate freely, but this assumption could not be extended to the crystaline state. Stern attributed the success of the Weiss hypothesis to its many adjustable parameters.

Free rotability was in clear contradiction with Born's theory of crystal structure, yet it seemed an indispensable ingredient to obtain the Curie law and spontaneous magnetization. Lenz tried to solve the contradiction using some sort of *quantum approach* (quantum in the very old sense of the first years of quantum mechanics). He assumed that the gas molecules were unable to rotate freely inside the crystal, however, they could perform *turnover* movements, and the positions allowed for each molecule were effectively quantized. He argued carefully that in the end, there were only two distinct positions available for these molecules.

In the case these molecules did not interact, Lenz found the Curie law for paramagnets. Lenz expected the interacting case to lead to spontaneous magnetization, nonetheless he never made computations on the interacting case, or specified any particular interaction among the molecules. He assigned this task to his student Ising.

Ising's intuition was the posibility of generating a non-local effect associated to spontaneous magnetization from a local nearest-neighbour interaction. He expected the forces acting between

[1] Interesting reviews of the Ising model can be found in [70, 71].

molecules to be short ranged, and deduced that qualitative physics could be extracted from a nearest-neighbour approximation. Ising solved the one-dimensional version of the model [76], the *chain model*, and found no signal of spontaneous magnetization. He obtained the same result in some variations of the model, including an arrangement of several chains in three dimensions; thence he incorrectly assumed that the three-dimensional case displayed no spontaneous magnetization.

Ising result was in some way dissappointing. People hoped that the main properties of ferromagnets could be described by such a simple model, and after the failure, they almost forsook it. It took some years for the scientific community to regain the faith in the Ising model[2], and the main responsible was Onsager, who solved analitically the two-dimensional case, and showed how spontaneous magnetization appeared below a critical temperature [80]. From that point on, the number of papers on the Ising model increased notably.

Onsager's solution is usually regarded as brilliant and extremely complicated. Indeed, up to this moment, there is no known solution for higher dimensional versions of the Ising model (except for the infinite-coupled model). Even the two-dimensional case in the presence of a magnetic field remains unbeaten.

Why the Ising model?

The Ising model is a good starting point to test our θ vacuum algorithms for several reasons. First of all, it is easy to treat and code into a computer, and the simulations are fast enough to allow us to generate large statistics, even in large lattices. Furthermore, the one-dimensional model in the presence of a magnetic field is exactly solvable, so we can check our results against analytic formulae in order to make sure they work. Then, the application of our methods to higher dimensions is straighforward. On the other hand, we can identify in some sense magnetization and topological charge on this model, and regard an imaginary external magnetic field as a θ term in the action. Finally, from the numerical point of view, it is even more challenging[3] than other complex systems suffering from the sign problem, as lattice QCD with a $\theta-$term, yet it remains more accessible. Therefore, it is a good idea to check the goodness of any algorithm in these toy models, prior to their application to more complex systems. From the pedagogical point of view, the Ising model as an introduction to the lattice is also a good start.

5.2 Solving the Ising model

Definition of the Ising model

The Ising model is an *statistical system* described by the following hamiltonian

$$H\left(\{s_i\}, J, B\right) = -J \sum_{\{i,j\}} s_i s_j - B \sum_i s_i, \tag{5.1}$$

where the s_i are Z_2 variables (*spins*[4] from now on) in the $\{1, -1\}$ representation, placed on a regular lattice, and $\{i, j\}$ means sum over nearest neighbours. J is the *coupling constant* among spins and B stands for the external magnetic field.

[2] See for instance [77, 78, 79].

[3] As the following sections show, the phase diagram of the Ising model within an imaginary magnetic field is richer than the one expected for QCD in presence of a θ–vacuum term.

[4] The spin nomenclature appeared a long time after the model was devised, probably linked to the apparition of the Heisenberg model. At that time, the Ising model became to be regarded as a simplification of the Heisenberg model.

As I said, this is an statistical system. By an statistical system I mean a system whose dynamics are completely irrelevant. We do not know the equations of motion of this model, and in fact, we do not need to. The kinetic term is even absent in the hamiltonian. We treat these systems by generating ensembles of configurations and then performing statistical analysis, which involves the computation of mean values and correlation functions. A configuration is a set of allowed values for the spin variables s_i. The usual way to represent a configuration is by assigning arrows ($\uparrow = +1$ and $\downarrow = -1$) to each value of the spin, and put one arrow per lattice site:

$$\begin{array}{c} \uparrow\uparrow\downarrow\uparrow\uparrow\uparrow\downarrow\downarrow\uparrow\downarrow \\ \uparrow\downarrow\downarrow\uparrow\downarrow\uparrow\uparrow\downarrow\downarrow\downarrow\uparrow \\ \downarrow\downarrow\downarrow\uparrow\downarrow\downarrow\uparrow\uparrow\uparrow\downarrow\uparrow \\ \downarrow\downarrow\uparrow\downarrow\downarrow\uparrow\downarrow\uparrow\uparrow\uparrow\downarrow \\ \uparrow\uparrow\uparrow\downarrow\uparrow\downarrow\downarrow\downarrow\downarrow\downarrow\downarrow \end{array}$$

The energy of each configuration is computed by using (5.1). It is obvious from (5.1) that, at zero magnetic field, the operation $s_i \to -s_i$ keeps the energy of the system unchanged. This fact is a consequence of the Z_2 symmetry the system enjoys in the case of vanishing magnetic field. The quantity

$$M = \sum_i^N s_i \tag{5.2}$$

is not invariant under Z_2 transformations, and defines an order parameter of the Z_2 symmetry. This quantity is called the *total magnetization of the system*, so for symmetry reasons we naively expect M to be zero in the thermodynamic limit. The total magnetization may be understood as a topological charge in those systems with an even number of spins[5], in the sense that $M/2$ is a quantized number, ranging from $-\infty$ to ∞ in the thermodynamic limit. We will use this property to analyze the Ising model as a toy model to test algorithms to simulate θ-vacuum theories.

Direct application of Boltzmann hypothesis gives us the probability $P(\{s_i\})$ of each configuration $\{s_i\}$,

$$\begin{array}{ll} P(\{s_i\}) & = \frac{e^{-\frac{H}{k_B T}}}{Z} = \frac{e^{F\sum_{\{i,j\}} s_i s_j + \frac{h}{2}\sum_i s_i}}{Z} \\ Z(F,h) & = \sum_{\{s_i\}} e^{F\sum_{\{i,j\}} s_i s_j + \frac{h}{2}\sum_i s_i} \end{array} , \tag{5.3}$$

and in the case of zero external field $h = 0$, the Z_2 symmetry forces explicitly the equality $P(\{s_i\}) = P(\{-s_i\})$. The quantity Z is the *partition function*, which encodes all the information of the system[6]. The expectation value of any observable can be computed, once we know Z. As we have marked in the last equation, Z is a function of the system parameters, $F = J/k_B T$ and $h = 2B/k_B T$, which I will call *reduced coupling* and *reduced magnetic field*. Thence, the average values of any observable or correlation function depend on these two parameters as well.

For instance, the *average density of magnetization* $\langle m \rangle = \frac{1}{N}\langle \sum_i^N s_i \rangle$ is

[5] This requirement is a natural imposition in antiferromagnetic systems, if we want to avoid frustration.

[6] To compute certain observables, however, it might be necessary to calculate the partition function *coupled to certain external sources*. For instance, in order to compute the correlation functions a site dependent magnetic field B_i is required, as we will see in the following pages.

$$\langle m\rangle = \sum_{\{s_i\}} P\left(\{s_i\}\right) m\left(\{s_i\}\right) = \sum_{\{s_i\}} m\left(\{s_i\}\right) \frac{e^{-\frac{H}{k_B T}}}{Z} = \frac{\frac{\partial Z}{\partial \frac{h}{2}}}{Z}. \tag{5.4}$$

At a finite volume, the partition funcion can not describe a phase transition of any kind. The proof is quite simple: The exponential[7] $e^{-\beta H}$ is a positive analitic function of the Hamiltonian parameters J and B, and of the temperature β; as Z is a finite sum of exponentials, it is a non-zero analitical function as well. No singularities occurr in the computation of any observable, and thence, no phase transition behaviour is displayed.

In order for the phase transition to appear, we need to reach the thermodynamic limit. Then, the partition function becomes a serie, and singular behaviour may happen. Unfortunately, the partition function is not well defined in the thermodynamic limit: When $N \to \infty$, Z usually diverges[8]. Therefore, it is convenient to work with the *free energy*

$$f\left(F,h\right) = \lim_{N\to\infty} \frac{1}{N} \ln\left(Z\left(F,h\right)\right). \tag{5.5}$$

No information is lost from $Z\left(F,h\right)$ to $f\left(F,h\right)$, thus we expect to be able to work out any expectation value from the free energy. In fact, taking derivatives with respect to the reduced magnetic field we find the *mean magnetization density* of the system,

$$\langle m\rangle = \frac{\partial f\left(F,h\right)}{\partial \frac{h}{2}} = \frac{1}{N} \frac{\partial \ln\left(Z\left(F,h\right)\right)}{\partial \frac{h}{2}} = \frac{1}{N} \frac{\frac{\partial Z}{\partial \frac{h}{2}}}{Z}. \tag{5.6}$$

The response of the mean magnetization density to the reduced magnetic field is the definition of the *magnetic susceptibility*

$$\chi = \frac{\partial \langle m\rangle}{\partial \frac{h}{2}} = \frac{1}{N}\left[\frac{\frac{\partial^2 Z}{\partial\left(\frac{h}{2}\right)^2}}{Z^2} - \left(\frac{\frac{\partial Z}{\partial \frac{h}{2}}}{Z}\right)^2\right] =$$

$$N\left[\left\langle m^2\right\rangle - \langle m\rangle^2\right] = N\left(\Delta m\right)^2. \tag{5.7}$$

The equality (5.7) is called *fluctuation-dissipation theorem.* It relates the fluctuations of the system with the sensitivity of the system to external fluctuations. The meaning is clear: A high sensitivity to external agents also implies high sensitivity to thermal fluctuations, hence a system that shows a great response under external fields fluctuates wildly in the absence of these fields, and vice-versa.

The magnetic susceptibility is inherently related to the spin-spin correlation functions. These functions measure the influence of the spin j over the spin k. In order to compute these spin-spin correlations, we introduce a site-dependent magnetic field

$$H\left(\{s_i\}, J, B_i\right) = -J \sum_{\{i,j\}} s_i s_j - \sum_i B_i s_i. \tag{5.8}$$

Now, the derivative of the free energy with respect to B_j yields the mean of the spin variable at the site j,

[7] As usual, $\beta = \frac{1}{k_B T}$.

[8] If a sign problem exists, the partition function becomes zero in the thermodynamic limit.

$$\langle s_j \rangle = \sum_{\{s_i\}} P\left(\{s_i\}\right) s_j = \sum_{\{s_i\}} s_j \frac{e^{\frac{H}{k_B T}}}{Z} = \frac{\frac{\partial Z}{\partial \frac{h_j}{2}}}{Z} = \frac{\partial f}{\partial \frac{h_j}{2}}. \tag{5.9}$$

It is straightforward to see that the taking of a second derivative with respect to the reduced magnetic field in another site produces the desired correlation function

$$\langle s_j s_k \rangle = \sum_{\{s_i\}} P\left(\{s_i\}\right) s_j s_k = \sum_{\{s_i\}} s_j s_k \frac{e^{\frac{H}{k_B T}}}{Z} = \frac{\frac{\partial^2 Z}{\partial \frac{h_j}{2} \partial \frac{h_k}{2}}}{Z}. \tag{5.10}$$

For this reason, the partition function is called the *generator of the correlation functions*.

This quantity measures effectively the influence of s_j in s_k whenever $\langle s_j \rangle = \langle s_k \rangle = 0$. However, if $\langle s_{j,k} \rangle \neq 0$, the correlation function may return non-zero values, even if the fluctuations of the spins s_j and s_k are completely unrelated. That is why we are usually more interested in the *connected correlation funcion*

$$G_{jk} = \langle s_j s_k \rangle - \langle s_j \rangle \langle s_k \rangle, \tag{5.11}$$

for this quantity measures the relations between the fluctuations of any pair of spins in any case. An easy way to compute G_{jk} is to use the free energy, instead of the partition function

$$G_{jk} = \langle s_j s_k \rangle - \langle s_j \rangle \langle s_k \rangle = \frac{\partial^2 f}{\partial \frac{h_j}{2} \partial \frac{h_k}{2}}, \tag{5.12}$$

and the free energy is the *generator of the connected correlation functions*.

Comparing (5.7) and (5.12), we can relate again the fluctuations of the spins with the response to a magnetic field

$$\chi = \sum_{j,k} G_{jk}, \tag{5.13}$$

and the fluctuation-dissipation theorem adquires its full meaning.

We qualitatively expect (5.11) and (5.12) to vanish as the distance between site j and k grows: If sites j and k are far away from each other, it is reasonable to think that the spins at the neighbourhood of site j are not affected by the fluctuations of the very distant spins of site k. We should expect then

$$lim_{|j-k| \to \infty} G_{jk} = \langle s_j s_k \rangle - \langle s_j \rangle \langle s_k \rangle = 0, \tag{5.14}$$

so, in this limit,

$$\langle s_j s_k \rangle = \langle s_j \rangle \langle s_k \rangle, \tag{5.15}$$

and applying translation invariance,

$$\chi \approx N \sum_k G_{jk}, \tag{5.16}$$

for G_{jk} should depend only on $|j-k|$, and not on the particular site j we are sitting.

Equation (5.15) profiles what is called the *cluster property*, and enables us to define *pure* and *mixed states* in our system.

The cluster property for the Ising model

Let us assume that at a given temperature, the system is in a disordered phase[9]. If we draw an histogram of the magnetization density, we observe something quite similar to figure 5.1.

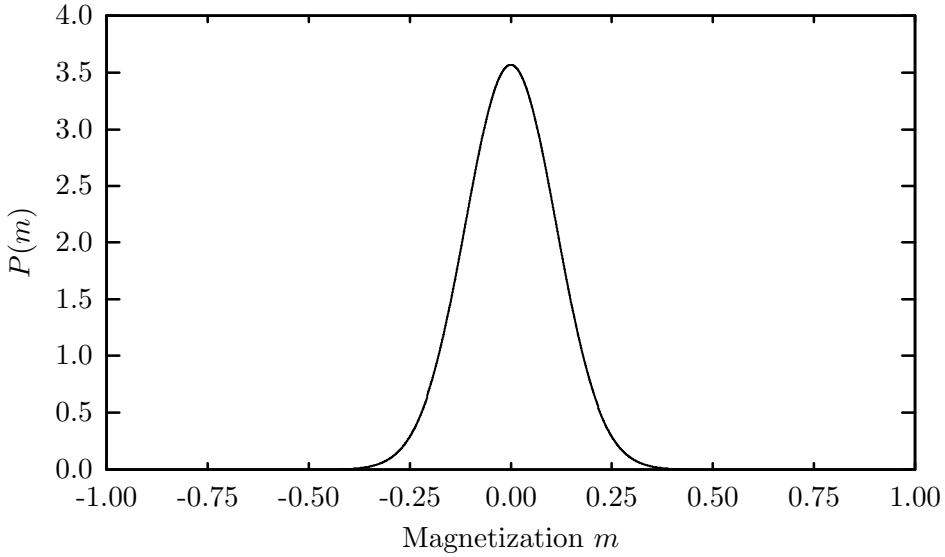

Figure 5.1: Magnetization density distribution function in the disordered phase of the finite volume Ising model.

As the number of spins increases, the width of the distribution narrows, until it becomes a Dirac delta. The position of the Dirac delta is uniquely determined by the intensity of the magnetic field. The important point to be noticed here is the fact that

$$\langle m^n \rangle = \langle m \rangle^n, \tag{5.17}$$

since the probability distribution function of the magnetization density is a Dirac delta

$$\int m^n \delta \left(m - m_0 \right) = m_0^n. \tag{5.18}$$

This is the *cluster property*, and as a consequence of it, wherever this property holds, *the intensive magnitudes of the system do not fluctuate in the thermodynamic limit.* The system is said to be in a *pure state.*

This is not in contradiction to a non-zero response of the system to a magnetic field. Recalling (5.7)

$$\frac{\partial \langle m \rangle}{\partial \frac{h}{2}} = N \left[\langle m^2 \rangle - \langle m \rangle^2 \right] = N \left(\Delta m \right)^2, \tag{5.19}$$

we observe that the vanishing of $\langle m^2 \rangle - \langle m \rangle^2$ is competing against the divergence $N \to \infty$. This clash of magnitudes results in a finite, non-zero value for the magnetic susceptibility.

This analysis is correct for the disordered phase. A breakdown of the Z_2 symmetry of the system (which may or may not happen at a given temperature) changes this picture drastically. The distribution function of the magnetization density now features two identical symmetric peaks (see fig. 5.2).

[9]By disordered phase I understand that no spontaneous Z_2 symmetry breaking has occurred, so $\langle s_i \rangle = 0$, the spins point up or down randomly, and the correlation functions die at long distances.

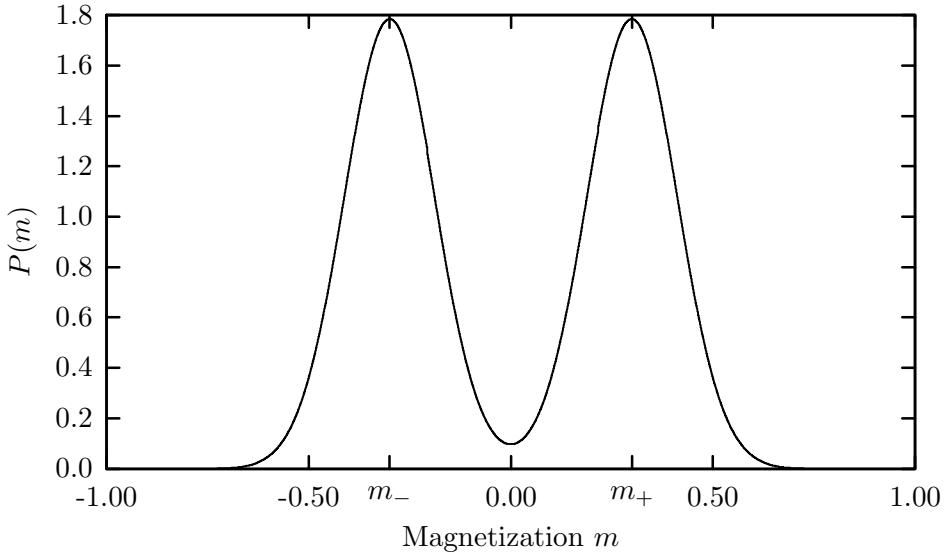

Figure 5.2: Magnetization density distribution function in the ordered (magnetized) phase of the finite volume Ising model.

The configuration space is divided, and this division becomes disconnected in the thermodynamic limit. Thus, if the system lies in the region of magnetization density m_+, it will remain there forever, never crossing to the region of configurations with magnetization density m_-. The connection only happens at a finite volume; then the transitions between these two distinct regions of the phase space are allowed. The effect of a magnetic field here is the selection of the favoured peak.

As we repeat the calculation of the equation (5.18), we discover that the cluster property is violated here

$$\int m^n \frac{1}{2} \left(\delta \left(m + m_-\right) + \delta \left(m - m_+\right)\right) = \frac{m_+^n + m_-^n}{2}, \tag{5.20}$$

for we have a set of vacua, as a consequence of the spontaneous Z_2 symmetry breaking. The fluctuation from one vacuum to another spoils the cluster property, and the susceptibility diverges. The system lies in a *mixed state*.

These kind of fluctuations only happen at the critical point. In the broken phase, as we reach the thermodynamic limit, the system is always in one of the two possible pure states[10] . On the other hand, for a finite volume, the transition can always take place, and the cluster property is not rigorously fulfilled; obviously, the cluster property only makes sense in the thermodynamic limit.

Analytic solution of the 1D Ising model

The one-dimensional case of the Ising model is exactly solvable, as Ernst Ising himself demonstrated in his PhD thesis in 1925. There are many ways to compute the free energy of the Ising model; the one we show here makes use of the transfer-matrix formalism, to illustrate how this technique can be applied to solve simple 1D models.

The clearest way to apply the transfer-matrix method to the one-dimensional Ising model requires a superficial modification of the Hamiltonian

[10]For a continuous symmetry, the Goldstone modes enable the system to change the vacuum in the thermodynamic limit as well. Then, both the susceptibility and the correlation length diverge in the broken phase.

$$H\left(\{s_i\}, J, B\right) = -J\sum_i^N s_i s_{i+1} - \frac{B}{2}\sum_i^N \left(s_i + s_{i+1}\right), \tag{5.21}$$

where I am taking two assumptions for granted: First, there exist some kind of spin ordering, so as to the spin s_i is a neighbour in the one-dimensional spin-chain of the spins s_{i-1} and s_{i+1}. Second, there are periodic boundary conditions, and the spin s_{N+1} is the same as the spin s_1. Then this Hamiltonian is completely equivalent to (5.1) with periodic boundary conditions.

Now we can decompose (5.21) in small site-dependent functions

$$H\left(\{s_i\}, J, B\right) = \sum_i^N I\left(s_i, s_{i+1}, J, B\right), \tag{5.22}$$

where

$$I\left(s_i, s_{i+1}, J, B\right) = -J s_i s_{i+1} - \frac{B}{2}\left(s_i + s_{i+1}\right). \tag{5.23}$$

After these modifications, the computation of the partition function can be easily done. We apply the definition

$$\begin{aligned} Z\left(F, h\right) &= \sum_{\{s_i\}} e^{-\beta H(J,B)} = \sum_{\{s_i\}} e^{-\sum_i^N \beta I(s_i, s_{i+1}, J, B)} \\ &= \sum_{\{s_i\}} \prod_i^N e^{-\beta I(s_i, s_{i+1}, J, B)} = \mathrm{tr}\left(T^N\right). \end{aligned} \tag{5.24}$$

where the matrix T is called the *transfer-matrix*. It is defined as a matrix of possible states, in this case restricted to a two spin configuration by construction

$$T = \begin{pmatrix} \uparrow\uparrow & \uparrow\downarrow \\ \downarrow\uparrow & \downarrow\downarrow \end{pmatrix}. \tag{5.25}$$

Multiplying T several times we construct higher spin chains

$$\begin{aligned} T^2 &= \begin{pmatrix} \uparrow\uparrow \times \uparrow\uparrow + \uparrow\downarrow \times \downarrow\uparrow & \uparrow\uparrow \times \uparrow\downarrow + \uparrow\downarrow \times \downarrow\downarrow \\ \downarrow\uparrow \times \uparrow\uparrow + \downarrow\downarrow \times \downarrow\uparrow & \downarrow\downarrow \times \downarrow\downarrow + \downarrow\uparrow \times \uparrow\downarrow \end{pmatrix} \\ &= \begin{pmatrix} \uparrow\uparrow\uparrow + \uparrow\downarrow\uparrow & \uparrow\uparrow\downarrow + \uparrow\downarrow\downarrow \\ \downarrow\uparrow\uparrow + \downarrow\downarrow\uparrow & \downarrow\downarrow\downarrow + \downarrow\uparrow\downarrow \end{pmatrix}. \end{aligned} \tag{5.26}$$

The taking of the trace is the result of the boundary condition $s_1 = s_{N+1}$. It is easy to see that this construction leads to the sum of all the configurations for a given N. The eigenvalues of the transfer-matrix give us the solution for the partition function Z. In fact

$$Z\left(F, h\right) = \mathrm{Tr}\left(T^N\right) = \sum_i \lambda_i^N. \tag{5.27}$$

but we are more interested in the result for the free energy

$$\begin{aligned} f\left(F, h\right) &= \lim_{N\to\infty} \frac{1}{N} \ln\left(Z\left(F, h\right)\right) = \lim_{N\to\infty} \frac{1}{N} \ln\left[\sum_i \lambda_i^N\right] \\ &= \lim_{N\to\infty} \frac{1}{N} \ln\left[\lambda_{Max}^N \sum_i \left(\frac{\lambda_i}{\lambda_{Max}}\right)^N\right] = \ln \lambda_{Max}, \end{aligned} \tag{5.28}$$

as the quantity $\left(\frac{\lambda_i}{\lambda_{Max}}\right)^N$ vanishes in the thermodynamic limit, except for the value $i = \text{Max}$[11]. Thence, the highest eigenvalue gives us the free energy of the system. Let us diagonalize T

$$\begin{aligned} |T - \lambda I| &= \begin{vmatrix} e^{F+\frac{h}{2}} - \lambda & e^{-F} \\ e^{-F} & e^{F-\frac{h}{2}} - \lambda \end{vmatrix} \\ &= \lambda^2 - 2\lambda e^F \cosh\frac{h}{2} - e^{2F}\left(e^{-4F} - 1\right) \\ \lambda &= \begin{cases} e^F\left(\cosh\frac{h}{2} + \sqrt{e^{-4F} + \sinh^2\frac{h}{2}}\right) \\ e^F\left(\cosh\frac{h}{2} - \sqrt{e^{-4F} + \sinh^2\frac{h}{2}}\right) \end{cases} \end{aligned} \tag{5.29}$$

Only the highest eigenvalue contributes to the free energy in the thermodynamic limit. Therefore, the final result is

$$f(F,h) = F + \ln\left(\cosh\frac{h}{2} + \sqrt{e^{-4F} + \sinh^2\frac{h}{2}}\right). \tag{5.30}$$

By using the free energy, any observable can be easily worked out. For instance, according to equation (5.6), the result for the magnetization is

$$\langle m\rangle = \frac{\partial f}{\partial \frac{h}{2}} = \frac{\sinh\frac{h}{2} + \frac{\sinh\frac{h}{2}\cosh\frac{h}{2}}{\sqrt{e^{-4F}+\sinh^2\frac{h}{2}}}}{\cosh\frac{h}{2} + \sqrt{e^{-4F} + \sinh^2\frac{h}{2}}} = \frac{\sinh\frac{h}{2}}{\sqrt{e^{-4F} + \sinh^2\frac{h}{2}}}. \tag{5.31}$$

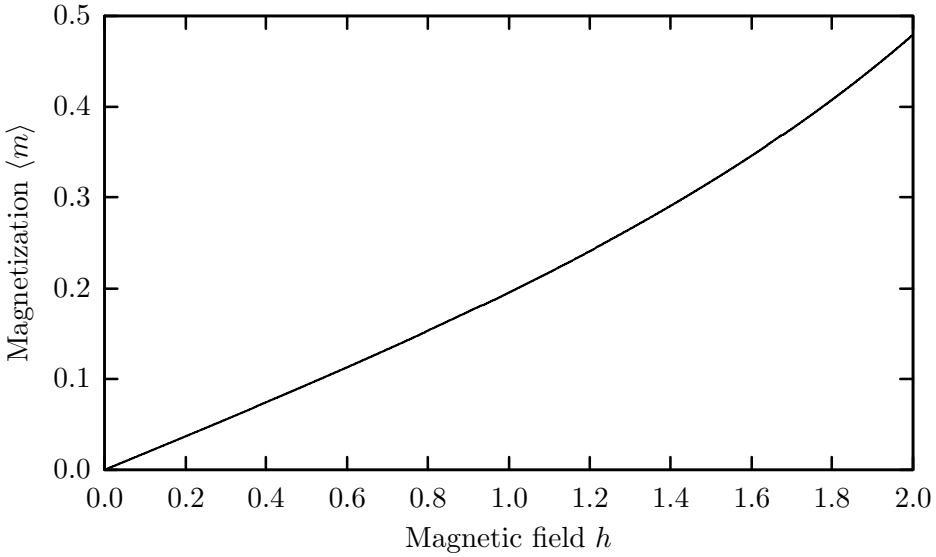

Figure 5.3: Magnetization density as a function of the external field h for the one-dimensional Ising model. F was set to $F = -0.50$; as $F < 0$, we are dealing with an antiferromagnetic coupling.

At vanishing magnetic field and non-zero temperature, $\langle m\rangle$ is always zero, so no spontaneous symmetry breaking happens for the one-dimensional model, as Ising proved in 1925[12].

[11] The eigenvalues are bounded for finite F (or, equivalently, non-zero temperature), so $\frac{\lambda_i}{\lambda_{Max}} \leq 1$. Unbound eigenvalues do not give rise to a well defined free-energy.

[12] Only at zero temperature ($F \to \infty$, a trivial fixed point) the transition happens.

Equation (5.31) for the magnetization is completely general, which means that we can apply it to the case of a pure imaginary magnetic field $h = i\theta$. For $\theta = \pi$, the Z_2 symmetry is restored (the magnetic field effect amounts to a sign σ, depending on the 'topological charge' $M/2$ of the configuration $\sigma = e^{i\pi M/2}$; this sign is invariant under a Z_2 transformation). Then, the question is whether there exist spontaneous symmetry breaking or not. The answer was given in (5.31): Substituting $h \to i\theta$

$$\langle m \rangle = \frac{i \sin \frac{\theta}{2}}{\sqrt{e^{-4F} - \sin^2 \frac{\theta}{2}}}. \tag{5.32}$$

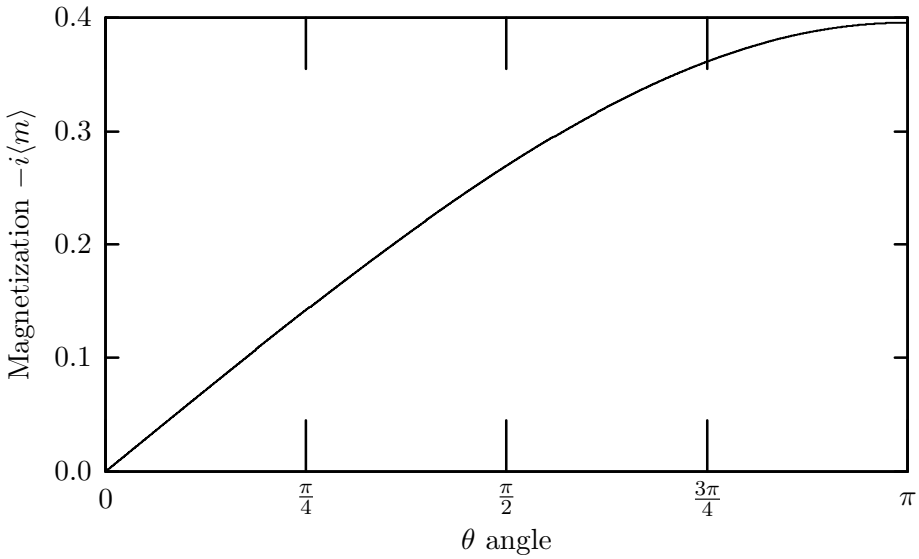

Figure 5.4: Magnetization density as a function of the θ angle for the one-dimensional Ising model. F was set to $F = -0.50$.

And the magnetization takes a non-zero expectation value for the one-dimensional Ising model at $\theta = \pi$, a fact that indicates spontaneous Parity breaking. It is quite remarkable that the Ising model within an imaginary external field is not properly defined with ferromangetic couplings [81]. Setting $F > 0$ we find that the denominator of 5.32 explodes if

$$e^{-4F} = \sin^2 \frac{\theta}{2},$$

holds, and the free energy

$$f(F, \theta) = F + \ln \left(\cos \frac{\theta}{2} + \sqrt{e^{-4F} - \sin^2 \frac{\theta}{2}} \right). \tag{5.33}$$

becomes undefined for certain values of θ, for the argument of the logarithm may vanish if $F > 0$. Hence, we will deal with the antiferromagnetic Ising model ($F < 0$) from now on, unless it is explicitly stated.

5.3 Systems with a topological θ term

Ways to simulate complex actions

Why analytic continuations fail in this case

For dimensions higher than one, the model within an external magnetic field is not exactly solvable[13]. Simulations can still be performed for real values of the reduced magnetic field, but the sign problem prevents us to do the same in the case of an imaginary external field. One well-known attempt to overcome this obstacle is the use of analytic continuations.

In the absence of phase transitions, the order parameter $m(h)$ should be a smooth function of the external field h without singularities. If $m(h)$ is measured for enough real values of h at a very high precision, a careful extrapolation to imaginary fields should be possible[14], provided an ansatz function for the behaviour of the order parameter. The kind of extrapolation has been a research topic during the last years, mostly in the framework of finite density QCD (see [82, 83, 84, 85, 86], also [87] and references therein).

A great caveat of this method is evident: It does not allow us to explore neither the critical points nor the region lying behind a phase transition. We are doomed to stay in the same phase, for the analitical prolongation does not account for the singularities and discontinuities linked to a phase transition. For the particular case of θ-vacuum, this fact should not be a major problem, as only transitions at the edge ($\theta = \pi$) are expected to happen[15].

Unfortunately, there is another serious problem: as a priori the behaviour of the models in the $\theta \neq 0$ is unknown, there is not a way to provide a sensible ansatz for the fitting function of the order parameter. In fact, it can be proved that two functions differing slightly in the real plane can diverge exponentially in the complex plane, and the results are bound to depend strongly on the ansatz functions. Therefore, the analytical continuations are not reliable for this particular problem –unless we only want to know the behaviour of the order parameter in the neighbourhood of $\theta = 0$–, and we need other sensible methods to compute the θ dependence of the theories.

The $p.d.f.$ computation at $\theta = 0$

On the other hand, the problem of θ-vacuum is set up in a way that suggests quite strongly a particular kind of dependence in θ. The partition function of any system in the presence of a θ term is periodic, and can be decomposed in sectors of different topological charge n as

$$Z_V(\theta) = Z_V(0) \sum_n p_V(n) e^{i\theta n}, \tag{5.34}$$

which resembles the Fourier transform of the probability distribution function ($p.d.f.$) of the topological charge at $\theta = 0$. The probability of the topological sector n is therefore given by $p_V(n)$, and this quantity can be measured from simulations at imaginary values of θ (i.e. real values of the external field $h = -i\theta$). Unfortunately, this is a very difficult task, for

i. Precision in a numerical simulation can not be infinite, is limited by statistical fluctuations. Thus the measurement of $p_V(n)$ suffers from errors.

ii. Small errors in $p_V(n)$ induce huge errors in the determination of $Z_V(\theta)$, for this quantity is exponentially small $Z_V \approx e^{-V}$ due to the sign problem.

[13] Onsager's solution is only valid for $h = 0$.

[14] Complex analysis proves that the analytic continuation *must exist and be unique*.

[15] Nonetheless, we will see in the Ising model a notable exception to this rule.

iii. Even if we were able to evaluate $p_V(n)$ with infinite accuracy, the terms on the sum (5.34) differs by many orders of magnitude (from 1 to e^{-V}).

In fact, the different groups that have tried to determine with high precision the *p.d.f.* of the topological charge by standard simulations, or by more sophisticated methods (re-weighting or multibinning techniques), have found artificial phase transitions[16] in the $U(1)$ model and in the CP^N models. The one to blame of these ghost transitions is the flattening of the free energy for θ-values larger than certain threshold. In [88, 89], this threshold is roughly evaluated, and the flattening behaviour demystified:

At zero external field and finite volume, usually the vanishing topological sector dominates. This implies that during the measurements

$$|\delta p_V(0)| \geq |\delta p_V(1)| \geq |\delta p_V(2)|. \tag{5.35}$$

Of course, this is not a theorem; in fact, the error in the determination of higher sectors might compete with that of sector zero. This statement only reflects what usually happens during simulations.

Thence, the most prominent error in the computation of the free energy is $\delta p_V(0)$, and the θ_b threshold is given by

$$f(\theta_b) \approx \frac{1}{V} |\ln |\delta p_V(0)||. \tag{5.36}$$

Consequently, if $\delta p_V(0) > 0$, then the free energy is given by a constant value

$$f(\theta) \approx \frac{1}{V} \ln \delta p_V(0) \qquad \theta > \theta_b. \tag{5.37}$$

A wavy behaviour can appear if the errors in other modes ($n = 1, 2 \ldots$) are competing with the zero mode $\delta p_V(0)$. If, on the other hand, $\delta p_V(0) < 0$, the free energy becomes impossible to be measured for $\theta > \theta_b$.

This way, the precision in the measurements limits how far can we go with θ. These are no news to us, but it is remarkable the severity of the problem: A reliable computation of the order parameter (or the free energy) to all values of θ is not feasible by direct measurement of the *p.d.f.*, due to the huge statistics required.

That is why other approaches (or at least, serious refinements of the *p.d.f.* approach) should be considered. The method I describe in the following lines succeeded to reproduce the θ dependence of the order parameter for those systems where $m(\theta)$ was a non-decreasing function in the $0 \leq \theta \leq \pi$ range.

An improvement over the standard *p.d.f.* methods

Let's write the partition function of any system with a topological charge term as a sum (integral in the infinite volume limit) over the density of topological charge $x_n = n/V$,

$$Z_V(\theta) = Z_V(0) \sum_n e^{-V f_V(x_n)} e^{i\theta V x_n}, \tag{5.38}$$

where we have set $p_V(n) = e^{-V f_V(x_n)}$. Assuming that CP-symmetry is preserved at vanishing[17] θ, we expect $e^{-V f_V(x_n)}$ to approach a delta distribution centered at the origin in the thermodynamic limit.

[16] Induced by the simulation method, or by the way the order parameter is computed, therefore this is not a real phase transition. Lack of precision, bad *p.d.f.* determinations due to poor sampling or rounding errors are some of the problems leading to these *ghost* transitions.

[17] Otherwise, the theory would be ill-defined at $\theta \neq 0$.

In the thermodynamic limit, $f_V(x_n)$ becomes $f(x)$. As all the coefficients entering in equation (5.38) are positive, the free energy for imaginary θ (that is, real field $h = -i\theta$) is given in the thermodynamic limit by the saddle point. We assume in the following that the first derivative of $f(x)$ is well-defined, except at most in isolated points. Then, we can write

$$f'(x) = h, \tag{5.39}$$

so the external field is given as a function of the topological charge density. The procedure to reconstruct $f(x)$ from (5.39) is the following

i. The mean value of the topological charge as a function of an external real field is measured with high accuracy (within a fraction of percent). The saddle point equation (5.39) is applied afterwards to obtain $f'(x)$.

ii. The function $f'(x)$ is fitted to the ratio of two polynomials. Then, the integral to compute $f(x)$ is performed analytically. This step is essentially different to what other groups proposed, and it solves the problems of the θ threshold in some systems.

iii. Finally, a multi-precision algorithm is used to calculate the partition function directly from (5.38), using the function $f(x)$ computed in point (ii).

Although $f(x)$ suffers from two different sources of errors, statistical and systematic coming from finite volume corrections to the saddle point equation (5.39), only statistical errors were important[18] in the determination of $f(x)$ in the whole range of θ's. To see why, we must analyze carefully the behaviour of $f_V(x_n)$ under correlated and uncorrelated errors.

If we call $f_V(x_n)$ the exact value of this function at a given volume V, and $\Delta f_V(x_n)$ the error, then the partition function computed with errors $Z'_V(\theta)$ is related to the exact partition function $Z_V(\theta)$ by

$$Z'_V(\theta) = Z_V(\theta) \left\langle e^{-V\Delta f_V(x_n)} \right\rangle. \tag{5.40}$$

Suppose that the error function $\Delta f_V(x_n)$ is an extremely uncorrelated function, vanishing everywhere except in a given value x_m. In this case, the error in the computation in the partition function is given by

$$\left\langle e^{-V\Delta f_V(x_n)} \right\rangle = 1 + 2e^{-V\left(f_V\left(\frac{m}{V}\right) - g_V(\theta)\right)} \left(e^{-V\Delta f_V\left(\frac{m}{V}\right)} - 1\right) \cos(m\theta), \tag{5.41}$$

where $g_V(\theta)$ is assumed to be the exact free energy density. As $g_V(\theta)$ increases with θ, the first exponential on the r.h.s. of (5.41) is doomed to be small near the origin, spanning corrections of order $\frac{1}{V}$. Unfortunately this pictures changes as θ increases, and the partition function might become negative.

On the other hand, if the errors are largely correlated, assuming for instance that $\Delta f_V(x_m)$ is almost constant, the errors propagated to $g_V(\theta)$ are almost constant as well, by virtue of (5.41); these errors amount to an irrelevant constant in the free energy. This picture is encouraging, for the fitting of (5.39) to a ratio of polynomials to perform the integration analitically is expected to produce largely correlated errors. Indeed, these ideas were successfully tested [90] in the one-dimensional Ising model and the two-dimensional $U(1)$ model, and it was used to predict the behaviour of the CP^3 model. The results were impressive by that time, solving completely the problem of the flattening of the order parameter beyond the critical value of θ. The key of this success was the aforementioned correlation among the errors: Test performed using the

[18] This statement was valid for the models studied in [90].

same method an adding an apparently negligible 0.1% random error to the measured free energy $f(x)$ led to disaster. Nonetheless, if the error was correlated, it could be as large as the 50% of the original value, and the final result would be quite reasonable.

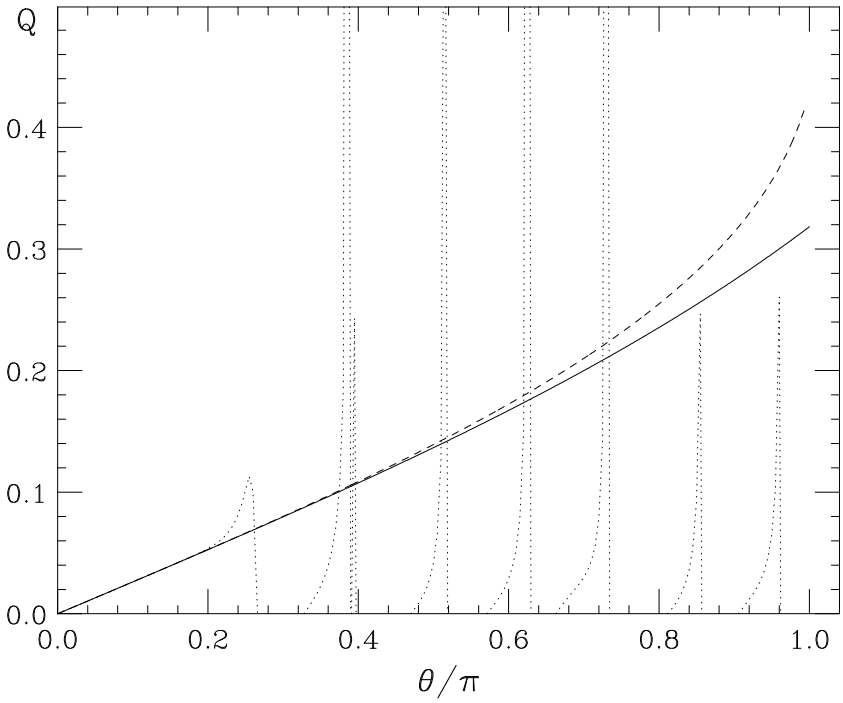

Figure 5.5: Effects of correlated and random errors on the θ dependence of the topological charge Q in the two-dimensional $U(1)$ model at $\beta = 0$. The continuous curve is the exact result, the dashed curve is the result obtained by substituting $f(x)$ by $f(x)(1 + \frac{1}{2}\sin(x^2))$, and the dotted curve is the result obtained by adding a random error of the order of 0.1% to $f(x)$.

However, this is not the final method to find out the θ dependence of the different models. The flattening behaviour can appear -and in fact, it does- whenever the behaviour of the order parameter is not monotonous. This is not a prediction, but seems to be a general rule. The flattening was first observed in a simple toy model which featured symmetry restoration at $\theta = \pi$

$$f(\theta) = \ln(1 + A\cos\theta). \tag{5.42}$$

For this model, the order parameter vanishes only at $\theta = 0, \pi$

$$-im(\theta) = \frac{A\sin\theta}{1 + A\cos\theta}, \tag{5.43}$$

but the method predicted an almost flat behaviour beyond the point $\theta = \frac{\pi}{2}$.

The problem might be solved by using a more suitable fitting funtion. In fact, we were able to reproduce qualitatively the behaviour of the order parameter in the two-dimensional Ising model, which –anticipating the result obtained in the following pages– features a vanishing order parameter at $\theta = \pi$.

The problem is the fact that the proper fitting function is not always integrable analitically. An odd polynomial always reproduces correctly the behaviour of the function $m(h)$, but we are seeking the solution to the saddle point equation (5.39), $h(m)$, which is the inverse. The exact solution to this inversion can be expressed in a closed form for polynomials of order 3 or less,

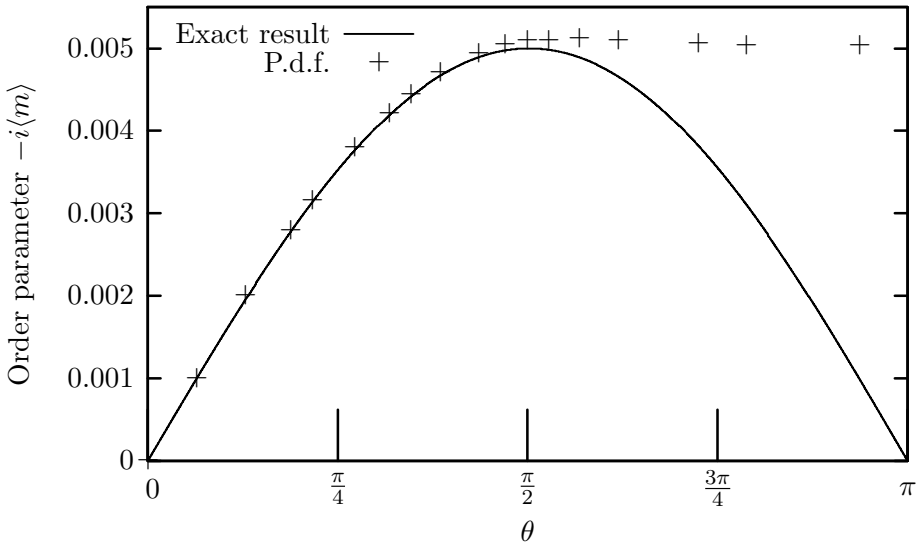

Figure 5.6: Attempt to solve the toy model defined in (5.42) using the improved $p.d.f.$ method. The feared flattening appears at $\theta \sim \frac{\pi}{2}$.

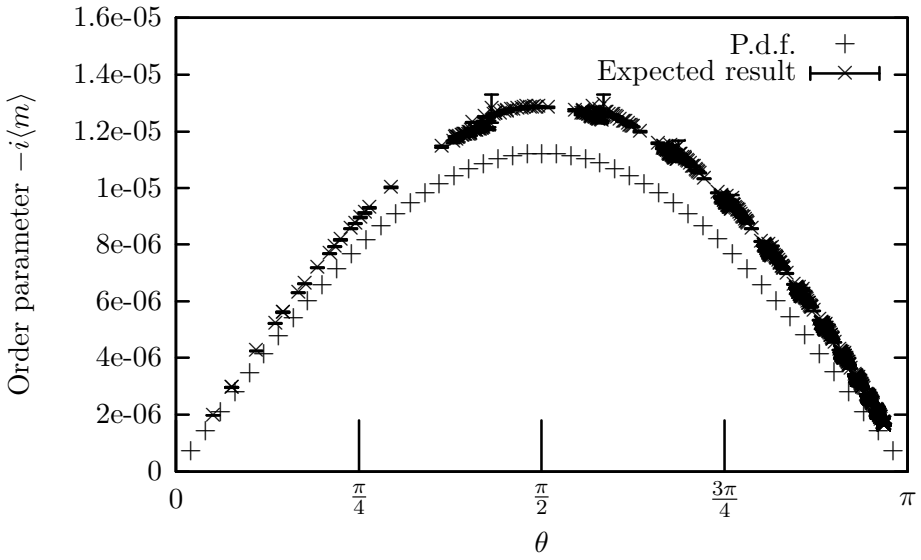

Figure 5.7: Ising's vanishing of the order parameter using the improved $p.d.f.$ method (crosses). The numerical results differ notoriously to those obtained in the next sections (circles), nonetheless the qualitatively correct behaviour of the order parameter suggest that further refinements might work properly. Errors were not estimated for the $p.d.f.$ method.

but the resulting function is not analitically integrable. A numerical approach to the problem introduces uncorrelated errors which spoil all the good properties of this approach. In the last example of fig. 5.7, an approximation to the most suitable fitting function was used, but clearly it was not enough to predict the values of $m\,(h)$ with high precision. In fact, fig. 5.7 represents a very well behaved case, usually the order parameter might differ from the expected case by an order of magnitude, or even give a wrong behaviour. As explained before, the result depends critically on the chosen fitting function.

This is not the only problem this method has. Another dark point in the method is the use of the saddle point relation, which has corrections at finite volume of order $O\left(\frac{1}{V}\right)$. These are uncontrolled sources of systematic errors. Even if these errors did not seems to affect too much

the final results in the models tested successfully, an upper bound for the errors could not be estimated in any way.

On the whole, although the method proposed in [90] represented a large improvement over what existed at that point, it was clear that another approach, one which was capable of estimating the magnitude of the errors, was necessary. The final conclusion was, further research should be made, and that is how the method described in the following sections was created.

Ising's miracle

As I explained before, the Ising model is a good toy-model for testing algorithms in development to simulate θ-vacuum systems in the computer. What was completely unexpected was the fact that the most successful method to deal with a θ term would come from a special property of the Ising model. This property was so useful and inspiring that it was called *the Ising's miracle*.

To find what is so miraculous about the Ising model, we have to pay atention to equations (5.31) and (5.32). If, instead of $\langle m \rangle$, the quotient $\frac{\langle m \rangle}{\tanh \frac{h}{2}}$ is computed, the outcoming function

$$y\left(z\right) = \frac{\langle m \rangle}{\tanh \frac{h}{2}} = \frac{\left(e^{-4F} - 1\right)^{-\frac{1}{2}} \cosh \frac{h}{2}}{\sqrt{\left(e^{-4F} - 1\right)^{-1} \cosh^2 \frac{h}{2} + 1}} = \frac{e^{-\frac{\lambda}{2}} z}{\sqrt{e^{-\lambda} z^2 + 1}}. \tag{5.44}$$

depends only on F and on the variable $z = \cosh \frac{h}{2}$ through a special combination of both $e^{-\frac{\lambda}{2}} z$, with $\lambda = -\ln\left(e^{-4F} - 1\right)$. Due to this somewhat simplified dependency on F and h, the transformation

$$y_\lambda\left(z\right) = y\left(e^{\frac{\lambda}{2}} z\right) \tag{5.45}$$

is equivalent to a change in the reduced coupling F, or in the temperature of the model. The interesting point here is the fact that this transformation can take the variable $z = \cosh \frac{h}{2}$ to the range $0 < z < 1$ for a negative value of λ, where z becomes a simple cosine $z = \cos \frac{\theta}{2}$, implying that we can measure $y\left(z\right)$ for imaginary values of the magnetic field by mean of numerical simulations at real values of h, which are free from the sign problem.

In other words, for the special case of the one-dimensional model, there exist an infinite number of triplets (m, h, F) such that verify

$$\frac{\langle m \rangle \left(F, h\right)}{\tanh \frac{h}{2}} = \frac{\langle m' \rangle \left(F', h'\right)}{\tanh \frac{h'}{2}}, \tag{5.46}$$

and we can extend this relationship to imaginary values of the magnetic field. The problem of performing a simulation with a complex action is thus reduced to the simulation of a real action.

In order to check if this property still holds for other systems (for instance, the Ising model in higher dimensions), simulations at different values of the external field have to be performed. Assuming $y\left(z, F\right) = y\left(g\left(F\right) z\right)$, then

$$\frac{\partial y}{\partial F} = \frac{\partial y}{\partial \left(g\left(F\right) z\right)} g'\left(F\right) z, \tag{5.47}$$

$$\frac{\partial y}{\partial z} = \frac{\partial y}{\partial \left(g\left(F\right) z\right)} g\left(F\right), \tag{5.48}$$

$$\frac{\frac{\partial y}{\partial F}}{\frac{\partial y}{\partial z}} = \frac{\frac{\partial y}{\partial (g(F) z)} g'\left(F\right) z}{\frac{\partial y}{\partial (g(F) z)} g\left(F\right)} = \frac{g'\left(F\right) z}{g\left(F\right)}. \tag{5.49}$$

For the miracle to be preserved in the model, the ratio $\frac{\partial y}{\partial F}/z\frac{\partial y}{\partial z}$ should be independent of h. Let's see how we can work this quantity out in a computer simulation. First we need to calculate $\frac{\partial y}{\partial F}$ and $\frac{\partial y}{\partial z}$ in terms of quantities we know:

$$\frac{\partial y}{\partial F} = \frac{\partial \frac{m}{\tanh\frac{h}{2}}}{\partial F} = \frac{1}{\tanh\frac{h}{2}}\frac{\partial m}{\partial F} =$$

$$\frac{1}{\tanh\frac{h}{2}}\left[\left\langle\left(\sum_i^N s_i s_{i+1}\right)\left(\sum_i^N s_i\right)\right\rangle - \left\langle\sum_i^N s_i s_{i+1}\right\rangle\left\langle\sum_i^N s_i\right\rangle\right], \tag{5.50}$$

$$z\frac{\partial y}{\partial z} = z\frac{\partial \frac{\langle m\rangle}{\tanh\frac{h}{2}}}{\partial \frac{h}{2}}\frac{\partial \frac{h}{2}}{\partial z} = \chi - \frac{\langle m\rangle}{\tanh\frac{h}{2}\,\sinh^2\frac{h}{2}}, \tag{5.51}$$

For the one-dimensional Ising model, the simulations reveal the constant ratio over a large range of fields h (see fig. 5.8).

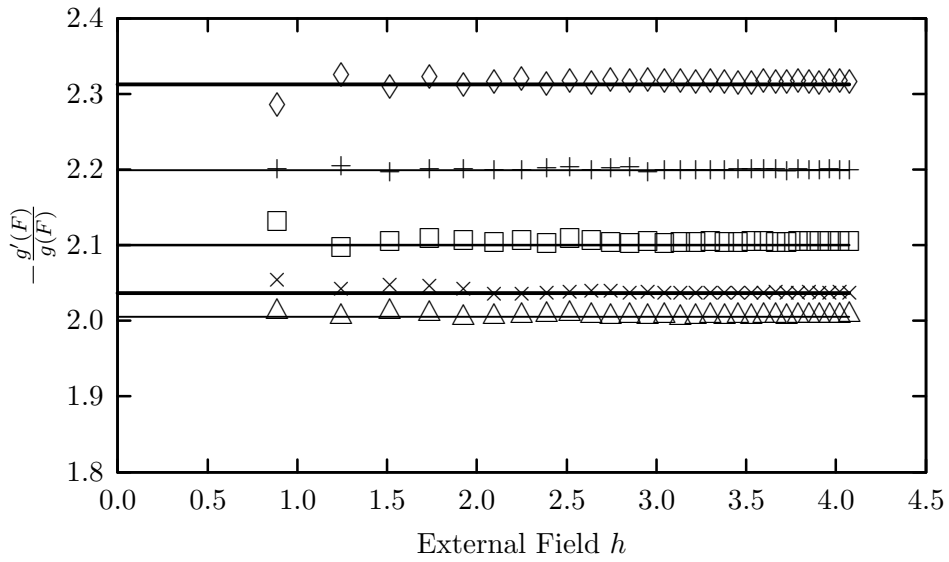

Figure 5.8: Ising's miracle check along formula (5.51). The continuous lines represent the analytical result, while the crosses stand for the numerical data. We performed short simulations (only ~ 100000 iterations) for several values of F in a $L = 100$ lattice. Errors are smaller than symbols.

Unfortunately, this property is exclusive of the one-dimensional case. For two dimensions, the order parameter $\langle m\rangle$ can not be written as a function of $g(F)\,z$ and the ratio shows a slightly dependence on the reduced magnetic field. For three dimensions, the dependence becomes a bit more pronounced. The peak in 5.9 is produced by the antiferromagnetic-ferromagnetic phase transition[19].

Computing the order parameter under an imaginary magnetic field

Although Ising's miracle is absent in higher dimensions, we can still take advantage from the methodology it profiles. For the one-dimensional case, a measurement of the order parameter

[19]The antiferromagnetic Ising model displays, for strong enough couplings, a phase transition at non-zero external magnetic field: the spin-coupling tries to put the system in an antiferromagnetic state, whereas the external field tries to order the spins in a ferromagnetic fashion. As the value of the external field increases, the ferromagnetic behaviour takes over.

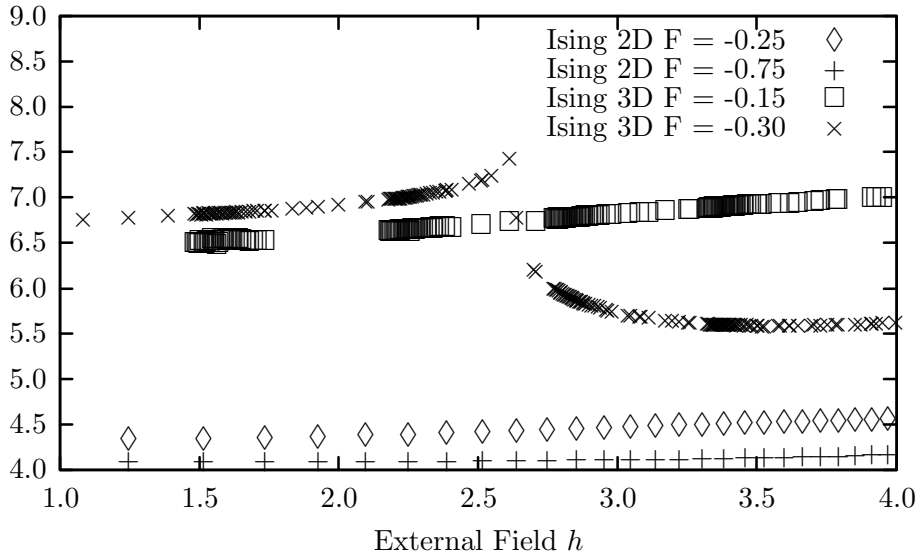

Figure 5.9: Ising's miracle realization in 2D and 3D. The miracle is approximate in 2D and 3D for low values of the field. The statistics of the simulations are 100000 iterations, and the lattice lengths are, for 2D $L = 50$ and for 3D $L = 25$. Errors are smaller than symbols.

produced at the point (F, z) is equivalent to a measurement done at (F', z') if the following relationship holds

$$g(F)\, z = g\left(F'\right) z',$$
$$g(F) = \left(e^{-4F} - 1\right)^{\frac{1}{2}}. \tag{5.52}$$

This way, and choosing carefully the value of F, a simulation performed at a real value of the reduced magnetic field $z \geq 1$ is equivalent to another simulation performed at imaginary values of h (where $z < 1$).

The procedure to find out the order parameter at imaginary values of the reduced magnetic field in non-miraculous systems relies on scaling transformations. We define the function $y_\lambda(z)$ as

$$y_\lambda(z) = y\left(e^{\frac{\lambda}{2}} z\right). \tag{5.53}$$

For negative values of λ, the function $y_\lambda(z)$ allows us to calculate the order parameter $\left(\tanh \frac{h}{2}\, y(z)\right)$ below the threshold $z = 1$.

If $y(z)$ is non-vanishing for any $z > 0$[20], then we can plot y_λ / y against y up to very small values of y. Furthermore, in the case that y_λ / y is a smooth function of y close to the origin, then we can rely in a simple extrapolation to $y = 0$. Of course, a smooth behaviour of y_λ / y can not be taken for granted; however no violations of this rule have been found in the exactly solvable models.

The behaviour of the model at $\theta = \pi$ can be ascertained from this extrapolation. The critical exponent

$$\gamma_\lambda = \frac{2}{\lambda} \ln\left(\frac{y_\lambda}{y}\right) \tag{5.54}$$

[20]Even though the possibility of a vanishing $y(z)$ for some value $z > 0$ can not be excluded completely, it does not happen for any of the analitically solvable models we know.

in the limit $y(z) \to 0 \quad (z \to 0)$ gives us the dominant power of $y(z)$ for values of z close to zero. As $z \to 0$, the order parameter $\tan\frac{\theta}{2}\, y\left(\cos\frac{\theta}{2}\right)$ behaves as $(\pi-\theta)^{\gamma_\lambda - 1}$. Then, a value of $\gamma_\lambda = 1$ implies spontaneous symmetry breaking at $\theta = \pi$, for at this point the broken symmetry by the external field is restored. A value between $1 < \gamma_\lambda < 2$ signals a second order phase transition, and the corresponding susceptibility diverges. Finally, if $\gamma_\lambda = 2$, the symmetry is realized (at least for the selected order parameter), there is no phase transition and the free energy is analytic at $\theta = \pi$[21].

We can take the information contained in the quotient $\frac{y_\lambda}{y}(y)$ to the limit, and calculate the order parameter for any value of the imaginary reduced magnetic field $h = -i\theta$ through an iterative procedure.

The outline of the procedure is the following:

i. Beginning from a point $y(z_i) = y_i$, we find the value y_{i+1} such that $y_\lambda = y_i$. By definition, $y_{i+1} = y\left(e^{\frac{-\lambda}{2}} z_i\right)$.

ii. Replace y_i by y_{i+1}, to obtain $y_{i+2} = y\left(e^{-\lambda} z_i\right)$.

The procedure is repeated until enough values of y are know for $z < 1$. This method can be used for any model, as long as our assumptions of smoothness and absence of singular behaviour are verified during the numerical computations.

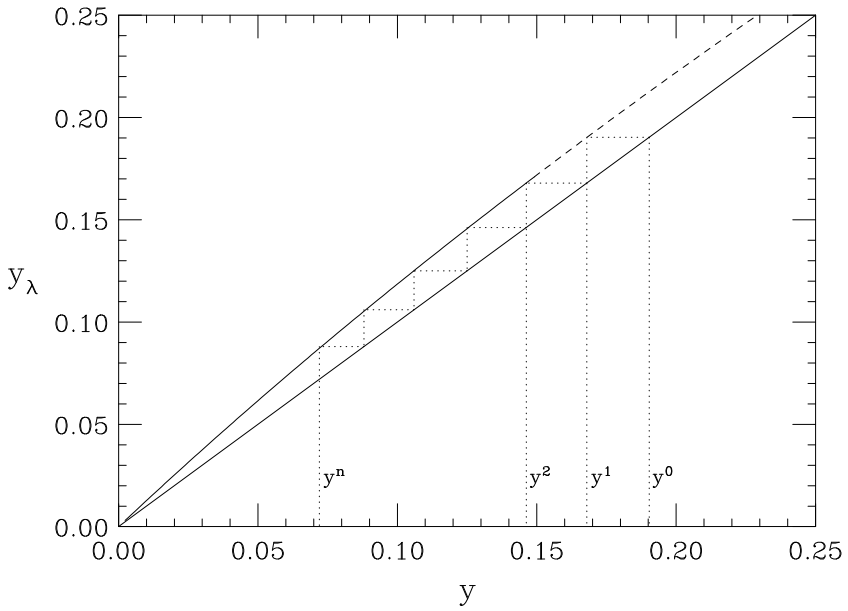

Figure 5.10: Iterative method used to compute the different values of $y(z)$. y_λ is ploted as a function of y using a dashed line in the region where direct measurements are available, and a continuous line in the extrapolated region. The straight continuous line represents $y_\lambda = y$.

[21] Other possibilities are allowed, for instance, any $\gamma_\lambda > 1, \quad \gamma_\lambda \in \mathbb{N}$ leads to symmetry realization for the order parameter at $\theta = \pi$ and to an analytic free energy. If γ_λ lies between two natural numbers, $p < \gamma_\lambda < q, \quad p, q \in \mathbb{N}$, then a transition of order q takes place.

Numerical work

The first thing to do is to check the correct implementation of the method, for its goodness has been already tested in a variety of models [91, 92, 93], and its validity, whenever the assumptions required are fullfiled, is beyond any question. The best way to verify the implementation is to apply the method to a solvable toy model, and compare the results with analytical formulae. In our case, we tested the method in the one-dimensional Ising model, and checked the results against (5.32).

The simulations were performed at a fixed volume, $N = 1000$ spins, and fixed reduced coupling $F = -2.0$. As in the one-dimensional Ising model there are no phase transitions, and the Ising's miracle is realized, there is no point in checking the method for several values of the reduced coupling. The parameter we varied was the reduced magnetic field h. As the simulations were done quite fast, we could obtain data for many values of h with large statistics. In fact, for each point in the plots we performed 10^7 metropolis iterations. In order to reduce autocorrelations, we performed at each iteration two sweeps over the lattice, proposing metropolis changes in the spins. The plots for the critical exponent and the order parameter are shown in fig. 5.11 and 5.12.

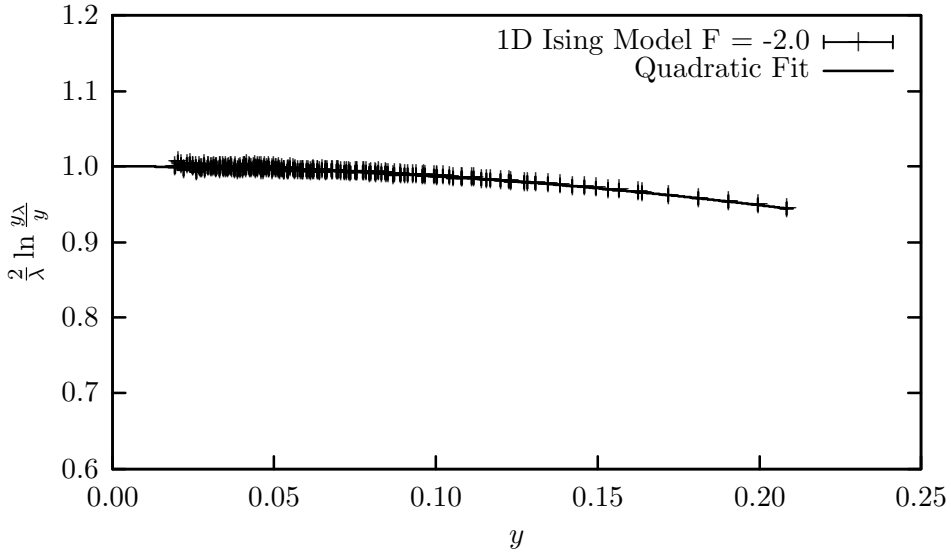

Figure 5.11: Calculation of the critical exponent γ_λ. The crosses correspond to the numerical simulation data, whereas the line is a quadratic fit. The extrapolation to zero seems quite reliable, as the function is smooth enough. Errors are smaller than symbols.

Our result for the critical exponent from the fit in fig. 5.11 is

$$\gamma_\lambda = 0.99980 \pm 0.00008,$$

which agrees with the analytical result. The fact that we obtained the right results in the one-dimensional model is not a big deal, as this model is miraculous, then it is expected to behave well under the scale transformations defined in this method.

Then we simulated higher dimensional models, expecting to see departures from this behaviour, as these models feature phase transitions between ordered (antiferromagnetic) and disordered phases. The two-dimensional simulations were done in a 100^2 lattice, after 100000 termalization sweeps. We spent 5000000 steps to measure each point accurately. The three-dimensional case, on the other hand, used a 50^3 volume, and measured each point for 2500000 steps after 100000 steps of thermalization. The outcoming results showed the expected depar-

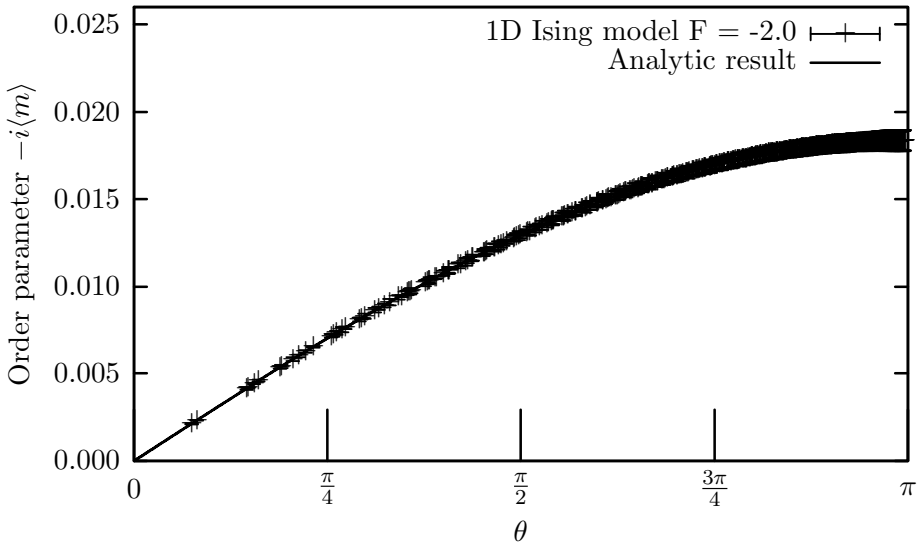

Figure 5.12: Order parameter as a function of θ. The non-zero value of the order parameter marks the spontaneous breaking of the Z_2 symmetry at $\theta = \pi$.

ture in the behaviour. Our prediction for the critical exponent $\gamma_\lambda \approx 2$ reveals a vanishing order parameter at $\theta = \pi$ in the ordered phase ($F = -1.50$ for $2D$ and $F = -1.00$ for $3D$)[22].

$$\gamma_\lambda^{2D} = 1.9997 \pm 0.0002$$

$$\gamma_\lambda^{3D} = 1.9998 \pm 0.0002$$

We can confirm this facts by plotting the order parameter against θ, as it is done in fig. 5.16 and 5.17.

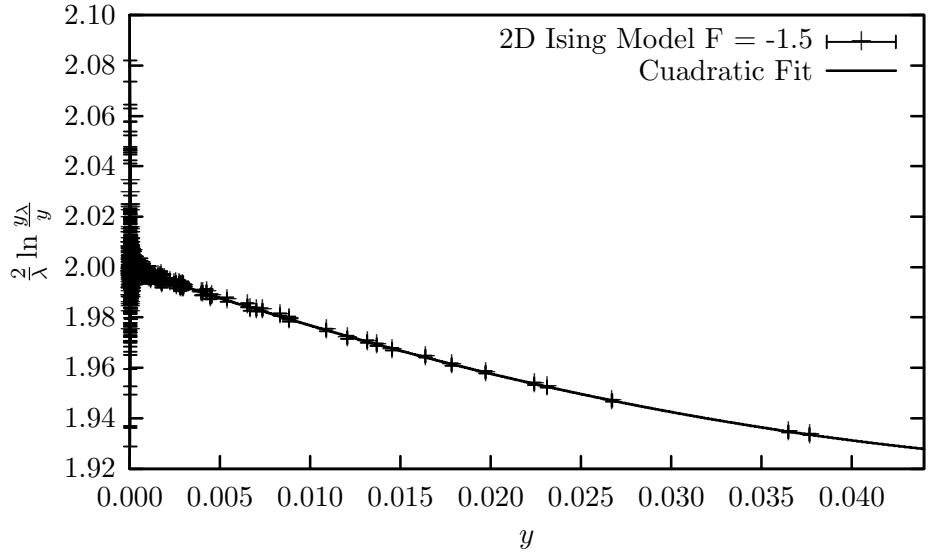

Figure 5.13: Calculation of the critical exponent γ_λ in the ordered phase of the two-dimensional model. The pluses correspond to the numerical simulation data, whereas the line is a cuadratic fit. Errors are much smaller than symbols, except for the points lying close to the origin.

[22] Actually the Z_2 symmetry is spontaneously broken, for the staggered magnetization $m_S \neq 0$ [94]. This point will be clarified in the mean-field approximation.

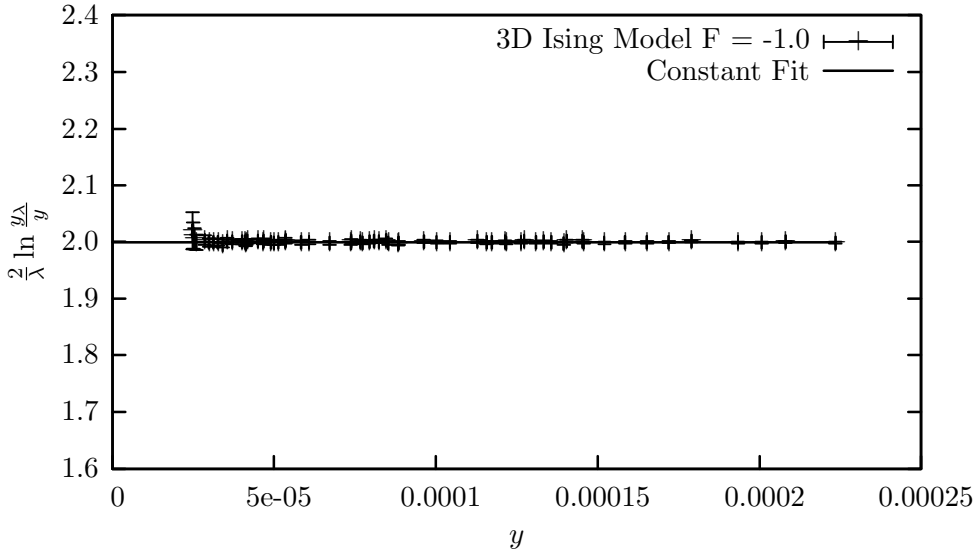

Figure 5.14: Calculation of the critical exponent γ_λ in the ordered phase of the three-dimensional model. The pluses correspond to the numerical simulation data, whereas the line is a constant fit. Errors are much smaller than symbols, except for the points lying close to the origin.

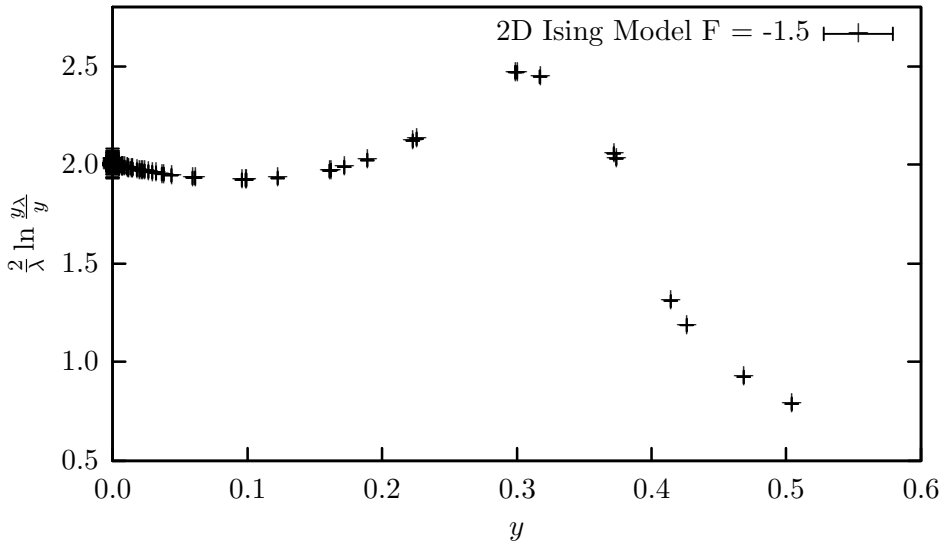

Figure 5.15: Due to the peaked behaviour of the quotient y_λ/y around $y = 0.3$, the extrapolation to zero required many simulations at small values of the magnetic field. Errors are much smaller than symbols, except for the points lying close to the origin.

The disordered phase revealed a caveat of this method, as it was impossible for us to extrapolate the function $\frac{y_\lambda}{y}(y)$ to zero. The reason is simple: at small values of F, y and y_λ approach the unity, for at vanishing F we recover the paramagnetic Langevin solution $m = \tan\frac{\theta}{2}$, which will be derived later. The smaller the value the F, the greater the gap between zero and our data becomes, and at some point, the extrapolation is not reliable any more, and the outcoming results depend strongly on the fitting function used. An example can be seen in fig. 5.18, where the data for the two-dimensional model at $F = -0.40$ are plotted. In this case, we are to far from zero to find out accurately the critical exponent, and the value of F could not be lowered much more, for the transition to the ordered phase is known to happen at $F \sim -0.44$. In 5.19 a similar example is shown for the ordered phase in the three-dimensional model, but this time

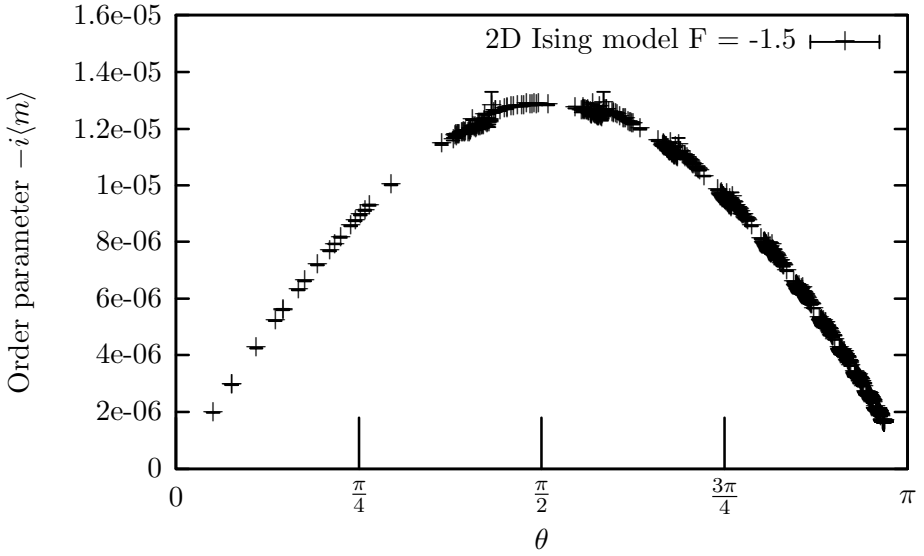

Figure 5.16: Order parameter as a function of θ in the ordered phase of the two-dimensional model. It vanishes at $\theta = \pi$.

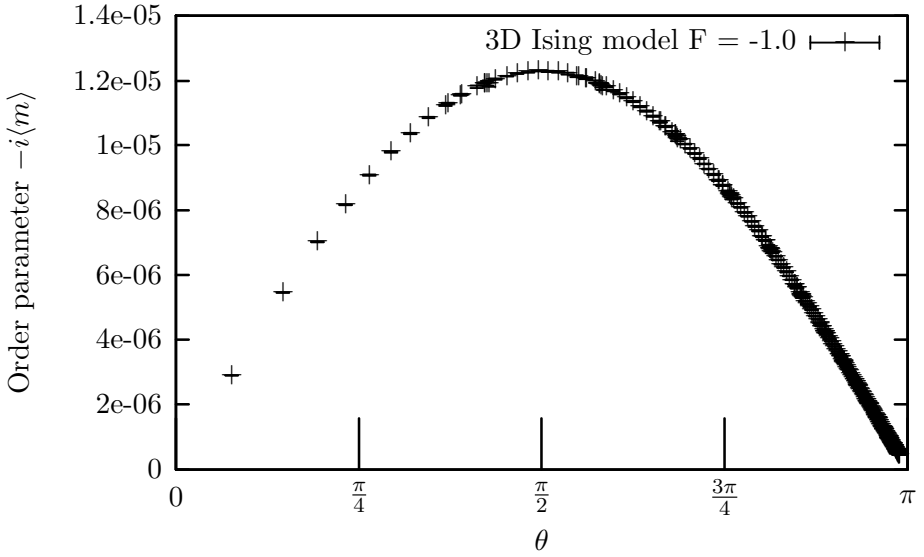

Figure 5.17: Order parameter as a function of θ in the ordered phase of the three-dimensional model. As in its two-dimensional counterpart, it vanishes at $\theta = \pi$. Errors are smaller than symbols.

a tentative extrapolation could be done, casting a reliable result.

This examples show how this method works fine when the antiferromagnetic couplings are strong enough. In general, the method performs well for asymptotically free theories, whose continuum limit lie in the region of weak coupling. In this region, the density of topological structures is strongly suppressed. Thus, the order parameter, and hence, $y\,(z)$, take small values, making the plot $\frac{y_\lambda}{y}\,(y)$ easily extrapolable to zero. In the particular case of the antiferromagnetic Ising model, the behaviour seems to be the contrary, for the coupling $F < 0$ opposes to the formation of topological structures, and large values of $|F|$ ensure a small magnetization. A high value of the dimension also helps, for instance, the three-dimensional model requires a lower value of the coupling than the two-dimensional case to make a reliable extrapolation of $\frac{y_\lambda}{y}\,(y)$ to $y \to 0$, for each spin is affected by a higher number of neighbours, so the topological

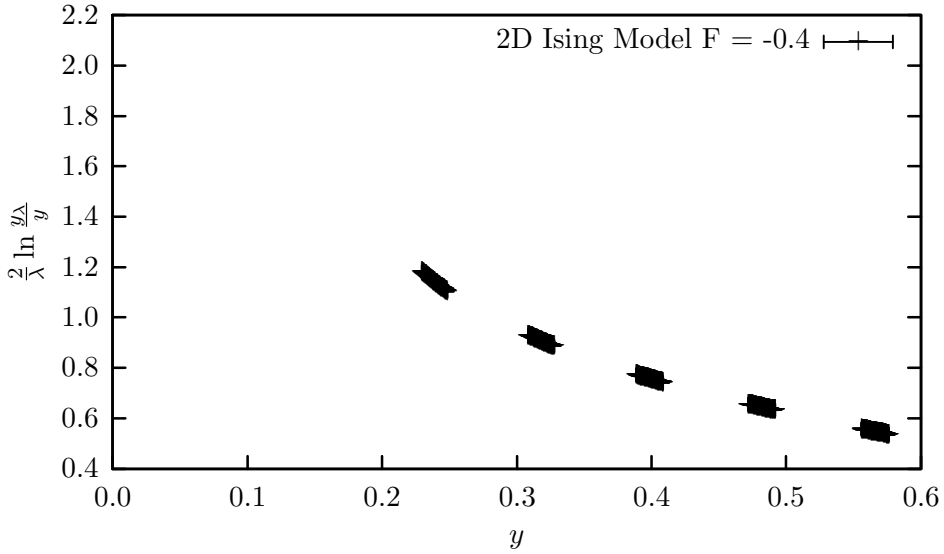

Figure 5.18: Failed calculation of the critical exponent γ_λ in the disordered phase for the two dimensional model. Our data is so far from the $y = 0$ axis, that an extrapolation can not be used to find out the value of γ_λ. A peak for lower values of y, as the one appearing in fig. 5.15, cannot be discarded 'a priori'. Errors are much smaller than symbols.

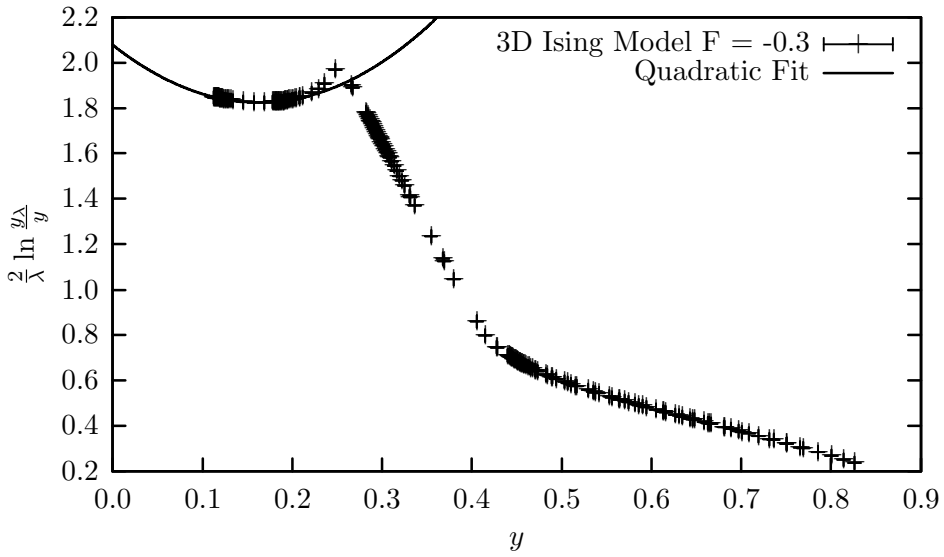

Figure 5.19: Another calculation of the critical exponent γ_λ in the ordered phase $F = -0.3$ for the three-dimensional model. Our data approaches the $y = 0$ axis enough to try an extrapolation, but the result suffers from much larger errors than in the $F = -1.0$ case. Here $\gamma_\lambda = 2.079 \pm 0.003$, and the measurement errors are much smaller than symbols.

structures are even more supressed.

As this method failed to deliver interesting results in the disordered phase, we tried a different approach: we expected naively that the two-dimensional model resemble the one-dimensional model at low values of the coupling. Since the *p.d.f.* method described in this chapter worked well for the one-dimensional case [90], it made sense that we applied it to the present scenario. What we found is an unstable behaviour: sometimes the method seems to predict the phase transition, in the sense that at finite volume there is not true phase transition, and an abrupt modification in the order parameter, linking the two expected behaviours, should happen. This

is what we observe in one of the data sets of fig. 5.20. Nonetheless, if a slightly different set of points is taken to fit the saddle point equation (5.39), the resulting data show a sharp departure from the expected behaviour at some θ.

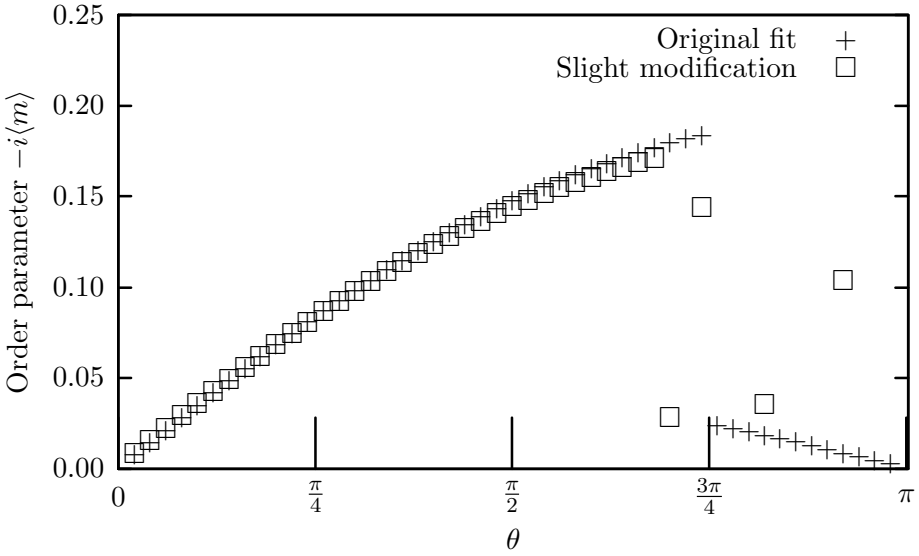

Figure 5.20: Failed calculation of the order parameter in the disordered phase using the *p.d.f.* method. In the first case, the points seem to predict a phase transition at $\theta \sim 2.35$, whereas in the second case the points depart sharply from a smooth function and never come back. The only difference between fits was the number of points used: in the second case, only half of the points (the closest to the origin) were used. Other modifications in the fitting procedures indicate us that the transition point is not stable. This might indicate either a failure in the fitting function, or a phase transition, and the impossibility for the method to precise the transition point, unless a perfect ansatz is made. Errors were not estimated.

There are two possible explanations to this behaviour: either the fitting function selected is completely wrong, or there is some hidden phenomena we are overlooking. The fitting function used was an odd quotient of polynomials

$$\frac{ax^3 - x}{cx^2 - b}$$

which should account perfectly for the behaviour of the order parameter, given the assumption that it is similar to the one-dimensional case. The addition of more terms to the fit did not do much to improve the result, hence this possibility was discarded.

The existence of a phase transition in the middle, however, was an interesting option. Indeed, the two-dimensional model in the presence of a θ term was solved exactly at the point $\theta = \pi$ almost sixty years ago by Yang and Lee in [94], and reviewed again in [95]. In those papers, a phase diagram was proposed were the antiferromagnetic model always stayed in an ordered phase at any non-zero value of F. Since the system is in a disordered state for low F's and zero field, some phase transition has to occur in the middle. Thence, the failure of the *p.d.f.* method should be due to a poor ansatz for the fitting function, caused by the presence of a phase transition at some θ_c.

The fact that the results for the two- and three-dimensional models are qualitatively the same in the ordered phase, makes us wonder whether for some value of the dimension $D > 3$ this behaviour is not observed. Moreover, the behaviour of this model in the disordered phase is completely unknown to us. That is why we decided to carry out a mean-field approximation

of the model, and compute the critical exponent γ_λ. As we know, mean-field results for other critical exponents are exact for the n-dimensional ferromagnetic Ising model, provided that $n \geq 4$. Thus we expect that, if the mean-field result for γ_λ is the same to that of the two- and the three-dimensional Ising model, then $\gamma_\lambda = 2$ for any value of the dimension.

5.4 The Mean-field approximation

An introduction to Mean-field theory

The mean-field approximation was introduced by Weiss in 1907, just two years after the appearance of Langevin's theory of paramagnets. Langevin's theory explains the paramagnetic phenomena assuming that paramagnetic materials are composed of a set of disordered magnetic dipoles[23]. The interaction among these dipoles is weak enough to be negligible against thermal fluctuations, and the only ordering agent is the external magnetic field,

$$H\left(B, \{s_i\}\right) = -B \sum_i^N s_i. \tag{5.55}$$

The model is easily solvable: As the spin do not interact with each other, the partition function factorizes:

$$Z\left(h\right) = \sum_{\{s_i\}} e^{-\beta H(h)} = \left[\sum_{s_i = \pm 1} e^{\frac{h}{2} s_i} \right]^N = 2^N \cosh^N \frac{h}{2}. \tag{5.56}$$

The free energy is given by

$$f\left(h\right) = \ln 2 + \ln \cosh \frac{h}{2}, \tag{5.57}$$

and the magnetization can be written in a closed form

$$m\left(h\right) = \tanh \frac{h}{2}. \tag{5.58}$$

The theory was quite a success for paramagnets, as it was able to predict Curie's law in its naive form $\chi = C/T$. Nevertheless, it could not explain ferromagnets, and spontaneous magnetization phenomena. The reason is quite straighforward: As the spin system describe by Langevin's theory is non-interacting, at zero external field, the magnetization should vanish. This can be readily checked in (5.58).

Weiss hypothesis improved Langevin's theory assuming a crude interaction among the spins. Each spin created a small magnetic field, called *molecular field*, which reinforced the effect of the external field. Once the external field is removed, the molecular field might be strong enough to give rise to spontaneous magnetization phenomena. The way to treat the molecular field was excessively simple: The spins interacted with an average magnetic field created by all the other spins. This effect is included on (5.55) just by writting

$$H\left(J, B, \{s_i\}\right) = -J \sum_{\{i,j\}}^N s_i \langle s_j \rangle - B \sum_i^N s_i, \tag{5.59}$$

[23]Originally, Langevin's theory was applied to classical vectors, instead of classical spins $S = 1/2$. Here we will apply the same ideas in the framework of the Ising model.

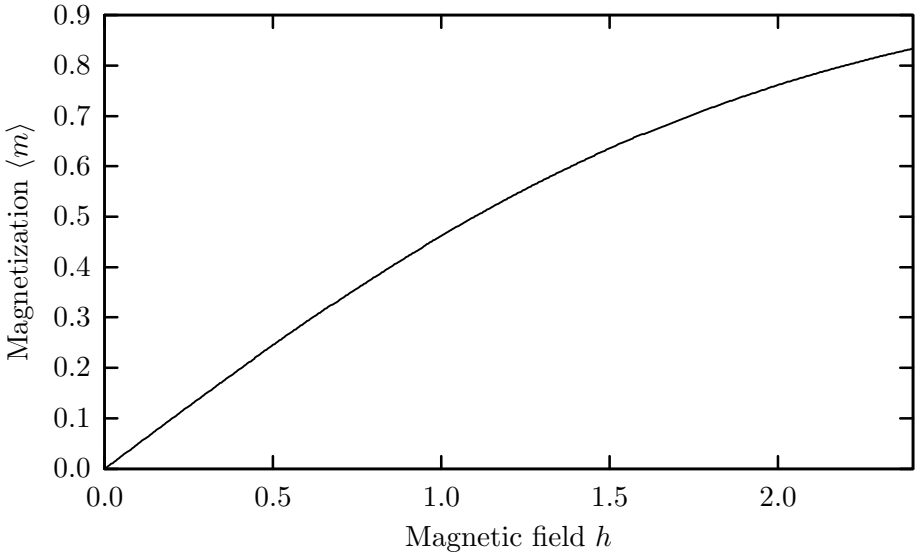

Figure 5.21: Langevin's prediction for the magnetization density distribution function of an $S = 1/2$ paramagnet.

which resembles the Hamiltonian for the Ising model (5.1). By using invariance under translations and the definition of the magnetization $m = \frac{1}{N}\sum_i^N s_i$ we find

$$H\left(J, B, m\right) = -NJm^2 - NBm. \tag{5.60}$$

So the mean-field hamiltonian is written as

$$H\left(J, B, m\right) = -N\left(Jm^2 + Bm\right). \tag{5.61}$$

We could have derived (5.61) directly from the infinite coupled Ising model, described by

$$H\left(J, B, \{s_i\}\right) = -\frac{J}{N}\sum_{i,j}^{N} s_i s_j - B\sum_{i}^{N} s_i. \tag{5.62}$$

Two comments are in order:

- The mean-field hamiltonian *depends only on the magnetization* m.
- A constant coupling J in (5.62) would lead to a N^2 divergence in the thermodynamic limit, and the energy would not be an extensive quantity. The reason is quite clear: Each spin is coupled to all the other spins[24] with the same strength. In the thermodynamic limit, this kind of coupling diverges, unless the coupling constant becomes increasingly small
$$J \to \frac{J}{N}.$$

As we can see in (5.62), the dimensionality of the system is completely irrelevant here, as every spin couples with every other spin. In fact, this system seems to feature an *infinite dimension*, for the coordination number[25] of each spin is, in an effective way, infinite in the

[24]Being rigorous, each spin is coupled to the other $N-1$ spins, but the difference is negligible in the thermodynamic limit.

[25]The coordination number q is the number of neighbours. In systems with nearest-neighbour interactions, it is an interesting property, and for the case of an square lattice, it is proportional to the dimensionality of the system $q = 2D$.

thermodynamic limit. This way to understand the mean-field approximation gives us some insight on what to expect from it. We can guess now that this approximation works better in higher dimensions, and in models with a great number of interacting neighbours per site. In any case, the approximation is very crude, for it does not depend on the dimension of the system we are considering[26].

Mean-field theory for the antiferromangetic Ising model

The Hamiltonian (5.59) refers to the ferromagnetic case. We could naively think that for negative values of the coupling J, this Hamiltonian is applicable to the antiferromangetic case, but this is not true. The problem lies in the fact that every spin couples to every other spin in the same way. An antiferromagnetic coupling in (5.59) would lead to a system where each spin tries to align in an opposite way to all the other spins, introducing frustration in the model. However, in antiferromagnetic compounds the spin-alignment pattern is staggered, like a chess board, and frustration is absent. The short-ranged model also lacks frustration for an even number of spins[27]. This is an essential difference, which may lead to qualitatively different behaviours. Thence, in order to define properly the mean-field version of the antiferromagnetic Ising model, we should divide the lattice in two sublattices, and define a coupling among spins whose sign depends on whether these two spins are on the same sublattice or not.

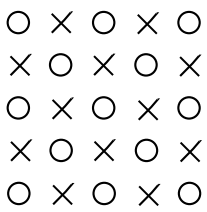

Figure 5.22: Representation of the two sublattices in a two-dimensional lattice. The lattice S_1 is indicated by the circles, whereas the lattice S_2 is marked by crosses. Note that, if there is only a nearest neighbour interaction, the circles do not interact among each other, but only with the four crosses that surrounds each circle. The antiferromagnetic mean-field approach must distinguish whether a circle/cross is interacting with a cross or a circle, and vice-versa.

For spins belonging to the same lattice, the coupling should be ferromagnetic ($J > 0$), but for spins belonging to different sublattices, the coupling should favour antiparallel ordering ($-J < 0$), according to the antiferromagnetic nature of the system. Therefore, two different mean-fields should appear, $\langle s_i \rangle_{i \in S_1} = m_1$ and $\langle s_i \rangle_{i \in S_2} = m_2$, referring to each one of the different sublattices. The corresponding Hamiltonian is a bit different than (5.62)

$$H\left(J, B, \{s_i\}\right) = -N\left[J\left(m_1 - m_2\right)^2 - B\left(m_1 + m_2\right)\right] =$$

$$= -\frac{J}{N}\left(\sum_{i \in S_1} s_i - \sum_{j \in S_2} s_j\right)^2 - B_1 \sum_{i \in S_1} s_i - B_2 \sum_{j \in S_2} s_j, \tag{5.63}$$

where we have separated the external magnetic fields acting on the different sublattice for computation purposes. In the end, the equality $B_1 = B_2$ is set. In this system, ferromagnetic

[26] In fact, a modification in the coordination number (which is the only dependence on the dimension the system might display) in a mean-field approximation for a given model only amounts to a rescaling of the coupling J. If we use the hamiltonian (5.62), the concept of coordination number does not make much sense anyway.

[27] With periodic boundary conditions.

interactions are stablished among the spins of the same sublattice, whereas antiferromagnetic forces appear among spins of different sublattices.

Let us solve this model. The partition function

$$Z\left(F,h\right)=\sum_{\{s_i\}}e^{\frac{F}{N}\left(\sum\limits_{i\in S_1}s_i-\sum\limits_{j\in S_2}s_j\right)^2+\frac{h_1}{2}\sum\limits_{i\in S_1}s_i+\frac{h_2}{2}\sum\limits_{j\in S_2}s_j} \tag{5.64}$$

can be summed up by applying the Hubbard-Stratonovich identity[28] to linearize the quadratic exponent

$$Z\left(F,h\right)=\frac{1}{\pi^{\frac{1}{2}}}\int_{-\infty}^{\infty}\sum_{\{s_i\}}e^{-x^2+2x\left[\frac{|F|^{\frac{1}{2}}}{N^{\frac{1}{2}}}+h_1\right]\sum\limits_{i\in S_1}s_i-\left[\frac{|F|^{\frac{1}{2}}}{N^{\frac{1}{2}}}-h_2\right]\sum\limits_{j\in S_2}s_j}dx. \tag{5.65}$$

At this point we see that the introduction of the θ term through the transformations

$$h_1\rightarrow i\theta_1,\qquad h_2\rightarrow i\theta_2,$$

render the hyperbolic cosines complex. The $\frac{1}{2}$ factor is allows us to define properly the quantized number $\frac{M}{2}$. The integrand factorizes, as there is no spin-spin interaction

$$\begin{aligned}Z\left(F,h\right)=\frac{2^Ne^F}{\pi^{\frac{1}{2}}}\int_{-\infty}^{\infty}e^{-x^2}\left[\cosh\left(2x\frac{|F|^{\frac{1}{2}}}{N^{\frac{1}{2}}}+i\frac{\theta_1}{2}\right)\times\right.\\ \left.\cosh\left(2x\frac{|F|^{\frac{1}{2}}}{N^{\frac{1}{2}}}-i\frac{\theta_2}{2}\right)\right]^{\frac{N}{2}}dx.\end{aligned} \tag{5.66}$$

Now we bring the transformation

$$\begin{aligned}x&\rightarrow&N^{\frac{1}{2}}y\\ dx&\rightarrow&N^{\frac{1}{2}}dy\end{aligned}$$

so (5.65) becomes

$$\begin{aligned}Z\left(F,h\right)=\frac{2^NN^{\frac{1}{2}}}{e^F\pi^{\frac{1}{2}}}\int_{-\infty}^{\infty}\left[e^{-y^2+}\right.\\ \left.^{\frac{1}{2}\ln\left[\cosh\left(2|F|^{\frac{1}{2}}y+i\frac{\theta_1}{2}\right)\cosh\left(2|F|^{\frac{1}{2}}y-i\frac{\theta_2}{2}\right)\right]}\right]^Ndy.\end{aligned} \tag{5.67}$$

where we have written the whole integral as an exponential. We can not solve the integral (5.67), but by using the *saddle-point technique*[29] we should be able to evaluate the free energy. The problem here lies in the validity of the saddle-point approach: were the argument of the logarithm in (5.67) real, then the saddle point technique would be completely valid, but the argument is, in general, complex[30]. Fortunately, the argument of the logarithm in (5.67) is real for the case $\theta_1=\theta_2=\theta$, as can be demonstrated by using some trigonometric transformations:

$$\cosh\left(2\left|F\right|^{\frac{1}{2}}y+i\frac{\theta}{2}\right)\cosh\left(2\left|F\right|^{\frac{1}{2}}y-i\frac{\theta}{2}\right)=$$

[28] See (B.4) Appendix B

[29] See Appendix B.

[30] There exists a complex version of the saddle-point technique, but it has several limitations, and seldom does it turn out to be useful.

$$\cosh^2\left(2\left|F\right|^{\frac{1}{2}}y\right)-\sin^2\frac{\theta}{2} \tag{5.68}$$

which never becomes negative. What we should realize is the fact that both hyperbolic cosines on the l.h.s. of (5.68) are conjugated quantities, so its product is bound to be real and non-negative, and we can apply the saddle-point technique

$$\lim_{N\to\infty}\frac{1}{N}\ln Z\left(J,B\right)=\ln 2+$$

$$+\lim_{N\to\infty}\frac{1}{N}\ln\int_{-\infty}^{\infty}\left[e^{-y^2+\frac{1}{2}\ln\left[\cosh^2\left(2\left|F\right|^{\frac{1}{2}}y\right)-\sin^2\frac{\theta_2}{2}\right]}\right]^N dy. \tag{5.69}$$

The maximum of

$$g\left(y\right)=-y^2+\frac{1}{2}\ln\left[\cosh^2\left(2\left|F\right|^{\frac{1}{2}}y\right)-\sin^2\frac{\theta}{2}\right] \tag{5.70}$$

gives us the saddle-point equations

$$-y_0+\frac{\left|F\right|^{\frac{1}{2}}}{2}\frac{\sinh\left(4\left|F\right|^{\frac{1}{2}}y_0\right)}{\cosh^2\left(2\left|F\right|^{\frac{1}{2}}y_0\right)-\sin^2\frac{\theta}{2}}=0, \tag{5.71}$$

$$-1+2\left|F\right|\frac{\cos^2\frac{\theta}{2}\cosh\left(4\left|F\right|^{\frac{1}{2}}y_0\right)-\sinh^2\left(2\left|F\right|^{\frac{1}{2}}y_0\right)}{\cosh^2\left(2\left|F\right|^{\frac{1}{2}}y_0\right)-\sin^2\frac{\theta}{2}}<0. \tag{5.72}$$

Thus, the free energy is

$$f\left(F,h\right)=\ln 2+g\left(y_0\right) \tag{5.73}$$

where y_0 verifies (5.71). The ghost variable y is related to m_S, the *staggered magnetization*. This relationship is obscure, in the sense that, in order to see this, we have to go back to (5.67), avoid the transformation (5.68) and set different magnetic fields θ_1 and θ_2

$$\left\langle m_j\right\rangle_{j=1,2}=m_j=\frac{\partial f}{\partial\frac{i\theta_j}{2}}=\left.\frac{\partial g}{\partial\frac{i\theta_j}{2}}\right|_{y=y_0}+\left.\frac{\partial g}{\partial y}\right|_{y=y_0}\frac{\partial y}{\partial\frac{i\theta_j}{2}}=\left.\frac{\partial g}{\partial\frac{i\theta_j}{2}}\right|_{y=y_0} \tag{5.74}$$

for the saddle-point equation forces $\left.\frac{\partial g}{\partial y}\right|_{y=y_0}$ to be zero.

Once m_1 and m_2 are well known, the calculation of m and m_S is straighforward. However, if the equality $\theta_1=\theta_2$ does not hold, the saddle point equation becomes complex again, so it is a bold step to consider the new function $g\left(y\right)$ as the free energy. Nevertheless, we regard this particular steps as an operational trick; since the final result should be evaluated at a y obtained with the true saddle-point equations (5.71), there is nothing wrong with this approach. After some calculus,

$$m_1 = \frac{1}{2}\frac{\cosh\left(2|F|^{\frac{1}{2}}y_0\right)\sinh\left(2|F|^{\frac{1}{2}}y_0\right)+i\sin\frac{\theta}{2}\cos\frac{\theta}{2}}{\cosh^2\left(2|F|^{\frac{1}{2}}y_0\right)-\sin^2\frac{\theta}{2}}, \tag{5.75}$$

$$m_2 = -\frac{1}{2}\frac{\cosh\left(2|F|^{\frac{1}{2}}y_0\right)\sinh\left(2|F|^{\frac{1}{2}}y_0\right)-i\sin\frac{\theta}{2}\cos\frac{\theta}{2}}{\cosh^2\left(2|F|^{\frac{1}{2}}y_0\right)-\sin^2\frac{\theta}{2}}, \tag{5.76}$$

$$m = \frac{i\sin\frac{\theta}{2}\cos\frac{\theta}{2}}{\cosh^2\left(2|F|^{\frac{1}{2}}y_0\right)-\sin^2\frac{\theta}{2}}, \tag{5.77}$$

$$m_S = \frac{\cosh\left(2|F|^{\frac{1}{2}}y_0\right)\sinh\left(2|F|^{\frac{1}{2}}y_0\right)}{\cosh^2\left(2|F|^{\frac{1}{2}}y_0\right)-\sin^2\frac{\theta}{2}}. \tag{5.78}$$

Therefore, and using (5.71),

$$y_0 = |F|^{\frac{1}{2}}\langle m_S\rangle. \tag{5.79}$$

This results are quite interesting: the magnetizations of the individual sublattices are, in general, complex, and they are related to each other by conjugation,

$$m_1 = -m_2^*.$$

On the other hand, the staggered magnetization

$$m_S = m_1 - m_2 = 2\mathrm{Re}\,(m_1)$$

is always real, and by virtue of (5.79), the solution y_0 to the saddle-point equation is real as well. The magnetization m becomes purely imaginary

$$m = m_1 + m_2 = 2i\mathrm{Im}\,(m_1)$$

in the presence of a θ term. For real external fields, the solution obtained here becomes the standard mean-field solution to the antiferromagnetic Ising model.

The resulting mean-field equations are quite similar to the standard ones (showed in appendix C), but the antiferromagnetic nature of the system makes them a bit more complicated[31].

$$m_1 = \frac{1}{4}\frac{i\sin\theta+\sinh(4|F|m_S)}{\cosh^2(2|F|m_S)-\sin^2\frac{\theta}{2}}, \tag{5.80}$$

$$m_2 = \frac{1}{4}\frac{i\sin\theta-\sinh(4|F|m_S)}{\cosh^2(2|F|m_S)-\sin^2\frac{\theta}{2}}, \tag{5.81}$$

$$m = \frac{1}{2}\frac{i\sin\theta}{\cosh^2(2|F|m_S)-\sin^2\frac{\theta}{2}}, \tag{5.82}$$

$$m_S = \frac{1}{2}\frac{\sinh(4|F|m_S)}{\cosh^2(2|F|m_S)-\sin^2\frac{\theta}{2}}. \tag{5.83}$$

The phase diagram in the mean-field approximation

All the magnitudes we have computed depend explicitly on the staggered magnetization m_S, which in turn depends on F and θ. Therefore the saddle-point equation (5.71), or its equivalent (5.83), must be solved first, in order to calculate the dependence of the other observables with θ. However, these are implicit equations, and in order to solve them we must rely on numerical

[31] In fact, another different set of mean-field equations were proposed to this system as an ansatz in [96]. For a discussion on the validity of these equations, see the Appendix C

methods. A simple way to see the solutions of (5.83) is a plot where the l.h.s. and the r.h.s. of (5.83) are represented as a function of m_S. The solutions are the coincident points of both functions. In 5.23, there is only one solution $m_S = 0$, which is a maximum of the free energy, but for other values of F the situation changes dramatically, and two new symetric solutions appear, which are maxima of the free energy, and the original solution $m_S = 0$ becomes a minimum, and it is no longer relevant.

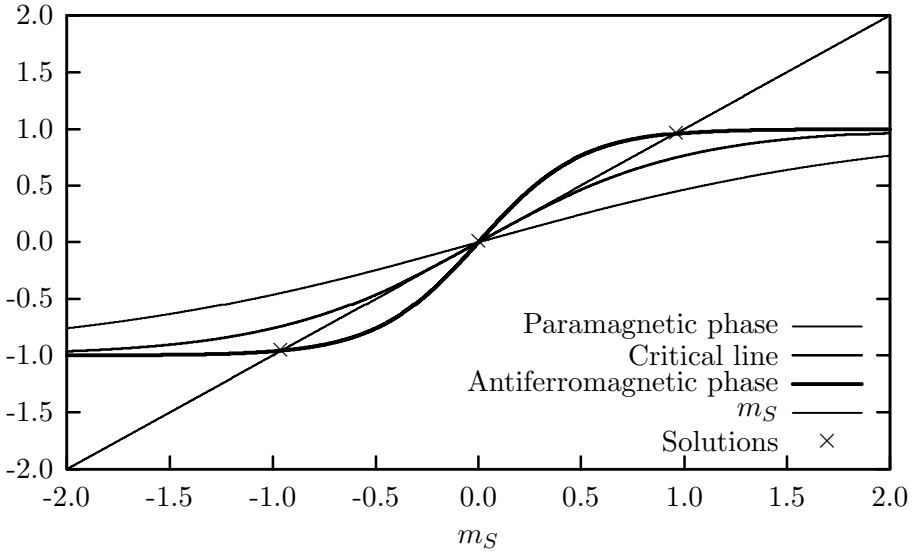

Figure 5.23: Plot done for $\theta = 0$ and three different F values corresponding to the two different phases plus the critical F_c. A solution to the saddle point equations can be found at those points marked by the circles.

From the two saddle point equations, (5.71) and (5.72), the critical value of F, F_c can be ascertained, and it depends on θ as

$$2F_c = \cos^2 \frac{\theta_c}{2}. \tag{5.84}$$

Consequently, for a given value of θ, there are values of F that make the system acquire a non-zero staggered magnetization. This last equation gives us the phase diagram on the $F - \theta$ plane
and there is a second order phase transition at the critical line (5.84). The behaviour of the system in the *paramagnetic phase* (given by $m_S = 0$ and $2F < \cos^2 \frac{\theta}{2}$) is the same as the Langevin theory, and the magnetization m (5.82) equals that of (5.58) after the proper substitution $h \to i\theta$. As $\theta \to \pi$ the paramagnetic phase narrows, until it is reduced to a single point $F = 0$ at $\theta = \pi$. The *staggered* phase (with antiparallel spin ordering $m_S \neq 0$ and $F > \frac{\cos^2 \frac{\theta}{2}}{2}$) on the other hand features Z_2 spontaneous symmetry breaking at $\theta = \pi$, as equation (5.83) indicates. The fact that this model features a phase transition at non-zero values of the external field is quite remarkable indeed. This kind of transitions would never appear in a ferromagnetic model, as the external field and the spin coupling work in the same direction: parallel spin alignment. On the contrary, in the antiferromagnetic case, the introduction of an external field produces frustration, whose origin comes from the competition of the spin coupling, trying to move the spins towards an antiparallel configuration, and the external field, favouring a completely parallel structure.

All the magnetizations are continuous functions, but the staggered susceptibility χ_S diverges,

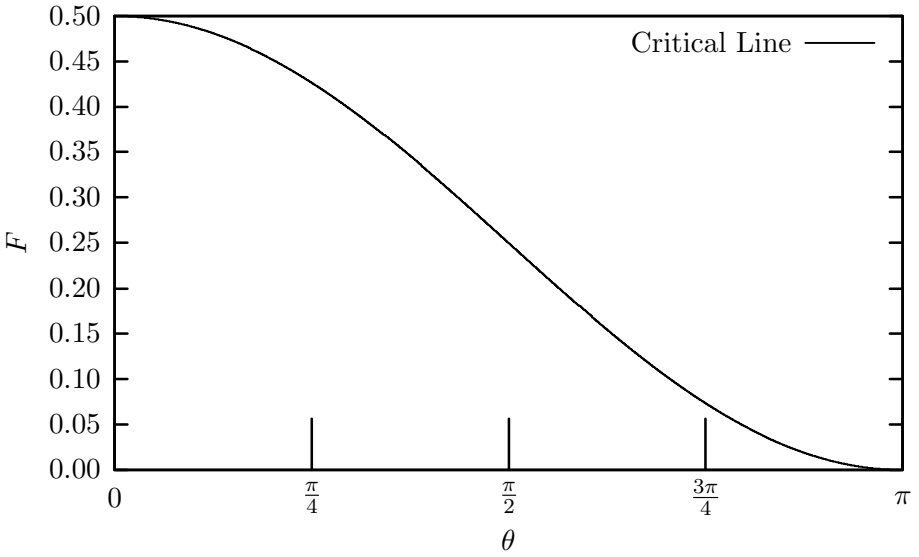

Figure 5.24: Phase diagram of the mean-field approximation to the antiferromagnetic Ising model in the $F-\theta$ plane.

as usually happens in a second order phase transition. The *topological*[32] susceptibility χ_T, on the other hand, displays a gap at the critical line. The computation is tedious, and has been moved to Appendix D. I only show here the final result

$$\Delta\chi_T = \lim_{\theta\to\theta_c^+}\chi_T - \lim_{\theta\to\theta_c^-}\chi_T = \frac{3}{4\left|F\right|}\frac{2\left|F\right|-1}{4\left|F\right|-3}. \tag{5.85}$$

Finally, the critical exponent γ_λ for this mean-field theory can be calculated, to see if it coincides with that obtained in simulations. In order to do so, we expand m in the neighbourhood of $\theta=\pi$

$$m\left(\theta\right) \sim m\left(\pi\right) + \left.\frac{\partial m}{\partial\theta}\right|_{\theta=\pi}\left(\pi-\theta\right) + \left.\frac{\partial^2 m}{\partial\theta^2}\right|_{\theta=\pi}\left(\pi-\theta\right)^2 + \ldots \tag{5.86}$$

If γ_λ is not natural number, we expect the first non-zero derivative to diverge. On the contrary, if γ_λ is a natural number, the order of the first non-vanishing derivative will give us the critical exponent. Taking derivatives

$$\begin{aligned}\left.\frac{\partial m}{\partial\theta}\right|_{\theta=\pi} &= \frac{i}{2}\frac{\left(2\cos^2\theta-1\right)\cosh^2\left(2\left|F\right|m_S\right)+1-\cos^2\frac{\theta}{2}}{\left(\cosh^2\left(2\left|F\right|m_S\right)-\sin^2\frac{\theta}{2}\right)^2} - \\ &\left. - \frac{i}{2}\frac{2\left|F\right|\sin\theta\sinh\left(4\left|F\right|m_S\right)\left.\frac{dm_S}{d\theta}\right|_{\theta=\pi}}{\left(\cosh^2\left(2\left|F\right|m_S\right)-\sin^2\frac{\theta}{2}\right)^2}\right|_{\theta=\pi} = \\ &= -\frac{i}{2}\left[\frac{1}{\sinh^2\left(2\left|F\right|m_S\right)} + \frac{2\left|F\right|\sin\theta\sinh\left(4\left|F\right|m_S\right)\left.\frac{dm_S}{d\theta}\right|_{\theta=\pi}}{\sinh^4\left(2\left|F\right|m_S\right)}\right]\end{aligned} \tag{5.87}$$

The first term on the r.h.s. of (5.87) does not diverge if m_S is not vanishing as $\theta\to\pi$. As $F_c\to 0$ in this limit, we expect a non-zero value for m_S if F is non-zero. Hence this term takes a finite, non-vanishing value. The next term is proportional to

[32]Topological in the sense that $M/2$ is a quantized charge, $m/2$ is its associated charge density, and χ_T the susceptibility.

$$\lim_{\theta \to \pi} \frac{dm_S}{d\theta} \sin\theta.$$

If $\frac{dm_S}{d\theta}$ diverges, then its product with $\sin\theta$ may yield a non-zero contribution to the final critical exponent. However, if it stays finite, the sine function kills this term at $\theta = \pi$. After a tedious calculation, it can be shown that the derivative vanishes, therefore

$$m(\theta) \sim i \frac{\pi - \theta}{2 \sinh(2F |m_S|)} = K(\pi - \theta), \tag{5.88}$$

with K a non-zero constant. The magnetization behaves as $(\pi - \theta)^{\gamma_\lambda - 1}$ in the neighbourhood of $\theta = \pi$. Thence, for mean-field antiferromagnetic theory $\gamma_\lambda = 2$, and the symmetry is always broken for $F \neq 0$. For $F = 0$ the behaviour is that of the Langevin theory, and $\gamma_\lambda = 0$.

Since mean-field theory works better in high dimensional systems (it reproduces all the critical exponents exactly for the ferromagnetic Ising model in dimension 4 and above), and the exponent γ_λ seems to have settled in $\gamma_\lambda = 2$ for the two- and three-dimensional models, and for the mean-field approximation, we expect this result to hold for any dimension of the system. This is not a proof, but in fact, it would be very remarkable if the behaviour of the antiferromagnetic Ising model in a higher dimension departed from $\gamma_\lambda = 2$.

5.5 Conclusions

Although the aim behind this investigation of the antiferromagnetic Ising model is to test our techniques for a future application to QCD in presence of a θ term, the results obtained through this chapter deserve attention on their own merit. Using the method described in section 5.3, the order parameter for the Z_2 symmetry can be calculated for any value of θ, and although there are some regions of the phase diagram where the method does not work very well, it provided us with enough information to make an educated guess on the phase diagram of the theory.

Our guess was later confirmed by a long mean-field calculation, which shares many properties with the original model. The mean-field result is quite interesting by itself, for it can be completely solved. The results of [94] and [95] supplied the remaining information for the two-dimensional case. In the end, we were able to reconstruct qualitatively the whole phase diagram of the theory for two-dimensions, and although we did not pursue to solve the model for higher dimensions, the mean-field calculations, and the fact that the behaviour for the two- and the three-dimensional models is the same for large values of F, give us strong indications that this phase diagram is qualitatively valid for any dimension of the model.

The method only has two caveats: (i.) it does not work properly (and can give wrong results) if there is a phase transition for some $\theta < \pi$, and (ii.) for small values of the coupling F the required extrapolations are not feasible. Fortunately for us, (i.) the standard wisdom on QCD, based on reasonable assumptions, expects no phase transitions for $\theta < \pi$, and (ii.) QCD is an asymptotic free theory, thus its continuum limit lies in the region where the extrapolations of the method work well. Therefore this method has become the perfect candidate to perform simulations of QCD with a θ term, which might provide the scientific community with precious information for the understanding of the strong CP problem.

Part II

Polymers and the chemical potential

Chapter 6

QCD and the chemical potential

"It is characteristic of wisdom not to do desperate things."

—Henry David Thoreau

Nowadays, the scientific community acknowledges the existence of new states of the hadronic matter at temperatures or densities higher than the energy scale of hadrons. In such conditions, the wave function of the quarks composing the nuclear matter begin to overlap notoriously, and the distance among quarks becomes small enough that the individual hadronic and mesonic particles are indistinguishible. Asymptotic freedom for QCD tell us that this new state of matter should behave as a free ideal gas of quarks and gluons, the so called quark-gluon plasma (QGP). It is also believed that in these regimes, the quark masses becomes irrelevant, and chiral symmetry is restored. Besides this well established phase, for very high densities and low temperatures, a color-superconducting phase transition is expected to take place: The large fermi spheres become unstable as the attractive force weakens, due to the asymptotic freedom, resulting in quark-pairing near the Fermi surface and a non-vanishing diquark condensate $\langle\psi\psi\rangle$. Both states of quark matter are not very common in our everyday-life, nonetheless they are of paramount importance to understand the behaviour of universe in its earlier stages. Moreover, the description of the complete phase diagram of QCD under these extreme conditions would help to understand the composition of many astrophysical objects, like neutron stars. But the application of these studies is not restricted to such entities; the heavy-ion collisions generated at large facilities like $RHIC$ and LHC are expected to be described accurately by assuming that the matter involved behaves as a QGP at high temperature and density, and then freezes into hadrons.

Of both fields (study of QCD at non-zero temperature and at non-zero densities), finite temperature QCD is far more developed. Lattice QCD simulations of finite temperature systems have been able to predict the critical temperature $T_C \approx 200 - 250$ MeV at which: (i.) the transition hadronic matter-QGP occurs, and (ii.) chiral symmetry is restored, and it seems that these two phenomena are inherently linked. On the other hand, finite temperature lattice calculations are used to predict or explain the data obtained in the heavy-ion colliders. It is clear that finite temperature QCD is an evolving field.

Sadly, and in spite of the community efforts, the same praise can not be given to finite density QCD. Direct lattice simulations are hindered by the well known *sign problem*, and every attempt to solve it ends in frustration. It seems that the state of the art of finite density QCD is almost the same than three decades ago, despite the continuous research performed during the last years.

But preseverance is rewarded, and step by step, new algorithms appear that seem to work, at least partially, and they can give us new insights on the behaviour of the matter at very high densities. The polymeric approach, or the complex Langevin are two examples of half-succeeding algorithms which, even if they fail to solve the problem completely, at least they keep the hope of finding the right solution one day.

6.1 Introducing the chemical potential on the lattice

The usual way to introduce new features on the lattice is to generalize continuum procedures or prescriptions to a discrete space-time. As we know very well the theories in the continuum, this method is often attempted in first place. Nevertheless, the results yielded by this schema are not always right. One clear example is the discretization of fermions on the lattice, leading to the well known problem of the doublers and the anomaly [8]. Another example is the introduction of a chemical potential on the lattice.

Naively, we expect the chemical potential to be coupled to the current associated with the fermion number $\bar{\psi}\gamma_4\psi$, so the lagrangian density of the theory is modified as

$$\mathcal{L} \to \mathcal{L} - a\mu\bar{\psi}\gamma_4\psi. \tag{6.1}$$

Then, we can calculate the μ-dependence of the energy density ϵ taking into account the new partition function Z,

$$\epsilon = -\frac{1}{V}\left.\frac{\partial Z}{\partial \beta}\right|_{\beta\mu=\text{Fixed}}, \tag{6.2}$$

where Z is written as a function of the new lagrangian density

$$Z = \int \prod_x d\psi_x \, d\bar{\psi}_x e^{\int d^4x \mathcal{L}}. \tag{6.3}$$

In the case of free fermions, the calculation for naive fermions[1] can be carried out exactly,

$$\epsilon = \left(\frac{\mu}{2a}\right)^2 \int_{-\pi}^{\pi} d^4p \frac{1}{\left(\sum_{j=0}^{3} \sin^2 p_j + (ma)^2\right)^2 - 2i\tilde{\mu}a \sin q_4 + 4\mu^2a^2}, \tag{6.4}$$

and this quantity diverges as $\epsilon \sim \left(\frac{\mu}{2a}\right)^2$ in the continuum limit $a \to 0$, which is in clear contrast with the continuum result for massless fermions $\epsilon \sim \mu^4$.

This divergence is not a lattice artifact. In fact, the continuum calculation leads to the same divergence at some point, but there, a prescription is used to remove it. We could proceed in the lattices as in the continuum, and add counterterms to get rid of the divergence [97], but this is, a priori, a very awkward way to proceed, that might lead to cumbersome formulations of finite density theories[2]. It is desirable to find a more elegant description of the chemical potential on the lattice.

The first successful attempt to circumvent this problem must be credited to P. Hasenfrazt and F. Karsch [98]. They observed that the chemical potential in the euclidean formulation of thermodynamics acted as the fourth component of an imaginary, constant vector potential, and that the standard way of introducing the chemical potential leads to gauge symmetry breaking.

[1] The inclusion of any other kind of fermions does not modify the final dependency. In fact, the problem always arises, regardless of the regularization. I choose here to show the results for naive fermions because of their simplicity.

[2] The formulation exposed in [97] however turned out to be quite manageable.

The clearest example is QED in the continuum, where the chemical potential is introduced as a shift μ/e in the time-component of the vector potential A, which can be thought as a gauge transformation[3].

This way, for naive fermions, the fermionic matrix looks like

$$\Delta_{xy} = m\delta_{xy} + \frac{1}{2}\sum_{\nu=1,2,3}\left\{\gamma_\nu\left[U_{x,\nu}\delta_{y,x+\hat{\nu}} - U^\dagger_{x-\nu,\nu}\delta_{y,x-\hat{\nu}}\right] + \right.$$

$$\left.\frac{1}{2}\gamma_4\left[e^{a\mu}U_{x,4}\delta_{y,x+\hat{4}} - e^{-a\mu}U^\dagger_{x-4,4}\delta_{y,x-\hat{4}}\right]\right\}, \tag{6.5}$$

Using this prescription,

$$\epsilon = \frac{1}{8\pi^3 a^3}\int_{-\pi}^{\pi} d^4p\theta\left(e^\mu - K - \sqrt{K^2+1}\right)\frac{K}{\sqrt{K^2+1}},$$

$$K = \sum_{i=1}^{3}\sin^2 p_i, \tag{6.6}$$

with $\theta(x)$ the heaviside step function. The continuum result for the momentum cut-off $\theta\left(\mu - \sqrt{p^2+m^2}\right)$ is recovered in the $a \to 0$ limit[4].

Unfortunately, neither the fermionic matrix (6.5), nor any of its variations (Kogut-Susskind, Wilson or Ginsparg-Wilson fermions, to give some examples) are suitable for numerical simulation. The reason is that hermiticity is lost for the Dirac operator. Then, any power of the determinant of the fermionic matrix becomes complex, and the sign problem appears. In the case of Wilson fermions, hermiticity is violated beforehand, even at zero chemical potential, but the following relation holds

$$\gamma_5 D = D^\dagger\gamma_5 \quad \Longrightarrow \quad \gamma_5 D = (\gamma_5 D)^\dagger, \tag{6.7}$$

so $\mathrm{Det}\left[\gamma_5 D\right]$ is real and although it can be negative, simulations can be performed for an even number of degenerated flavours, for $\mathrm{Det}^2\left[\gamma_5 D\right]$ is always positive.

The problem of the chemical potential is that it breaks completely the relation (6.7) by introducing the asymmetry between forward and backward links. This asymmetry is necessary, for it enhances the propagation of quarks and hinders that of antiquarks, but indeed it is not of any help when it comes to do the lattice simulations.

In fact, during the 90's [100, 101, 102, 103], several groups tried to perform simulations at finite density by means of the quenched approximation, but they obtained results in clear contradiction with the intuitive expectations: It is expected that the observables be almost μ-independent as long as μ is smaller than a certain threshold value, given by $\mu_c = m_B/3$, where m_B is the lightest baryon mass. For $\mu > \mu_c$, a finite baryon density populates the system, as it is more convenient from the energetical point of view. But the quenched approximation set the critical value of the chemical potential at $m_\pi^2/2$, with m_π the mass of the pion. In the chiral limit, the baryons stay massive, whereas the pions become massless. Then μ_c is set to zero. This is completely inacceptable.

[3]The physical effect of the chemical potential in QED is irrelevant, as the introduction of μ amounts to a constant shift in the energy. In general, any $U(N)$ theory lacks baryons, and therefore, do not truly depend on μ.

[4]R. V. Gavai wrote a beautiful paper [99] where he shows a general action leading to the correct implementation of the chemical potential. Sadly it seems that there are no realizations of this general action with a real and positive determinant.

A common explanation for this behaviour is to understand the quenched approximation as the theory of the modulus (the one that solves the sign problem taking the modulus of the determinant, this theory treats equally the quark **3** and the antiquark 3^* representations) for zero flavours [104]. As the theory of the modulus features a diquark baryon, the critical value for the chemical potential is expected to be around $m_\pi^2/2$. Nonetheless, we can arrive to the quenched approximation from very different limits for instant, the zero flavour theory of full QCD, and in this case the quarks and the antiquarks are treated in a different way, so there must be other explanation for this behaviour. In fact, the differences between the theory of the modulus, full QCD and the quenched approximation has been investigated in the large quark mass limit [105], and for vanishing temperature, full QCD and the theory of the modulus coincide, whereas the quenched approximation gives very different results.

The conclusion is that the sea-quarks are of paramount importance in finite density calculations, and they can not be neglected happily, as the quenched approximation does. In the beginning era of lattice QCD, where no much computer power was available, this was translated in the necessity of developing competent algorithms to simulate fermionic actions: Lattice QCD simulations were commonly performed without dynamical fermions, either in its pure gauge form, or including the fermions using the quenched approximation. Except for a few shy attempts, most of the lattice practitioners thought there were no satisfactory algorithms to deal with the problem of the Grassman variables in a computer, and some of them were actively researching new computational methods for fermionic degrees of freedom.

6.2 Polymeric models

The problem which arises with fermions is how to make them comply with Pauli's exclusion principle inside the lattice. Although theoretically a representation of anticommuting variables could be set up in the computer, this is not feasible in practice [19]. Thence, we should remove our Grassman variables from our theory, thus we integrate them out to yield a determinant. But the determinant is a non-local quantity, which render the simulations slow, and in some cases (like finite density) is intractable, due to the sign problem.

The first steps

One interesting attempt to circunvent these problems was the polymer representation of fermions. The polymerization of fermions, although young, was quite promising, and had been applied successfully to some models [106, 107, 108]. It provided a method to simulate fermions without computing the fermionic determinant, and this property was quite appealing, for it would speed up the fermionic simulations by a large factor. However, there was a key handicap: A severe sign problem appeared where it has never been. The polymerization transformed the fermionic determinant into fermionic loops, whose sign depended on the gauge group and on their particular shape. In fact, the pioneers of polymeric simulations [106] did notice the abrupt decreasing of the mean sign, but they did not worry too much about it, as long as their numerical results were consistent with the expected results. QCD performs no better, and the simplest negative fermionic loop is very simple indeed [109] (see fig. 6.1), causing the negative configurations to be almost as usual as the positive ones. As a result, the observables fluctuate wildly, and are impossible to measure reliably. Some clustering techniques were introduced to avoid the sign flipping, but these rendered the algorithm as slow as the standard determinant computation, thus the idea was forsaken.

P. Rossi and and U. Wolff recovered it in a shy attempt to applicate the polymerization to the strong coupling limit of $U(N)$ gauge theories with staggered fermions [107]. They observed

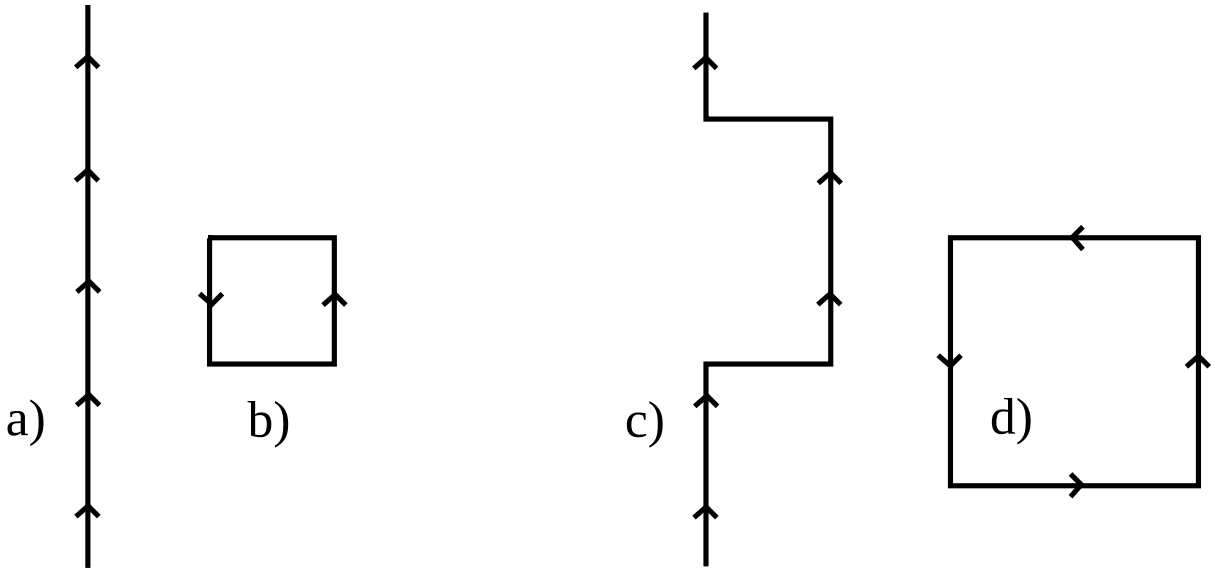

Figure 6.1: Example of loops with positive and negative weights (assuming anti-periodic boundary conditions in the y direction). The loops a) and b) are the simplest of their kind, and carry a positive weight. On the other hand, the loops c) and d) contribute with negative terms to the partition function.

that the family of gauge groups $U(N)$ were not affected by the sign problem, since they lacked baryonic loops[5]. They used this advantage to establish a relation between the chiral symmetry breaking and confinement. Later on, U. Wolff introduced the chemical potential for a $SU(2)$ gauge theory in this polymeric model [110]. Baryonic loops appeared, but they were always positive, due to the nature of the $SU(2)$ gauge group. As the fermionic loops were hard to implement, he decided to add an external source, and compute the quantities in the vanishing source limit.

Karsh and Mütter took the baton from Wolff and faced the $SU(3)$ gauge group (QCD) [109], introducing a key modification: By cleverly clustering the polymers and the baryonic loops, they found a way not only to create baryonic loops easily by simulating only polymer degrees of freedom, but also to solve the sign problem at zero chemical potential. It was possible to simulate a non-zero chemical potential in a wide range of μ's as well, and they found a first order phase transition between two clear different states, at a critical μ which was very close to the mean field predictions. The Monomer-Dimer-Polymer model (MDP) was born.

Fall and rise of the MDP model

Unfortunately, there was something wrong with Karsch and Mütter method. A forecoming article by Azcoiti et al [111] proved that Karsch and Mütter computer implementation of the polymer theory (which was that of Rossi and Wolff) featured a poor ergodicity when baryonic loops were added, and therefore, their simulations where no longer reliable. Being more specific, it was impossible to simulate a lattice whose temporal length (L_T) was higher than four. In those cases, the system would freeze in one of the two states, regardeless of the chemical potential value, resulting in a inacceptably large hysteresis cycle. Moreover, the algorithm was extremely inefficient when dealing with low masses, and even Karsch and Mütter reckoned in their article that ergodicity could not be proved. The idea, again, was abandoned.

[5] A derivation of this statement will be done later.

Recently, Ph. de Forcrand and collaborators rescued the Karsch and Mütter polymerization of the action, and substituted their naive algorithm by a world-line approach [112]. The world-line algorithms were first brought to the scientific mainstream by N. Prokof'ev and B. Svistunov [113, 114, 115] long time ago, but they didn't draw too much attention. Chandrasekaran took them back to life in his later works [116], arguing that this kind of algorithms may solve the sign problem for certain actions. The first results of Ph. de Forcrand were both promising and deceptive. On the bright side, they broke the zero mass limit, and the simulations performed well. On the dark side, they never showed results beyond $L_T > 2$, so the low temperature (and the most interesting) region of the phase diagram was never explored. Later on, they pushed the worm algorithm trying larger lattices in temporal extent and playing with the temperature, obtaining some remarkable results [117]. It seems that different algorithms yield different results, and work well in different ranges. This leads us to the conclusion that, there is nothing wrong with Karsch and Mütter way to rewrite the action, or the partition function. The problem is related to the simulation algorithm.

Starting from Karsch and Mütter algorithm, both ergodicity and efficiency can be improved by adding new possibilities of interaction among polymers, even at zero mass. These modifications allow us to simulate strong coupling QCD with any temporal length. Our conclusion is that the Karsch and Mütter regrouping of configurations does not solve the sign problem for the chemical potential, although there are some interesting regions where simulations can be performed.

6.3 Karsch and Mütter original model

The starting point of the polymeric formulation of strong coupling QCD is the partition function including both, gauge and fermion fields

$$\mathcal{Z}\left(m,\mu,\beta\right)=\int[dU]\;d\bar{\psi}\,d\psi e^{S_G}e^{S_F} \tag{6.8}$$

where ψ and $\bar{\psi}$ are, as usual, the fermionic Grassman variables, and U belongs to the gauge group ($SU(3)$ for QCD). The gauge action S_G is no longer relevant, for we are in the strong coupling regime ($\beta \to 0$). The fermionic action, on the other hand, is responsible for the complete dynamics of the system. We choose, as P. Rossi and U. Wolff did [107], the staggered formulation of fermions, although we are aware of the fact that the polymerization of Wilson fermions is not an untreated problem [118, 119]. The fermion action reads

$$\begin{aligned} S_F\left(\beta\right) &= \sum_{n,\nu}\left[\xi_{n,\nu}(\mu)\left(\bar{\psi}_n U_{n,\nu}\psi_{n+\nu}-\bar{\psi}_{n+\nu}U_{n+\nu,-\nu}\psi_n\right)+2m\bar{\psi}\psi\right] \\ &= \bar{\psi}_m\Delta_{mn}\psi_n \end{aligned} \tag{6.9}$$

where the factor $\xi_{n,\nu}(\mu)$,

$$\xi_{n,\nu}(\mu)=\eta_\nu(n)\begin{cases} e^{\mu} & \nu=4 \\ e^{-\mu} & \nu=-4 \\ 1 & \text{otherwise}\end{cases} \tag{6.10}$$

encloses both the staggered sign

$$\eta_\mu(n)=(-1)^{\sum_{i<\mu}x_i}, \tag{6.11}$$

which depends on the point n, the link direction ν and the chemical potential factor e^{μ}. We are considering $\nu = \pm 1, \pm 2, \pm 3, \pm 4$ in $3+1$ dimensions, being $\nu = \pm 4$ the positive (negative) temporal direction.

As we are in the strong coupling regime, the direct integration of the partition function should be feasible. Of course we know that the fermionic action reduces to the determinant of the fermionic matrix

$$\mathcal{Z}\left(m, \mu, \beta = 0\right) = \int [dU] \, \det \Delta_{mn}, \tag{6.12}$$

but we are interested in integrating the gauge fields as well, so let's go back one step and try another approach. We expand the exponential of the fermion action

$$e^{S_F} = \sum_{i=0} \frac{S_F^i}{i!}, \tag{6.13}$$

and then integrate the gauge fields usign the group integration rules. The big problem here arises from the powers of S_F. The fermionic action (6.9) is a sum over all possible points n and directions ν, and any power of this large sum involves an even larger number of sumands. What we want to do is to integrate all these sumands, one by one.

Let's perform the integration step by step. First of all, we expand the mass term.

$$J_n\left(m\right) = e^{2m \sum_{k=1}^{N} \bar{\psi}_n^k \psi_n^k} = \sum_{i=0} \frac{\left(2m \sum_{k=1}^{N} \bar{\psi}_n^k \psi_n^k\right)^i}{i!}. \tag{6.14}$$

where k stands for a color index. We have called this term $J_n\left(m\right)$, for further reference. Following the standard notation on the subject,

$$M_k(n) = \bar{\psi}_n^k \psi_n^k, \qquad M(n) = \sum_k \bar{\psi}_n^k \psi_n^k, \tag{6.15}$$

and we will call a *monomer* to the first one, M_k, for any k. The expansion (for QCD, $N = 3$) in terms of these new fields looks like

$$\begin{aligned} J_n\left(m\right) = 1 + 2m \left(M_1(n) + M_2(n) + M_3(n)\right) \\ +(2m)^2 \left(M_1(n)M_2(n) + M_2(n)M_3(n) + M_3(n)M_1(n)\right) \\ +(2m)^3 M_1(n)M_2(n)M_3(n). \end{aligned} \tag{6.16}$$

Monomers are discrete, ultralocal objects which consume some Grassman variables of the point n they belong to, in particular the pair $\bar{\psi}_n^k \psi_n$ for a given value of the color k. For $SU(N)$, the monomer occupation of a site number is an integer whose maximum value is N, the number of colors. In this case (maximum monomer occupation number), all the Grassman variables of the point are used to construct monomers. The other extreme case is zero occupation number, and the Grassman variables may serve other purposes.

These other purposes are related to the terms which involve gauge fields. The integration of these turns out to be fairly easy, for in the strong coupling regime only the annihilating fields survive. For any $U(N)$ gauge group, this set of annihilating fields reduce to the product of a link $U_{n,\nu}$ and its adjoint $U_{n,\nu}^{\dagger} = U_{n+\hat{\nu},-\nu}$, which equals unity, but in the special case of $SU(N)$, the group integral of the N^{th} power of a field is also the identity, so the combination $U_{n,\nu}^N$ should be taken into account as well.

After the gauge integration, only a sum of different products of Grassman variables remain, and we must assure that every Grassman variable appears once and only once in each sumand, otherwise the corresponding summand becomes zero. Translating the result into monomer operators (6.15), what we find for QCD is

$$\begin{aligned} I_{n,\nu}(\mu) &= \int [dU] \exp\left[\xi_{n,\nu}(\mu)\left(\bar{\psi}_n U_{n,\nu}\psi_{n+\hat{\nu}} - \bar{\psi}_{n+\hat{\nu}} U_{n+\hat{\nu},-\nu}\psi_n\right)\right] \\ &= 1 + \frac{1}{3}M(n)M(n+\hat{\nu}) + \frac{1}{12}\left(M(n)M(n+\hat{\nu})\right)^2 + \frac{1}{36}\left(M(n)M(n+\hat{\nu})\right)^3 \\ &\quad + \xi^3_{n,\nu}(\mu)\bar{B}(n)B(n+\hat{\nu}) + \xi^3_{n+\hat{\nu},-\nu}(\mu)\bar{B}(n+\hat{\nu})B(n). \end{aligned} \tag{6.17}$$

The quantities

$$B(n) = \psi_1(n)\psi_2(n)\psi_3(n) \qquad \bar{B}(n) = \bar{\psi}_1(n)\bar{\psi}_2(n)\bar{\psi}_3(n) \tag{6.18}$$

can be regarded as baryon-antibaryon fields. These fields come from the cubic terms $\left(\bar{\psi}_n U_{n,\nu}\psi_{n+\nu}\right)^3$, and do not appear in the $U(N)$ gauge groups. As we shall see later, these fields are related to baryons, so an interesting conclusion we anticipated before is the fact that $U(N)$ gauge groups do not allow the creation of baryons[6].

Following Karsch and Mütter program, and in order to complete the interpretation of the resulting partition function, we translate the product of monomers $M(x)M(n+\nu)$ into dimer fields $D_i(n,\nu)$. A dimer field arises from the cancelation of the gauge fields in the terms $\bar{\psi}_n U_{n,\nu}\psi_{n+\nu}$ and $\bar{\psi}_{n+\nu}U_{n+\nu,-\nu}\psi_n$. This cancellation gives way to the Grassman product $\bar{\psi}_n\psi_{n+\nu}\bar{\psi}_{n+\nu}\psi_n$, a product of Grassman variables which involve two points joined by a link $U_{n,\nu}$; so the dimers are not ultralocal entities, as the monomers, but they link two neighbouring points.

The double dimer field

$$D_2(n,\nu) = \left(\frac{M(n)M(n+\hat{\nu})}{2!}\right)^2 \tag{6.19}$$

can be written as

$$\begin{aligned} D_2(n,\nu) &= \left[M_1(n)M_2(n) + M_1(n)M_3(n) + M_2(n)M_3(n)\right] \\ &\quad \times \left[M_1(n+\hat{\nu})M_2(n+\hat{\nu}) + M_1(n+\hat{\nu})M_3(n+\hat{\nu}) + \right. \\ &\quad \left. M_2(n+\hat{\nu})M_3(n+\hat{\nu})\right], \end{aligned} \tag{6.20}$$

for the other Grassman products involve powers higher than one of at least one of the Grassman variables, and therefore, they cancel after integration. The factorials are introduced for convenience. The triple dimer field is easier to build

$$\begin{aligned} D_3(n,\nu) &= \frac{\left(M(n)M(n+\hat{\nu})\right)^3}{(3!)^2} \\ &= M_1(n)M_2(n)M_3(n)M_1(n+\hat{\nu})M_2(n+\hat{\nu})M_3(n+\hat{\nu}) \end{aligned} \tag{6.21}$$

as there is only one possibility to make use of all the Grassman variables. On the other hand, the one dimer field involve nine terms in the $SU(3)$ formulation

$$D_1(n,\nu) = M(n)M(n+\hat{\nu}) = \left[M_1(n) + M_2(n) + M_3(n)\right]$$

[6]Another way to visualize the lack of baryons in $U(N)$ groups is to notice that a baryon would not be a gauge invariant object.

$$\times [M_1(n+\hat{\nu}) + M_2(n+\hat{\nu}) + M_3(n+\hat{\nu})] \tag{6.22}$$

Let's put these new fields in the integral $I_{n,\nu}(\mu)$ (6.17)

$$I_{n,\nu}(\mu) = 1 + \frac{1}{3}D_1(n,\nu) + \frac{1}{3}D_2(n,\nu) + D_3(n,\nu)$$
$$+\xi^3_{n,\nu}(\mu)\bar{B}(n)B(n+\nu) + \xi^3_{n+\nu,-\nu}(\mu)\bar{B}(n+\nu)B(n). \tag{6.23}$$

Note that there is a ξ^3 factor weighting the baryonic terms, which can become negative. The third power comes from the number of colors $N = 3$; which means that for N even, there is no sign problem for the baryons in this formulation. This is not a great surprise: The sign problem is intrinsecally related to fermi statistics, but the baryons of $SU(N)$ for N even are bosons.

In the end, the partition function is written as a product of dimer, monomer and baryonic fields:

$$Z_{MDP}(m,\mu,\beta=0) = \sum_{n,\nu}\int d\bar{\psi}\, d\psi\, I_{n,\nu}(\mu)\, J_n(m)\,. \tag{6.24}$$

The only terms counting in this integral are those which make use of all the Grassman variables in each point, in one way or another. This fact leave us a simple rule: The number of monomers (nM) and outgoing links (nD, number of dimers) in any point of the lattice must equal the number of colors N

$$nM(n) + \sum_{\nu} nD(n,\nu) = N \tag{6.25}$$

For QCD, $N = 3$, and there is a finite set of point types, shown in Table 6.1. The factor $w(x)$ appearing in the last row is a statistical weight derived from the integrals $J_n(m)$ and $I_{n,\nu}(\mu)$. In simple words, the number $w(x)$ takes into account the colour-multiplicity allowed for each link, except for the 1/3 factor of equation (6.23), associated to single and double dimers; this has to be taken into account separately.

Node type	0	1	2	3	4	5	6
							
$n_D(x)$	3	2	1	0	2	3	3
$n_M(x)$	0	1	2	3	1	0	0
$w(x)$	3	6	3	1	3	6	1

Table 6.1: Allowed node types for the $SU(3)$ theory.

The later rule (6.25) is violated in presence of baryonic loops, for these entities consume all the Grassman variables available, so there is no place for a monomer or a dimer. Let's see why: A baryonic loop $\bar{B}(n)B(n+\nu)$ uses the $\bar{\psi}_k$ of all colors ($k = 1 \ldots N$) of a point n, and the ψ_k of its neighbour $(n+\nu)$. In order to kill the N Grassman fields $\bar{\psi}$ that dwell in the point n, we need to put there N Grassman fields ψ, i.e., we have to close the baryonic loop at some point.

On the whole: We have rewritten the partition function of a strong coupling gauge $SU(N)$ theory by integrating both, Grassman and gauge fields. As a result, we have obtained a discrete

set of configurations consisting on graphs of monomers, dimers and baryonic loops. Then we perform a Montecarlo simulation in the space of graphs.

So far we have described Rossi and Wolff's modelization of strong coupling $U(N)$ and $SU(N)$. In their first article, Rossi and Wolff restricted their simulations to $U(N)$ gauge groups, for it is very hard to implement baryonic loops. As we have explained before, whenever a baryonic loop populates a site, this site becomes saturated, and no other structure (monomer or dimer) can be there. Given a configuration with monomers and dimers, the addition of a baryonic loop involves a non-trivial change in all the neighbouring sites of the loop, and this change may extend to even further sites, in order to preserve the rule (6.25), rendering the algorithm highly non–local.

But Wolff developed a way to include baryonic loops, and tested it in $SU(2)$ [110]. He added to $I_{n,\nu}(\mu)$ an external source like this

$$I_{n,\nu}(\mu)^W = I_{n,\nu}(\mu) + \lambda B(n) + \lambda \bar{B}(n). \tag{6.26}$$

We recover the standard action in the limit $\lambda \to 0$. The external source allows the baryonic loops to be open, for now their endings are annihilated by the external source terms. But there may be a severe sign problem in this formulation, for the open baryonic chains acquire arbitrary sign, due to the ξ^N Kogut-Susskind weights. This problem can be eliminated in $SU(2)$ easily: Being all the Kogut-Susskind weights squared, we can forget about the sign of the open chains. Nevertheless, it is impossible to implement $SU(3)$ this way, and the sign problem hinders any attempt of simulation. Moreover, the dynamical creation of baryonic loops relies on the interaction of the open baryonic chains, generated by the external baryonic field. As the external field is removed (which is the interesting limit), these open chain interactions are reduced as well, slowing down the algorithm. This does not seem like the best way to introduce the baryonic loops on the lattice.

The solution came from the hands and the minds of Karsch and Mütter. They realized that the points of type zero (see table 6.1) could be arranged in closed loops (polymers), as shown in fig. 6.2. These polymers consumed all the Grassman variables available along the loop, so they behaved like a baryonic loop. By associating a baryonic loop to each polymer, they found a way to avoid this non-locality in the generation of configurations procedure. The key point here is the clustering of two configurations into one: the polymer configuration A and the baryonic loop configuration B. This new configuration has a weight equivalent to the sum of the weights of A and B, and we can create polymers easily, by proposing local changes.

In addition there is a further advantage, let's compute the weight of a baryonic loop C in a configuration, being C the set of points and directions that result in a closed loop. There are two main possibilities for C: It may wind around the temporal direction of the lattice or not. Since the net temporal displacement is zero in the later case (we will assign the subindex *SL, spatial loop* to it), the accumulating e^{μ} factors cancel the $e^{-\mu}$, and only a product of staggered sign factors remain, regardeless of the orientation of the loop,

$$w_{SL} = \prod_{n,\nu \in C} \eta_\nu^3(n) = \prod_{n,\nu \in C} \eta_\nu(n). \tag{6.27}$$

On the other hand, a winding loop (or *TL, temporal loop*) keeps the exponential factors, so does its weight, and the final result is

$$w_{TL}^{\pm} = \prod_{n,\nu \in C} \eta_\nu^3(n) e^{\pm 3\mu} = -(-1)^k e^{\pm 3\mu k L_T} \prod_{n,\nu \in C} \eta_\nu(n). \tag{6.28}$$

where k is the winding number. The factor $(-1)^k$ arises from the antiperiodic boundary conditions in the temporal coordinate. The exponent $\pm 3\mu k L_T$ is positive in the case of a baryon,

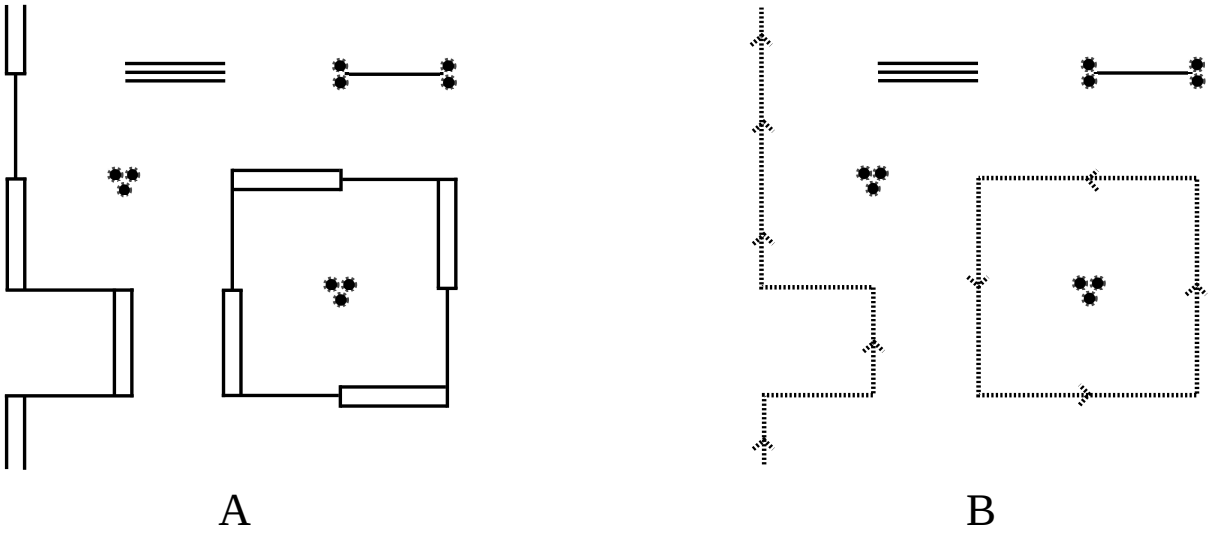

Figure 6.2: Configuration A shows a temporal polymer, winding around the lattice through the boundary, and a spatial polymer. In configuration B the fermionic loops equivalent to the polymers of configuration A are shown. In the Karsch and Mütter model, these two configurations are the same, and we have to add their weights in order to calculate its contribution to the partition function.

and negative in the case of an antibaryon. Clearly, the simulation of baryonic loops "out of the box" features a sign problem, even at zero chemical potential. The configuration weight is negative whenever there exists an odd number of negative loops, and given the point weight (in Table 6.1), this possibility seems rather plausible.

Fortunately, the clustering method of Karsch and Mütter solves the problem for $\mu = 0$. Adding weights of a spatial loop and a polymer results in

$$w_{SL} + w_{Poly} = 1 + \prod_{n,\nu \in C} \eta_\nu^3(n) = \begin{cases} 2 & \text{if} \quad w_{SL} = 1 \\ 0 & \text{if} \quad w_{SL} = -1 \end{cases}, \tag{6.29}$$

and the negative spatial loops do never appear, as they have vanishing weight. We can distinguish the orientation of the loop looking at the orientation of the polymer, but there is no advantage in doing so.

The case of a temporal loop is more subtle. First of all, Karsch and Mütter clustered the baryon and the antibaryon loop into one entity, so we do not distinguish the orientation of the loop.

$$w_{TL}^+ + w_{TL}^- = -(-1)^k 2 \cosh(3\mu k L_T) \prod_{n,\nu \in C} \eta_\nu(n). \tag{6.30}$$

Two polymer configurations are clustered with this one, so the final weight is

$$w_{Poly}^+ + w_{Poly}^- + w_{TL}^+ + w_{TL}^- = 2 - (-1)^k 2 \cosh(3\mu k L_T) \prod_{n,\nu \in C} \eta_\nu(n), \tag{6.31}$$

which doubles that of the spatial loop in the $\mu = 0$ case, for we have clustered the *two possible orientations* of the loops. Now, Karsch and Mütter decide to distinguish between the different polymers, so they split this macroconfiguration into two different ones, each of these comprising a polymer and half a baryon-antibaryon sum. The partition function is the same, but the weight now is divided by two

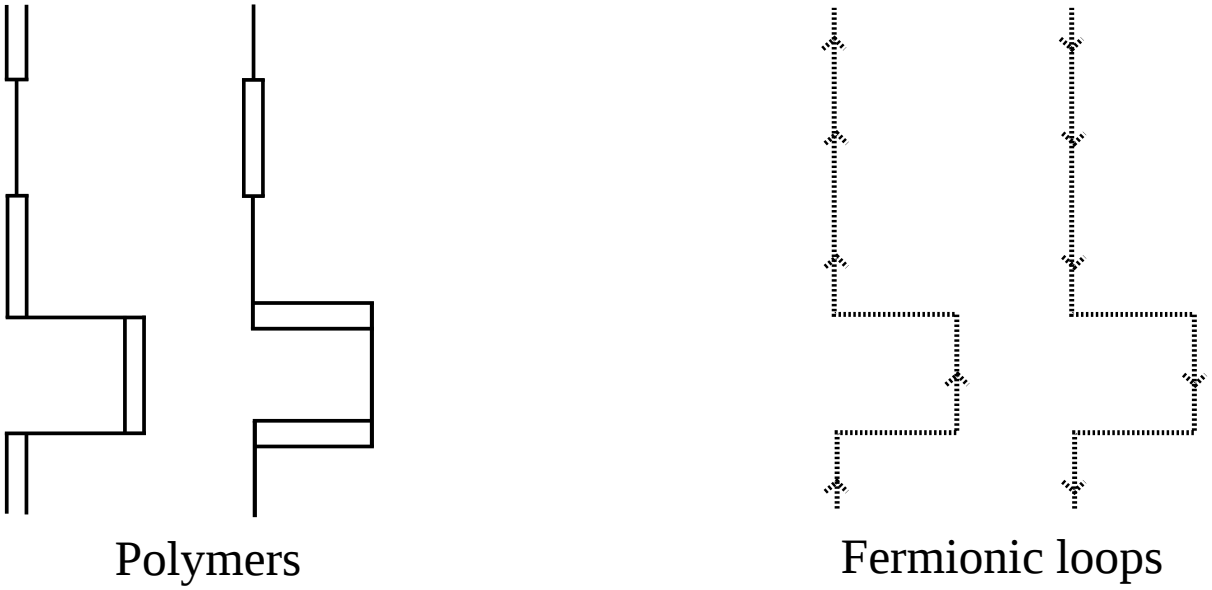

Figure 6.3: The fermionic loops are oriented, so for a given closed path, there are two fermionic loops associated to it (right). Fortunately, the number of polymers associated to a closed path is two as well (left), so we can even distinguish the orientation of the loops in our clustering of configurations. As explained in the text, Karsch and Mütter chose to cluster all the configurations, making the orientation of the loops irrelevant.

$$w^{\pm}_{Poly} + \frac{w^{+}_{TL} + w^{-}_{TL}}{2} = 1 - (-1)^k \cosh\left(3\mu k L_T\right) \prod_{n,\nu \in C} \eta_\nu(n) = 1 + \sigma\left(C\right) \cosh\left(3\mu k L_T\right). \tag{6.32}$$

where $\sigma\left(C\right) = \pm 1$ gathers all the terms contributing to the sign of the loop.

On the whole, the contribution of a given MDP configuration, labeled K, to the partition function is

$$w_K = (2m)^{N_M} \left(\frac{1}{3}\right)^{N_{D1}+N_{D2}} \prod_x w(x) \prod_C w(C) \tag{6.33}$$

where N_M refers to the total number of monomers, N_{Dj} is the number of type j dimers ($j = 1$ single dimer, $j = 2$ double dimer), $w(x)$ is the specific weight of each type of point, and $w(C)$ is the weight of each loop present in the configuration. The equivalence with the original partition function (before configuration clustering) is straightforward.

We have conserved most of the notation of Karsch and Mütter, as their paper [109] is the base of this work.

Observables

The interesting observables in finite density QCD are those which signal a phase transition, namely the baryonic density and the chiral condensate.

i. The chiral condensate can be readily calculated using the expression

$$\left\langle \bar{\psi}\psi \right\rangle = \frac{1}{V} \frac{d \ln Z}{d\left(2m\right)} = \frac{\langle N_M \rangle}{2mV}, \tag{6.34}$$

which equals the monomer density up to a normalization constant. Here V represents the total volume.

ii. The baryonic density is related to the baryonic loops, winding k times around the lattice in the time direction

$$n = \frac{1}{3V_S}\frac{d\ln Z}{d(\mu)} = \frac{\sinh(3\mu k L_T)}{\cosh(3\mu k L_T) + \sigma(C)}, \tag{6.35}$$

and this quantity saturates as $\mu \to \infty$, for in that limit, $\cosh x \approx \sinh x \gg 1$. The factor V_S factor represents the spatial volume only, and the $1/3$ normalizes by the number of colors.

As there are negative weights in the partition function, we must evaluate these logarithms with care. Actually, what we are doing is taking the modulus in the measure, and introducing the sign in the observables

$$\langle \mathcal{O} \rangle = \frac{\langle \sigma_K \mathcal{O} \rangle_+}{\langle \sigma_K \rangle_+} \tag{6.36}$$

with σ_K the sign carried by the weight of the configuration K in the partition function sum. The symbol $\langle\rangle_+$ indicates that we are using the modulus of the measure.

Implementation

After a random configuration of monomers and dimers was generated, the updating schema of the algorithm was quite simple: It only tried to increase or decrease the occupation number of each site by transforming dimers connecting two sites x and y into two monomers, or two monomers belonging to neighbouring sites x and y into a dimer. It is clear that this approach slows down critically when taking the chiral limit. The reason is simple: In order to reach the configuration B of fig. 6.4 from configuration A, the system is forced to create monomers. But the probability of creating a pair of monomers is proportional to the square of the quark mass m. Thus, when close to the chiral limit, the system is doomed to stay in configuration A. In other words, the acceptance of the original algorithm drops to zero in the chiral limit.

This rendered the algorithm useless for small masses. Even if the chemical potential is ridiculously high, a system beginning in a completely random configuration never develops baryonic loops, if the fermion mass is small enough, but freezes in a bizarre configuration of dimers. Moreover, starting from a random configuration and simulating with a low mass, the system will be depleted of monomers soon. But this does not mean that all the monomers are eliminated. In fact, it might happen that, as the monomers are eliminated randomly, some monomers become *isolated*, I mean, without other monomers in their neighbourhood. The algorithm can neither eliminate nor move these monomers if the mass is too low, leading to persistent dislocations and point defects in the lattice. This behaviour derives in undesired defects in the lattice, that can not be eliminated.

The problem is accentuated with the cold configurations and the inclusion of fermionic loops, which are entities with great weights in the partition function. The only way to break a loop is to introduce a pair of monomers therein. Thanks to the m^2 factor, as $m \to 0$ the probability of breaking a loop becomes completely negligible, and the baryonic loops become superstable entities. This can lead to wrong results for the critical point, or to incredible large hysteresis cycles, as observed in [111].

Finally, the baryonic loops cannot interact among them in any way, unless they are first broken and then reconstructed. So two neighbouring loops of winding number $k = 1$ cannot become a loop of winding number $k = 2$ easily, and vice-versa. This fact implies that the loops

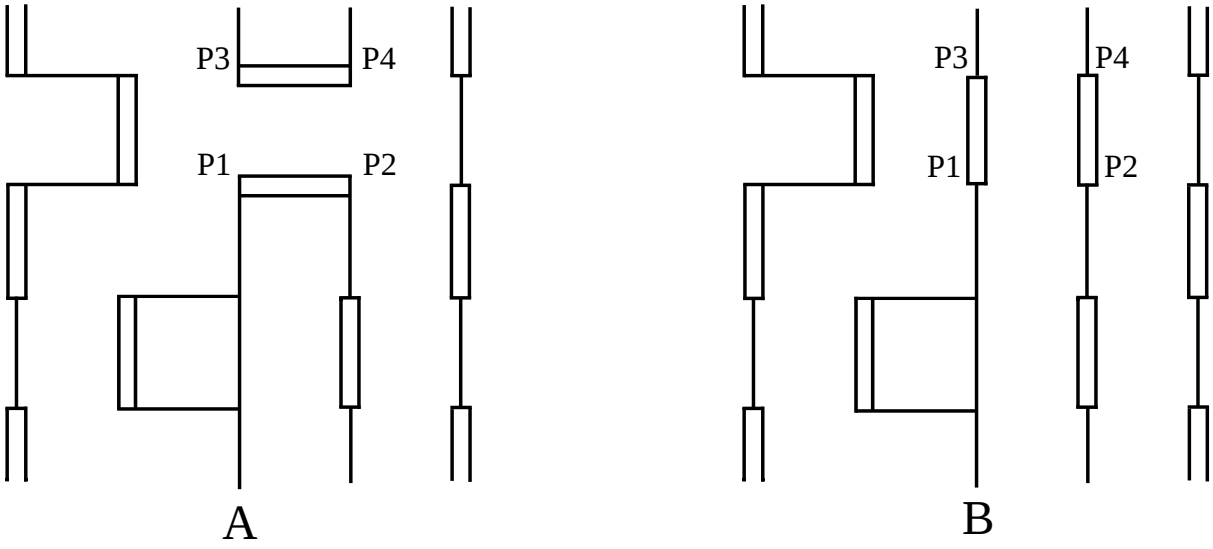

Figure 6.4: Example of bottleneck in the algorithm proposed by Karsch and Mütter. The probability of transition A→B should be large $O(1)$, for in B a new baryonic loop is created. Nonetheless, in order to go from A to B, the double dimers P1-P2 and P3-P4 must be destroyed. This is impossible if the mass $m \to 0$, and the system is frozen in the A state.

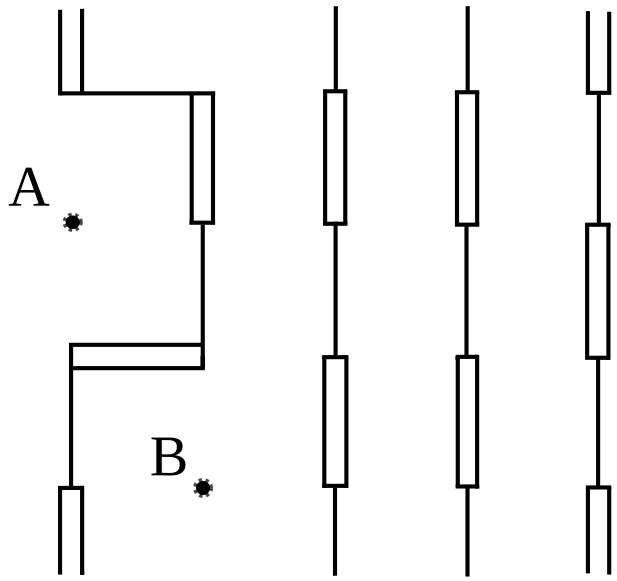

Figure 6.5: An almost saturated configuration of polymers (baryonic loops). Monomers A and B are not neighbours, so in order to eliminate them, the surrounding baryonic loops must be rearranged. This is quite unlikely to happen if the mass is very low and the chemical potential high, producing unexpected defects in the lattice.

of high winding number are rarely produced (by the dynamics of the simulation). Nevertheless, even at large masses, at some point one of these large baryonic loops with high winding number can be constructed by chance. Although the longer the loop, the higher the probability of being destroyed in the next Monte Carlo step, the great weight of loops with high winding number outcomes by far the increase of Monte Carlo attacks due to the length of the loop: They are superstable and non-interacting objects, which stay in our lattice during the whole simulation.

These loops are sometimes twisted in strange ways, wasting a large volume, and preventing the formation of new loops, even at great values of μ. This twisting truly can spoil simulation results, for the loops are not allowed to be deformed without being broken and rebuilt.

On the whole, the algorithm proposed by Karsch and Mütter is bound to lead to many artifacts, which are not related to the polymerization formulation of QCD at strong coupling, but on the particular implementation of this polymerization on the computer. We expect to obtain relable results with this algorithm only for largely massive fermions $m \approx 1$. For large masses, however, the sign problem does not seem to be relevant [120].

Indeed this naive implementation was used by Rossi and Wolff, and Karsch and Mütter; and their results, albeit remarkable, are far from satisfactory. The whole idea of combining polymerization of the fermionic action with the clustering of configurations to remove the sign problem is brilliant, but the implementation at that time was poor. This is what we tried to fix.

6.4 The Improved Monomer-Dimer-Polymer ($IMDP$) algorithm

It is clear that we need a proposal to modify the configuration which can deal with these bootlenecks. At first, one can think of keeping the dimer $\leftrightarrow$ monomer modification and try to perform several changes around a site before the metropolis accept/reject step. This enhacenment decreases the locality, and therefore, the acceptance rate, but it should improve the ergodicity. It happens that the decrease in the acceptance rate is too large (at some point in our simulations, it would drop to zero) to be considered a feasible solution. The only remaining possibility is to play with dimers.

The first modification, allows a single monomer to be displaced freely around the lattice by rotating a dimer of an opposite point around (see fig. 6.6). This possibility allows two freshly created monomers to be separated, and two distant monomers to be rejoined. The probability of this kind of modification to happen is of order $O(1)$ (unless the creation or annihilation of fermionic loops is involved).

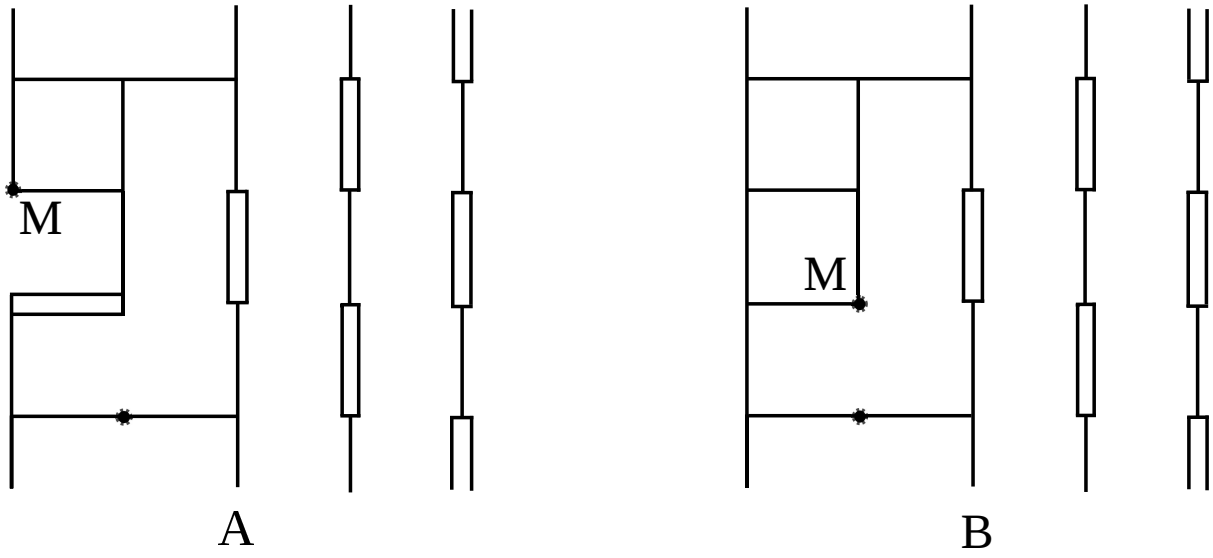

Figure 6.6: An example of monomer displacement. The monomer M moves freely around the allowed sites, and after one montecarlo step is in position to annihilate with the other lonely monomer, removing the point defects of the lattice.

This solves the problem of the isolated monomers.

Our second proposal deals with only dimers, and thus it becomes quite handy when dealing with small, or even vanishing masses. A dimer is allowed to be displaced around any closed path in this formulation, and we choose the simplest closed path (the plaquette) as proposal to modify configurations, as any other larger closed path can be constructed from plaquettes. Again, the probability of accepting the new configurations generated using this modification is of order $O(1)$, if the baryonic loops do not enter in the calculus. This way, the problem of the chiral limit is solved, and the ergodicity of the algorithm, almost completely restored.

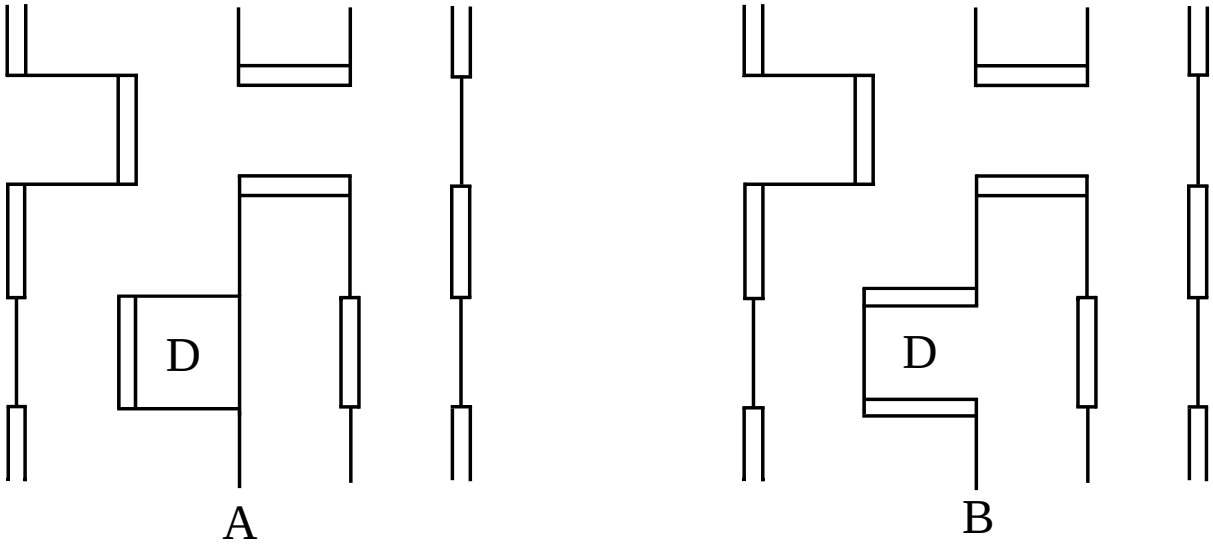

Figure 6.7: An example of dimer rotation around a closed path. The difference between A and B lies in the loop marked as D. Example 6.4 can also be solved without creating monomers in two steps of dimer rotations.

The last modification deals with the lack of interaction among baryonic loops. It would be interesting to be able to split or merge neighbouring loops, as the modulus of the weight of the configurations with the loops merged/splitted is of the same order of magnitude[7], but the modifications proposed up to now require the participant loops to be broken and then rebuilt. Taking into account the high weight of a baryonic loop, this represents a significant bottleneck in the simulation procedure.

Thence, the following merge/splitting options where added. In fact, this modification also enables the algorithm to deform existing loops, by combination of spatial loops baryonic loops with temporal loops. Thanks to this last modification, loops of very high winding number can be created and destroyed at ease by the algorithm. Indeed we observed non-permanent loops of large winding numbers (≈ 50) in our simulations.

The probability of all these modifications is (in most cases) of order $O(1)$, that is why they are so important. At high masses, they compete with the original dimer $\leftrightarrow$ monomers transformation of Karsch an Mütter, but at low masses, they become dominant and rule the dynamics of the system.

IMPD vs Worm Algorithm

The similarities of these modifications with the worm algorithm are, at least, notorious. It seems that we have implemented some sort of worm algorithm without worms, i.e., without

[7]If the loops merged are both temporal loops, the sign of the configuration might change after this modification. This enhancement of sign switching, which is necessary for ergodicity, might play against us later.

open chains. All the configurations generated by our procedure are physical, opposing what happens in the worm algorithm. This similarity is, surprinsingly, completely accidental. In fact, we learned on the worm algorithm after developing these modifications. We would probably have used the worm algorithm directly to treat the MDP model (as Ph. de Forcrand did in [112, 117]) if we had known about it.

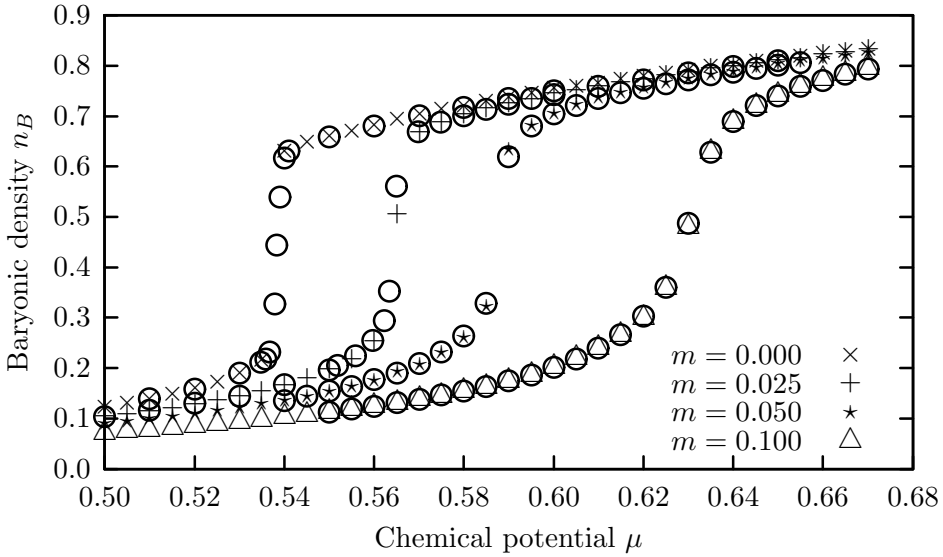

Figure 6.8: Comparison of our results to those of Philippe de Forcrand in [112]. Ph. de Forcrand results are always marked in circles. The agreement is good within errors, being the errorbars smaller than symbols. To obtain the plotted data, we used 100000 thermalization steps, followed by 100000 measurement steps.

The question of which of the two, the worm algorithm or our approach, bests the other in numerical simulations is not very important. As they are based in similar principles, we expect both of them to perform almost equally, after doing the corresponding optimizations. And we expect both of them to share the same problems in the same situations. We have, however, to give the worm algorithm an edge when it comes to computing correlation functions, for the non-physical configurations generated during the update procedure of the worm algorithm become quite handy for this task.

Numerical results

We performed simulations at several volumes to check whether the sign problem was a real issue on this model or not, mainly in the chiral limit (for high values of the mass, the Karsch and Mütter algorithm should work properly). Our simulations were performed starting from a cold configuration (system filled up with baryonic loops, $n_B = 1$, and high initital value of the chemical potential μ, that decreases along the simulation), and from a hot configuration (system empty of loops, $n_B = 0$, and a low value of μ, increasing as the simulation goes on). We left the system thermalize for 1000000 iterations, allowing it to relax to a new configuration, and then performed measurements in 200000 montecarlo steps. The results for the smaller volume began to reveal a sign problem after the introduction of our modifications of the algorithm, although for $V = 4^4$ only in a small region of μ's the average sign takes problematic values.

This behaviour contrasts with the disparition of the sign problem for high values of μ observed in the old algorithm. The reason why the sign problem was tractable in the original work of Karsch and Mütter is the fact that the system easily saturates with baryonic loops, and there is only one saturated state, which carries a positive weight. If the system spents most of

the time in this state, the mean sign will take high values. In fact, the system usually stays in the saturation state forever, unless the chemical potential is reduced.

In our simulations, the system did not always succeeded in finding a saturated state, due to the presence of dislocations and strange geometries for the loops, allowed by the new improvements of the algorithm. It stayed in an *almost* saturated state, where the system evolved quite slowly, for there was no room in the configurations to propose modifications without breaking a large number of baryonic loops. So at first glance, the improvements in the ergodicity of the algorithm turn out to *increase* the severity of the sign problem, or at least, the extension of the region where it appears.

The saturated (or almost saturated) state seems a finite volume effect, rather than a physical property of QCD [101]. In fact, after increasing the spatial volume we observe how the saturation effect is relaxed, and the mean sign drops.

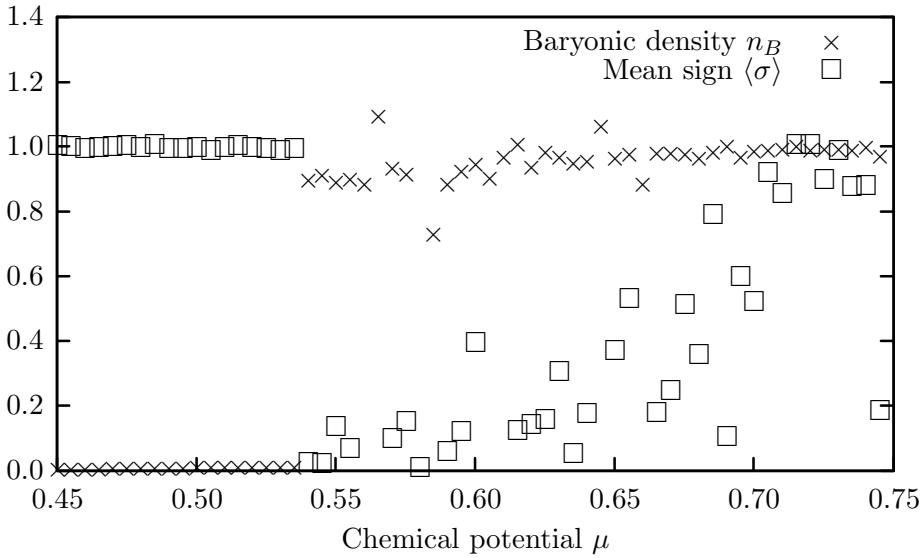

Figure 6.9: Baryonic density and mean sign for 4^4 volume at zero mass, hot start. The system does not saturate completely, probably because some long-lived complex loop structures are created. This allows a sign flipping, even at very high $\mu's$. Errors are not shown to improve readability, but they are smaller than symbols in those regions where the mean sign $\langle\sigma\rangle \sim 1$ and huge where $\langle\sigma\rangle$ is small or fluctuates strongly.

The explanation of the lowering of the mean sign value as the spatial volume increases is quite intuitive: As μ increases, baryonic loops are more likely to be created and stay. Nonetheless, these loops have a higher life expectancy if they are packed. This is because, in order to destroy a loop inside a pack of loops, we usually need to mess with the neighbouring loops. Since those loops have quite large weights, proportional to $\cosh(3L_T\mu)$, the greater the number of loops involved in the modification of the configuration, the harder to destroy them. In other words, the loops which are close together protect each other. So the loops tend to pack, and the straight loop (which carries a positive weight) is the best loop for packing, achieving a greater loop density. But the loops at the boundaries of the pack are more exposed to modifications, deformations and annihilation. These boundary loops change easily of shape, and so does the sign associated to them, that keeps flipping during the simulation. Indeed, for very large volumes, the saturation state is difficult to reach, for the loops tend to disorder, merge and arrange in complicated geometrical ways. Dislocations and defects are produced, and the system never saturates. It seems that the loop entropy plays a role here.

The saturation also introduces large autocorrelation times in the simulations, slowing down

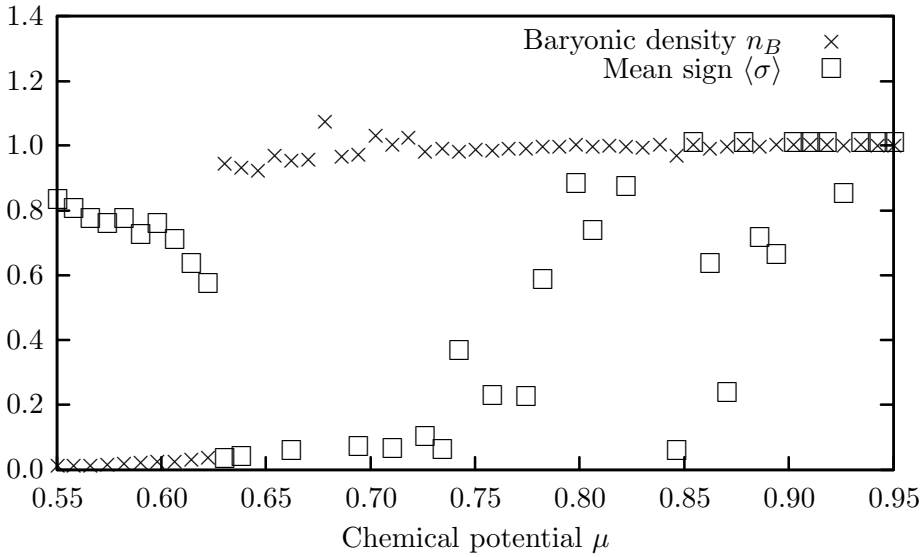

Figure 6.10: Baryonic density and mean sign for $8^3 \times 4$ volume at zero mass, hot start. Only when the system saturates completely $\mu \sim 0.87$, the mean sign stops fluctuating wildly. Errors are not shown to improve readability, but they are smaller than symbols in those regions where the mean sign $\langle\sigma\rangle \sim 1$ and huge where the $\langle\sigma\rangle$ is small or fluctuates strongly.

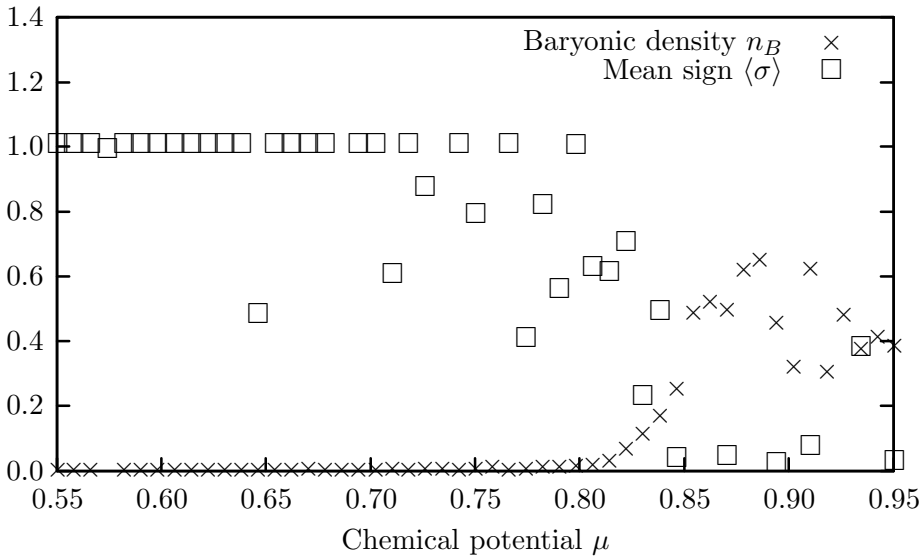

Figure 6.11: Baryonic density and mean sign for 8^4 volume at zero mass, hot start. The system does not saturate at the μ values simulated, and the mean sign fluctuates without control, mostly after the critical chemical potential $\mu \sim 0.8$ has been reached. Errors are not shown to improve readability, but they are smaller than symbols in those regions where $\langle\sigma\rangle \sim 1$ and huge where $\langle\sigma\rangle$ is small or fluctuates strongly.

the measurements. Almost saturated states show great stability, leading to highly correlated measurements. This is a point where one might expect the worm algorithm to perform better than ours, but the advantage is not very clear, for each time the worm algorithm creates a new valid configuration, non-local modifications are introduced, and when the system is in an almost saturated state, these modifications are bound to involve many loops, and therefore, to be discarded[8].

[8]The low autocorrelation times shown in [112] happen at very high temperatures $L_T = 2$, where the barynonic

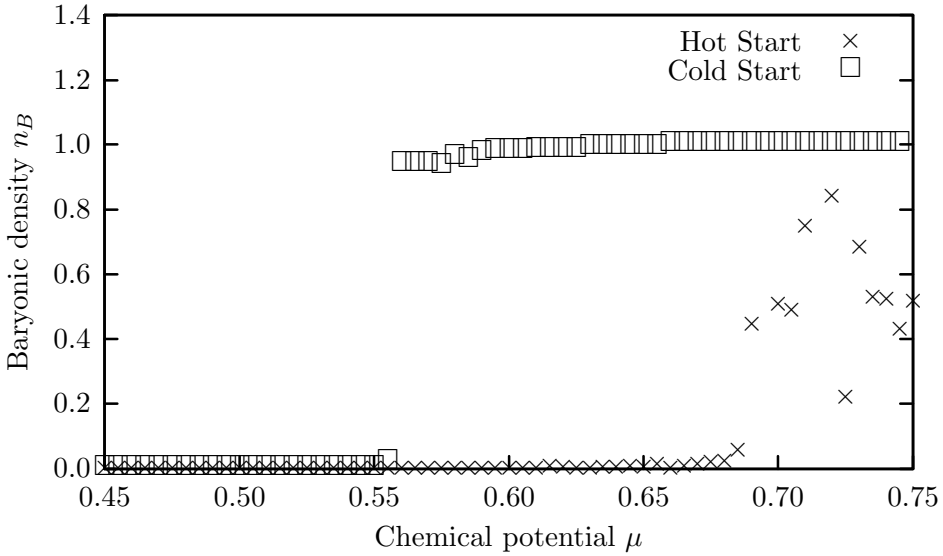

Figure 6.12: Hysteresis cycle for 6^4 at zero quark mass. The cycle is greatly reduced with respect to [111]. The errorbars are not plotted to improve the readability of the figure. These are smaller than symbols in the saturated ($n_B = 1$) and empty (no loops, $n_B \sim 0$) states, and incredibly large in the region in between. The simulation starting from a hot configuration never reaches the saturation state due to the presence of dislocations and complex structures of loops.

Another feature of this model is the hystheresis cycle it presents. The hysteresis cycle was first observed and discussed in [111]. In our improved algorithm, it is greatly reduced, but it exists as well. This large hysteresis seems related to the saturation of loops as well: The saturation state is superstable, and any modification aimed to destroy it must either create a pair of monomers, which is a quite improbable process for low masses, or destroy several loops at the same time.

This two features, (i.) a superstable saturated state produced by a finite spatial volume effect, and (ii.) the presence of a severe sign problem in the region close to the critical value of μ, makes us conclude that this model does not solve in any way the sign problem for QCD at finite density. However, all these effects are relaxed for very high temperatures, where the weight of the loops is greatly reduced, and the model works well, as fig. 6.8 shows. This is not a great deal, and there are other procedures which also work at high temperatures for any value of β [121].

6.5 Conclusions

The MDP model developed by Karsch and Mütter was quite successful at solving the sign problem in a polymer formulation of QCD at $\mu = 0$ and for non-zero masses. As this system seemed quite manageable, the extension to $\mu \neq 0$ was mandatory; unluckily the original MDP implementation suffered from ergodicity problems at small values of the mass, which only allow the system to live in two distinct states: Either complete saturation or complete depletion of baryonic loops. Each one of those states does not suffer from the sign problem, this is quite evident in the depleted configuration, and almost trivial in the saturated one: In order to saturate the lattice, only the simplest loops (the straight ones) are allowed. These loops are the

loops are easy to break, and our algorithm is also expected to perform well.

most important contribution to the partition function, and carry positive weights. Thence, no sign problem seems to appear in the MDP model.

Nonetheless, once the ergodicity problem has been solved by improving the simulation algorithm, this picture changes. Now there are more allowed states, and these states need not be positive-weighted. In order to see this effects we need large volumes, for the system sees the walls[9] of our box very soon. This last point 'solves' the sign problem for small volumes and low temperatures[10], because it leads to saturation of baryonic loops, but this is an unrealistic effect which leads to unrealistic results [101, 102, 103]. If the volume becomes larger, we see a bunch of baryonic loops in the center of our box, but the borders are empty, and the system is not saturated, but free to evolve. As the loops can move and change its shape at the borders, and at large μ the loops carrying negative weight are as important as the ones which carry positive weight, both kind of loops are expected to be created and destroyed at the border of the box, leading to a severe sign problem. If, on the contrary, the volume is too small, the system saturates easily. As in total saturation, only positive loops are allowed, the sign problem dissapears. But this is rather a finite volume effect.

Every advocate of this model wields the same argument to defend the model, and to explain why it works: The positive-weighted loops are more important than the negative counterparts in the partition function, so eventually, the positive-weighted loops will take over, and the sign problem will disappear. This argument is quite naive. The larger weight of the positive-weighted loops might not be enough to overcome the sign problem. In fact, the positive-weighted loops must have weights much larger than those of the negative-weighted loops in the thermodynamic limit if we want to see a mean sign different from zero, and for sure this is not the case of the MDP model as the temperature $T \to 0$ while $\mu \neq 0$. This fact can be checked in a very simple model featuring a severe sign problem.

Imagine a linear chain of non-interacting spins. Each spin can point either upwards or downwards, as in the Ising model. If a spin points upwards, it contributes with a factor $p > 0$ to the configuration weight, and if it points downwards, it contributes with a factor $q < 0$. Let $p - q = 1$ to normalize those probabilities, and let us try to compute the mean sign $\langle \sigma \rangle$ of this model for a given volume V:

$$\langle \sigma \rangle = \left(\frac{p+q}{p-q} \right)^V = (p+q)^V .$$

As $p+q < 1$ always, the mean sign (and Z itself) exponentially vanishes in the thermodynamic limit. It does not matter how greater is p against $|q|$ (take for instance values $p = 0.99$ and $q = -0.01$), the sign problem is severe, unless, in an effective way

$$\lim_{V \to \infty} \left| \frac{q}{p} \right| = 0$$

For this to happen, the ratio q/p must become small as the volume increases. Imagine that

$$p = 1 - \kappa V^{-\alpha} \qquad q = -\kappa V^{-\alpha},$$

being α an arbitrary number higher than zero. Then the mean sign would become

[9] For the (anti-)periodic boundary conditions used in this work, there are no walls, but nonetheless the system sees itself through the boundary, and finite volume effects become important.

[10] At high temperatures (small L_T) the MDP model work well in general, giving high values for the mean sign. The temperature can be fine tuned using a parameter, introduced in the original paper of Karsch and Mütter [109]. As we wanted to perform simulations at zero temperature, we have not included this parameter in this work, although Ph. de Forcrand made use of it [112, 117].

$$\langle\sigma\rangle = \left(1 - 2\kappa V^{-\alpha}\right)^V = \left[\left(1 + \frac{1}{-\frac{V^\alpha}{2\kappa}}\right)^{-\frac{V^\alpha}{2\kappa}}\right]^{-2\kappa V^{1-\alpha}} = e^{-2\kappa V^{1-\alpha}}.$$

For $\alpha > 1$, $\langle\sigma\rangle \to 1$ in the thermodynamic limit, and there is no sign problem at all. For $\alpha = 1$ the sign problem can be handled in the infinite volume limit, as $\langle\sigma\rangle \to$ tends to a fixed value. If $1 > \alpha > 0$, the sign problem is *almost* exponentially severe, and can be treated by using the theory of the modulus, i.e., taking all the weights as positive and hoping that the resulting theory is equivalent to the original one in the thermodynamic limit; and this is what happens indeed, although the convergence might be slow. Only in the case $\alpha = 0$ the mean sign goes to zero exponentially with the volume. In the case of the MDP model, the loops carrying negative weights are almost as simple as the positive ones, and have weights which are almost equally large. If the configurations carrying positive weights took over the negative ones, the theory of the modulus would be equivalent to the original theory. But we know for sure that this is not the case: the negative weights in the configurations come from the loop expansion of the fermionic determinant, and are necessary in order to reproduce correctly the anticommutation rules. As we expect at very high densities the quark dynamics to be ruled mostly by Fermi-Dirac statistics, it is quite natural to find a severe sign problem in this formulation. In the $\mu = 0$ case, the model has the same problem, but the fermionic cancelations are introduced by hand explicitly, thence it can be simulated. If we removed these cancellations, and took the modulus of the resulting theory (dropping the sign on the negative weighted configurations), then the resulting theory would feature hard-core bosons[11] instead of fermions. Therefore, the theory of the modulus can not be equivalent to the original one. On the whole. things seem to be more complicated than what the advocates of this model defend.

The failure of the MDP model, showing a severe sign problem for $\mu \neq 0$, is a heavy blow to the finite density QCD practitioners. However, there are other possibilities, some of them open only to discrete systems, that we have not explored: Merom algorithms, a refinement of the clustering techniques, or the addition of other terms to the action which, in combination with clustering, might help reduce the sign problem. That is why we should keep investigating these models.

[11] A hard-core boson is a field ϕ with Bose statistics, but verifying a nilpotency rule $\phi^2 = 0$.

Chapter 7

Algorithms for the pure gauge action

"Calculation never made a hero."
—John Henry Newman

Although the $MDP-QCD$ does not work very well for $\mu \neq 0$, it can be taken as an alternative for fermion simulations at zero chemical potential. Since the MDP model escapes from the computation of the determinant, it should represent a great algorithmic advance for simulating fermions on a lattice. Moreover, for non-zero μ, there are still some unexplored possibilities (like mixing merom cluster algorithms with this formulation) that can reduce the severity of the sign problem. Nevertheless, the model has an important drawback which constrains its range of application: It is only valid at strong coupling. As the continuum limit of QCD lies in the weak coupling limit, this restriction can not be regarded slightly, and must be faced seriously, if we aspire to make from the MDP approach a competitive model for QCD. In other words, we need to treat the gauge action.

One way to confront the problem is to mimic the procedure applied to fermions, i.e., (i.) the expansion of the fermionic action and (ii.) the integration of the Grassman variables to yield a set of graphs, and try to apply this method to the pure gauge action. We can expand the gauge exponential in β powers, and integrate the link variables of each term of the expansion.

In fact, this procedure defines a general transformation of the terms of the partition function which can be applied to any model. This transformation maps a continuous system into a discrete one, usually with a sign problem, except for some particular cases. Nonetheless, there are several techniques, ready to be applied to discrete systems, which might reduce or even solve completely the sign problem, like configuration clustering, or the merom algorithm, yet the integration of the latter with polymeric models remains unexplored.

Another advantage of the simulations of these discrete systems –when compared to their standard counterparts- is the fact that, when it comes to fermions, they become *fast*. In the former section, devoted to the MDP model of Karsch and Mütter, we transformed a rather heavy computational object, the fermionic determinant, into a set of balls and sticks (monomers and dimers), and as we will see, the graphs do not get much more complicated when we introduce gauge fields.

Thence, although the polymeric models at this point are not completely developed, for they must face a sign problem in order to be useful for the lattice community, there are many possibilities in the horizon to fix this caveat. It is reasonable to start the research on the gauge part of the action, and try to reconcile it with the fermionic part.

7.1 The strong coupling expansion for Abelian groups

To begin with, we consider only abelian groups. Of course, we are interested in applying this ideas to $SU(3)$ in the end, but in order to develop a systematic method to construct the graphs, we decided to start from the easiest models we could. These are the $U(1)$ and Z_n gauge field theories on the lattice, formulated with the usual Wilson action

$$S_{PG} = -\mathrm{Re}\left[\beta \sum_{n,\mu,\nu\mu<\nu} U(n)_\mu U(n+\hat{\mu})_\nu U^\dagger(n+\hat{\nu})_\mu U(n)^\dagger_\nu\right] =$$

$$-\frac{\beta}{2}\sum_{k=1}^{N_P}\left(U_k + U_k^\dagger\right), \tag{7.1}$$

where k indexes the N_P plaquettes of the lattice, and U_k and $U_k^\dagger$ are the oriented product of gauge fields around the plaquette k, and its complex conjugated, which I will call *anti-plaquette*. The partition function can be expanded in powers of the inverse of the coupling β

$$Z = \int [\mathcal{DU}] \prod_{k=1}^{N_P} e^{\frac{\beta}{2}\left(U_k + U_k^\dagger\right)} = \int [\mathcal{DU}] \prod_{k=1}^{N_P} \left\{ \sum_{n=0}^{\infty} \frac{\left(\frac{\beta}{2}\right)^n}{n!} \left(U_k + U_k^\dagger\right)\right\} =$$

$$\int [\mathcal{DU}] \prod_{k=1}^{N_P} \left\{ \sum_{n=0}^{\infty} \frac{\left(\frac{\beta}{2}\right)^n}{n!} \left[\binom{n}{j} (U_k)^j \left(U_k^\dagger\right)^{n-j}\right]\right\} =$$

$$\int [\mathcal{DU}] \prod_{k=1}^{N_P} \left\{ \sum_{j_1,j_2=0}^{\infty} \frac{\left(\frac{\beta}{2}\right)^{j_1+j_2}}{(j_1+j_2)!} \left[\binom{j_1+j_2}{j} (U_k)^{j_1} \left(U_k^\dagger\right)^{j_2}\right]\right\}. \tag{7.2}$$

The next step consist on the expansion of the product over the plaquettes, to find a sum over products of different powers of the plaquettes, multiplied by constant factors. After this expansion has been done, the integration of each summand of plaquettes can be carried out just by following the group integration rules: *The integral of every non-trivial product of links is zero.* In other words, the only surviving terms are those where each plaquette U_k is, either annihilated by its corresponding anti-plaquette $U_k^\dagger$, or belongs to a close surface of oriented plaquettes[1]. In the case of the Z_n groups, the n-th power of a (anti-)plaquette is non-trivial as well[2]. Thus, we can label each term of the expansion with two numbers $(n_k^\alpha, \bar{n}_k^\alpha)$, being α a labels referring to a specific term in the expansion, k the label for the plaquette on the lattice, and consequently, n_k^α (or $\bar{n}_k^\alpha$) the power of the k plaquette U_P (or anti-plaquette $U_P^\dagger$) in the term α of the product expansion. After integration, the partition function is a sum of different terms indexed by α,

$$Z = \sum_{\alpha\in\mathcal{C}} C^\alpha(\beta), \tag{7.3}$$

[1] By oriented I mean that half of the faces are plaquettes, and the other half anti-plaquettes, placed in a certain way to ensure that every link is annihilated.

[2] This non-triviality of the n-th power of a link was the origin of baryons in the MDP model. We expect any Z_n gauge theory to feature baryons composed of n quarks as well.

with $\mathcal{C}$ standing for the space of graphs (the different summand terms in the partition function). The particular value of $C^\alpha(\beta)$ is given by the group integration of the term α of the expansion, and its result can be computed analytically

$$C^\alpha(\beta) = \prod_k \frac{\beta^{n_k^\alpha + \bar{n}_k^\alpha}}{2^{n_k^\alpha + \bar{n}_k^\alpha} n_k^\alpha! \bar{n}_k^\alpha!}. \tag{7.4}$$

The key point underlying this expansion (and the MDP one) is the interpretation of these C^α as configurations of a new system, equivalent to the original one. Each configuration α is given by the set of numbers $(n_k^\alpha, \bar{n}_k^\alpha)$, and its probability is given by $w^\alpha = C^\alpha/Z$. Montecarlo simulations can be performed in this configuration space, instead of using the original one.

The configurations are translated in our lattice into a set of closed surfaces of plaquettes and anti-plaquettes. The simplest closed surface that we can imagine on the lattice is the cube, and we can regard any other closed surfaces as a particular spatial arrangement of cubes. This is one of the most beautiful properties of this algorithm: The fact that it allows a geometrical interpretation. We can think of a lattice where there are open surfaces made of plaquettes and antiplaquettes, closed surfaces (volumes) and other more complex structures, evolving as time goes by. To create, destroy and modify these surfaces in all the imaginable ways, we only need two transformations acting as building blocks for the $U(1)$ group, and three for the Z_n groups[3]:

(i.) The transformation $(n_k^\alpha, \bar{n}_k^\alpha) \to (n_k^\alpha + 1, \bar{n}_k^\alpha + 1)$, and its inverse (when $n_k^\alpha, \bar{n}_k^\alpha > 0$) $(n_k^\alpha, \bar{n}_k^\alpha) \to (n_k^\alpha - 1, \bar{n}_k^\alpha - 1)$. This transformation creates a pair plaquette/anti-plaquette at a given place k of the lattice.

(ii.) The addition of a closed cube of oriented plaquettes, for dimensions higher than two. Any closed surface can be constructed by adding cubes and removing the touching faces using the first transformation.

(iii.) In the case of a Z_n group, the addition of n plaquettes or anti-plaquettes to the same place k, that is, $(n_k^\alpha, \bar{n}_k^\alpha) \to (n_k^\alpha + n, \bar{n}_k^\alpha)$ or $(n_k^\alpha, \bar{n}_k^\alpha) \to (n_k^\alpha, \bar{n}_k^\alpha + n)$. This transformation keeps the rule $n_k^\alpha = \bar{n}_k^\alpha \pmod n$.

A Monte Carlo designed with these transformations for the configurations can generate almost any possible configuration; the only exception are the plaquette foils, which will be treated later. The efficiency of our particular implementation will be compared against the standard heat-bath algorithm.

We must be careful with the implementation of cubes. In three dimensions, there is only one possible cube per lattice site[4], and the orientation of the plaquettes does not matter, providing the gauge links are annihilated as the Bianchi identity dictates (if there is a plaquette in one face, there must be an anti-plaquette in the opposing face). But in four dimensions, there are four possible cubes per lattice site. The orientation of the plaquettes of the first cube can be chosen arbitrarily, as long as we comply with the Bianchi identity (in which face there is a plaquette, and in which face there is an antiplaquette), but this imposes constraints in the orientation of the other three cubes, for they share common faces. All the cubes must have consistent orientations.

[3]The addition or removal (when possible) of a single surface of plaquettes or anti-plaquettes which wraps around the lattice should be an allowed transformation as well; however, this is a finite volume correction, and we decided to ommit it in the simulation program.

[4]Assuming a cubic lattice.

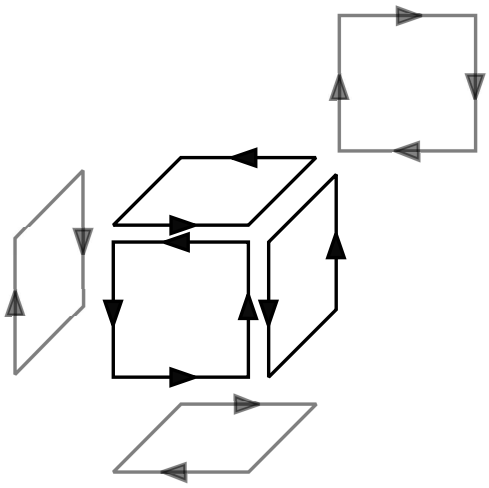

Figure 7.1: Fixing the orientations of the plaquettes for a single cube. Once a face is locked in orientation, its opposite face must be inversely oriented.

7.2 Measuring observables

The computation of observables is quite easy in this representation. The definition of the observable plaquette[5] is

$$\langle P_\square \rangle = \frac{1}{N_P} \partial_\beta \ln (Z) \tag{7.5}$$

Using (7.3) and (7.4), we obtain

$$\langle P_\square \rangle = \frac{1}{N_P} \partial_\beta \ln \left(\sum_{\alpha \in \mathcal{C}} C^\alpha \right) = \frac{1}{N_P} \frac{1}{Z} \sum_{\alpha \in \mathcal{C}} \frac{(n^\alpha + \bar{n}^\alpha)}{\beta} C^\alpha \tag{7.6}$$

with

$$n^\alpha = \sum_{k=1}^{N_P} n_k^\alpha \qquad \bar{n}^\alpha = \sum_{k=1}^{N_P} \bar{n}_k^\alpha$$

The quantity C^α / Z is the probability w^α of each configuration α. The mean of the observable plaquette is then

$$\langle P_\square \rangle = \frac{1}{\beta N_P} \sum_{\alpha \in \mathcal{C}} w^\alpha \, (n^\alpha + \bar{n}^\alpha) \tag{7.7}$$

that is to say, the observable plaquette is equal to the mean value of the sum of the occupation numbers n^α plus $\bar{n}^\alpha$, divided by β and normalized by N_p.

Another interesting observable is the specific heat:

$$C_V = \partial_\beta \langle P_\square \rangle \tag{7.8}$$

We can profit from the previous expression of $P_\square$ (7.7) to find the following equation

[5] We must remark that the observable plaquette and the plaquettes living in our lattice are not the same, although they are strongly related. The observable plaquette refers to the minimal Wilson loop, whereas the plaquettes refers to geometric entities, living on the lattice. In order to keep the discussion clear, we will always refer to the minimal Wilson loop as *observable plaquette*.

$$C_V = \frac{1}{N_P}\left\{\sum_{\alpha\in\mathcal{C}} w^\alpha \frac{(n^\alpha+\bar{n}^\alpha)^2}{\beta^2} - \left(\sum_{\alpha\in\mathcal{C}} w^\alpha \frac{(n^\alpha+\bar{n}^\alpha)}{\beta}\right)^2 - \right.$$

$$\left.\sum_{\alpha\in\mathcal{C}} w^\alpha \frac{(n^\alpha+\bar{n}^\alpha)}{\beta^2}\right\} = N_P\left[\left\langle P_\square^2\right\rangle - \langle P_\square\rangle^2 - \frac{N_P^2}{\beta}\langle P_\square\rangle\right] \tag{7.9}$$

Sometimes, it is interesting to compute correlation observables, such as the Wilson loop (larger than the single observable plaquette), or the plaquette–plaquette correlation function. To compute these it will prove helpful to introduce a pair of variable coupling constants $\{\beta_k, \bar{\beta}_k\}$, which depend on the plaquette site k, in such a way that the partition function reads now

$$Z(\beta_j,\bar{\beta}_j) = \int [dU] \prod_k e^{\left(\frac{\beta_k}{2}U_k + \frac{\bar{\beta}_k}{2}U_k^\star\right)} \tag{7.10}$$

The weight of the configurations changes accordingly

$$C^\alpha(\beta_j,\bar{\beta}_j) = \prod_{k=1}^{N_P} \frac{\beta_k^{n_k^\alpha}\bar{\beta}_k^{\bar{n}_k^\alpha}}{2^{n_k^\alpha+\bar{n}_k^\alpha}\left(n_k^\alpha!\right)\left(\bar{n}_k^\alpha!\right)} \tag{7.11}$$

Now the correlation functions or the Wilson loops are computed by simple derivation, and then taking all the β_k, $\bar{\beta}_k$ to the same value. For instance, the 2×1 Wilson loop can be calculated as

$$\langle P_{W_{2\times 1}}\rangle = 2^2 \lim_{\beta_j,\bar{\beta}_j\to\beta} \frac{\sum_{\alpha\in\mathcal{C}} \partial_{\beta_k}\partial_{\beta_{k+1}} C^\alpha\left(\beta_j,\bar{\beta}_j\right)}{\sum_{\alpha\in\mathcal{C}} C^\alpha\left(\beta_j,\bar{\beta}_j\right)} =$$

$$2^2 \sum_{\alpha\in\mathcal{C}} \frac{n_k^\alpha n_{k+1}^\alpha}{\beta^2} w^\alpha \tag{7.12}$$

where k and $k+1$ are contiguous plaquette sites. The generalization of this result to larger planar Wilson loops is straightforward. Indeed, the expectation value of any planar Wilson loop can be computed as the mean value of the product of the occupation numbers of the plaquettes enclosing the loop, multiplied by a factor $2/\beta$ to a power which is the number of plaquettes involved. This observable is quite remarkable, for it is computed as a product of occupation numbers, and features a $(2/\beta)^{Area}$ factor, which eventually may become exponentially large or small as the size of the loop increases. All these particular facts render this observable hard to compute, as we will see in the numerical results.

In the same way we can also obtain the correlation functions for two arbitrary plaquettes on the lattice:

$$\langle U_k U_l\rangle = 2^2 \lim_{\beta_j,\bar{\beta}_j\to\beta} \frac{\sum_{\alpha\in\mathcal{C}} \partial_{\beta_k}\partial_{\beta_l} C^\alpha\left(\beta_j,\bar{\beta}_j\right)}{\sum_{\alpha\in\mathcal{C}} C^\alpha\left(\beta_j,\bar{\beta}_j\right)} = 2^2 \sum_{\alpha\in\mathcal{C}} \frac{n_k^\alpha n_l^\alpha}{\beta^2} w^\alpha \tag{7.13}$$

and

$$\langle U_k U_l^*\rangle = 2^2 \lim_{\beta_j,\bar{\beta}_j\to\beta} \frac{\sum_{\alpha\in\mathcal{C}} \partial_{\beta_k}\partial_{\bar{\beta}_l} C^\alpha\left(\beta_j,\bar{\beta}_j\right)}{\sum_{\alpha\in\mathcal{C}} C^\alpha\left(\beta_j,\bar{\beta}_j\right)} = 2^2 \sum_{\alpha\in\mathcal{C}} \frac{n_k^\alpha \bar{n}_l^\alpha}{\beta^2} w^\alpha \tag{7.14}$$

These expressions are quite analogous to the formulae derived for the Wilson loop.

Finally from (7.13) and (7.14), and taking into account the symmetry of the model, we can write:

$$\langle \mathrm{Re}U_k \mathrm{Re}U_l \rangle_c = \frac{1}{\beta^2} \langle (n_k + \bar{n}_k)(n_l + \bar{n}_l) \rangle - \langle n_k + \bar{n}_k \rangle \langle n_l + \bar{n}_l \rangle \quad (7.15)$$

$$\langle \mathrm{Im}U_k \mathrm{Im}U_l \rangle_c = -\frac{1}{\beta^2} \langle (n_k - \bar{n}_k)(n_l - \bar{n}_l) \rangle \quad (7.16)$$

where the brackets denote average over configurations.

Plaquette foils and topology

There is an allowed object we have not make used of in our expansion: A foil of (anti-)plaquettes, forming a surface, which wraps around itself through the boundary conditions. It is an object containing roughly L^2 plaquettes, with L the length of our lattice, and thence, the probability of creating such an object is negligible for $\beta < 2$ as $V \to \infty$. For higher values of β however, this objects become important. The problem is the fact htat we can not generate such a plaquette sheet using cubes and standard plaquettes. We can only create pairs of sheets[6]. We might whink at first that this difference might give some contribution, but as we expect to create the same number of foils and anti-foils[7], the contribution should cancel out. If we have chosen to remove the sheets from our simulation programs is because they lead to important finite volume effects, related to those happening in the heat-bath [122]: if a sheet is created during a simulation, and it is deformed by the addition of plaquettes and cubes, it might be quite hard to remove, slowing down the simulation critically. As the contribution of these foils should not be important (they take the system to a *local* minimum), it is better to left them behind.

Numerical work

In order to see our algorithm (which we should call, from now on, *geometric algorithm*) at work, we have performed numerical simulations of several lattice gauge theory systems in three and four dimensions. Our aim is to check the goodness of our approach, comparing the results we obtain using the geometric algorithm with those coming from more standard ones; hence we want to compare the properties of the algorithm itself, in terms of numerical efficiency and autocorrelation times with, for example, the usual heat-bath algorithm. We have in mind the results of [123], where it was claimed that, with a similar algorithm, at a second order critical point in a non-gauge system, there is a very strong reduction in the critical slowing down.

Let us start with the three dimensional U(1) lattice gauge model: this model is known to have a single phase from strong to weak coupling. We have chosen to measure two simple observables, namely the plaquette observable and the specific heat, following the definitions given in the preceeding Section. We have simulated the model with our algorithm and with a standard heat-bath for a large interval of β values using a 12^3 lattice; we allowed the system to reach thermalization for 5×10^4 iterations and then measured the observables for 10^6 iterations. Errors were evaluated using a Jackknife procedure. The results are shown in Fig 7.2.

We can easily see in this figure that the two simulations give essentially the same results.

Almost the same situation can be depicted also for the four dimensional U(1) model; the results of a similar set of simulations, performed with the two algorithms on a 16^4 lattice, are shown in Fig 7.3.

Here the only difference can be seen near the phase transition point. Remember that due to the difference in finite volume terms between the two algorithms, the precise pseudo-critical

[6]For instance, filling a plane with cubes and removing the edges at the boundaries of the lattice would result in a pair foil/anti-foil.

[7]We do not expect a breaking of the symmetry plaquette/anti-plaquette.

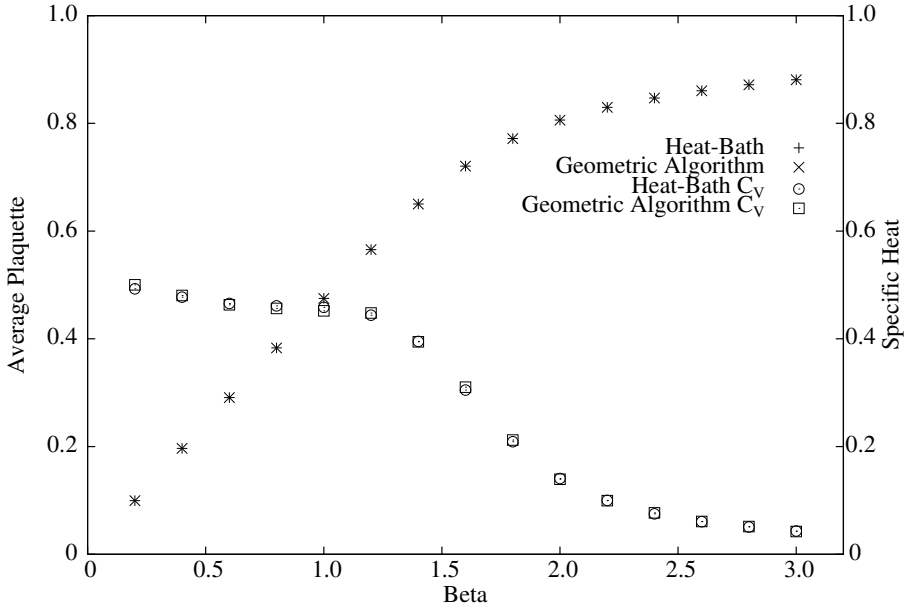

Figure 7.2: Three dimensional U(1) lattice gauge system. Errors are smaller than symbols.

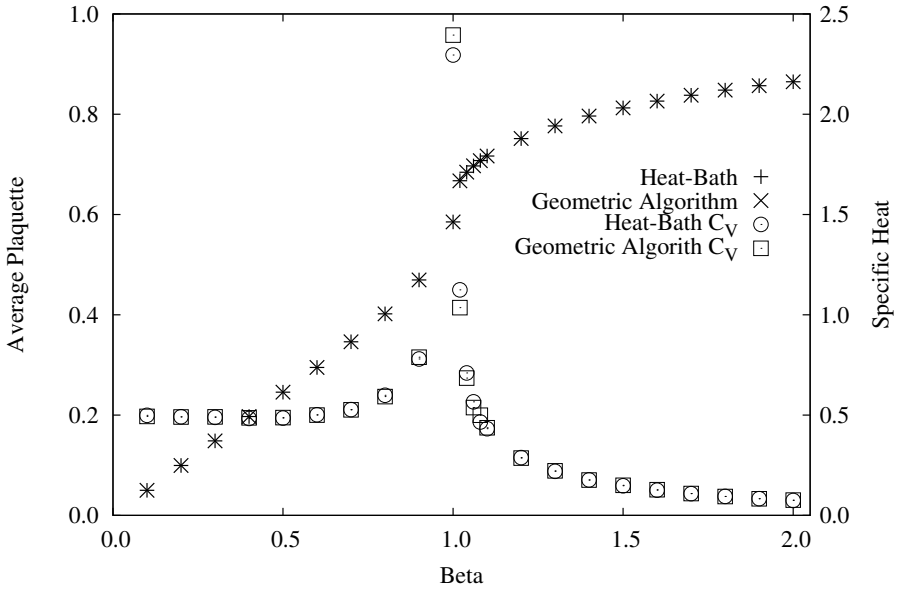

Figure 7.3: Four dimensional U(1) lattice gauge system; please note the different scale for the specific heat on the right. Largest errors (those on the pseudo-critical point) are smaller than symbols.

coupling value at finite volume has to be slightly different. We have calculated a few more points very close to the critical beta for each algorithm, and the results can be seen in tables 7.2 and 7.2. It seems that the peaks are sharper (narrower and larger) in the heath-bath algorithm (take notice of the much larger value of the specific heat for some of these points as compared with fig.7.3).

These results allow us to infer that the geometric approach is able to reproduce all the features of the models under investigation, and when differences are seen, they can be easily explained on the difference between finite volume terms. To study more carefully these differences

β	Plaquette	C_v
1.010700	0.62545(34)	24.1(3)
1.010850	0.64014(143)	88.2(2)
1.010900	0.64940(54)	47.9(4)
1.011100	0.65473(6)	2.6034(1)
1.011600	0.65576(12)	2.5559(2)

Table 7.1: Heat-bath results near β_c.

β	Plaquette	C_v
1.011120	0.6373(45)	67.2(7)
1.011160	0.6423(46)	67.4(3.6)
1.011420	0.6549(1)	2.9660(2)

Table 7.2: Geometric results near β_c.

we have calculated $\beta_c(L)$, the critical coupling for each algorithm at different lattice sizes. We present in table 7.3 the results. We also include in the table the results of a fit of $\beta_c(L)$ for the three largest lattices from each set to the finite-size scaling law expected for a first-order phase transition [124], in order to obtain the value $\beta_c(L = \infty)$. This gives a good fit and consistent results for the infinite volume limit.

L	$\beta_c(L)$ (heat-bath)	$\beta_c(L)$ (geometric)
6	1.00171(8)	1.00878(20)
10	1.00936(11)	1.01062(7)
12	1.01027(8)	1.01100(7)
14	1.01064(4)	1.01103(20)
16	1.01084(17)	1.01116(14)
∞	1.01108(10)	1.01120(22)

Table 7.3: $\beta_c(L)$ for heat-bath and geometric algorithm respectively.

The presence of two clearly different phases in this model, namely a confining and a Coulomb one, allows us to study the behaviour of the Wilson loop results in two different physical situations; as above, we have also performed standard simulations for a cross check between the two approaches. In Figs. 7.4 and 7.5 we report the behaviour of the Wilson loop in both phases (confining in Fig. 7.4 and Coulomb in Fig. 7.5) and in lattices of different size (12^4, 14^4, 16^4).

These figures deserve some comments. The geometric algorithm seems to suffer from larger statistical errors than the heat-bath method, regardless of the phase of the system. To understand this result, we should have a close look at the inner machinery of the algorithm, in particular, the way the Wilson loop is computed (see eq. (7.12)). First of all, the mean value of the Wilson loop is computed as a sum of integer products, implying the existence of large fluctuations between configurations. For example, doubling the occupation number of a single plaquette doubles the value of the loop. This is a quite common fluctuation at the β values of our simulations, and the fluctuations will increase as the loop (and therefore the number of plaquettes) grows. To complicate the computation further, we are trying to calculate an exponentially small quantity by summing integer numbers. The discrete nature of this computation tells us that non-zero values of the quantity must appear with an exponentially small probability. This explains the inherent difficulties of the large Wilson loops (4×4 and greater) measurement in the confining phase. The result is shown in Fig. 7.4: the mean value of the 5×5 Wilson loop was exactly zero in the geometric algorithm, which is of course wrong. Finally, the expectation value of the Wilson loop is proportional to a $(2/\beta)^A$ factor, with A the loop area. This value may become huge (or tiny) for large loops and low (or high) values of beta, thus enhancing the problems that arise from the discreteness of the algorithm [8].

[8] See [125, 126] for a discussion of some numerically efficient algorithms for the calculation of large Wilson

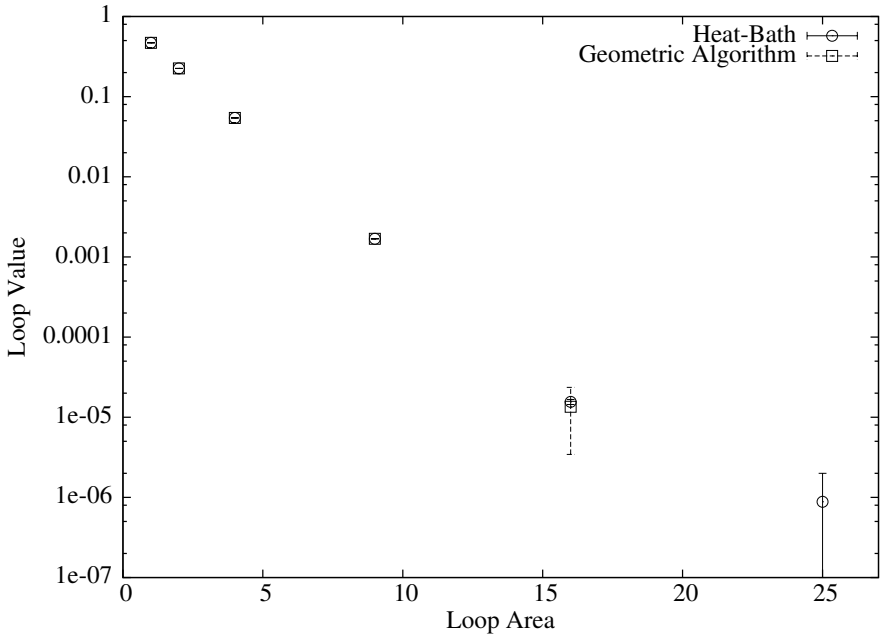

Figure 7.4: Real part of the Wilson loop versus the loop area for the confining phase ($\beta = 0.9$) in the four-dimensional U(1) gauge model. Notice the absence of the 5×5 loop in the geometric algorithm. The lattice volume was 16^4.

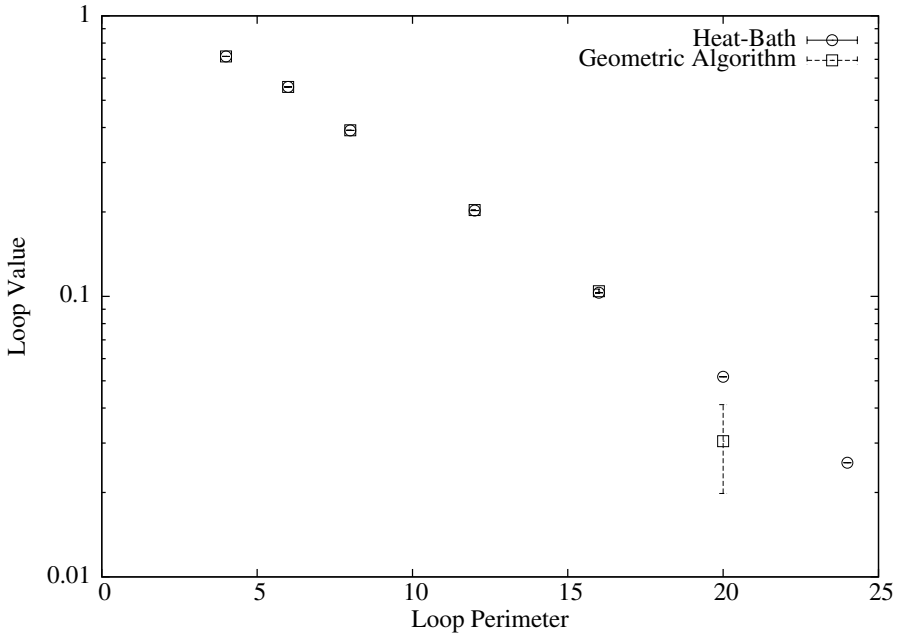

Figure 7.5: Real part of Wilson loop versus the loop perimeter for the Coulomb phase ($\beta = 1.1$) in the four-dimensional U(1) gauge model. The lattice volume was 16^4.

Notwithstanding the stronger fluctuations in the large Wilson loops within the geometric algorithm discussed above, it has a clear advantage against heat-bath: it does not suffer from ergodicity problems. Indeed the results for the Wilson loop at $\beta = 3$ reported in Fig. 7.6 strongly support the previous statement. The points obtained with the geometric algorithm

loops and Polyakov loop correlators.

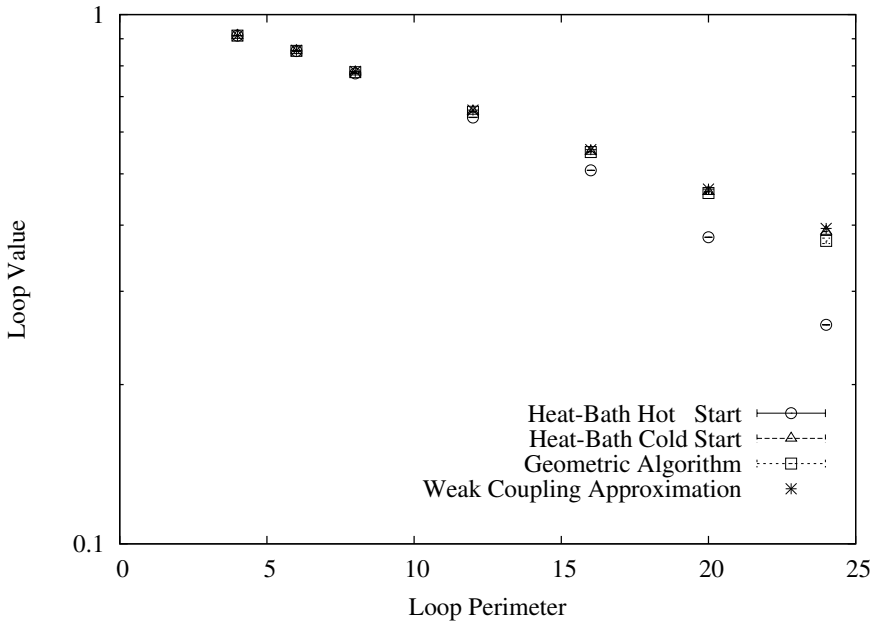

Figure 7.6: Real part of Wilson loop versus the loop perimeter for a large β value ($\beta = 3.0$) in the four-dimensional $U(1)$ gauge model. Notice the difference in performance between the hot and the cold starts of the heat-bath algorithm. The lattice volume was 12^4.

nicely follow the weak coupling prediction of [127], whereas the heat-bath results for large Wilson loops, obtained from a hot start, clearly deviate from the analytical weak coupling prediction. The origin of this anomalous behavior in the heat-bath case is related to the formation of vortices, which are metastable states, that become extremely long lived in the Coulomb phase [122]. These vortices seem to be related to the topological sheets of plaquettes of our model. As we removed them in our simulation algorithm, the GA is expected to perform better than the heat-bath.

We have also calculated the plaquette–plaquette correlation (of the real (7.15) and of the imaginary (7.16) parts) in both phases and for plaquettes living in the same plane. Here we expect a much milder behaviour for the geometrical algorithm, for there is no large $(2/\beta)^A$ factor, and the fluctuations are reduced to a couple of plaquettes. The results are shown in Figs. 7.7, 7.8, 7.9 and 7.10.

In all the cases, the numerical results obtained with the geometric and heat-bath algorithms essentially agree, except for the correlations of the imaginary part of the plaquettes in the Coulomb phase (Fig. 7.10), where a clear discrepancy for distances larger or equal than 4 is observed. Again in this case the reason for this discrepancy is related to the formation of extremely long-lived metastable states [122] in the heat-bath simulations, which seem to be absent in the geometric algorithm. Indeed we have verified, with simulations in 12^4 lattices, that when we start the heat-bath runs from a cold configuration, the disagreement on the correlations of the imaginary part of the plaquettes in Coulomb phase at large distances basically disappear. There are still small discrepancies in this case, but they can be reasonably attributed to the difference in finite volume terms between the two algorithms.

To compare computational costs we define a figure of merit, which is the product of the squared error times the cpu time. We expect the error to vanish like $1/\sqrt{N_{\text{Monte Carlo}}}$, and therefore the quantity defined above should tend asymptotically to a constant. We show the value of this quantity for several observables in both phases and for both algorithms in Fig. 7.11.

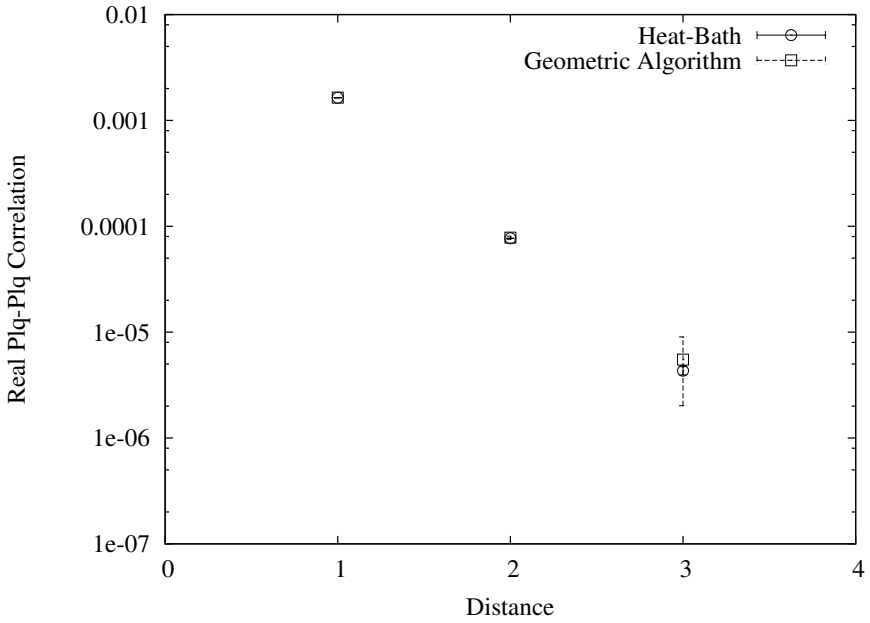

Figure 7.7: Correlation function of the real part of the plaquette versus plaquette–plaquette distance in lattice units, for the four-dimensional $U(1)$ lattice gauge model in the confining phase ($\beta = 0.9$). Beyond distance 4, the error became far larger than the expectation value of the correlation. The lattice volume was 16^4.

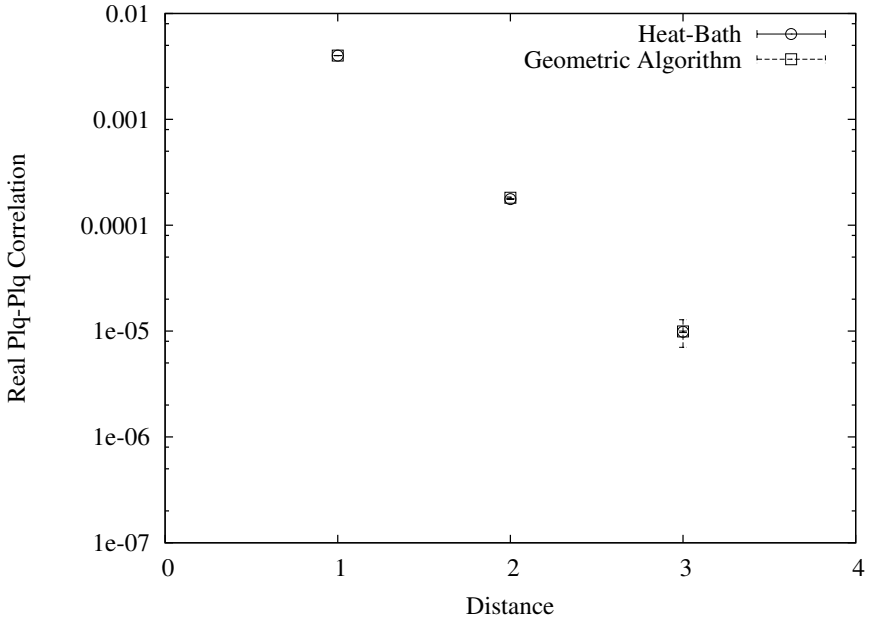

Figure 7.8: Correlation function of the real part of the plaquette versus plaquette–plaquette distance in lattice units, for the four-dimensional $U(1)$ lattice gauge model in the Coulomb phase ($\beta = 1.1$). Beyond distance 4, the error became far larger than the expectation value of the correlation. The lattice volume was 16^4.

We can see that the performance of both algorithms is quite comparable. The differences that are seen could conceivably change if one were to optimize the specific implementations, but none is obviously much more efficient than the other for the models studied.

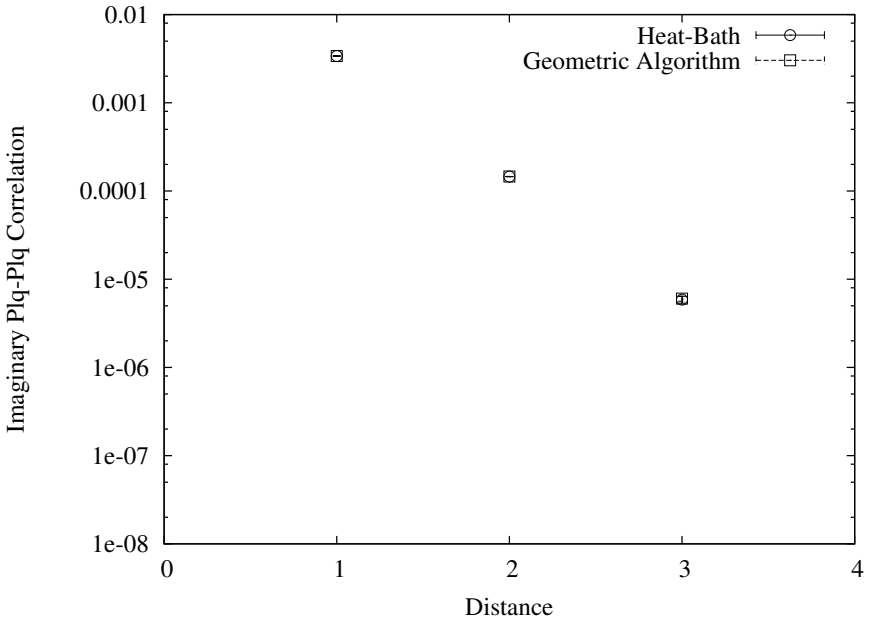

Figure 7.9: Correlation function of the imaginary part of the plaquette versus plaquette–plaquette distance in lattice units, for the four-dimensional $U(1)$ lattice gauge model in the confining phase ($\beta = 0.9$). Beyond distance 4, the error became far larger than the expectation value of the correlation. The lattice volume was 16^4.

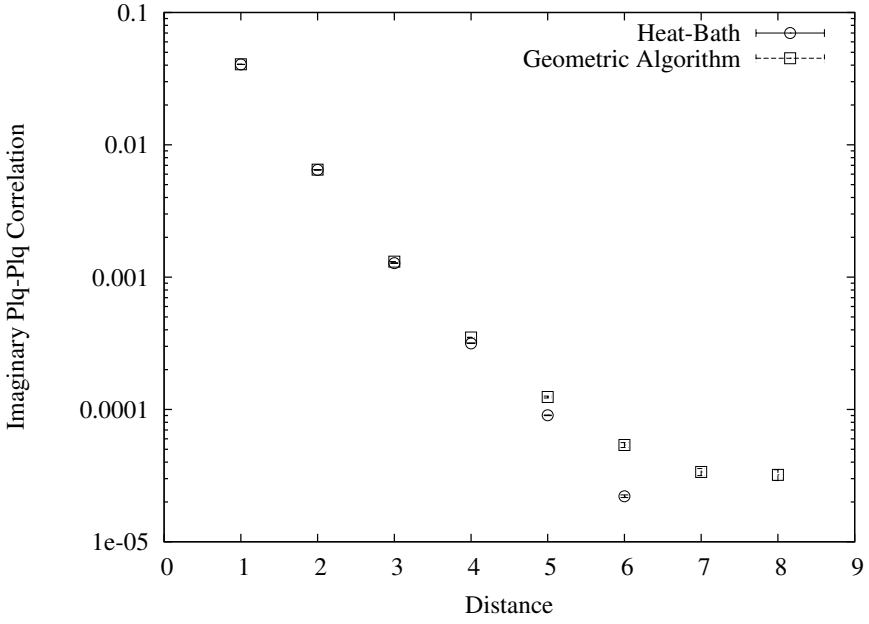

Figure 7.10: Correlation function of the imaginary part of the plaquette versus plaquette–plaquette distance in lattice units, for the four-dimensional $U(1)$ lattice gauge model in the Coulomb phase ($\beta = 1.1$). Notice the different behaviour of the algorithms at large distances. The lattice volume was 16^4.

In particular, for the plaquette observable and the specific heat, both algorithms have a similar figure of merit. From our point of view, the differences are not quite significant, and could change with careful optimizations. The real plaquette-plaquette correlation is quite another

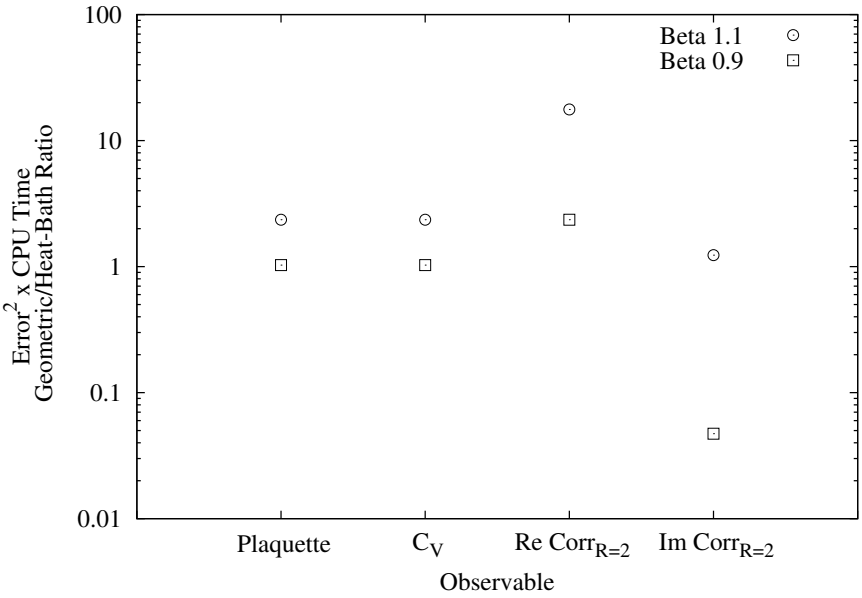

Figure 7.11: Ratios of figures of merit for different observables between geometric and heat-bath algorithms. Re $\mathrm{Corr}_{R=2}$ and Im $\mathrm{Corr}_{R=2}$ stand for Real and Imaginary plaquette–plaquette correlations at distance 2.

story, for the differences become significative in the Coulomb phase (a factor ≈ 20), but they do not become worse as β increases, as we test in a 12^4 simulation at $\beta = 3.0$.

On the other hand, the geometric algorithm seems to perform much better for the imaginary plaquette-plaquette correlation in the confining phase, whereas in the Coulomb phase all the advantage vanishes. Again, our 12^4 computation at $\beta = 3.0$ reveals that the ratio slowly decreases as β increases (being ≈ 0.8 at $\beta = 3.0$).

Of course, this analysis assumes that both algorithms have no ergodicity problems. We must be careful to start from a cold configuration when running the heat-bath simulations in the Coulomb phase, in order to avoid metastable states which could spoil the reliability of the simulation.

7.3 The three dimensional Ising gauge model

Let us finally come to the point of critical slowing down: This is a major issue, as any improvement in this field can be of paramount importance in term of the cost of large scale simulations of (statistical) systems at a critical point. Beating critical slowing down is one of the main motivations in the development of new Monte Carlo algorithms.

Typically what is found in Monte Carlo simulations of system both in statistical physics and gauge theories is that the autocorrelationtime τ diverges as we approach a critical point, usually as a power of the spatial correlation length: $\tau \sim \xi^z$, where ξ is the correlation length and z is a dynamical critical exponent. The typical local algorithm has a value of $z \gtrsim 2$, making it very inefficient to simulate close to the critical point. For spin systems there are well known cluster algorithms with much smaller z. Previously published results [123] on an algorithm similar to ours, but applied to a non-gauge model, have claimed a similarly smaller value for z. Having also this motivation in mind, we have investigated the autocorrelation properties of our numerical scheme on the critical point of a system that undergoes a second order phase transition (with diverging correlation length). Our model of choice has been the

three dimensional Ising-gauge model. We have performed extensive simulations in the critical zone of this model for several values of the lattice size (and hence correlation length), using both the geometric algorithm and the standard Monte Carlo approach, the latter known to have a lower bound for the autocorrelation exponent z equal to 2, a value typical of all local algorithms. For lattices up to $L = 24$ we have in all cases more than 5×10^5 Monte-Carlo iterations, which increase to more than 1×10^6 for $L = 32, 48$, and to more than 4×10^6 iterations for the largest lattice $L = 64$.

For an observable O we define the autocorrelation function $\rho(t)$ as

$$\rho(t) = \frac{\langle (O(i) - O_A)\,(O(i+t) - O_B) \rangle}{\sqrt{\sigma_A^2 \sigma_B^2}} \tag{7.17}$$

where the mean values are defined as $O_A = \langle O(i) \rangle$, $O_B = \langle O(i+t) \rangle$, and the variances $\sigma_A^2 = \left\langle (O(i) - O_A)^2 \right\rangle$, $\sigma_B^2 = \left\langle (O(i+t) - O_B)^2 \right\rangle$, denoting $\langle\rangle$ average over i. We then define the integrated autocorrelation time by

$$\tau = \rho(0) + 2 \sum_{t=1}^{N} \rho(t) \frac{N - t}{N} \tag{7.18}$$

where N is fixed, but with $N < 3\tau$ and $N < 10\%$ of the total sample. In Fig. 7.12 we report the results for the integrated autocorrelation time of the plaquette versus lattice size in logarithmic scale for both algorithms.

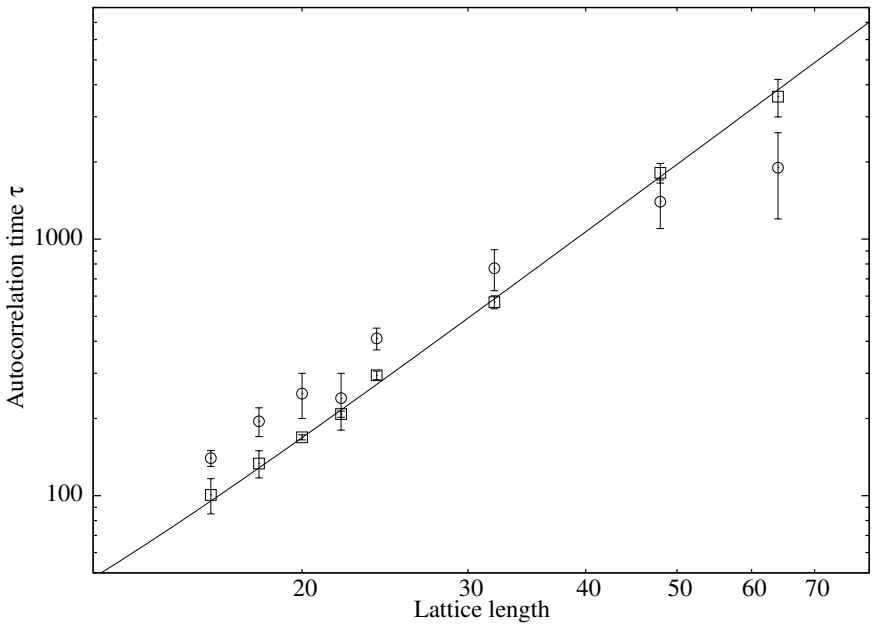

Figure 7.12: Autocorrelation times at the critical point (of each algorithm) versus lattice length; boxes stand for standard algorithm results, with a linear fit to guide the eye, while circles represent the results of the geometric algorithm. The errors were obtained by a jack-knife procedure.

The results of our simulations hint to a different asymptotic behaviour of the autocorrelation time, although with our present data we cannot obtain a conclusive result. The points for the heat-bath algorithm seem to fall nicely on a straight line, which would correspond to a simple

exponential dependence of τ on L, with $z = 2.67 \pm 0.08$, but the geometric algorithm presents a more complicated behaviour, as well as larger errors. There are signs that the asymptotic behaviour might be better than for the heat-bath, but much more extensive simulations, outside the scope of this work, would be needed to get a definite value for z.

7.4 Conclusions and Outlook

Inspired by the sign problem, we have developed a geometric algorithm, based on the strong coupling expansion of the partition function, which can be applied to abelian pure gauge models[9]. We have checked in the $U(1)$ model in 3 and 4 dimensions that the algorithm can be implemented efficiently, and is comparable with a standard heat-bath algorithm for those models. It seems however that the geometric algorithm does not suffer lack of ergodicity due to the presence of vortices, as can be the case for heat-bath, depending on the starting point.

We have also studied the algorithm in the 3 dimensional Ising gauge model at the critical point, where we have seen hints that the asymptotic behaviour of the geometric algorithm may be better than standard heat-bath. This would be very interesting, because in contrast to spin systems, where there exists cluster algorithms that can greatly reduce critical slowing-down, to our knowledge no similar algorithm is known for gauge systems. Our results are however not enough to establish this, and much more extensive simulations should be done to clarify this point.

This algorithmic advance must not be regarded as an isolated contribution, but more precisely as the first step of a more ambitious program, which aims to simulate QCD at finite chemical potential, but which also could be applied to other systems suffering from the sign problem, as for example systems with a θ vacuum term. New ideas are clearly needed in order to make significant advances in this problem, and one possibility is the development of new simulation algorithms that might circumvent the difficulties of conventional approaches. So our next logical step would be to combine the fermionic expansion of the MDP of Karsch and Mütter with this strong coupling expansion for pure gauge fields, and try to build a completely new algorithm, capable of dealing with fermions and gauge fields for $\mu = 0$, and maybe, through an intelligent clustering procedure, for $\mu \neq 0$ as well.

[9] I must reckon that, some time before our development took place, S. Chandrasekharan had come across a similar idea in [116], where he succeeded to simulate QED in four dimensions by using a worm algorithm and a world-sheet approach. Indeed, the conclusions he reports in his papers are remarkably the same as ours.

Chapter 8

Further applications of polymers

"Defeat is not the worst of failures. Not to have tried is the true failure."

—George Edward Woodberry

8.1 Mixing fermions and gauge theories: QED

The fermionic contributions of the MDP model share a common property: They all have trivial contributions from the gauge links. In the case of dimers, the gauge link involved $U_{n,\mu}$ is annihilated by the reverse link $U_{n+\hat{\mu},-\mu} = U^{\dagger}_{n,\mu}$; the baryonic loops consist of concatenated trivial powers of the gauge links (in the case of $SU(3)$, the third power $U^{3}_{n,\mu}$); and the monomers have no gauge links to play with. There are no closed loops of links contributing to the partition function, even though some closed fermionic loops, giving non-vanishing contribution to the Grassman integral, carry a gauge loop associated. This happens because the group integral of any closed, non-annihilating gauge loop is zero.

The addition of the strong coupling expansion of the gauge action changes this picture dramatically. Now the non-annihilating gauge loops associated to fermionic loops can be cancelled by other gauge loops coming from the pure gauge action expansion. Fermions however, follow Fermi statistics and anticommutation rules, hence we expect a sign problem to appear, for there are fermionic-gauge loops which carry a negative weight. The simplest of them all, for two dimensions, is shown if fig. 8.1, but indeed there are many other examples. As we will see, the dynamical simulations of fermions and gauge fields with polymeric models are untractable at this moment. In the following sections I will develop the model of the polymeric expansion of QED with fermions, and show how the sign problem spoils the measurements of observables.

Pairing gauge and fermionic terms

As we previously solved the strong coupling expansion for abelian groups, we can afford to construct the partition function of the complete system, with fermions and gauge fields out of the strong coupling regime. The procedure to follow is the expansion of the exponentials which define the partition function, in the same fashion we did in the previous chapters. To avoid repetition, I just explain the differences. The whole partition function can be decomposed in three terms

$$Z = Z_{MDP} \times Z_{GA} + Z_{\text{Mixed}} \tag{8.1}$$

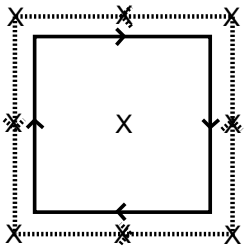

Figure 8.1: Simplest fermionic loop in the theory mixing fermions and gauge fields out of the strong coupling regime. The solid line indicated a gauge loop, which annihilates the gauge contribution of the fermionic loop, marked by a dashed line. The $\times$ mark lattice points, this loop is larger than the simplest plaquette.

where Z_{GA} is exactly given in (7.2), Z_{MDP} comes from the $U(1)$ version of (6.24) and Z_{Mixed} aglomerates all the contributions which are not included in the previous partition functions. The new expression for Z_{MDP} becomes quite simple in $U(1)$ for two reasons: First, there are no baryons; and second, there are no colours, only one degree of freedom is allowed per site, and this degree of freedom can be either a dimer or a monomer

$$Z_{MDP} = \sum_{\alpha \in \mathcal{C}_F} C_F^{\alpha} = (2m)^{N_M^{\alpha}} . \tag{8.2}$$

where $\mathcal{C}$ denotes the whole space of configurations, and C_F^{α} is a factor which gathers the contribution of monomers and dimers only. The terms encoded by Z_{Mixed} are those which involve products of gauge and fermionic loops. Now, a closed fermionic loop which does not annihilate all its gauge links can give rise to a contribution in the final partition function. For instance, a plaquettte loop,

$$\bar{\psi}_n U_{n,\mu} \psi_{n+\hat{\mu}} \bar{\psi}_{n+\hat{\mu}} U_{n+\hat{\mu},\nu} \psi_{n+\hat{\mu}+\hat{\nu}} \bar{\psi}_{n+\hat{\mu}+\hat{\nu}} U^{\dagger}_{n+\nu,\mu} \psi_{n+\hat{\nu}} \bar{\psi}_{n+\hat{\nu}} U^{\dagger}_{n,\nu} \psi_n$$

gives zero contribution to the MDP partition function because, even if the Grassman integral is non-zero, the gauge group integral of the plaquette defined by the fermionic line vanishes. The difference is that now, we can complete this term by multiplying it by the complementary gauge loop, coming from the gauge action,

$$U_{n,\nu} U_{n+\hat{\nu},\mu} U^{\dagger}_{n+\hat{\mu},\nu} U^{\dagger}_{n,\mu}.$$

This way all the Grassman variables and the gauge links are killed, and the integral over the gauge group becomes trivial again. As these fermionic loops consume all the anticommuting degrees of freedom, they are self-avoiding, and cannot mix with monomers. The new rule for the occupancy numbers of each site is

$$nM(n) + \sum_{\nu} [nD(n,\nu) + nF(n,\nu)] = 1, \tag{8.3}$$

which takes into account the fermionic lines nF which produce the fermionic loops. Since there is only a pair $\bar{\psi}, \psi$ of Grassman variables for each site, the dimers become self-avoiding as well. This fact will prove a handicap in the clustering process.

The weight carried by these fermionic loops comprises a contribution coming from the gauge plaquette, and a contribution coming from the closed fermionic line which defines the loop. The former can be absorbed in Z_{GA}, whereas the latter is just a sign given by the Kogut-Susskind phases

$$w\left(C^{\alpha}\right) = \prod_{\{x,\mu\}\in C^{\alpha}_{\text{Loops}}} \eta(x)\mu \tag{8.4}$$

where $C^{\alpha}_{\text{Loops}}$ is the set of fermionic loops belonging to the configuration C^{α}. Therefore, the contribution of a general configuration involving monomers, dimers, gauge plaquettes and anti-plaquettes, and these new kind of fermionic loops is a product of the former contributions C^{α}_{F} and C^{α}_{G}, multiplied by the fermionic loop weights

$$Z = (2m)^{N^{\alpha}_{M}} \prod_{k} \frac{\beta^{n^{\alpha}_{k}+\bar{n}^{\alpha}_{k}}}{2^{n^{\alpha}_{k}+\bar{n}^{\alpha}_{k}} n^{\alpha}_{k}!\bar{n}^{\alpha}_{k}!} \prod_{\{x,\mu\}\in C^{\alpha}_{\text{Loops}}} \eta(x)\mu. \tag{8.5}$$

As we can see, the sign associated to each fermionic loop gives rise to a potential sign problem. When close to the strong coupling limit, the sign problem becomes milder as expected, for the strong coupling limit of this theory without baryons should be free of sign problems. But if we keep increasing the coupling β, at certain point the sign problem becomes severe. This behaviour is related to the relative importance of each fermionic loop: At strong coupling, there are no fermionic loops, as they involve gauge plaquettes, whose weight is proportional to a power of β. The configuration is basically a bunch of dimers and monomers, depending on the mass of the fermion. As β increases, the simplest fermionic loops (plaquettes) appear, which are positive. But at certain point, the negative loops (see fig. 8.1) become non-negligible, and the sign problem becomes severe.

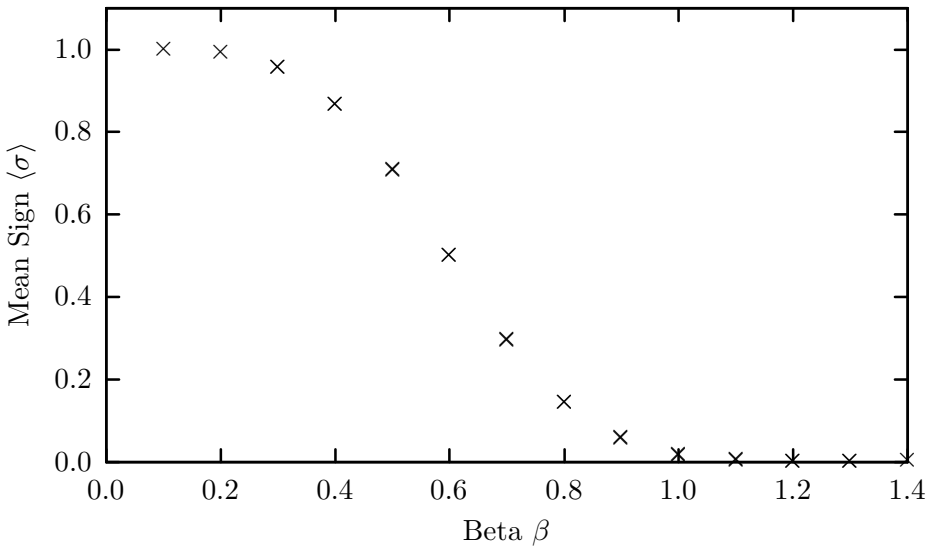

Figure 8.2: Mean sign as a function of the coupling β for the Schwinger model with polymerized Kogut-Susskind fermions, keeping the ratio m/e fixed. We used a 100^2 lattice, with 250000 thermalization steps and 1000000 measurement steps. The sign problem seems severe beyond $\beta \sim 1.1$.

Some ideas for configuration clustering

The way Karsch and Mütter solved the sign problem for the MDP model at zero chemical potential should be an example of the power of the discrete models to deal with the sign problem. Configuration clustering could be the way out to solve this long-standing problem, as foretold long time ago [128]. As this model, involving gauge fields and fermions, is richer than

the previous models analyzed in terms of objects which live in our lattice, we expect to find more possibilities for the clustering.

Our clustering attempt gathered dimers, fermionic and gauge loops in the same term of the partition function, that is, for each fermionic loop, a pair of dimers using the same number of Grassman variables are associated to it, and a pair of gauge plaquette/anti-plaquette. The addition of such an object to an existing configuration would have a transition probability proportional to

$$P_{i\to j} \propto \frac{\beta}{2}\left[\sigma + \frac{\beta}{2}\right]$$

where sigma is the sign of the loop. For $\beta \geq 2$, the sign problem could be overcome. Yet this turned out to be an unnatural choice, for a set of dimers cannot be mirrored into fermionic loops in some cases. We need a one-to-one correspondence between fermionic loops, and dimers plus pairs of gauge plaquettes, but we can think of a very simple configuration of dimers and gauge plaquettes with no correspondence: A single dimer populating the lattice.

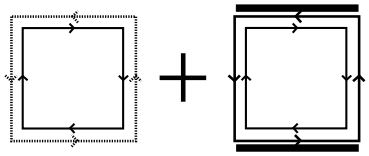

Figure 8.3: Attempt to cluster configurations in the new model. We add a gauge loop with two dimers (right, the horizontal thick solid lines represent the dimers) and a fermionic loop (left) into a single entity. Unfortunately, there is no one-to-one correspondence in this case, and an isolated single dimer has no correspondence with the proposed system.

In the end, we did not find a satisfactory way to cluster configurations and to solve the sign problem; however, this does not mean that the problem cannot be solved.

A word on Wilson fermions

The discussion has been restricted to Kogut-Susskind fermions up to now, but also a system featuring Wilson fermions can be translated into a set of monomers, dimers and fermionic loops. The pioneer on this field is M. Salmhofer [118][1], which succeeded in solving the Schwinger model at strong coupling with Wilson fermions. The procedure to follow in this taks is the same, but due to the inclusion of the γ matrices, the Grassman rules which the points of the lattice must comply with are far more complex, and the number of possible points increase notoriously. In fact, M. Salmhofer mapped QED_2 to an eight vertex model, where each vertex has a different (and positive) weigth, but the inclusion of gauge fields increases the number of vertex to 49 [130][2], and a great number of these vertex are negative. The result is a sign problem, which worsens as the dimension of the model increases, thus the models were dropped at some point, although it seems that no one ever tried to overcome the sign problem with the clustering of configurations. This failure contrast with the success of other fermionic models, like the Gross-Neveu model, or the Karsch and Mütter proposal for $\mu = 0$.

[1] K. Scharnhost solved the two flavoured version in [129]. U. Wenger has recently worked on this topic as well [119], but it seems that no significant advances where made on his papers.

[2] It is remarkable the effort spend by the group of Graz –particularly C. Gattringer- in the implementation of polymeric models on the lattice. Some examples are colleted in [130, 131, 132].

8.2 Other interesting models

The polymerization procedure can be applied to several interesting models, where it can be used to try to solve the sign problem by clustering, or to reduce the critical slowing down. Indeed, taking into account the limited success of this kind of models and algorithms to reduce the severity of the sign problem, the scientific community regard them as a way to avoid the critical slowing down, as the authors of the worm algorithm explicitly state in [114]. The applicability of the method to statistical systems is quite wide.

The Ising model

I will briefly summarize the steps necessary to construct the equivalent polymeric model. Recalling (5.3), we apply the identities

$$e^{Fs_is_j} = \cosh F \left[1 + s_i s_j \tanh F\right],$$
$$e^{hs_i} = \cosh h \left[1 + s_i \tanh h\right],$$

to Z. The new partition function is written as

$$Z(F,h) = (\cosh F)^N \sum_{\{s_i\}} \left[\prod_{\{i,j\}} (1 + s_i s_j \tanh F)\right] \times$$
$$(\cosh h)^N \left[\prod_i (1 + s_i \tanh h)\right]. \tag{8.6}$$

There are two kinds of graphs derived from this expansion:

- Closed loops of dimers. The product of different $s_i s_j \tanh F$ terms give non-zero contributions only when every spin is squared, for $s_i^2 = 1$. Otherwise, the sum over all configurations which involve the unpaired spin $s_i = \pm 1$ vanishes. In order to find a nonzero contribution, we need to construct a chain like

  $$s_{i_1} s_{i_2} \tanh F \times s_{i_2} s_{i_3} \tanh F \times s_{i_3} s_{i_4} \tanh F \ldots s_{i_n} s_{i_1} \tanh F,$$

  where every spin appears twice. As s_{i_j} and $s_{i_{j+1}}$ are neighbours (as indicated in the product over $\{i,j\}$ in (8.6)), this lead to a closed loop. The loops are not self-avoiding, and two loops may cross at a given lattice site, but overlapping dimers are not allowed, because we have used all the spin variables available. The weight of this kind of loops is given by the coupling F

  $$w_{Cl}^{Is} = (\tanh F)^L, \tag{8.7}$$

  with L the length of the loop. As L is always an even number, there is no sign problem, even at negative values of the coupling (the antiferromagnetic model).

- Open chains with two heads. The latter expansion need not give rise to a closed loop, if we cap both ends of the growing spin chain with monomers, coming from the external field term

  $$s_{i_1} \tanh h s_{i_1} s_{i_2} \tanh F \times s_{i_2} s_{i_3} \tanh F \ldots s_{i_{n-1}} s_{i_n} \tanh F \times s_{i_n} \tanh h.$$

The result is an open string, whose ends carry monomers (heads). The weight of this chain

$$w_{Op}^{Is} = (\tanh F)^L (\tanh h)^2 , \tag{8.8}$$

can become negative, if the length of the string is odd and the coupling F is negative (antiferromagnetic coupling). Then a severe sign problem appears.

The model was tested successfully for the ferromagnetic case. A parallel work of U. Wolff was published in [133], where the absence of critical slowing down is emphasized.

The Antiferromagnetic Ising model at $\theta = \pi$

Although in general the Ising model under an imaginary magnetic field has a severe sign problem, this is a special case where simulations can be performed. The equivalence relations that are used here are

$$\begin{aligned} e^{F s_j s_k} &= \cosh F + s_j s_k \sinh F, \\ e^{-1 \frac{\theta}{2} s_j} &= \cos \frac{\theta}{2} - i s_j \sin \frac{\theta}{2}. \end{aligned} \tag{8.9}$$

In general, the open chains in this model may have negative weights, but for $\theta = \pi$ the system is greatly simplified. The former relations become

$$\begin{aligned} e^{F s_j s_k} &= \cosh F + s_j s_k \sinh F, \\ e^{-1 \frac{\pi}{2} s_i} &= -i s_j. \end{aligned} \tag{8.10}$$

In the one-dimensional case, the chains of dimers are removed, no matter if they belong to a closed or to an open loop, for the inner points of these chains are multiplied by $-is_j$ factors (per site j) which can not be annihilated, and therefore its weight in the partition function vanishes after summing up all the possibilities for the spin. Thus, only dimers with their heads capped with monomers are the allowed objects of this theory, and their weight is simply

$$w_D = \sinh F. \tag{8.11}$$

For higher dimensions, an odd number of dimers (up to $2D-1$) can touch a site j: this structure brings up an odd number of s_j factors, that are cancelled by the $-is_j$ factor coming from the external field. Thus complex structures like nets can be constructed. The system of dimers can be summed up analytically for one and two dimensions [94, 95], and can be simulated for higher dimensions easily. This special case, which seems pretty accidental, give us however a strong reason to keep believing in polymeric models.

The Hubbard model

The Hubbard model is a simple model, describing tighly coupled charged fermions (electrons or holes) on a crystal. It is quite interesting due to its relationship to superconductivity: It was thought than the main properties of the superconductors at high temperature should be described by this model [134, 135].

The one-dimensional model can be analytically solved, and shows no superconducting phase. The two-dimensional model was expected to behave better, with supercoducting behaviour when the chemical potential surpassed some critical value [136].

We were interested in the two-dimensional repulsive Hubbard model with chemical potential, for it features a sign problem. The lattice formulation of the model was taken from [137], developed by M. Creutz. The quantum Hamiltonian of the Hubbard model, written in terms of creation and annihilation operators, is transformed into a lattice system of Grassman variables, after a discretization of the time direction. The original Hubbard Hamiltonian follows:

$$H = -K \sum_{\{i,j\},\sigma} a^\dagger_{i\sigma} a_{j\sigma} - \frac{U}{2} \sum_i \left(a^\dagger_{i\uparrow} a_{i\uparrow} - a^\dagger_{i\downarrow} a_{i\downarrow} \right)^2 + h \sum_i \left(a^\dagger_{i\uparrow} a_{i\uparrow} - a^\dagger_{i\downarrow} a_{i\downarrow} \right) + \mu \sum_{i,\sigma} a^\dagger_{i\sigma} a_{i\sigma}, \tag{8.12}$$

where K is the hopping parameter, U is the repulsion term (attractive if $U < 0$) between fermions, h is the magnetic field affecting the electrons according to their spin, μ the chemical potential which introduces an asymmetry in the spin distribution, and $a^\dagger_{i\sigma}$ and $a_{i\sigma}$ are the creation and annihilation operators, verifying the anticommutation relation

$$\left\{ a_{i\sigma} a^\dagger_{j\rho} \right\} = \delta_{ij} \delta_{\sigma\rho}. \tag{8.13}$$

After performing the transformations described in [137], which involve the addition of a Gaussian scalar field, the final result for the partition function is

$$Z = \lim_{\frac{K}{L_T} \to 0} \frac{e^{V^2 \beta \left(\frac{U}{2} + h - \mu \right)}}{(2\pi)^{\frac{V^2 L_T}{2}}} \int (dA)\, e^{-\frac{A^2}{2}} e^{-\psi^* M_+ \psi} e^{-\psi^* M_- \psi}, \tag{8.14}$$

with

$$\psi^* M_\pm \psi = \lim_{\frac{K}{L_T} \to 0} \frac{K\beta}{L_T} \left[\sum_{\{i,j\},t} \psi^*_{i,t} \psi_{j,t} - \sum_{i,t} \psi^*_{i,t} \psi_{i,t-1} + \sum_{i,t} \psi^*_{i,t} \psi_{i,t} e^{\left(\frac{\beta U}{L_T} \right)^{\frac{1}{2}} A_{i,t} - \frac{\beta}{L_T}(h + U \pm \mu)} \right]. \tag{8.15}$$

Take into account that, in this model, no explicit regularization of fermions is used, only a set of Grassman variables to reproduce Fermi statistic.

The bosonic field is integrated out exactly, and the result is absorbed in the value of the weights for the monomers. After integrating the Grassman variables, we are left with four kinds of objects

- Monomers, ultralocal objects living in a site, whose weight depends on the monomer occupation number n_M of that site and of the spin of the monomer as

$$w_D \propto \begin{cases} e^{\frac{\sigma^2}{-} \Lambda_{pm}} & n_M = 1 \\ e^{\frac{2\sigma^2}{-} \Lambda_+ - \Lambda_-} & n_M = 2 \end{cases} \tag{8.16}$$

  where σ and Λ are two constants

$$\sigma^2 = \frac{\beta U}{L_T}, \qquad \Lambda_{pm} = \frac{\beta \left(U + h \pm \mu \right)}{L_T},$$

  depending on the parameters of the theory.

- Spatial loops, extending only in the spatial plane, carrying a negative weight. This breaks completely the possibility of simulating the model in the computer, for the number of loops in a given configuration is compeltely arbitrary, and a configuration contributes negatively to the partition function if it has an odd number of spatial loops. The weight of a loop is given by

$$w_{SL} \propto -\left(\frac{\beta K}{L_T}\right)^C, \tag{8.17}$$

  with C the length of the loop.

- Temporal loops, winding around the lattice k times. These loops need not be straight, and can turn around in the spatial directions, but must always move forward in the time direction. Due to the antiperiodic boundary conditions required for the time direction, the sign associated to the weight of these loops is $(-1)^{k+1}$. The weight of these loops depends on the displacements on the spatial direction as

$$w_{TL} \propto (-1)^{k+1}\left(\frac{\beta K}{L_T}\right)^D, \tag{8.18}$$

  where D is the number of displacements in the spatial directions. In order to close the loop, D must always be an even number. As the only loop which is not displaced is the positive weighted, straight loop with $k = 1$, this is the predominant loop, and loops of higher winding numbers are suppresed with powers of K/L_T, which should vanish in the thermodynamic limit.

The behaviour of this model, regarding the mean sign of a simulation, is quite similar to that of the MDP model at $\mu \neq 0$: The sign problem is a real problem, as long as the configurations are far from saturation of loops (in this case, straight temporal loops). In a large lattice, this sign problem always appears. We did not come across a clusterization of configurations which could solve this sign problem, even at zero chemical potential, where the standard theory does not suffer from a sign problem.

This case is an example of complete failure of the polymerization procedure: It takes a well-behaved model (the $2+1$ Hubbard model at zero chemical potential), and transforms it into a model with a severe sign problem. What we can learn from this story is the fact that, as a rule, a polymeric version of a given fermionic or spin theory does not solve the sign problem, and even might worsen it. On the other hand, for some systems this procedure might give unvaluable help, speeding up simulations, reducing the critical slowing down, or even allowing us to perform simulations in a system with the sign problem.

8.3 Conclusions

The polymerization procedure arised originally as a method to simulate fermions in the early days of the lattice. Although it allowed to perform simulations of fermions at a low computer cost, it introduced a sign problem, severe in most cases. Nonetheless, the polymerized systems are discrete, and this property enables us to play with the clustering of configurations. It has been demonstrated that a clever clustering can solve completely the sign problem. Sadly, the addition of a chemical potential usually breaks the sign equilibrium of the configuration clusters, bringing back the sign problem. That is why the MDP model works so fine at zero chemical potential, but when $\mu \neq 0$, no matter what we do, the sign problem comes back for low

temperatures and large volumes. In fact, the configurations unbalanced by a chemical potential are very hard to cluster into useful groups. Therefore, and unless a lattice researcher comes with a brilliant idea, the polymerization of fermions do not seem to be the solution to the problem of chemical potential, even though there is still some hope lying in the utilisation of specific techniques for discrete systems, like the merom algorithm.

This conclusion takes us back to the original purpose of the polymers: to simulate fermions at a very low cost. Gauged models in the strong coupling regime seem to work fine, and pure abelian[3] theories also are tractable [139]. But when one mixes fermions and gauge fields, the sign problem is back, and the clustering becomes difficult. Nevertheless, this kind of models have a great advantage with respect to the non-zero chemical potential case: the configurations are not strongly unbalanced by the addition of $e^{\pm\mu}$ factors to some configurations. This way, I find quite plausible to think that a sensible way to cluster configurations exists, like the one that Karsch and Mütter found in the MDP model. In addition, from time to time this procedure surprises us finding a model with a sign problem, which can be completely solved after the polymerization, like the $n-$dimensional Ising model at $\theta = \pi$.

On the whole, the polymerization is a technique very easy to apply which might prove to be very useful in some systems, and that should not be discarded at first glance, but certainly it will not solve the sign problem.

[3]Non-abelian pure gauge theories seem to have a sign problem [138].

Summary

In this work, several long-standing problems of QCD have been analysed from the lattice point of view. Although the main motivation driving this research was the sign problem, the variety of topics treated here is more extense, covering the realization of symmetries in QCD and alternative methods to simulate fermions on the computer. Here an overview of the conclusions drawn in this dissertation is exposed, classified by chapter number. Since the first two chapters are introductory, they lack conclusions, so our enumeration will begin from chapter three:

Chapter 3: *The Aoki phase*

Up to now, all the dynamical fermionic simulations of lattice QCD, done inside the Aoki phase with the aim of investigating the spontaneous breaking of Parity and Flavour, used a twisted mass term $hi\bar{\psi}\gamma_5\tau_3\psi$, which broke explicitly both symmetries [38, 39, 41, 42]. The zero external field limit $h \to 0$ was taken afterwards, in order to see if the breaking of the symmetries still remained in the absence of the source. In principle, this method (the addition and removal of an external source) is a valid method to investigate SSB, mostly in analytical calculations; nonetheless it has some handicaps when we put it in the computer:

- Since the thermodynamic $V \to \infty$ and the zero external source $h \to 0$ limits do not commute, a great number of simulations must be performed in order to reach the thermodynamic limit for each value of the external source, and at the end an uncontrolled extrapolation to zero external field must be made. These two facts introduce large systematic errors, quite difficult to handle.
- On the other hand, the addition of an external source like $hi\bar{\psi}\gamma_5\tau_3\psi$ enforces the standard Aoki vacuum, verifying

$$\left\langle i\bar{\psi}\gamma_5\psi\right\rangle = 0, \qquad \left\langle i\bar{\psi}\gamma_5\tau_3\psi\right\rangle \neq 0.$$

- Moreover, not all the external sources are allowed with this method; those introducing a sign problem can not be simulated. This was an obstacle to prove our claims of new phases, for we could not select one of the new vacua we claim to have discovered.

The $p.d.f.$ formalism allows us to study the vacuum structure of the Aoki phase *without adding external sources to the action*, thus it circumvents all the aforementioned dangers and problems of the external source method. However, the $p.d.f.$ requires previous knowledge of the spectrum of the hermitian Dirac operator $\gamma_5 D$, therefore several possibilities appeared, depending on the behaviour of the eigenvalues μ_i of $\gamma_5 D$:

(i.) If the spectral density of $\gamma_5 D$ of each configuration U, $\rho_U(\mu,\kappa)$ is asymmetric in the thermodynamic limit, and the symmetry is only recovered in the continuum limit $a \to 0$, then the expectation value

$$\left\langle \left(i\bar{\psi}\gamma_5\psi\right)^2 \right\rangle$$

may become negative. This fact would complicate the η meson measurements in the physical phase (outside Aoki's), unless the measurements are done when close to the continuum limit, where the spectral symmetry is expected to be recovered. Moreover, assuming that the Aoki phase disappears at some finite value of the coupling β, as some authors suggest [45, 58], the physical interpretation of the Aoki phase could be compromised, for if the expected value of the square of the hermitian pseudoscalar operator $\left\langle \left(i\bar{\psi}\gamma_5\psi\right)^2 \right\rangle$ can be negative, then the correlation function that defines the η meson mass may cast incongruous results. This possibility was discarded after performing quenched simulations of lattice QCD, inside and outside the Aoki phase, for several volumes (4^4, 6^4 y 8^4).

(ii.) The second possibility assumes that the spectral symmetry is recovered in the thermodynamic limit. Then, the standard Aoki phase,

$$\left\langle i\bar{\psi}\gamma_5\psi \right\rangle = 0, \qquad \left\langle i\bar{\psi}\gamma_5\tau_3\psi \right\rangle \neq 0;$$

is not the only possibility, but new vacua appear, characterized by

$$\left\langle i\bar{\psi}\gamma_5\psi \right\rangle \neq 0.$$

These vacua are not connected to Aoki's original one by Flavour or Parity transformations. The result is quite unexpected, for both, Aoki's approximate calculations [27, 28] and χPT [32, 33], support unambiguously $\left\langle i\bar{\psi}\gamma_5\psi \right\rangle = 0$, in spite of the spontaneous breaking of Parity. The reason explaining why $\left\langle i\bar{\psi}\gamma_5\psi \right\rangle$ vanishes in a vacuum with broken Parity is the existence of a symmetry called P', which is a composition of Parity and a discrete Flavour rotation.

The existence of that symmetry can be called into question thanks to some inconsistencies. The first one is related to the fact that both, Parity and Flavour, are spontaneously broken, therefore, we expect any symmetry, composition of Parity and Flavour, to be broken as well. This argument is not very strong, but is reasonable. On the other hand, the non-local gluonic operator

$$W = \frac{1}{V}\sum_i^N \frac{1}{\mu_i}$$

is an order parameter of the P' symmetry. Were W intensive, $\langle W^n \rangle$ should vanish in the thermodynamic limit for any natural n in a P' conserving scenario. Nevertheless, W contributes to the expectation value $\left\langle \left(i\bar{\psi}\gamma_5\psi\right)^2 \right\rangle$ in such a way that, if $\langle W^2 \rangle$ vanishes, $\left\langle \left(i\bar{\psi}\gamma_5\psi\right)^2 \right\rangle$ must forcibly become non-zero *inside* the Aoki phase. The operator W scales with the volume in the same way as an intensive operator, thus this is an strong argument supporting the existence of new phases.

In any case, the *p.d.f.* calculations are *exact*, hence (i.) either the calculations of Aoki, Sharpe and Singleton use approximations which are not accurate enough to predict the existence of new phases, or (ii.) there must exist forcibly a way to reconcile the *p.d.f.* results with these calculations. In fact, an attempt has been proposed in [43]; in this paper a solution involving the realization of an infinite set of sum rules for the eigenvalues of the

$\gamma_5 D$ is introduced, however there are no theoretical arguments supporting the realization of these sum rules.

In order to find which of the two possibilities (sum rules or new phases) actually happens in QCD simulations, we performed dynamical fermionic simulations inside the Aoki phase *without external sources*. From the technical point of view, this simulations are quite challenging for the Dirac operator develops small eigenvalues inside the Aoki phase, its condition number grows with V, and becomes hard to invert. That is why a new algorithm, using recent techniques [52], was specailly develop to address this problem. The numerical results are not conclusive: although the expectation value $\left\langle \left(i\bar{\psi}\gamma_5\psi\right)^2 \right\rangle$ is clearly non-zero in the smallest volume 4^4, the measurements for a higher volume 6^4 are noisy enough to prevent us from obtaining a final result.

Chapter 4: *Parity conservation in QCD from first principles*

In spite of the tacit assumption that QCD does not break spontaneously neither Parity nor any global vector symmetry, there is a notorius lack of proofs of this hypothesis. The well-known theorems of Vafa and Witten [59, 60] –in particular, the one dedicated to Parity [59]– have been called into question several times in the literature [32, 61, 62, 63, 65, 66], and nowadays everybody agrees on the lack of a proof of Parity conservation in QCD. Regarding the vector-symmetry conservation theorem [60], it requires such demanding conditions, that only the naive and the Kogut-Susskind regularizations of fermions on the lattice comply with them. Moreover, the theorem is not applicable neither to Wilson fermions (one of the most widespread regularizations in QCD simulations), nor to Ginsparg-Wilson fermions. Remarkably, the Wilson fermions violate both theorems, breaking Parity and Flavour spontaneously in the so-called Aoki phase.

The probability distribution function formalism $p.d.f.$, combined with an appropiate regularisation, is capable of proving Parity and Flavour conservation (and in general. if the $p.d.f.$ is correctly used, the conservation of any other vector symmetry) in QCD. By *appropiate* one must understand that in this regularisation, the eigenvalues of the Dirac operator have a lower bound for a non-zero value of the quark mass. Wilson fermions violate this condition, and the small eigenvalues of the Dirac operator are responsible for the breaking of Parity and Flavour in the Aoki phase. Nevertheless, the Ginsparg-Wilson fermions have good chiral properties, so the masses are multiplicatively renormalized. Then the eigenvalues of the Dirac operator are bounded from below for massive quarks, and the conservation of Parity and Flavour in QCD can be proved within the $p.d.f.$ framework, overcoming the difficulties found in the earlier attemps of Vafa and Witten.

Chapter 5: *The antiferromagnetic Ising model within an imaginary magnetic field*

Even though the final aim of the study of the antiferromagnetic Ising model within an imaginary magnetic field is to test techniques and algorithms to simulate the more relevant case of QCD with a θ term, the results obtained for the Ising model deserve attention on their own. By using the method described in section 5.3, the order parameter of the Z_2 symmetry can be computed for any value of θ in the ordered phase. In spite of the failure of the method to deliver sensible results for the low-coupling region, the data obtained allow us to make reasonable assumptions on the phase diagram of the theory, assumptions that were corroborated in a mean-field calculation.

If one adds to this information the existing results for the antiferromagnetic Ising model at $\theta = \pi$ [94, 95], the phase diagram of the two-dimensional model can be reconstructed qualitatively, matching that of the mean-field theory, and although higher dimensions were not pursued in this work, we expose some convincing arguments, which strongly suggest that this phase diagram holds for higher dimensions.

Sadly the method employed here to solve the model is not exempt from flaws: firts, it does not work properly if there is a phase transition for $\theta < \pi$; in this case it could give wrong results. Lastly, the extrapolations required by the method are only reliable for high values fo the coupling $|F|$. Fortunately for us, a transition in $\theta < \pi$ is not expected in QCD, therefore the first point should not be relevant for our future work. Regarding the second point, QCD is an asymptotically free theory, thus its continuum limit lies in the region were the extrapolations of the method work well. That is why this method profiles itself as the perfect candidate to explore with the computer QCD with a θ term, possibly a necessary deed in order to understand the topological properties of QCD.

Chapter 6: *QCD and the chemical potential μ*

The MDP model, developed by Karsch and Mütter [109], successfully solved the sign problem of the polymeric formulation of QCD at $\mu = 0$ for non-vanishing masses. The model could be easily modified to admit non-zero values for the chemical potential, so the extension was compulsory. However, the original MDP implementation of Karsch and Mütter displayed ergodicity problems for small values of the quark mass, and the dynamics were ruled mainly by two states of the system: a saturated state, were all the space points are taken up by a baryonic loop, resulting in maximum baryonic density, and a depleted state with no baryonic loops at all. As these two states carry a positive weight, the sign problem aparently dissappeared, thanks to the ergodicity problems of the original implementation.

Nevertheless, once the ergodicity problem is solved, the system is allowed to be in much more states, which could carry a positive or a negative weight; then, the sign problem comes back. In order to see these effects, we need a large spatial volume, otherwise the system interacts with the walls or with itself (depending on the boundary conditions), resulting in a saturation state right after the transition. The observed saturation seems not to be a physical property of the system[4] [101, 102, 103]; in fact it can be solved by increasing the spatial volume of the system. For larger volumes, a core of baryonic loops can be observed in the dense phase (for $\mu \gtrsim \mu_c$), whereas the borders are empty. It is this emptiness that allows for the creation and annihilation of loops on the surface of the baryonic core; as for high values of μ the loops carrying positive and negative weights are almost equally important in the partition function, both kind of loops are expected to appear on the core surface, creating large sign fluctuations. If, on the contrary, the spatial volume is small, the core takes up all the available space, saturation occurrs, and the sign problem disappears, but this is a finite volume effect. Indeed, the sign problem seems unavoidable, for it is created by the Fermi statistics, and Fermi statistics rule the dynamics of the dense phase.

The failure of the MDP model is a heavy blow for all the finite density QCD practitioners. Nonetheless, there still remain unexplored possibilities, applicable to discrete systems as the MDP model, that might mitigate or even solve the sign problem. That is why it is a sensible idea to keep researching in those kind of models.

Chapter 7 and 8: *Algorithms for the pure gauge action and Further applications of polymers*

The polymerization of the fermionic action appeared as a method to simulate fermions on the lattice. Even if this approach allowed us to simulate fermions at a low computational cost, it introduced a (severe in most cases) sign problem. However, the polymeric systems are discrete systems as well, and this property proved quite useful when it comes to clustering configurations with opposite signs, in order to cancel the sign fluctuations by hand. It was demonstrated [109] that if one performs a clever clustering in some polymeric models, the severe sign problem disappears completely. But the addition of a chemical potential to the action breaks the fragile equilibrium between positive and negative weighted configurations, bringing the sign problem back to the game. This is the case of the MDP model, which works properly (after a clever clustering of configurations) at zero chemical potential, but for $\mu \neq 0$ the sign problem returns and spoils the behaviour of the system. Indeed, a set of configurations which has been unbalanced by a chemical potential is quite difficult to cluster in such a way that the sign problem disappears. That is why, unless a new brilliant idea go on stage, the polymerization of fermions seems not to offer a solution to the problem of finite density QCD, although it is true that not every possibility of this technique has been explored yet.

[4] Although saturation may occurr for very high values of μ.

This conclusion takes us back to the original purpose of the polymers: to simulate fermions on the lattice at low computational cost. The pure gauge models in the strong coupling regime can be simulated with polymers, even those that feature baryonic loops, thanks to the contribution of Karsch and Mütter [109]. It happens that the abelian gauge theories are polymerizable[5] without introducing a sign problem [139]. But when one mixes polymerized fermions with polymerized gauge fields, the sign problem comes back, and a new clustering that might solve the sign problem seems difficult to find. Nevertheless, this case has an important advantage with respect to the chemical potential case: the configurations are not strongly unbalanced by the exponential $e^{\pm\mu}$ factors. This way it seems plausible that a sensible way to cluster configurations should exist, following the steps of Karsch and Mütter, who found a way in the MDP model. In addition, the polymerization gives us some surprises from time to time: some systems featuring a severe sign problem can be completely solved or simulated by using this technique, like, for instance, the Ising model at $\theta = \pi$.

On the whole, the polymerization technique can be applied easily to any system, and although it does not represent the definitive solution for the sign problem, it can prove useful for some particular systems, and should not be discarded a priori.

[5]The polymerization of non-abelian gauge theories introduce a severe sign problem [138].

Outlook

Although in some particular cases we have achieved a remakable success, most of the problems of QCD treated here remain unsolved after our analysis. Nonetheless this contribution should be very useful to anybody interested in these topics. In the following lines I explain what remains unsolved, and which are going to be our future lines of investigation.

- **The structure of the Aoki phase** remains unclear. Neither us nor the advocates of the standard picture of the Aoki phase have provided enough arguments to clarify this issue. Future research is needed to find out what happens in this region.
- **Parity and Flavour** have been proved from first principles in this work, by a clever use of the $p.d.f.$ formalism. This topic is closed.
- **Regarding QCD with a θ term,** the methods used in chapter five seem quite promising, and will be applied to QCD with the aim of finding more about the topology of QCD, and maybe, about the strong CP problem.
- **The problem of the chemical potential in QCD** can not be solved using polymers. Another approach must be taken.
- **On the other hand, the polymers** might prove useful to analyze other systems involving fermions, spins or gauge fields. We have not explored thoroughly the possibility of simulating non-abelian gauge fields, for instance. Many trends of investigation are still open, and shall be pursued.

Appendix A

Nöther's theorem

In classical field theories, the existence of continuous symmetries is associated to conserved quantities. This relationship was established long time ago by Emmy Nöther [140]. Her theorem states:

"For any differentiable symmetry of the action of a physical system, there corresponds a conservation law"

In general, given a field $\phi(x)$, one can perform a *coordinate transformation*, involving only the coordinates x^μ, an *internal transformation* involving only the field ϕ, or a *general transformation* which combines both. It is convenient to compute the total variation of a local function under an infinitesimal general transformation:

$$\phi(x) \to \phi'(x')$$

$$\Delta\phi = \phi'(x') - \phi(x) = \phi'(x+\delta x) - \phi(x) \cong$$

$$\cong \phi'(x) - \phi(x) + \delta x^\mu \phi_{,\mu} = \underbrace{\delta\phi}_{\substack{\text{Internal} \\ \text{transformation}}} + \underbrace{\delta x^\mu \phi_{,\mu}}_{\substack{\text{Coordinate} \\ \text{transformation}}} , \tag{A.1}$$

were we are using the standard notation $\phi_{,\mu} = \partial_\mu \phi$.

Let's consider a general lagrangian density $\mathcal{L}$, which depends on the coordinatex x^μ, some fields and their first derivatives. We concentrate on the effects of transforming a single field ϕ and computing the variation of the corresponding action

$$\delta S = \int d^4x' \tilde{\mathcal{L}}(\phi', \partial'_\mu \phi', x') - \int d^4x \mathcal{L}(\phi, \partial_\mu \phi, x).$$

As we are dealing with an infinitesimal transformation, we can write $x' \cong x + \delta x$, so the new jacobian becomes

$$\frac{\partial x'}{\partial x} = 1 + \partial_\mu \delta x^\mu,$$

and then expand $\tilde{\mathcal{L}}$ around $\mathcal{L}$. For the shake of clarity, we will call $\tilde{\mathcal{L}}(\phi', \partial'_\mu \phi', x')$ just $\tilde{\mathcal{L}}$ and $\mathcal{L}(\phi, \partial_\mu \phi, x)$ simply $\mathcal{L}$. Then,

$$\int d^4x' \tilde{\mathcal{L}} = \int d^4x \left(1 + \partial_\mu \delta x^\mu\right) \mathcal{L}\left(\phi(x) + \delta\phi, \phi_{,\mu} + \delta\phi_{,\mu}, x + \delta x\right) \cong$$

$$\cong \int d^4x \left[\mathcal{L} + \frac{\partial \mathcal{L}}{\partial \phi}\delta\phi + \frac{\partial \mathcal{L}}{\partial \phi_{,\mu}}\delta\phi_{,\mu} + \frac{\partial \mathcal{L}}{\partial x^\mu}\delta x^\mu\right] + \int d^4x \mathcal{L}\partial_\mu \delta x^\mu.$$

The expression above can be simplified enormously. First of all, we integrate by parts the last term:

$$\int d^4x \partial_\mu \delta x^\mu \mathcal{L} = \int d^4x \partial_\mu \left(\mathcal{L}\partial x^\mu\right) - \int d^4x \frac{\partial \mathcal{L}}{\partial x^\mu}\delta x^\mu,$$

which leaves us with

$$\int d^4x' \tilde{\mathcal{L}} \cong \int d^4x \left[\mathcal{L} + \frac{\partial \mathcal{L}}{\partial \phi}\delta\phi + \frac{\partial \mathcal{L}}{\partial \phi_{,\mu}}\delta\phi_{,\mu}\right] + \int d^4x \partial_\mu \left(\mathcal{L}\partial x^\mu\right).$$

After this, we use the following property of our continuous infinitesimal transformation

$$\delta\phi_{,\mu} = \partial_\mu \delta\phi,$$

which allows us to integrate by parts the last term inside the brackets,

$$\int d^4x \frac{\partial \mathcal{L}}{\partial \phi_{,\mu}}\delta\phi_{,\mu} = \int d^4x \partial_\mu \left(\delta\phi \frac{\partial \mathcal{L}}{\partial \phi_{,\mu}}\right) - \int d^4x \partial_\mu \left(\frac{\partial \mathcal{L}}{\partial \phi_{,\mu}}\right)\delta\phi_{,\mu}.$$

Combining both, we compute the total variation of the action

$$\delta S \cong \int d^4x \left[\frac{\partial \mathcal{L}}{\partial \phi} - \partial_\mu \left(\frac{\partial \mathcal{L}}{\partial \phi_{,\mu}}\right)\right]\delta\phi + \int d^4x \partial_\mu \left(\mathcal{L}\partial x^\mu + \delta\phi \frac{\partial \mathcal{L}}{\partial \phi_{,\mu}}\right).$$

The term in brackets vanishes by virtue of the equations of motion. Thence, if our transformation is a symmetry of the action, $\delta S = 0$, and the following equation holds

$$\int d^4x \partial_\mu \left(\mathcal{L}\partial x^\mu + \delta\phi \frac{\partial \mathcal{L}}{\partial \phi_{,\mu}}\right) = 0.$$

Recalling (A.1), the case of a general transformation can be explicitly solved

$$\delta\phi \to \Delta\phi = \delta\phi + \delta x^\mu \frac{\partial \phi}{\partial x^\mu}$$

$$\int d^4x \partial_\mu \left(\mathcal{L}\partial x^\mu + \delta\phi \frac{\partial \mathcal{L}}{\partial \phi_{,\mu}} + \delta x^\mu \phi_{,\mu} \frac{\partial \mathcal{L}}{\partial \phi_{,\mu}}\right) = 0,$$

but in general we are not interested in coordinate frame changes, and our concerns sway around the internal transformations. Therefore we set δx^μ to zero to find

$$\int d^4x \partial_\mu \left(\delta\phi \frac{\partial \mathcal{L}}{\partial \phi_{,\mu}}\right) = 0. \tag{A.2}$$

As this result must hold for *any* value of $\delta\phi$, the integral is irrelevant here, and we define the *current* associated to our internal symmetry j^μ as

$$j^\mu = \delta\phi \frac{\partial \mathcal{L}}{\partial \phi_{,\mu}}. \tag{A.3}$$

Equation (A.2) immediately imposes

$$\partial_\mu j^\mu = 0,$$

and the current is conserved. Integrating j^0 in a time-slice we find the *conserved charge* associated to the current

$$Q = \int d^3x j^0.$$

Appendix B

Hubbard-Stratonovich identity and Saddle-Point Equations

B.1 The Hubbard-Stratonovich identity

The Hubbard-Stratonovich identity is used to linearize quadratic exponents. The derivation is quite simple: Let's begin from the equality

$$\pi^{\frac{1}{2}} = \int_{-\infty}^{\infty} e^{-x^2} dx. \tag{B.1}$$

The definite integral on the r.h.s. of (B.1) is invariant under translations, due to the infinite limits. Thence

$$\pi^{\frac{1}{2}} = \int_{-\infty}^{\infty} e^{-(x-a)^2} dx = \int_{-\infty}^{\infty} e^{-x^2+2ax} e^{-a^2} dx. \tag{B.2}$$

The factor e^{-a^2} is a constant, and we can move it out of the integral to the l.h.s.

$$e^{a^2} = \frac{1}{\pi^{\frac{1}{2}}} \int_{-\infty}^{\infty} e^{-x^2+2ax} dx. \tag{B.3}$$

By substituting $a \to ia$ we can deal with negative exponents

$$e^{-a^2} = \frac{1}{\pi^{\frac{1}{2}}} \int_{-\infty}^{\infty} e^{-x^2+2iax} dx. \tag{B.4}$$

In the infinite ranged Ising model, $a = \left(\frac{F}{N}\right)^{\frac{1}{2}} \sum_i^N s_i$, and the quadratic term in the exponential is substituted by an integral in a ghost variable x

$$e^{\frac{F}{N}\left(\sum_i^N s_i\right)^2} = \frac{1}{\pi^{\frac{1}{2}}} \int_{-\infty}^{\infty} e^{-x^2+2x\left(\frac{F}{N}\right)^{\frac{1}{2}} \sum_i^N s_i} dx. \tag{B.5}$$

B.2 The Saddle-Point Equations

Let $f(x)$ be a continuous function whose absolute maximum lies at x_0. Let Z_N be

$$Z_N = \int_{-\infty}^{\infty} e^{Nf(x)} dx. \tag{B.6}$$

Then

$$\lim_{N\to\infty}\frac{1}{N}\ln Z_N = f\left(x_0\right). \tag{B.7}$$

Proof:

First we take out of the exponential a common factor

$$Z_N = \int_{-\infty}^{\infty} e^{Nf(x)}dx = e^{Nf(x_0)}\underbrace{\int_{-\infty}^{\infty} e^{-N(f(x_0)-f(x))}\,dx}_{I_N}, \tag{B.8}$$

so as to make the integrand ≤ 1 for any value of x. Now we compute

$$\lim_{N\to\infty}\frac{1}{N}\ln Z_N = f\left(x_0\right) + \lim_{N\to\infty}\frac{1}{N}\ln\left[I_N\right]. \tag{B.9}$$

Since Z_N is finite for finite N, the integral I_N is also finite for a finite value of N. Moreover, as N increases, the value of the integral should stay or decrease. Therefore

$$\forall N > N_0 \quad I_{N_0} \geq I_N \quad \Longrightarrow \quad \frac{1}{N}\ln I_N \leq \frac{1}{N}\ln I_{N_0},$$

and as $N\to\infty$, the quantity $\frac{1}{N}\ln I_{N_0}$ vanishes, thus we impose the condition

$$\lim_{N\to\infty}\frac{1}{N}\ln I_N \leq 0. \tag{B.10}$$

This completes the first part of the proof.

Now we take advantage of the continuity of $f\left(x\right)$:

$$\forall\varepsilon \quad \exists\delta > 0 \| \quad |x - x_0| < \delta \implies |f\left(x\right) - f\left(x_0\right)| < \varepsilon.$$

Given a number ε, I find a δ satisfying the continuity condition, and divide the integral I_N in three parts,

$$I_N = \int_{-\infty}^{\infty} e^{-N(f(x_0)-f(x))} = \int_{-\infty}^{x_0-\delta} e^{-N(f(x_0)-f(x))}dx + \int_{x_0-\delta}^{x_0+\delta} e^{-N(f(x_0)-f(x))}dx + \int_{x_0+\delta}^{\infty} e^{-N(f(x_0)-f(x))}dx. \tag{B.11}$$

As all these integrals are positive, the following inequality,

$$I_N \geq \int_{x_0-\delta}^{x_0+\delta} e^{-N(f(x_0)-f(x))}dx, \tag{B.12}$$

is straightforward, but $f\left(x_0\right) - f\left(x\right)$ is bounded by ε, so

$$I_N \geq \int_{x_0-\delta}^{x_0+\delta} e^{-N\varepsilon}dx = e^{-N\varepsilon}2\delta. \tag{B.13}$$

Taking logarithms and dividing by N

$$\frac{1}{N}I_N \geq \frac{1}{N}\left(\ln 2 + \ln\delta\right) - \varepsilon. \tag{B.14}$$

The first term of the r.h.s. dies in the limit $N\to\infty$. The second term can be arbitrarily small, thence

$$\lim_{N\to\infty} \frac{1}{N} \ln I_N \geq 0. \tag{B.15}$$

which is the second part of the proof. Combined with the first piece

$$0 \geq \frac{1}{N} \ln I_N \geq 0, \tag{B.16}$$

and we can rewrite equation (B.9) taking into account (B.16),

$$\lim_{N\to\infty} \frac{1}{N} \ln Z_N = f(x_0) + \lim_{N\to\infty} \frac{1}{N} \ln [I_N] = f(x_0), \tag{B.17}$$

which is the desired result.

Appendix C

Mean-field theory

Let us solve the infinite coupled, ferromagnetic Ising model, described by the Hamiltonian

$$H\left(J,B,\{s_i\}\right)=-\frac{J}{N}\sum_{i\neq j}^{N}s_is_j-B\sum_{i}^{N}s_i. \tag{C.1}$$

Defining $F=\beta J$ and $h=\beta B$, the partition function

$$Z\left(F,h\right)=\sum_{\{s_i\}}e^{\frac{F}{N}\sum_{i\neq j}^{N}s_is_j+h\sum_{i}^{N}s_i} \tag{C.2}$$

can be summed up by noticing the following equality

$$\sum_{i\neq j}^{N}s_is_j=\left[\sum_{i}^{N}s_i\right]^2-N \tag{C.3}$$

and it is this equality that allow us to recover (5.61) up to a constant. Now the quadratic exponent is linearized using the Hubbard-Stratonovich identity[1]

$$Z\left(F,h\right)=\frac{e^{-F}}{\pi^{\frac{1}{2}}}\int_{-\infty}^{\infty}\sum_{\{s_i\}}e^{-x^2+\left(2x\left(\frac{F}{N}\right)^{\frac{1}{2}}+h\right)\sum_{i}^{N}s_i}dx. \tag{C.4}$$

The integrand factorizes, as there is no spin-spin interaction

$$Z\left(F,h\right)=\frac{2^Ne^{-F}}{\pi^{\frac{1}{2}}}\int_{-\infty}^{\infty}e^{-x^2}\cosh^N\left[2x\left(\frac{F}{N}\right)^{\frac{1}{2}}+h\right]dx. \tag{C.5}$$

Let us remove N factors by rescaling the variable x

$$\begin{array}{rcl} x & \rightarrow & N^{\frac{1}{2}}y \\ dx & \rightarrow & N^{\frac{1}{2}}dy \end{array}$$

so (C.4) becomes

$$Z\left(F,h\right)=2^Ne^{-F}\left(\frac{N}{\pi}\right)^{\frac{1}{2}}\int_{-\infty}^{\infty}\left[e^{-y^2+\ln\left[\cosh\left(2F^{\frac{1}{2}}y+h\right)\right]}\right]^N dy. \tag{C.6}$$

[1] See Appendix B

Again, the integral (C.6) is not solvable by standard means, but the *saddle-point technique*[2] enables us to work out the free energy

$$\lim_{N\to\infty}\frac{1}{N}\ln Z\left(F,h\right)=\ln 2+$$
$$\lim_{N\to\infty}\frac{1}{N}\ln\int_{-\infty}^{\infty}\left[e^{-y^2\ln\left[\cosh\left(2F^{\frac{1}{2}}y+h\right)\right]}\right]^N dy. \tag{C.7}$$

And the saddle-point equations

$$-y_0+F^{\frac{1}{2}}\tanh\left(2F^{\frac{1}{2}}y_0+h\right)=0, \tag{C.8}$$
$$-1+\frac{2F}{\cosh^2\left(2F^{\frac{1}{2}}y_0+h\right)}<0, \tag{C.9}$$

maximize the following function

$$g\left(y\right)=-y^2+\ln\left[\cosh\left(2F^{\frac{1}{2}}y+h\right)\right]. \tag{C.10}$$

Thus, the free energy is

$$f\left(F,h\right)=\ln 2+g\left(y_0\right) \tag{C.11}$$

and y_0 complies with the saddle-point equations (C.9). It is straightforward to link the ghost variable y to the magnetization of the system

$$\langle m\rangle=m_0=\frac{\partial f}{\partial h}=\left.\frac{\partial g}{\partial h}\right|_{y=y_0}+$$
$$\left.\frac{\partial g}{\partial y}\right|_{y=y_0}\frac{\partial y}{\partial h}=\tanh\left(2F^{\frac{1}{2}}y_0+h\right)=F^{-\frac{1}{2}}y \tag{C.12}$$

This way we arrive to the standard mean-field equation[3]

$$m_0=\tanh\left(2Fm_0+h\right). \tag{C.13}$$

The dependency of the free energy on the external field is hidden in $m_0\left(h\right)$.

Equation (C.13) is the standard mean-field equation. Indeed, when performing mean field calculations, people usually try an ansatz like (C.13), instead of deriving it, as it has been done in this work, and this ansatz normally guesses right.

The ansatz method is based on physical grounds, and begins with equation (5.58) for paramagnetic substances

$$m=\tanh\left(h\right). \tag{C.14}$$

This equation only takes into account the external magnetic field, neglecting the magnetic field that might appear if the magnetic dipoles of the substance align to h. This induced field is called *molecular field*, and we expect it to be proportional to the current magnetization of the sample m. As magnetic interactions are quite short ranged, we expect each dipole to interact

[2] See Appendix B.

[3] In some text, a $2D$ factor appears accounting for the coordination number, leaving the equation as $m_0=\tanh\left(4DFm_0+h\right)$. This factor can be absorbed in the coupling constant F, and does not modify qualitatively the physics of the model.

only with surrounding dipoles, so the strength of the molecular field is also proportional to the coordination number q and to a coupling constant dipole-magnetization F. Therefore, our guess is

$$m = \tanh\left(qFm + h\right). \tag{C.15}$$

which is essentially the same as (C.13).

These equations are valid for the ferromagnetic case, however, the antiferromangetic case is not so straightforward to guess. A simple but effective way would be to substitute the magnetization m by the staggered magnetization m_S in (C.15). But this must be wrong, for the magnetic field affects the spins in the same way as the staggered magnetization, even though the external field is not staggered itself.

There are other approaches, like the one showed in [96], where the lattice is divided in two different sublattices S_1 and S_2, and the following mean-field equations are proposed

$$m_1 = \tfrac{1}{2}\tanh\left(2Fm_2 + h\right), \tag{C.16}$$
$$m_2 = \tfrac{1}{2}\tanh\left(2Fm_1 + h\right). \tag{C.17}$$

These equations are suspicious in the sense that, for a ferromagnetic coupling $F > 0$, they fail to deliver the original equation (C.13) in the limit $m_1 = m_2 = \frac{m}{2}$, giving instead

$$m = \tanh\left(Fm + h\right). \tag{C.18}$$

On the contrary, our derivation

$$m_1 = \tfrac{1}{2}\tanh\left(h + 2Fm_S\right), \tag{C.19}$$
$$m_2 = \tfrac{1}{2}\tanh\left(h - 2Fm_S\right). \tag{C.20}$$

leads to the right result if we tweak the couplings a bit. We divide Fm_S into

$$m_1 = \tfrac{1}{2}\tanh\left(2\left(F_{11}m_1 + F_{12}m_2\right) + h\right), \tag{C.21}$$
$$m_2 = \tfrac{1}{2}\tanh\left(2\left(F_{21}m_1 + F_{22}m_2\right) + h\right). \tag{C.22}$$

where F_{ij} represents the coupling of spins belonging to the sublattice S_i to the ones belonging to the sublattice S_j. The ferromagnetic case is represented by $F_{11} = F_{22} = F_{12} = F_{21} > 0$, whereas the antiferromagnetic case appears when $F_{11} = F_{22} = -F_{12} = -F_{21} > 0$. The main difference between the two approaches is the fact that we have taken into account all the spins when computing the molecular field, whereas our colleagues in [96] took only into account the spins of the opposite sublattice. Indeed, if in our original result for the antiferromagnetic model we introduce a *staggered reduced magnetic field* h_S, which enhances the staggered magnetization[4] instead of a standard field h, we find for m_S an equation which is analogous to the one for m in the ferromagnetic case

$$m_S = \tanh\left(2Fm_S + h_S\right). \tag{C.23}$$

This is an expected result, an indicates that we are moving along the right track, for the models are completely equivalent.

[4]This effect can be achieved by allowing the field to couple differently to the two sublattices.

Coming back to the ferromagnetic model, equation (C.13) displays spontaneous magnetization for certain values of the coupling F. The best way to check this is by solving equation (C.13) graphically, as it is done in fig. C. Fig. C tells us which solutions of (C.13) are stable (maxima) and which are not (minima).

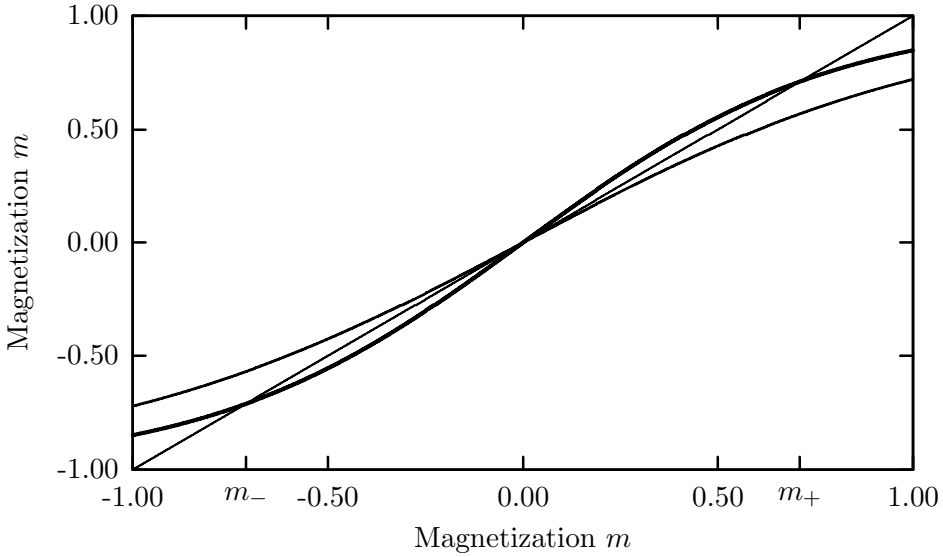

Figure C.1: Graphical solution to equation (C.13). The existence of spontaneous symmetry breaking depends on the slope of the function $\tanh(2Fm_0)$ at the origin, as discussed in this chapter.

The parameter who determines the right number of solutions to the saddle-point equation is F, through the first derivative of the function $\tanh(2Fm_0)$ at the origin

$$\frac{\partial}{\partial m_0}\tanh(2Fm_0)\bigg|_{m_0=0} = 2F. \tag{C.24}$$

Depending on the behaviour close to the origin, we have several possibilities

- If the slope of $\tanh(2Fm_0)$ is higher than the slope of the function $y = m_0$

$$2F > 1 \quad \rightarrow \quad F > \frac{1}{2},$$

  there are three solutions to the saddle point equation, $m_0 = \{m_+, m_-, 0\}$, two of them symmetric to keep the original Z_2 symmetry of the action.

- On the contrary, a small slope of $\tanh(2Fm_0)$, $F < \frac{1}{2}$, leads to only one solution at the origin, adn the Z_2 symmetry is preserved.

The value $F_C = \frac{1}{2}$ is called the *critical coupling*, and marks a second order phase transition with diverging susceptibility

$$\lim_{F\to F_C^-}\chi|_{m_0=0} = \lim_{F\to F_C^-}\frac{\partial m_0}{\partial h}\bigg|_{m_0=0} = \frac{1-m_0^2}{(1-2F)\left(1-m_0^2\right)} \implies \chi\to\infty, \tag{C.25}$$

and the critical exponent γ for this divergence is $\gamma = 1$. It can be proved that the exponent remains the same if we approach the critical point from above ($F \to F_C^+$).

Finally, the effect of the reduced external field on the broken phase is to select a vacuum from the two distinct possibilities.

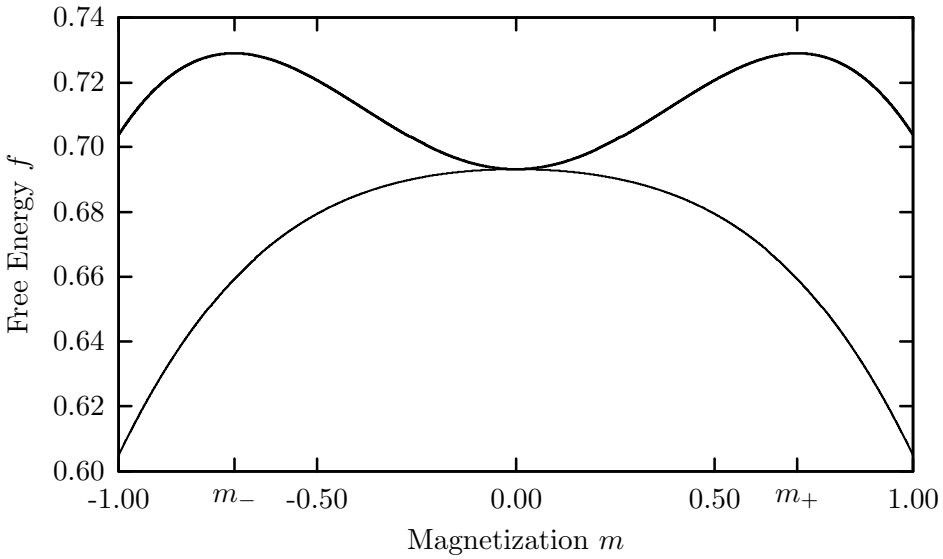

Figure C.2: Free energy (C.11) as a function of the magnetization m_0. Whenever spontaneous symmetry breaking occurrs, the stable vacua are those far from the origin, which violate Z_2 symmetry. For the non-SSB scenario, the only stable vacua is at the origin, and the mean magnetization is zero. Whether the first or the second condition happens depends only on F.

Appendix D

Some mean-field results for the Ising model

In order to compute the gap in the susceptibilities at the critical line, it is compulsory to find out the behaviour of the variable y_0 in the neighbourhood of θ_c. What we must do is solve the saddle-point equation

$$y_0 = \frac{|F|^{\frac{1}{2}}}{2} \frac{\sinh\left(4\,|F|^{\frac{1}{2}}\, y_0\right)}{\cosh^2\left(2\,|F|^{\frac{1}{2}}\, y_0\right) - \sin^2\frac{\theta}{2}}. \tag{D.1}$$

The way to proceed is to expand the hyperbolic functions as a power series in y, and drop all the higher order terms. As for $\theta < \theta_c$ the only solution to the saddle point equation is $y_0 = 0$, we can expand around this point

$$\sinh\left(4\,|F|^{\frac{1}{2}}\, y_0\right) = 4\,|F|^{\frac{1}{2}}\, y_0 + \frac{32}{3}\,|F|^{\frac{3}{2}}\, y_0^3 + O\left(y^5\right), \tag{D.2}$$

$$\cosh\left(2\,|F|^{\frac{1}{2}}\, y_0\right) = 1 + 2\,|F|\, y_0^2 + O\left(y^4\right), \tag{D.3}$$

so the saddle-point equation becomes

$$y_0 \sim 2\,|F|\, \frac{y_0 + \frac{8}{3}\,|F|\, y_0^3}{4\,|F|\, y_0^2 + \cos^2\frac{\theta}{2}} \qquad y_0 << 1. \tag{D.4}$$

Now we expand again the denominator of (D.4) up to y_0^2,

$$\frac{1}{4\,|F|\, y_0^2 + \cos^2\frac{\theta}{2}} = \frac{1}{\cos^2\frac{\theta}{2}} - \frac{4\,|F|}{\cos^4\frac{\theta}{2}} y_0^2 + O\left(y_0^4\right). \tag{D.5}$$

Therefore, for $\theta \gtrsim \theta_c$,

$$y_0 \sim \frac{2\,|F|}{\cos^2\frac{\theta}{2}} y_0 + 8\,|F|^2\, \frac{2\cos^2\frac{\theta}{2} - 3}{3\cos^4\frac{\theta}{2}} y_0^3. \tag{D.6}$$

We already know of the $y_0 = 0$ solution. Solving the quadratic equation that is left,

$$y_0 = \sqrt{\frac{3}{8\,|F|^2} \frac{\left(\cos^2\frac{\theta}{2} - 2\,|F|\right)\cos^2\frac{\theta}{2}}{2\cos^2\frac{\theta}{2} - 3}}. \tag{D.7}$$

Thus y_0 tends to zero as θ approaches the critical value for a given F. Its derivative with respect to θ, on the other hand,

$$\frac{dy_0}{d\theta} = -\sqrt{\frac{3}{32\left|F\right|^2}}\frac{\sin\theta\left(\cos^4\frac{\theta}{2} - 3\cos^2\frac{\theta}{2} + 3\left|F\right|\right)}{\sqrt{\left(2\cos^2\frac{\theta}{2} - 3\right)^3\left[\left(\cos^2\frac{\theta}{2} - 2\left|F\right|\right)\cos^2\frac{\theta}{2}\right]}}, \tag{D.8}$$

diverges as

$$\frac{1}{\sqrt{\left(\cos^2\frac{\theta}{2} - 2\left|F\right|\right)\cos^2\frac{\theta}{2}}},$$

for at the critical line $\cos\frac{\theta_c}{2} = 2F$. The divergence cancels in the product $y_0\frac{dy_0}{d\theta}$. As $y_0 = \sqrt{|F|}m_S$, this also applies to $m_S\frac{dm_S}{d\theta}$.

The solution obtained in (D.7) can be used to calculate the behaviour of the susceptibilities around the critical point. The 'topological' susceptibility

$$\chi_T = \frac{dm}{di\frac{\theta}{2}} = \frac{dm}{d\theta}\frac{d\theta}{di\frac{\theta}{2}} = \frac{\left(\cos^2\frac{\theta}{2} - 1\right)\cosh\left(2\left|F\right|m_S\right) + 1 - \cos^2\frac{\theta}{2}}{\left(\cosh^2\left(2\left|F\right|m_S\left(\theta\right)\right) - \sin^2\frac{\theta}{2}\right)^2} -$$
$$-\frac{2\left|F\right|\sin\theta\sinh\left(4\left|F\right|m_S\right)\frac{dm_S}{d\theta}}{\left(\cosh^2\left(2\left|F\right|m_S\right) - \sin^2\frac{\theta}{2}\right)^2}, \tag{D.9}$$

takes the value

$$\lim_{\theta\to\theta_c^-}\chi_T = \frac{1}{\cos^2\frac{\theta_c}{2}} = \frac{1}{2\left|F\right|}, \tag{D.10}$$

as we approach θ_c from below. However, if we come from the antiferromagnetic phase $\theta > \theta_c$, the second term gives a non-zero contribution, for the derivative $\frac{dm_S}{d\theta}$ diverges at the critical line. The divergence is cancelled exactly by the factor $\sinh\left(4\left|F\right|m_S\right)$, as explained before, and what remains is a finite contribution

$$m_S\frac{dm_S}{d\theta}\bigg|_{\theta=\theta_c} = -\frac{3\sin\theta_c}{16\left|F\right|^2\left(4\left|F\right| - 3\right)}$$
$$\frac{2\left|F\right|\sin\theta\sinh\left(4\left|F\right|m_S\right)\frac{dm_S}{d\theta}}{\left(\cosh^2\left(2\left|F\right|m_S\right) - \sin^2\frac{\theta}{2}\right)^2} \sim -\frac{3\sin^2\theta_c}{32\left|F\right|^2\left(4F - 3\right)}$$

In the end

$$\lim_{\theta\to\theta_c^+}\chi_T = \frac{1}{2\left|F\right|} + \frac{3}{4\left|F\right|}\frac{2\left|F\right| - 1}{4\left|F\right| - 3}, \tag{D.11}$$

and the gap is

$$\Delta\chi_T = \lim_{\theta\to\theta_c^+}\chi_T - \lim_{\theta\to\theta_c^-}\chi_T = \frac{3}{4\left|F\right|}\frac{2\left|F\right| - 1}{4\left|F\right| - 3}. \tag{D.12}$$

The staggered susceptibility diverges at the critical line. This is quite expected, as for $\theta = 0$ the susceptibility diverges at the critical point. The computation for any value of θ is complicated, for in order to obtain χ_S, we need to take derivatives with respect to a staggered field θ_S, and the take the $\theta_S \to 0$ limit. To this purpose, we use the original form of the free energy (5.67) with a θ_S term

$$f\left(F, m_S, \theta, \theta_S\right) = -\left|F\right| m_S^2 + \frac{1}{2}\ln\left[\cosh\left(2\left|F\right| m_S + \frac{i\theta + i\theta_S}{2}\right)\times\right.$$
$$\left.\cosh\left(2\left|F\right| m_S - \frac{i\theta - i\theta_S}{2}\right)\right] \tag{D.13}$$

Taking derivatives with respect to m_S we should recover the saddle-point equation with the addition of the θ_S source

$$\frac{df}{dm_S} = 0 = -2\left|F\right| m_S + \left|F\right|\left[\tanh\left(2\left|F\right| m_S + \frac{i\theta + i\theta_S}{2}\right) + \right.$$
$$\left.\tanh\left(2\left|F\right| m_S - \frac{i\theta - i\theta_S}{2}\right)\right]. \tag{D.14}$$

This time the saddle point equation is complex, therefore a working solution is not guaranteed at first glance. Nevertheless, we are using θ_S as a mathematical tool to find out the staggered susceptibility. In the end the $\theta_S \to 0$ limit is taken, and the validity of the saddle-point solution is recovered.

From (D.14) a new equation for the staggered magnetization is obtained

$$m_S = \frac{1}{2}\left[\tanh\left(2\left|F\right| m_S + \frac{i\theta + i\theta_S}{2}\right) + \right.$$
$$\left.\tanh\left(2\left|F\right| m_S - \frac{i\theta - i\theta_S}{2}\right)\right]. \tag{D.15}$$

The derivative with respect to θ_S gives us the longed susceptibility

$$\chi_S = \frac{dm_S}{d\frac{i\theta_S}{2}} = \frac{1 + 2\left|F\right|\chi_S}{2\cosh^2\left(2\left|F\right| m_S + \frac{i\theta + i\theta_S}{2}\right)} +$$
$$\frac{1 + 2\left|F\right|\chi_S}{2\cosh^2\left(2\left|F\right| m_S - \frac{i\theta - i\theta_S}{2}\right)} = \frac{1 + 2\left|F\right|\chi_S}{2} X, \tag{D.16}$$

where

$$X = \frac{1}{2\cosh^2\left(2\left|F\right| m_S + \frac{i\theta + i\theta_S}{2}\right)} + \frac{1}{2\cosh^2\left(2\left|F\right| m_S - \frac{i\theta - i\theta_S}{2}\right)}.$$

Moving all the terms proportional to χ_S to the l.h.s.

$$2\chi_S\left(1 - \left|F\right| X\right) = X, \tag{D.17}$$

we can find the value of χ_S

$$\chi_S = \frac{X}{2 - 2\left|F\right| X}. \tag{D.18}$$

The quantity X must be evaluated at the point $\theta = \theta_c$ and $\theta_S = 0$. This is not a difficult task and the final value is

$$X = \frac{1}{\left|F\right|}.$$

Therefore

$$\chi_S = \frac{1}{2\left|F\right| - 2\left|F\right|} = \infty, \tag{D.19}$$

and the susceptibility diverges at the critical line.

Finally, and to elucidate the behaviour of $m\left(\theta\right)$ as $\theta \to \pi$, we need to work out the following limit

$$\lim_{\theta \to \pi} \frac{dm_S}{d\theta} \sin\theta. \tag{D.20}$$

As $\sin\theta \to 0$ when θ approaches π, only if the derivative $\frac{dm_S}{d\theta}$ diverges at $\theta = \pi$ is the product (D.20) non-vanishing. The expansion we performed previously is not very useful here, as the point $\theta = \pi$ is far from the critical line (unless we are taking the $F \to 0$ limit as well). The way to solve this problem is to compute implicitly the derivative from the saddle-point equation (5.83) at $\theta = \pi$

$$\begin{aligned}
\left.\frac{dm_S}{d\theta}\right|_{\theta=\pi} = \left.\frac{dm_S}{d\theta}\frac{2\left|F\right|\cosh\left(4\left|F\right|m_S\right)}{\cosh^2\left(2\left|F\right|m_S\right) - \sin^2\frac{\theta}{2}}\right|_{\theta=\pi} - \\
- \sinh\left(4\left|F\right|m_S\right)\left.\frac{\frac{dm_S}{d\theta}\left|F\right|\sinh\left(4\left|F\right|m_S\right) - \frac{\sin\theta}{4}}{\left(\cosh^2\left(2\left|F\right|m_S\right) - \sin^2\frac{\theta}{2}\right)^2}\right|_{\theta=\pi} = \\
= \left.\frac{dm_S}{d\theta}\right|_{\theta=\pi} 4\left|F\right| \operatorname{cotanh}\left(2\left|F\right|m_S\right)\left[1 - \operatorname{cotanh}\left(2\left|F\right|m_S\right)\right].
\end{aligned} \tag{D.21}$$

Moving all the terms to the l.h.s. of the equation we find that either

$$1 - 4\left|F\right| \operatorname{cotanh}\left(2\left|F\right|m_S\right)\left[1 - \operatorname{cotanh}\left(2\left|F\right|m_S\right)\right] = 0, \tag{D.22}$$

or

$$\left.\frac{dm_S}{d\theta}\right|_{\theta=\pi} = 0. \tag{D.23}$$

The first case is impossible, for the solution to the saddle-point equation at $\theta = \pi$ imposes

$$m_S\left(\pi\right) = \operatorname{cotanh}\left(2\left|F\right|m_S\right), \tag{D.24}$$

which is non-zero and verifies

$$\left|m_S\right| \geq 1,$$

so the l.h.s. never vanishes, for the second summand is always positive. Therefore, (D.23) applies and the derivative vanishes at $\theta = \pi$.

Appendix E

Spectrum of the Ginsparg-Wilson operator on the lattice

Years ago Ginsparg and Wilson (Ginsparg-Wilson) [11] suggested, in order to avoid the Nielsen and Ninomiya non go theorem [8] and to preserve chiral symmetry on the lattice, to require the following condition for the inverse Dirac operator

$$\gamma_5 D^{-1} + D^{-1}\gamma_5 = 2aR\gamma_5, \tag{E.1}$$

where a is the lattice spacing and R is a local operator. Accordingly D should satisfy, instead of the standard anticommutation relation of the continuum formulation, the Ginsparg-Wilson relation

$$\gamma_5 D + D\gamma_5 = 2aDR\gamma_5 D. \tag{E.2}$$

Fifteen years after this proposal, Hasenfratz [141] and Neuberger [142] found that the fixed point action for QCD and the overlap fermions satisfy respectively the Ginsparg-Wilson relation, the last with $R = 1/2$. Furthermore, Hasenfratz, Laliena and Niedermayer [143] realized that Ginsparg-Wilson fermions have nice chiral properties, allowing us to establish an exact index theorem on the lattice. Indeed if we define a local density of topological charge as

$$q(x) = aRTr\left(\gamma_5 D\left(x, x\right)\right), \tag{E.3}$$

the corresponding topological charge is

$$Q = aRTr(\gamma_5 D), \tag{E.4}$$

which is a topological invariant integer that approaches the continuum topological charge in the continuum limit. Finally by replacing the Ginsparg-Wilson Dirac operator $D + m$ by

$$\Delta + m = \left(1 - \frac{am}{2}\right) D + m, \tag{E.5}$$

in order to define an unsubtracted proper order parameter [144]

$$\bar{\psi}\left(1 - \frac{aD}{2}\right)\psi, \tag{E.6}$$

then the Ginsparg-Wilson fermionic action possesses an exact symmetry which is anomalous for the flavour singlet transformations, but exact for the flavour non-singlet case (see [145]); a property which allows us to introduce also a θ parameter in the Ginsparg-Wilson action, as in the continuum.

In this dissertation, the value $R = 1/2$ is used, as well as the massive Dirac operator (E.5) associated to the unsubtracted chiral order parameter (4.39), but the choice is irrelevant for the final results, as they hold as well for the standard, substracted order parameters, and for any other constant values of $R > 0$.

Let us start with the Ginsparg-Wilson relation for $R = 1/2$,

$$\gamma_5 D + D\gamma_5 = aD\gamma_5 D. \tag{E.7}$$

One also chooses D such that

$$\gamma_5 D \gamma_5 = D^\dagger. \tag{E.8}$$

Merging (E.7) and (E.8),

$$D + D^\dagger = aDD^\dagger = aD^\dagger D. \tag{E.9}$$

Hence D is a normal operator, and as such, it has a basis of orthonormal eigenvectors. Also eigenvectors corresponding to different eigenvalues are necessarily orthogonal. From (E.9) it is immediate to check that the operator $V = 1 - aD$ is unitary, $V^\dagger V = I$. Therefore the spectrum of V lies in the unit circle with center in the origin, and the spectrum of D must then lie in the shifted and rescaled circle of radius $\frac{1}{a}$ centered in the real axis at $(\frac{1}{a}, 0)$. Then, the possible eigenvalues of D are of the form

$$\lambda = \frac{1}{a}\left(1 - e^{i\alpha}\right), \alpha \in \mathbb{R}, \tag{E.10}$$

and the following identity is satisfied

$$\lambda + \lambda^* = a\lambda\lambda^*. \tag{E.11}$$

Let $\mathbf{v}$ be an eigenvector of D with eigenvalue λ, $D\mathbf{v} = \lambda\mathbf{v}$. Taking into account (E.7), a relationship between the eigenvalues of $\mathbf{v}$ and $\gamma_5\mathbf{v}$ can be found,

$$D\gamma_5\mathbf{v} = -\gamma_5 D\mathbf{v} + aD\gamma_5 D\mathbf{v} = -\lambda\left(\gamma_5\mathbf{v} + aD\gamma_5\mathbf{v}\right), \tag{E.12}$$

and using (E.11) we arrive to the final expression

$$D\left(\gamma_5\mathbf{v}\right) = -\frac{\lambda}{1 - a\lambda}\left(\gamma_5\mathbf{v}\right) = \lambda^*\left(\gamma_5\mathbf{v}\right). \tag{E.13}$$

Thus, if $\mathbf{v}$ is an eigenvector of D with eigenvalue λ, then $\gamma_5\mathbf{v}$ is another eigenvector with eigenvalue λ^*, and when λ is not real, then those two eigenvectors correspond to different eigenvalues and must be orthogonal. On the other hand, restricting ourselves to the subspace corresponding to real eigenvalues, $\lambda = 0$ or $\lambda = \frac{2}{a}$, γ_5 and D commute, and therefore we can find a common basis of eigenvectors; in other words, we can find an orthonormal basis for which the eigenvectors of D corresponding to real eigenvalues are chiral. If we denote by n^+ (n^-) the number of eigenvectors of positive (negative) chirality in the subspace corresponding to $\lambda = 0$, and similarly n'^+ (n'^-) for the subspace corresponding to $\lambda = \frac{2}{a}$, then the fact that $Tr(\gamma_5) = 0$ and $Q = \frac{a}{2}Tr(\gamma_5 D)$ imply

$$n^+ - n^- = n'^- - n'^+, \tag{E.14}$$

$$Q = n^- - n^+. \tag{E.15}$$

Let us call V the size of the matrix D. Then the density of topological charge, defined as $\frac{Q}{V}$, is bounded in absolute value by 1, $\left|\frac{Q}{V}\right| \leq 1$.

The operator in the fermion action is

$$\Delta + m = \left(1 - \frac{am}{2}\right) D + m \tag{E.16}$$

Its spectrum is trivially related to the spectrum of D; if λ are as before the eigenvalues of D, then the eigenvalues of (E.16) are $\left(1 - \frac{am}{2}\right)\lambda + m$. They still lie in a circle with the center in the real axis, and the possible real eigenvalues are now m and $\frac{2}{a}$. We will always require that $0 < m < \frac{2}{a}$, then the operator (E.16) preserves the position of the higher real eigenvalue [69].

We will also need the spectrum of $H = \gamma_5 (\Delta + m)$. It is easy to see that H is an hermitian operator, $H^\dagger = H$, and therefore has real spectrum μ_j. This spectrum can be worked out by noting that the matrix $\gamma_5 (\Delta + m)$ is block diagonal in the basis of eigenvectors of D. Calling $\mathbf{v}_\lambda$ such and eigenvector with non-real eigenvalue λ, then

$$\begin{array}{ll} H\mathbf{v}_\lambda & = \gamma_5 \left(1 - \frac{am}{2}\right) \lambda \mathbf{v}_\lambda + m \mathbf{v}_{\lambda^*} \quad = \left(m + \lambda \left(1 - \frac{am}{2}\right)\right) \mathbf{v}_{\lambda^*}, \\ H\mathbf{v}_{\lambda^*} & = \gamma_5 \left(1 - \frac{am}{2}\right) \lambda^* \mathbf{v}_{\lambda^*} + m \mathbf{v}_\lambda \quad = \left(m + \lambda^* \left(1 - \frac{am}{2}\right)\right) \mathbf{v}_\lambda. \end{array} \tag{E.17}$$

This is a block diagonal matrix, decomposable in 2×2 blocks like

$$\begin{pmatrix} 0 & m + \lambda \left(1 - \frac{am}{2}\right) \\ m + \lambda^* \left(1 - \frac{am}{2}\right) & 0 \end{pmatrix}. \tag{E.18}$$

The diagonalization of this block yields a pair of real eigenvalues $\pm\mu$,

$$\mu^2 = m^2 + \lambda\lambda^* \left(1 - \frac{am}{2}\right)^2 + m \left(\lambda + \lambda^*\right) \left(1 - \frac{am}{2}\right) \tag{E.19}$$

For the case $\lambda \in \mathbb{R}$, the results become quite different. Let $\mathbf{v}_\lambda$ be an eigenvector of D of chirality $\chi = \pm 1$, that is, $\gamma_5 \mathbf{v}_\lambda = \chi \mathbf{v}_\lambda$. Then

$$H\mathbf{v}_\lambda = \gamma_5 \left(1 - \frac{am}{2}\right) \lambda \mathbf{v}_\lambda + m\chi \mathbf{v}_\lambda = \left(m + \lambda \left(1 - \frac{am}{2}\right)\right) \chi \mathbf{v}_\lambda, \tag{E.20}$$

and the expression for μ reads

$$\mu = \left(m + \lambda \left(1 - \frac{am}{2}\right)\right) \chi. \tag{E.21}$$

More explicitly, as $\lambda \in \mathbb{R}$ implies that either $\lambda = 0$ or $\lambda = \frac{2}{a}$, the only allowed values for μ are $\mu = \pm m$ for $\lambda = 0$, with degeneracy n^+ and n^-, and similarly $\mu = \pm\frac{a}{2}$ with degeneracy n'^+, n'^- when $\lambda = \frac{2}{a}$.

The above calculations imply a bound for μ at finite mass, as was remarked in [69],

$$\mu^2 \geq m^2, \tag{E.22}$$

valid only if $ma < 2$, which is a reasonable requirement. Otherwise, the spectrum of the Ginsparg-wilson operator breaks down.

The importance of the mass bound (E.22) can not be overemphasized. It is essential in the proofs developed in this dissertation on symmetry conservations, and also rules out the existence of an Aoki phase for Ginsparg-Wilson fermions. We might wonder how this happens in the Ginsparg-Wilson formulation, given the fact that the Ginsparg-Wilson operator does not anticommunte with γ_5. The answer is related to equation (E.1): we can write a similar equation for Wilson fermions, $\left\{\gamma_5, \Delta^{-1}\right\} = 2aR\gamma^5$, where R is a *non-local* operator, but in the case of Ginsparg-Wilson fermions, this R turns out to be local. It is this locality that enforces

the depletion of the spectrum of small real eigenvalues, close to the origin, for the eigenvectors of Δ look like chiral solutions at long distances, and effectively it is *as if* the anticommutator was realized. So, no quasi-chiral, exceptional configurations are allowed, the Aoki phase is completely forbidden, and therefore, the symmetries are respected.

-Another interesting results are straightforward from this point on. For instance, we know that there exist an index theorem for Ginsparg-Wilson fermions [143], thus we can relate the zero modes of $\bar{\Delta}$ to the topological density and the topological susceptibility,

Let's consider now the determinant of the operator

$$\Delta + m + \frac{q}{V}\gamma_5 \left(1 - \frac{aD}{2}\right). \tag{E.23}$$

Proceeding as before, another block-diagonal structure is found in the basis of eigenvectors of D, and the contribution to the determinant coming from the block corresponding to a complex pair $\mathbf{v}_\lambda$, $\mathbf{v}_{\lambda^*}$ is given by

$$\det \begin{pmatrix} \left(1 - \frac{am}{2}\right)\lambda + m & \frac{q}{V}\left(1 - \frac{a\lambda}{2}\right) \\ \frac{q}{V}\left(1 - \frac{a\lambda^*}{2}\right) & \left(1 - \frac{am}{2}\right)\lambda^* + m \end{pmatrix} = \\ m^2 + \left[1 - \left(\frac{am}{2}\right)^2\right]\lambda\lambda^* - \frac{q^2}{V^2}\left(1 - \frac{a^2\lambda\lambda^*}{4}\right), \tag{E.24}$$

where we have used the identity (E.11). The determinant of this block gives the contribution of a pair of eigenvalues to the determinant

$$1 - \alpha\frac{q^2}{V^2}, \tag{E.25}$$

with

$$\alpha = \frac{1 - \frac{a^2\lambda\lambda^*}{4}}{m^2 + \left[1 - \left(\frac{am}{2}\right)^2\right]\lambda\lambda^*}. \tag{E.26}$$

The minimum achievable value for the determinant of the block (E.24) is obtained by setting $\lambda = 0$. In that case, the product equals m^2. As a result, the determinant is bounded from below for any non-zero value of the mass, and the following relationship applies

$$|\alpha| \leq \frac{1}{m^2} \tag{E.27}$$

Regarding the chiral modes of chirality χ, they contribute with a factor

$$\left(1 - \frac{am}{2}\right)\lambda + m + \frac{q}{V}\left(1 - \frac{a\lambda}{2}\right)\chi \tag{E.28}$$

For $\lambda = \frac{2}{a}$ the final factor is just $\frac{2}{a}$, whereas for a zero mode $\lambda = 0$ with chirality χ, the outcoming value is $m + \chi\frac{q}{V}$.

Bibliography

[1] S. Weinberg, *Phys. Rev. D* **11**, (1975) 3583.

[2] S. Adler, *Phys. Rev.* **177**. (1969) 2426; J. S. Bell and R. Jackiw, *Il Nuovo Cimento A* **60**, (1969) 47.

[3] G. 't Hooft, *Phys. Rev. Lett.* **37**, (1976) 8; *Phys. Rev. D* **14**, (1976) 3432.

[4] C. A. Baker, D. D. Doyle, P. Geltenbort, K. Green, M. G. D. van der Grinten, P. G. Harris, P. Iaydjiev, S. N. Ivanov, D. J. R. May, J. M. Pendlebury, J. D. Richardson, D. Shiers, and K. F. Smith, *Phys. Rev. Lett.* **97**, 131801 (2006).

[5] R. D. Peccei, *Lect. Notes Phys.* **741** (2008), 3.

[6] J. Schwinger, *The Quantum Theory of Fields I*, 1950.

[7] R. F. Streater and A. S. Wightman, *PCT, spin and statistics, and all that*, Benjamin/Cummings (1964). ISBN 0-691-07062-8.

[8] N.B. Nielsen and M. Ninomiya, *Phys. Lett. B***105**, (1981) 219; *Nucl. Phys. B***185**, (1981) 20.

[9] K. G. Wilson, *Phys. Rev. D***10**, (1974) 2445.

[10] K. G. Wilson, Lectures given in the Cargese Summer Inst., Cargese, France. Published in *Cargese Summer Inst.*, (1976) 0143.

[11] P.H. Ginsparg and K. G. Wilson, *Phys. Rev. D* **25**, (1982) 2649.

[12] S. Sharpe, *PoS(LAT2006)022*; C. Bernard, M. Golterman, Y. Shamir and S. Sharpe, *Phys. Lett. B* **649**, (2007) 235 [arXiv:hep-lat/0603027]; A. Kronfeld, *PoSLAT2007:016*, [arXiv:0711.0699 [hep-lat]] C. Bernard, M. Golterman, Y. Shamir, and S. Sharpe, *Phys. Rev. D* **77**, (2008) 114504.

[13] V. Azcoiti, G. Di Carlo, A. Galante, A. F. Grillo and V. Laliena, *Phys. Rev. D* **50**, (1994) 6994 [arXiv:hep-lat/9401032]; V. Azcoiti, G. Di Carlo, A. Galante, A. F. Grillo and V. Laliena, *Nucl. Phys. B (Proc. Suppl.)* **34**, (1994) 747.

[14] M. Creutz, *PoS(LAT2006)208* [arXiv:hep-lat/0608020]; M. Creutz, *Phys. Lett. B* **649**, (2007) 230 [arXiv:hep-lat/0701018]; M. Creutz, *Phys. Lett. B* **649**, (2007) 241 [arXiv:0704.2016 [hep-lat]]; M. Creutz, *PoS(LAT2007)007*, [arXiv:0708.1295 [hep-lat]]; M. Creutz, *Ann. of Phys.* **323**, (2008) 2349, [arXiv:0711.2640 [hep-th]]; M. Creutz, [arXiv:0804.4307v2 [hep-lat]]; M. Creutz, *Phys. Rev. D* **78**, (2008) 078501.

[15] V. A. Miranski, *Dynamical Symmetry Breaking in Quantum Field Theories*, World Scientific 1993. ISBN 981-02-1558-4. *Phys. Rev. D* **70**, (2004) 114504.

[16] J. Goldstone, *Nuovo Cimento* **19**, (1961) 154.

[17] J. Goldstone, A. Salam and S. Weinberg, *Phys. Rev.* **127**, (1962) 965.

[18] Y. Nambu, *Phys. Rev.* **117**, (1960) 648.

[19] M. Creutz, *Phys. Rev. Lett.* **81**, (1998) 3555 [arXiv:hep-lat/9806037]; *Nucl. Phys. B (Proc. Suppl.)* **73**, (1999) 819 [arXiv:hep-lat/9809024].

[20] R. Aloisio, V. Azcoiti, G. Di Carlo, A. Galante and A. F. Grillo, *Nucl. Phys. B* **606**, (2001) 322 [arXiv:hep-lat/0011079].

[21] V. Azcoiti, V. Laliena and X.Q. Luo, *Phys. Lett. B* **354**, (1995) 111.

[22] W. Lee and S. Sharpe, *Phys. Rev. D* **60**, (1999) 114503.

[23] C. Aubin and Q. Wang,

[24] S. Aoki, S. Böttcher and A. Gocksh, *Phys. Lett. B* **331**, (1994) 157 [arXiv:hep-lat/9312084];

[25] S. Aoki, *Phys. Rev. D* **30**, (1984) 2653;

[26] S. Aoki, *Phys. Rev. Lett.* **57**, (1986) 3136.

[27] S. Aoki, *Phys. Rev. D* **33**, (1986) 2399.

[28] S. Aoki, *Phys. Rev. D* **34**, (1986) 3170.

[29] S. Aoki, *Nucl. Phys. B* **314**, (1989) 79.

[30] M. Golterman, S. Sharpe and R. Singleton, Jr., *Nucl. Phys. Proc. Supp.* **140** (2005) 335 [arXiv:hep-lat/0409053].

[31] (GN) R. Kenna, C. Pinto and J.C. Sexton, *Phys. Lett. B* **505** (2001) 125 [arXiv:hep-lat/0101005].

[32] S. Sharpe and R. Singleton, Jr., *Phys. Rev. D* **58**, 074501 (1998) [arXiv:hep-lat/9804028v2].

[33] S. Sharpe and R. Singleton, Jr., *Nucl. Phys. B (Proc. Suppl.)* **73**, (1999) 234 [arxiv:hep-lat/9808047].

[34] M. Creutz, *Talk at Brookhaven Theory Workshop on Relativistic Heavy Ions*, July 1996 [arXiv:hep-lat/9608024].

[35] S. Aoki and A. Gocksh, *Phys. Lett. B* **231**, (1989) 449; *Nucl. Phys. B (Proc. Suppl.)* **17**, (1990) 378;

[36] S. Aoki and A. Gocksh, *Phys. Lett. B* **243**, (1990) 409;

[37] S. Aoki, *Phys. Lett. B* **190**, (1987) 140.

[38] S. Aoki and A. Gocksh, *Phys. Rev. D* **45**, (1992) 3845.

[39] S. Aoki, *Prog. Theor. Phys. Suppl.* **122** (1996) 179 [arXiv:hep-lat/9509008].

[40] S. Aoki, A. Ukawa and T. Umemura, *Phys. Rev. Lett.* **76**, (1996) 873 [arXiv:hep-lat/9508008]; *Nucl. Phys. B (Proc. Suppl.)* **47**, (1996) 511 [arXiv:hep-lat/9510014]; *Nucl. Phys. B (Proc. Suppl.)* **53**, (1997) 438 [arXiv:hep-lat/9612010];

[41] E.-M. Ilgenfritz, W. Kerler, M. Mueller-Preussker, A. Sternbeck and H. Stueben, *Phys. Rev. D* **69** (2004) 074511 [arXiv:hep-lat/0309057]; *Nucl. Phys. B (Proc. Suppl.)* **129&130** (2004) 898 [arXiv:hep-lat/0309059].

[42] E.-M. Ilgenfritz, W. Kerler, M. Mueller-Preussker, A. Sternbeck and H. Stueben, [arXiv:hep-lat/0511059].

[43] S. Sharpe, *Phys. Rev. D* **79**, (2009) 054503 [arXiv:0811.0409].

[44] T. Banks and A. Casher, *Nucl. Phys. B* **169**, (1980) 103.

[45] K. M. Bitar, U. M. Heller and R. Narayanan, *Phys. Lett. B* **418**, (1998) 167.

[46] H. Leutwyler and A. Smilga, *Phys. Rev. D* **46**, (1992) 5607.

[47] R. G. Edwards, U. M. Heller, R. Narayanan and R. L. Singleton, Jr., *Nucl. Phys. B***518**, (1998) 319, [arXiv:hep-lat/9711029v2].

[48] R. Narayanan and H. Neuberger, *Nucl. Phys. B***443**, (1995) 305 [arXiv:hep-th/9411108].

[49] R. G. Edwards, U. M. Heller and R. Narayanan, *Nucl. Phys. B***535**, (1998) 403 [arXiv:hep-lat/9802016].

[50] P. Hernández, *Nucl. Phys. B***536**, (1998) 345 [arXiv:hep-lat/9801035].

[51] V. Azcoiti, G. di Carlo and A. Vaquero, *Phys. Rev. D* **79**, (2009) 014509 [arXiv:0809.2972].

[52] M. Lüscher, *Comput. Phys. Commun.* **156**, (2004) 209.

[53] V. Azcoiti, G. Di Carlo and A. F. Grillo, *Phys. Rev. Lett.* **65**, (1990) 2239.

[54] V. Azcoiti, G. Di Carlo, A. F. Grillo, V. Laliena and X.Q. Luo, *Nucl. Phys. B (Proc. Suppl.)* **34**, (1994) 750.

[55] V. Azcoiti, G. Di Carlo, A. Galante, A. F. Grillo and V. Laliena, *Phys. Rev. D* **50**, (1994) 6994; *Phys.Rev. D* **53**, (1996) 5069.

[56] V. Azcoiti, G. Di Carlo, L.A. Fernandez, A. Galante, A.F. Grillo, V. Laliena, X.Q. Luo, C.E. Piedrafita and A. Vladikas, *Phys. Rev. D* **48** (1993) 402.

[57] S. Aoki and H. Fukaya, *Phys. Rev. D***81**, (2010) 034022 [arXiv:0906.4852 [hep-lat]].

[58] K. Bitar, *Phys. Rev. D***56**, (1997) 2736 [arXiv:hep-lat/9709086].

[59] C. Vafa and E. Witten, *Phys. Rev. Lett.* **53**, (1984) 535.

[60] C. Vafa and E. Witten, *Nucl. Phys. B* **234**, (1984) 173.

[61] T. D. Cohen, *Phys. Rev. D* **64**, (2001) 047704.

[62] X. Ji, *Phys. Lett. B* **554**, (2003) 33.

[63] V. Azcoiti and A. Galante, *Phys. Rev. Lett.* **83**, (1999) 1518.

[64] T. D. Lee and C. N. Yang, *Phys. Rev.* **87**, (1952) 404; *ibid.* **87**, (1952) 410;

[65] M. Asorey, *Phys. Rev. D* **80**, (2009) 127702 [arXiv:hep-lat/0204130].

[66] P. R. Cromptom, *Phys. Rev. D* **72**, (2005) 076003.

[67] V. Azcoiti, G. di Carlo and A. Vaquero, *JHEP* **0804**, (2008) 035 [arXiv:0804.1338].

[68] V. Azcoiti, G. di Carlo, E. Follana and A. Vaquero, *JHEP* **1007**, (2010) 047 [arXiv:1004.3463 [hep-lat]].

[69] Ferenc Niedermayer, *Nucl. Phys. B (Proc. Suppl.)* **73**, (1999) 105 [hep-lat/9810026].

[70] S. G. Brush, *Rev. Mod. Phys.* **39**, (1997) 883.

[71] M. Niss, *Arch. Hist. Exact. Sci.* **59**, (2005) 267.

[72] W. Lenz, *Phys. Zeitschr.* **21**, (1920) 613.

[73] P. Curie, *Ann. Chim. Phys.* **5**, (1895) 289; *Oeuvres*, p. 232.

[74] P. Weiss, *J. de Physique* **6**, (1907) 667.

[75] P. Langevin, *J. de Physique* **4**, (1905) 678; *Annales de Chimie et Physique* **5**, (1905) 70.

[76] E. Ising, *Zeitschr. f. Physik* **31**, (1925) 253.

[77] R. Peierls, *Proc. Cambridge Phil. Soc.* **32**, (1936) 477.

[78] H. A. Kramers and G. H. Wannier, *Phys. Rev.* **60**, (1941) 252.

[79] E. Montroll, *J. Chem. Phys.* **9**, (1941) 706; *J. Chem. Phys.* **10**, (1942) 61;

[80] L. Onsager, *Phys. Rev.* **65**, (1944) 117.

[81] V. Azcoiti, V. Laliena, and A. Galante, Proceedings of the *International Workshop on Non-Perturbative Methods and Lattice QCD*, Guangzhou, China, (2000) 161 [hep-lat/0007045].

[82] M. P. Lombardo, *Nucl. Phys. B (Proc. Suppl.)* **83**, (2000) 375.

[83] P. de Forcrand and O. Philipsen, *Nucl. Phys. B***642**, (2002) 290.

[84] M. D'Elia and M. P. Lombardo, *Phys. Rev. D***67**, (2003) 014505.

[85] V. Azcoiti, G. Di Carlo, A. Galante and V. Laliena, *JHEP* **0412**, (2004) 010.

[86] V. Azcoiti, G. Di Carlo, A. Galante and V. Laliena, *Nucl. Phys. B***723**, (2005) 77.

[87] M.-P. Lombardo, *PoS(LAT2005)* 168 [arXiv:hep-lat/0509181].

[88] J. Plefka and S. Samuel, *Phys. Rev. D* **56**, (1997) 44.

[89] M. Imachi, S. Kanou and H. Yoneyama, *Prog. Theor. Phys.* **102**, (1999) 653.

[90] V. Azcoiti, G. Di Carlo, A. Galante and V. Laliena, *Phys. Rev. Lett.* **89**, (2002) 141601.

[91] V. Azcoiti, G. Di Carlo, A. Galante and V. Laliena, *Phys. Lett. B* **563**, (2003) 117.

[92] V. Azcoiti, G. Di Carlo, A. Galante and V. Laliena, *Phys. Rev. D* **69**, (2004) 056006.

[93] V. Azcoiti, G. Di Carlo and A. Galante, *Phys. Rev. Lett.* **98**, (2007) 257203 [arXiv:0710.1507 [hep-lat]].

[94] T. D. Lee and C. N. Yang, *Phys. Rev.* **87**, (1952) 410.

[95] V. Matveev and R. Shrock, *J. Phys. A* **28**, (1995) 4859.

[96] R. Agra, F. van Wijland and E. Trizac, *Eur. J. Phys.* **27**, (2006) 407.

[97] N. Bilić and R. V. Gavai, *Z. Phys. C***23**, (1984) 77.

[98] P. Hasenfratz and F. Karsch, *Phys. Lett. B***125**, (1983) 308.

[99] R. V. Gavai, *Phys. Rev. D***32**, (1985) 519.

[100] I. Barbour, *Nucl. Phys. B(Proc. Suppl.)* **26**, (1992) 22. E. Mendel, *Nucl. Phys. B***387**, (1992) 485. N. Bilić and K. Demeterfi, *Phys. Lett. B***212**, (1988) 83. J. Vink, *Nucl. Phys. B***323**, (1989) 399. C. T. H. Davies and E. G. Klepfish, *Phys. Lett. B***256**, (1991) 68. J. B. Kogut, M.-P. Lombardo and D. K. Sinclair, *Phys. Rev. D***51**, (1995) 1282; *Nucl. Phys. B(Proc. Suppl.)* **34**, (1994). I. Barbour, N-E. Behilil, E. Dagotto, F. Karsch, A. Moreo, M. Stone and H. W. Wyld, *Nucl. Phys. B***275**, (1986) 296. P. H. Damgaard, D. Hochberg and N. Kawamoto, *Phys. Lett. B***158**, (1985) 239.

[101] J. B. Kogut, M.-P. Lombardo and D. K. Sinclair, *Phys. Rev. D***54**, (1996) 2303.

[102] H. Matsuoka and M. Stone, *Phys. Lett. B***136**, (1984) 204.

[103] J. B. Kogut, H. Matsuoka, M. Stone, H. W. Wyld, S. Shenker, J. Shigemitsu and D. K. Sinclair, *Nucl. Phys. B***225**, (1983) 93.

[104] M. A. Stephanov, *Nucl. Phys. B (Proc. Suppl.)* **53**, (1997) 469.

[105] R. Aloisio, V. Azcoiti, G. Di Carlo, A. Galante and A.F. Grillo, *Phys. Lett. B***453**, (1999) 275.

[106] M. Karowski, R. Schrader and H. J. Thun, *Commun. Math. Phys.* **97**, (1985) 5.

[107] P. Rossi and U. Wolff, *Nucl. Phys. B***248** (1984) 105.

[108] F. Palumbo, *Phys. Rev. D* **60** 074009 (1999).

[109] F. Karsch and K. H. Mutter, *Nucl. Phys. B***313** (1989) 541.

[110] U. Wolff, *Phys. Lett. B***153** (1985) 92.

[111] R. Aloisio, V. Azcoiti, G. Di Carlo, A. Galante and A. F. Grillo, *Nucl. Phys. B* **564**, (2000) 489 [arXiv:hep-lat/9910015].

[112] Ph. de Forcrand and M. Fromm, *PoS(LAT2008)*, 191 [arXiv:0811.1931].

[113] N. V. Prokof'ev, B. V. Svistunov, and I. S. Tupitsyn, *Sov. Phys. JETP* **87**, (1998) 310.

[114] N. V. Prokof'ev, B. V. Svistunov, and I. S. Tupitsyn, *Phys. Lett. A***238**, (1998) 253;

[115] N. V. Prokof'ev and B. V. Svistunov, *Phys. Rev. Lett.* **87**, (2001) 160601 [arXiv:cond-mat/0103146]

[116] S. Chandrasekharan, *PoS(LAT2008)*, 003 [arXiv:0810.2419 [hep-lat]].

[117] Ph. de Forcrand and M. Fromm, *PoS(LAT2009)* 193. *Phys. Rev. Lett.* **104**, (2010) 112005.

[118] M. Salmhofer, *Nucl. Phys. B***362**, (1991) 641.

[119] U. Wenger, *Phys. Rev. D***80**, (2009) 071503 [arXiv:0812.3565v1 [hep-lat]]; *PoS(LAT2009)*022 [arXiv:0911.4099 [hep-lat]].

[120] R. Aloisio, V. Azcoiti, G. Di Carlo, A. Galante and A. F. Grillo, *Phys. Rev. D***61**, (2000) 111501 [arXiv:hep-lat/9903004].

[121] Vicente Azcoiti, Giuseppe Di Carlo, Angelo Galante and Victor Laliena, In proceedings of *"Non-Perturbative Quantum Field Theory: Lattice and Beyond"*, Guangzhou (China), [arXiv:hep-lat/0505021]; *Nucl.Phys. B***723**, (2005) 77 [arXiv:hep-lat/0503010].

[122] V. Azcoiti, J.L. Cortes, G. Di Carlo, A. F. Grillo and A. Tarancon, *Z. Phys. C* **47**, (1990) 247.

[123] Y. Deng, T. M. Garoni and A. D. Sokal, *Phys. Rev. Lett.* **99** (2007) 110601.

[124] V. Azcoiti, G. Di Carlo and A. F. Grillo, *Phys. Lett. B* **268**, (1991) 101.

[125] M. Panero, *JHEP* **0505**, (2005) 066.

[126] M. Caselle, M. Hasenbusch and M. Panero, *JHEP* **0301**, (2003) 057.

[127] R. Horsley and U. Wolff, *Phys. Lett. B* **105**, (1981) 290.

[128] I. Montvay, DESY-89-051, April 1989

[129] K. Scharnhorst, *Nucl. Phys. B***479**, (1996) 727 [arXiv:hep-lat/9604024v1].

[130] J. Steiner, *Study of the One-Flavour Lattice Schwinger Model with Wilson Fermions in therms of a 49-Vertex Model*, Diplomarbeit U. Graz, 2000.

[131] C. Gattringer, *Nucl. Phys. B***559**, (1999) 539 [arXiv:hep-lat/9903021v2]; *Nucl. Phys. B***543**, (1999) 533 [arXiv:hep-lat/9811014v1].

[132] C. Gattringer, V. Hermann and M. Limmer, *Phys. Rev. D***76**, (2007) 014503 [arXiv:0704.2277v1 [hep-lat]].

[133] U. Wolff, *Nucl. Phys. B***810** (2009) 491 [arXiv:0808.3934 [hep-lat]]

[134] Ph. W. Anderson, *Phys. Scr.***2002**, (2002) 10 [arXiv:cond-mat/0201429].

[135] E. Arrigoni, E. Fradkin and S. A. Kivelson, *Phys. Rev. B***69**, (2004) 214519 [arXiv:cond-mat/0309572].

[136] T. A. Maier, M. Jarrell, T. C. Schulthess, P. R. C. Kent, and J. B. White, *Phys. Rev. Lett.***95**, (2005) 237001.

[137] M. Creutz, *Phys. Rev. D***38**, (1988) 1228.

[138] I. G. Halliday and P. Suranyi, *Phys. Lett. B***350**, (1995) 189.

[139] V. Azcoiti, G. Di Carlo, E. Follana and A. Vaquero, *JHEP* **0908**, (2009) 008 [arXiv:0905.0639 [hep-lat]].

[140] E. Nöther, [arXiv:physics/0503066].

[141] P. Hasenfratz, *Nucl. Phys. B(Proc. Suppl.)* **63** (1998) 53.

[142] H. Neuberger, *Phys. Lett. B***417** (1998) 141; *Phys. Lett. B***427** (1998) 353.

[143] P. Hasenfratz, V. Laliena and F. Niedermayer, *Phys. Lett. B* **427**, (1998) 125 [hep-lat/9801021].

[144] S. Chandrasekharan, *Phys. Rev. D***60**, (1999) 074503 [arXiv:hep-lat/9805015].

[145] M. Lüscher, *Phys. Lett. B* **428** (1998) 342.